Identification and Development of Novel Optics for Concentrator Photovoltaic Applications

Submitted by Katie May Agnes Shanks to the University of Exeter

as a thesis for the degree of

Doctor of Philosophy in Renewable Energy

In February 2017

I certify that all material in this thesis which is not my own work has been identified and that no material has previously been submitted and approved for the award of a degree by this or any other University.

Signature: ……..

ABSTRACT

Concentrating photovoltaic (CPV) systems are a key step in expanding the use of solar energy. Solar cells can operate at increased efficiencies under higher solar concentration and replacing solar cells with optical devices to capture light is an effective method of decreasing the cost of a system without compromising the amount of solar energy absorbed. CPV systems are however still in a stage of development where new designs, methods and materials are still being created in order to reach a low levelled cost of energy comparable to standard silicon based photovoltaic (PV) systems.

This work outlines the different types of concentration photovoltaic systems, their various design advantages and limitations, and noticeable trends. Comparisons on materials, optical efficiency and optical tolerance (acceptance angle) are made in the literature review as well as during theoretical and experimental investigations. The subject of surface structure and its implications on concentrator optics has been discussed in detail while highlighting the need for enhanced considerations towards material and hence the surface quality of optics. All of the findings presented contribute to the development of higher performance CPV technologies. Specifically high and ultrahigh concentrator designs and the accompanied need for high accuracy high quality optics has been supported.

A simulation method has been presented which gives attention to surface scattering which can decrease the optical efficiency by 10-40% (absolute value) depending on the material and manufacturing method. New plastic

optics and support structures have been proposed and experimentally tested including the use of a conjugate refractive-reflective homogeniser (CRRH). The CRRH uses a reflective outer casing to capture any light rays which have failed total internal reflection (TIR) due to non-ideal surface topography. The CRRH was theoretically simulated and found to improve the optical efficiency of a cassegrain concentrator by a maximum of 7.75%. A prototype was built and tested where the power output increase when utilising the CRRH was a promising 4.5%. The 3D printed support structure incorporated for the CRRH however melted under focused light, which reached temperatures of 226.3°C, when tested at the Indian Institute of Technology Madras in Chennai India.

The need for further research into prototyping methods and materials for novel optics was also demonstrated as well as the advantages of broadening CPV technology into the fields of biomimicry. The cabbage white butterfly was proven to concentrate light onto its thorax using its highly reflective and lightweight wings in a basking V-shape not unlike V-trough concentrators. These wings were measured to have a unique structure consisting of ellipsoidal pterin beads aligned in ladder like structures on each wing scale which itself is then tiled in a roof like pattern on the wing. Such structures of a reflective material may be the answer to lightweight materials capable of increasing the power to weight ratio of CPV technology greatly. Experimental testing of the large cabbage white wings with a silicon solar cell confirmed a 17x greater power to weight ratio in comparison to the same set up with reflective film instead of the wings.

An ultrahigh design was proposed taking into account manufacturing considerations and material options. The geometrical design was of 5800x of which an optical efficiency of either ~75% with state of the art optics should produce and effective concentration of ~4300x. Relatively standard quality optics on the other hand should give an optical efficiency of ~55% and concentration ratio ~3000x. A prototype of the system is hypothesised to fall between these two predictions. Ultrahigh designs can be realised if the design process is as comprehensive as possible, considering materials, surface structure, component combinations, anti-reflective coatings, manufacturing processes and alignment methods. Most of which have been addressed in this work and the accompanied articles. Higher concentration designs have been shown to have greater advantages in terms of the environmental impact, efficiency and cost effectiveness. But these benefits can only be realised if designs take into account the aforementioned factors. Most importantly surface structure plays a big role in the performance of ultrahigh concentrator photovoltaics.

One of the breakthroughs for solar concentrator technology was the discovery of PMMA and its application for Fresnel lenses. It is hence not an unusual notion that further breakthroughs in the optics for concentrator photovoltaic applications will be largely due to the development of new materials for its purpose.

In order to make the necessary leaps in solar concentrator optics to efficient cost effective PV technologies, future novel designs should consider not only

novel geometries but also the effect of different materials and surface structures. There is still a vast potential for what materials and hence surface structures could be utilised for solar concentrator designs especially if inspiration is taken from biological structures already proven to manipulate light.

Acknowledgements

Firstly, I would like to express my sincere gratitude to my supervisor Prof. Tapas Mallick for the continuous support of my Ph.D study, for his patience, motivation, and immense knowledge. His guidance helped me throughout my research and writing. His as well as the advice and insights from my second supervisor, Dr. Senthil Sundaram, were invaluable to my progression as a researcher overall.

I would like to also thank Prof. Richard Ffrench-Constant for his guidance in the butterfly related research. He encouraged me to widen my research from various perspectives and brought a different point of view and aim to the interdisciplinary research. His enthusiasm was always a driving force for the research and its applicability in a commercial sense.

My sincere thanks goes to James Yule who helped me understand the mechanical difficulties in building prototypes, for the long discussions on material and structural supports required for the optical designs presented here and for giving me his precious time when deadlines for prototypes were approaching.

Appreciation also goes to Dr. Eduardo Fernandez at the University of Jaen in Spain and to Prof. K.S. Reddy at the Indian Institute of Technology Madras in India who both provided me an opportunity to join their teams and gave me access to their laboratory and research facilities.

Last but not the least, I would like to thank my family for their support, my fellow lab mates for the stimulating discussions and suggestions, and my friends for the times in and out of university. My PhD experience would not have been the same without any of them.

Table of Contents

List of Figures

Abbreviations, symbols and nomenclature

ABS	Acrylonitrile Butadiene Styrene	-
AM	Atmosphere	-
ASAP	Advanced Systems Analysis Program	-
ASTM	American Society of Testing and Materials	-
BICPV	Building Integrated Concentrator Photovoltaic	-
BRDF	Bidirectional Reflectance Distribution Function	-
BSDF	Bidirectional Scatter Distribution Function	-
BTDF	Bidirectional Transmittance Distribution Function	-
C	Concentration	X or Suns
CAP	Concentration Acceptance Product	-
CNC	Computer Numerical Control	-
CPC	Compound Parabolic Concentrator	-
CPV	Concentrator Photovoltaic	-
CRRH	Conjugate Refractive Reflective Homogeniser	-
EVA	Ethylene-vinyle Acetate	-
f	Focal Length	m
G	Spectral Irradiance	$W/m^2/nm$
GaAs	Gallium Arsnide	-
H	Height	m
HCPV	High Concentrator Photovoltaic	-
I	Current	Amps
LCO	Low Concentrator Optics	-
LSC	Luminescent Solar Concentrator	-
n	Refractive Index	-
O-I	Oranic-Inorganic	-

PC	Polycarbonate	-
PDMS	Polu(dimethylsiloxane)	-
PET	Polyethylene Terepthalate	-
PMMA	Poly (methylmethacrylate)	-
PSD	Power Spectral Density	-
PV	Photovoltaic	-
r	Radius	m
SD	Separation Distance	-
SHE	Square Elliptical Hyperboloid	-
Si	Silicon	-
SOG	Silicon on Glass	-
TiO2	Titanium Dioxide	-
TIR	Total Internal Reflection	-
TIS	Total Integrated Scatter	-
UHCPV	Ultra-High Concentrator Photovoltaic	-
V	Voltage	Volts
W	Width	m
α_1	Angle of Incidence	°
α_2	Angle of Refraction/Reflection	°
θ_C	Critical Angle	°
λ	Wavelength	nm
σ or RMS	Route Mean Square (RMS)	-

List of Accompanying Material

In the Appendix the following published and submitted articles are given.

Journal Papers Published:

Article 1. K. Shanks, S. Senthilarasu, and T. K. Mallick, “Optics for concentrating photovoltaics: Trends, limits and opportunities for materials and design,” *Renew. Sustain. Energy Rev.*, vol. 60, pp. 394–407, Jul. 2016.

The complete review was performed and written by the author under the guidance of the supervisors.

Article 2. K. Shanks, N. Sarmah, J. P. Ferrer-Rodriguez, S. Senthilarasu, K. S. Reddy, E. F. Fernández, and T. Mallick, “Theoretical investigation considering manufacturing errors of a high concentrating photovoltaic of cassegrain design and its experimental validation,” *Sol. Energy*, vol. 131, pp. 235–245, Jun. 2016.

The initial design concept was proposed by the first and second author. The optimisation procedure, theoretical simulations and paper was completed by the first author under the guidance of the supervisor. The experimental work was carried out by the first author and third author with the supervision of the sixth author.

Article 3. K. Shanks, H. Baig, S. Senthilarasu, K. S. Reddy, and T. K. Mallick, “Conjugate refractive–reflective homogeniser in a 500× Cassegrain concentrator: design and limits,” *IET Renew. Power Gener.*, vol. 10, no. 4 (Special Issue - Invited from PVSAT-11), pp. 440–447, Apr. 2016.

This initial concept was suggested by the second author. The methods, simulations, experimental work and paper writing was carried out by the first author with advice from the other authors on presentation and how to carry out an easy validation experiment.

Article 4. K. Shanks, H. Baig, N. P. Singh, S. Senthilarasu, K. S. Reddy, and T. K. Mallick, “Prototype fabrication and experimental investigation of a conjugate refractive reflective homogeniser in a cassegrain concentrator,” *Sol. Energy*, vol. 142, pp. 97–108, Jan. 2017.

The design, molding of the optics, assembly of the prototype and paper writing was completed by the first author. The second author suggested using 3D printing for the support structure of the CRRH’s reflective sleeve. The experimental and thermal measurements were carried out with the help of the third author and supervision of the fifth and sixth authors.

Article 5. K. Shanks, S. Senthilarasu, R. H. Ffrench-Constant, and T. K. Mallick, “White butterflies as solar photovoltaic concentrators,” *Sci. Rep.*, vol. 5, p. 12267, Jul. 2015.

The concept, experimental plan and manuscript preparation was initiated by the first author and discussed by all authors. The first author performed all practical experimentation and analysis and first contacted the third author on the possibility of the overlapping research.

Article 6. K. Shanks, J. P. Ferrer-Rodriguez, E. F. Fernández, P. Pérez-Higueras, S. Senthilarasu, and T. K. Mallick, “An Ultrahigh Concentrator Photovoltaic Design based on multiple Fresnel Lens Primarys focusing to one central Solar cell,” *Optica*, 2017 *(submitted).*

The initial concept was conceived jointly between the first, second, third and fourth authors. The work was performed and written by the author under the guidance of the supervisors.

Book Chapters:

Article 7. Shanks, K., Senthilarasu, S., Mallick, T.K.: ‘High-Concentration Optics for Photovoltaic Applications’, in Pérez-Higueras, P., Fernández, E.F. (Eds.): ‘High Concentrator Photovoltaics:

Fundamentals, Engineering and Power Plants' (Springer International Publishing, 2015, 1st edn.), pp. 85–113

The complete chapter was written by the author under the guidance of the supervisors and the editors.

Conference Papers:

Article 8. N. Sarmah, K. Shank, L. Micheli, K. S. Reddy, and K. M. Tapas, "Design and Optical Performance Analysis of a Reflective Type High Concentrating Photovoltaic System," in *9th International Conference on Concentrator Photovoltaic Systems (CPV-9)*, 2013.

Half of the results and graphical representations were completed by the second author. The article was written by the first author under the guidance of their supervisors.

Article 9. K. Shanks, N. Sarmah, and T. K. Mallick, "The Design and Optical Optimisation of a Two stage Reflecting High Concentrating Photovoltaic Module using Ray Trace Modelling," in *PVSAT-9*, 2013, pp. 4–7.

The complete work was performed and written by the author under the guidance of the second author and supervisors.

Article 10. K. Shanks, N. Sarmah, K. S. Reddy, and T. Mallick, “The design of a parabolic reflector system with high tracking tolerance for high solar concentration,” in *AIP -10th International Conference on Concentrator Photovoltaic Systems (CPV-10)*, 2014, October 2015, pp. 211–214.

The complete work was performed and written by the author under the guidance of the second author and supervisors.

Article 11. K. Shanks, H. Baig, and T. K. Mallick, “The Conjugate Refractive-Reflective Homogeniser in a 500X Cassegrain Concentrator : Design, Limits and Optical Surface Losses,” in *11th Photovoltaic Science Application and Technology Conference (PVSAT-11)*, 2015, October.

The complete work was performed and written by the author under the guidance of the second author and supervisors.

Article 12. P. Pérez-Higueras, J. P. Ferrer-Rodríguez, K. Shanks, F. Almonacid, and E. F. Férnández, “Thin photovoltaic modules at ultra high concentration,” in *AIP -11th International Conference on Concentrator Photovoltaic Systems (CPV-11)*, 2015, no. 1679, p. 130004.

The design was discussed by all others, the work and paper was written by the second author with guidance from the other authors.

Article 13.P. K. Shanks, S. Senthilarasu and Tapas K. Mallick, “Reliability Investigations for a Built Ultrahigh Concentrator Prototype,” *13th International Conference on Concentrator Photovoltaic Systems (CPV-13)*, 2017. (Abstract accepted).

The complete work was planned and untaken by the first author with guidance from the second and third authors.

CHAPTER 1: Introduction

Solar energy is one of the most abundant resources upon the earth which can produce clean and efficient energy to many locations. Photovoltaics (PV) can convert absorbed sunlight into electricity at efficiencies ranging up to almost 50%. However to achieve these high conversion efficiencies the sunlight incident upon the PV material must be concentrated and the cells themselves typically made of expensive 'rare earth' materials such as gallium and indium. Some semiconductor materials and combinations utilised for solar cells are GaAs, AlGaInP, GaNAsSb, GaInAsP and GaInP. The manufacturing of cells themselves can involve toxic materials such as Arsenic, cadmium telluride and lead. Silicon cells can also be used with concentrated light but are best suited to low concentration optics and will not produce as high conversion efficiencies as the systems utilising multijunction cells. Concentrator Photovoltaics (CPV's) reduce the amount of PV material required by replacing it with optical devices that collect and redirect the light towards the smaller PV. In this way the cost of the system can be reduced, especially if multi-junction cells are being used, and there is less demand for the mined elements required for the PV materials. In comparison to standard flat plate solar panels which are typically of much lower efficiencies (~20-30% commercially available at present) CPV's are more environmentally friendly due to the reduced PV material and higher conversion efficiencies.

There are however many challenges in CPV design and manufacturing.

This work outlines these challenges and provides a number of solutions to overcome them. The importance of surface structure and material choice in the design and manufacturing stages of CPV production is proven. Effective methods and solutions to the accounting and capturing of lost energy due to surface scattering is provided. This includes the development of the conjugate refractive reflective homogeniser (CRRH) which is a simple optic that can increase the optical efficiency. The effect and practicality of using plastic optics has also been investigated as another option to combat conventional material and surface flaws. Lightweight plastic optics or support structures can be used as long as no more than low concentration light is incident on them. Pioneering work into biomimicry, specifically of the cabbage white butterfly's reflective wings, for developing lightweight reflective materials has been presented. A novel ultrahigh concentrator design is given which accounts for optical losses and gives realistic minimum and maximum performance predictions depending on the quality of optics employed.

The methods and results presented should be useful to many areas of CPV optical research, designers, manufacturers and even some biologically based science which requires a different view point to confirm behaviour or structural hypothesis. With the increasing encouragement for renewable energy as a means against reducing fossil fuel usage and global warming, the advancement of solar energy technology is beneficial. Solar energy technology, specifically concentrator photovoltaics have a vast potential for higher efficiency, cost effective and aesthetically pleasing designs. This work aims to branch out from the current field of CPV optics and initiate focus onto

biomimicry, surface pattern considerations and simplified cost effective prototyping methods. Ultimately it is the practicality of CPV technology which will determine its application reach, popularity and impact.

Aims and Objectives of Research

- Reviewing current concentrator photovoltaic technology, disseminating the technology into its multiple constituents and identifying routes to designing higher performing CPV systems.
- Understanding and developing effective modelling methods to accurately predict the performance of an optical system for CPV use. This includes gaining expertise in current ray tracing software to simulate accurately CPV deigns.
- Designing, optimising and building novel low concentration and high concentration optics for CPV applications. Comparing how successful prototypes perform experimentally with their theoretical predictions and what causes the results to differ. By doing this specific materials and manufacturing methods may be less effective than others in building novel optics. Methods to mitigate loss in the final built CPV designs can hence also be found in each stage of development, from simulation to manufacturing.
- To broaden the scope of design and optical material use within the area of CPV research. Proposing new reflective (including coating and substrate) materials, structures, geometries and simple solutions to improving the performance of CPV technology.

1.1. Research Methodology

1.1.1. Reviewing Literature

Past milestones in CPV technology and current developments in optical design were reviewed to gain an understanding of the most established technologies and identify development trends. Research into the potential for materials and biomimicry was also undertaken and highlighted as an untapped area for CPV development. Methods for theoretically and experimentally investigating a design were explored and key parameters to analyse identified.

1.1.2. Design and performance investigations of concentrator optics

First, a cassegrain design was investigated using the ray trace modelling software ASAP. This Monte Carlo based simulation software has both a high level of accuracy and fast rendering speeds. Optical geometries were built using a combination of imported Solidworks geometries and by being built within the ASAP software itself. The cassegrain design was then optimised, built and tested. The prototype was experimentally tested under solar simulators at the University of Exeter and at the University of Jaen in Spain. The results helped to develop a more thorough and accurate method of ray trace simulation. The need for attention to surface structure was highlighted from this work and the prototype redesigned to take this into account. The optics within the simulations were adjusted to study various material and surface quality effects. This lead to research into the manufacturing capabilities for concentrator optics and the need for a more thorough

simulation method incorporating specific refractive index plots, scattering profiles and other optical properties of the optics to be used.

1.1.3. Ray Trace Simulation Method

A simulation environment was developed which included a suitable sun source and appropriate analysis steps for designing low and high concentrator optics. The edge-ray principle was utilised for wavelength ranges appropriate to the intended solar cell to be used. Absorption, refraction and reflection losses were included and linked to each optics material specific refractive index behaviour. This included Fresnel reflection and incomplete total internal reflection (TIR) due to surface errors. Particular attention was given to understanding and developing the scattering profiles of different optical materials and shapes due to their surface structure and refractive index.

1.1.4. Extending Material considerations with Biomimicry

From the surface structure results and understanding developed previously, investigations were made into the wings of the Cabbage White Butterfly. The basking behaviour of this butterfly (wings in a V-shape) was compared to V-trough concentrators in the literature, especially those with grooved microstructures or facets. The wings were measured using a spectrophotometer and found to be highly reflective. Experiments were carried out matching these extremely lightweight wings with single junction solar cells and testing the cells output under a solar simulator with an I-V tracer. Concentration was also proven utilising a thermal camera and the wings in a V-shape. Overall the wings and solar cell configuration reduced the power to weight ratio significantly in comparison to the system with reflective film wings.

1.1.5. Prototype Manufacturing and Experimental testing

Using the optimised designs from the ray trace simulations, prototypes of low and high concentration optics were built and tested. Various materials and methods of manufacturing were explored including moulds, polishing and 3D printed plastic mirrors with reflective coatings or films. Some of the optics geometrics or moulds were ordered from external companies but where possible they were made in house. Again there was always the aim of improving the surface quality (smoothness) of the optics. Manufactured optics were tested separately and together for their optical efficiency, acceptance angle and I-V performance utilising state of the art spectrophotometers, external quantum efficiency machines and solar simulators.

1.1.6. Ultrahigh Concentration

Ultrahigh concentration requires high quality optics and precise alignment accuracy for optimal performance. From the investigations into surface structures, manufacturing techniques and optical tolerance an ultrahigh concentration design was developed. This design takes into account the challenges of obtaining high optical efficiencies as well as high acceptance angles and the limitations of current materials and manufacturing methods. A detailed analysis is given of the designs characteristics and optical measurements taken to ensure the theoretical matches the experimental. Suggestions for improvement are given for all designs presented here and for future research.

1.2. Contribution of the papers in the field

- A thorough characterisation and dissemination of solar concentrator designs and how they should be grouped and compared as well as noticeable trends and their future outlook.
- A design and modelling method aimed at optimising acceptance angle while incorporating realistic surface errors of optics as well as other practical concerns.
- Understanding of the impact of surface structures; specifically of non-ideal optics, materials and manufacturing methods on the performance of a prototype in comparison to its theoretical predictions.
- Cheap, easy and effective methods at the prototyping stage to improve optical efficiency using conjugate refractive reflective methods to trap light.
- The practicality of using plastic mirrors and 3D printed structures in concentrator devices of high concentration ratios and high temperatures.
- Experimentally confirmed concept of the cabbage white butterfly concentrating light using its white wings in a V-shape and the potential for a material based on their wing structure for high power-weight ratio devices.

1.3. Outline of the thesis

Chapter 1 introduces the topic of solar energy, solar concentrators, their benefits and the many challenges in harvesting light for electricity. An updated literature review of different solar concentrator designs is given, expanded

from article 1 and 7. The importance of material choice and surface structure is highlighted along with suggestions for furthering CPV research by investigating natural structures.

Chapter 2 demonstrates the challenges and limitations of optics through the design of a cassegrain concentrator. Again, surface structure and scattering effects introduced in chapter 1 are expanded upon and the simulation methods used for reproducing the effects given. An optimisation procedure is proposed for incorporating the surface roughness of optics into designs when working with ray trace software such as Breaults ASAP. The work presented here, and in articles 2 and 8-10, identify the complex challenges facing CPV optical design. Specifically, the need for more material options and manufacturing methods, which can produce high quality but cost effective smooth surfaces, is demonstrated.

Chapter 3 Proposes a solution to surface imperfections described in chapter 2. A conjugate refractive reflective homogeniser (CRRH) is designed and investigated as presented in articles 3 and 11. The CRRH utilises an outer reflective casing surrounding a solid refractive homogeniser such that any light rays which fail total internal reflection within the refractive part of the homogeniser are still captured by the reflective outer sleeve. Different refractive materials and scattering profiles are also given and tested to see their associated optical losses. The benefit of the CRRH compared to its purely refractive homogeniser counterpart is also demonstrated theoretically and a simple proof of concept experiment also carried out.

Chapter 4 carries on from chapters 2 and 3, detailing the manufacturing and assembly challenges of the cassegrain concentrator (article 2) and CRRH (article 4). Again, the challenge of obtaining smooth surfaces for the optics are highlighted, especially in the prototyping stage which do not benefit from mass production cost savings. The use of reflective films, plastic mirrors and support structures are discussed and presented in this chapter. Plastic substrates for reflective optics are explored and their limitations in high temperatures demonstrated. 3D printing is also investigated for support structure use as part of the CRRH. A complete 3 by 3 array of the cassegrain concentrator with CRRH is presented along with its installed performance at the Indian Institute of Technology Madras in Chennai, India. This chapter, and articles 2 and 4, substantiate the scattering losses projected from the theoretical parts of chapters 2 and 3 due to surface quality and material choice.

Chapter 5 gives a thorough example of interdisciplinary research by showing how complex surface structures developed by nature could be used for solar concentrator optics. This chapter differs from the previous chapters by demonstrating specific surface patterns as enhancing optics for CPV use. The wings of the cabbage white butterfly are both highly reflective and extremely lightweight. Biomimicry of such a structure could greatly improve the power to weight ratio of CPV technology and vastly expand its application. The work presented in this chapter and the accompanying article 5 sets a route for research to expand into biomimetic optics for CPV applications. There is great

potential for CPV optics to be found in this untapped resource and this chapter gives one example of how to measure and deduce such potential from natural materials.

Chapter 6 introduces and summarises the results from article 6; detailing the design of a novel ultrahigh concentrator photovoltaic system. This chapter links to previous chapters due to the increased importance of optical accuracy for ultrahigh concentrator systems. In this way the surface structure, material choice, manufacturing challenges, prototyping techniques and practical considerations all must be matched and optimised for best performance. The cases for relatively standard quality optics and state of the art optics are both presented with the associated optical efficiency for each. For both cases ultrahigh concentration is reached and the choice of priority between efficiency, cost or land cover is discussed as also done in article 13.

Chapter 7 concludes the chapters and gives recommendations for future work.

Overall this work identifies novel surface structures, materials and optics for use as CPV optics. A broad literature review explores the potential in the faceting of designs and potential of biomimicry. Challenges have been clearly demonstrated theoretically and experimentally, mainly due to optical quality and etendue limitations. Solutions have been proposed including the CRRH optic and the ultrahigh concentrator design. Future work has been suggested to continue the investigation into biomimicry for CPV optics and to develop

cost effective efficient CPV technology. The methods and results presented should be useful to many areas of CPV optical research, designers, manufacturers and even some biologically based science which requires a different view point to confirm behaviour or structural hypothesis.

1.4. Literature Review:

1.4.1. Solar Energy

Energy from the sun is one of the most abundant on the planet. In 1 second the sun delivers 120 petajoules of energy to the earth and in 1 hour the sun gives more energy to the earth than humanity consumes over the course of a year [Article 1]. In comparison to other forms of renewable energy technology solar energy also has the most potential as discussed by Timilsina et al. [1]. Solar energy is the only renewable energy that can be captured in space and has been installed in varying scales, from calculators to power plants. It has the greatest flexibility and at present is the leading renewable energy technology for domestic power generation. There are however many complexities and challenges to harvesting solar energy for our own use.

The direct normal solar radiation spectrum is shown in Figure 1 labelled as AM = 1.5. This is the standard spectrum assumed as the input to most photovoltaic devices. This spectrum is the energy from the sun after parts of it have been absorbed by the atmosphere due to water vapour, oxygen and carbon dioxide [2]. As can be seen from Figure 1 different solar zenith angles (angle between the sun and the vertical) will give different effective incident irradiance as the light rays pass through different thicknesses of the earth's atmosphere.

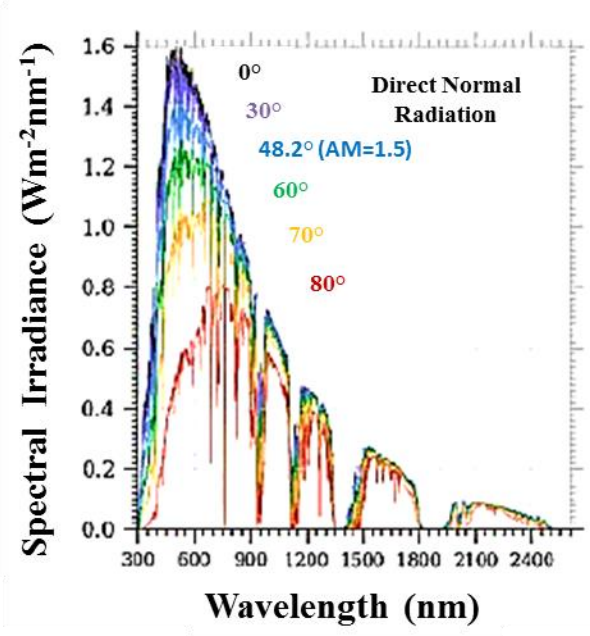

Figure 1: Spectral direct radiation for varying solar zenith angles and the American Society of Testing and Materials (ASTM) G173 AM1.5 standard [2].

Light from the sun also has a divergence angle of ±0.27° due to the diameter of the sun which means alignment with the sun will also have this error range as a minimum. Brendt and Rabl [3] investigated the variation in radiance across the sun's disc (called limb darkening) and proposed the radiance distribution as shown in Figure 2. This distribution and specifically the divergence angle play a key role in concentration ratio limits and attainable accuracy of solar concentrator designs as discussed later.

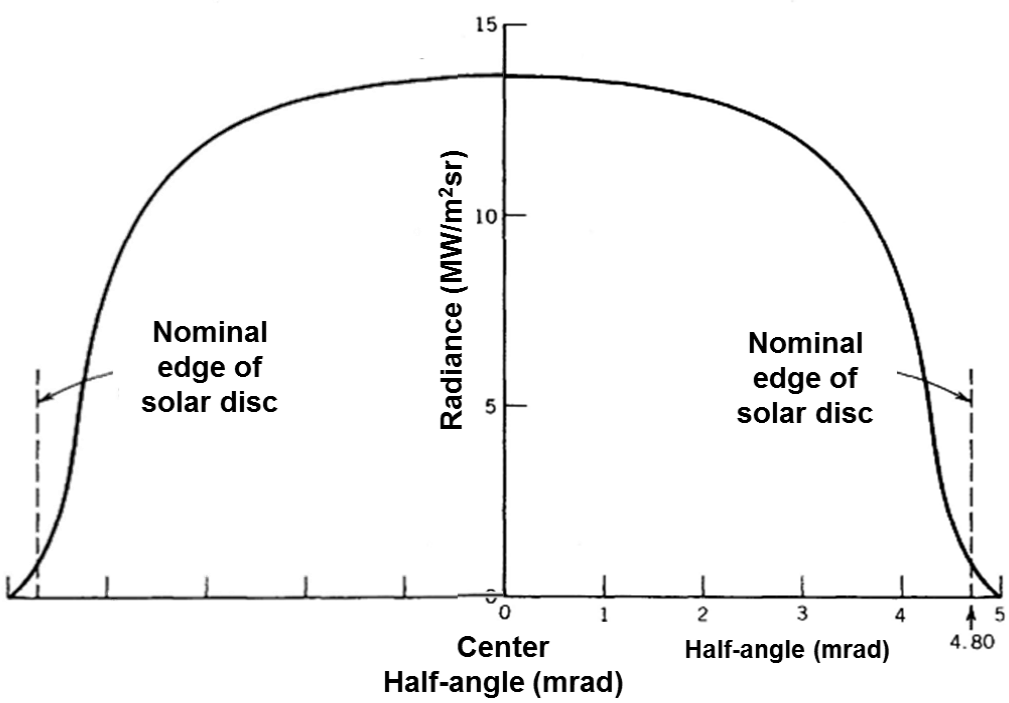

Figure 2: The sun shape showing the divergence angle of solar light [3].

In recent years, the bivariate Gaussian distribution is often used as an approximate representation of the sun shape for error calculations [3], [4] and the variation in this shape and the solar "constant" power has been investigated further [2]. Many other contributing factors such as location, temperature, humidity, pollution (e.g. aerosols, soot and dust) and much more can affect the exact irradiance spectra for a device as described by Perez-Higueras et al. [2]. There has been some case studies on modelling these effects but no model so far has been proven to be accurate for all locations [2] To capture this incident energy, solar photovoltaic or solar thermal technology can be used to convert the sunlight into electricity or heat respectively.

1.4.1. Etendue

Etendue is the term given to characterise the size and angular spread of a beam of light. It literally translates from French as ‘extension’ and can come under many other names such as acceptance, view factor and Lagrange invariant [5], [6]. It can be described and derived in various forms such as in terms of optical momentum, phase space, optical path length and as a geometrical quantity [7]. Most importantly, the law of Etendue can be thought of as the optical equivalent to the law of entropy which can never be decreased, only conserved at a minimum. Derivations of the various forms of etendue are given in sources such as by Winston et. al. [6] and Julio Chaves [7]. Here we will give a simple derivation which is also covered by Julio chaves and apply it to the concentration limit to aid understanding in the context of solar concentrators.

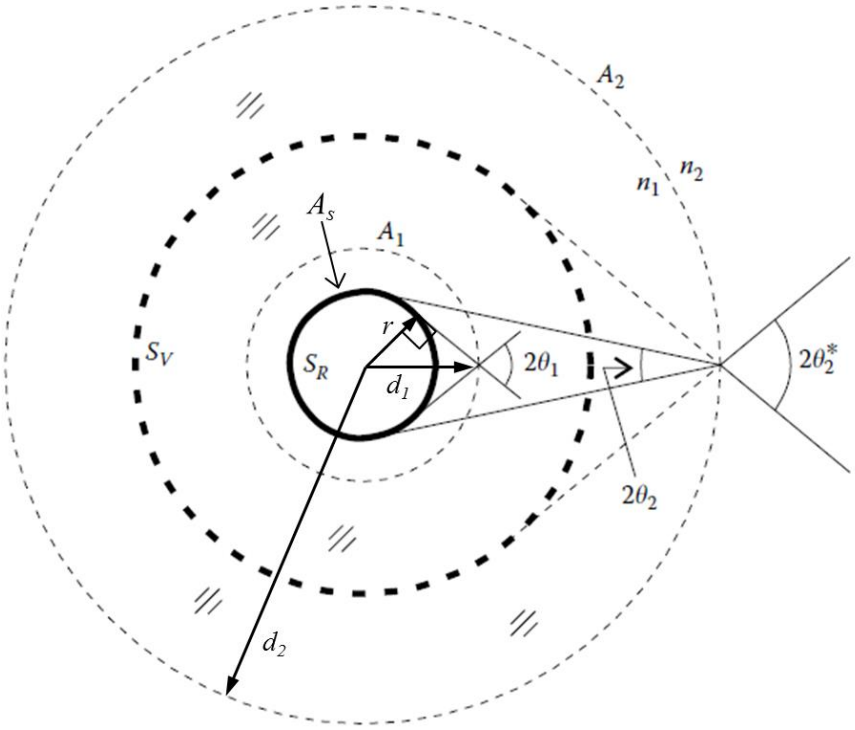

Figure 3: Representation of 3D light cones formed from source S_R when hitting surface A_1 and A_2 where A_2 is an interface between two refractive

indices n_1 and n_2 and refraction takes place. The light cone spreading after refraction at A_2 can be represented as coming from a virtual spherical source S_V [7].

As can be seen in Figure 3 there is a relationship between the minimum distance travelled of a cone of light rays (d_1 or d_2) and the maximum incidence angle of the light rays upon a surface (A_1 or A_2). When the distance travelled from a source (d) is increased the angle (θ) is decreased as shown by small d_1 with large θ_1 and large d_2 with small θ_2 in Figure 3. The maximum angle of light from the source is a line tangential to the radius of the source and hence the following relationship links the parameters of the source S_R and surface A_1.

$$\frac{r}{d_1} = \sin\theta_1 \tag{1}$$

Where r is the radius of the source S_R, d_1 is the shortest distance travelled by a light ray from the source S_r to the surface A_1 and θ_1 is the maximum incidence angle of a light ray from the source incident on the surface. The same can be said for light rays incident on surface A_2 using d_2 and θ_2. The area of the spherical surface A_1 is given by:

$$A_1 = 4\pi d_1^2 \tag{2}$$

Which if we substitute for d from equation 1 we can acquire:

$$A_1 \sin^2\theta_1 = 4\pi r^2 = A_s \tag{3}$$

Where A_S is the area of the source providing the illumination. The above equation is similar for A_2 and θ_2 in Figure 3 which means that both equations can be related through A_S to give:

$$A_1 \sin^2 \theta_1 = A_s = A_2 \sin^2 \theta_2 \quad (4)$$

From this and Figure 3 we can see that as light travels further, the area (or distance) it uses increases but the angle of the light cone decreases. This happens in such a way that the quantity A $\sin^2\theta$ is conserved.

Now if we include an optical stage such as refraction at A2 where light refracts from n_1 to n_2 and the angle of spreading light increases from $2\theta_2$ to $2\theta_2$* then we can say that the light appears to come from a virtual source S_V. We can then write a similar equation to equation 3.

$$A_2 \sin^2 \theta_2^* = A_V \quad (5)$$

We can then relate this equation to equation 4 through snells law:

$$n_1 \sin\theta_2 = n_2 \sin\theta_2^*$$

$$\sin\theta_2 = \frac{n_2}{n_1}\sin\theta_2^*$$

$$A_1 \sin^2\theta_1 = A_2 \sin^2\theta_2 = A_2\left(\frac{n_2}{n_1}\sin\theta_2^*\right)^2 = A_2\frac{n_2^2}{n_1^2}\sin^2\theta_2^*$$

$$A_1 n_1^2 \sin^2\theta_1 = A_2 n_2^2 \sin^2\theta_2^* \quad (6)$$

In this way the quantity n^2A $\sin^2\theta$ is conserved as light travels through space. The étendue of the radiation crossing area A within a cone of angle $\pm\theta$ is given the equation

$$U = \pi n^2 A \sin^2\theta \quad (7)$$

and is conserved in the geometry presented in Figure 3.

1.4.1.1. Maximum Concentration Ratio

From equation 6 we can rearrange such that we get the concentration ratio of a system:

$$\frac{A_1^2}{A_2^2} = \frac{n_2^2 \sin^2 \theta_2^*}{n_1^2 \sin^2 \theta_1} \tag{8}$$

In a realistic concentration system we can assume that a light ray will not be absorbed if it begins to point away from the receiver (θ*>π/2) and so we obtain:

$$3D\,Concentration\,Ratio = \frac{n_2^2}{n_1^2 \sin^2 \theta_1} \tag{9}$$

Similarly for a 2D system we would have:

$$2D\,Concentration\,Ratio = \frac{n_2}{n_1 \sin \theta_1} \tag{10}$$

Where n_2 is the refractive medium in contact with the solar cell. Now for the maximum concentration ratio obtainable on earth, ignoring scattering and absorption losses, we can assume an ideal system perfectly normal to the light rays coming from the distant source of the sun and immersed in air. These rays as already mentioned in 1.4.1 have a fundamental uncertainty angle of ±0.27° which when inserted as the incidence angle into equation 9, and taking $n_1=n_2=1$ in air, gives us the maximum concentration ratio of ~46000 Suns. This is also explained in Article 7 and in further detail elsewhere [6], [7].

1.4.2. Photovoltaic Solar Cells

There are now many types of photovoltaic solar cells with varying record efficiencies as shown in Figure 4. Single p-n junction solar cells can only

absorb one wavelength band of the incident irradiance. This limits their efficiency to ~33%, first calculated and named as the Shockley-Queisser limit in 1961 [8]. Multi-junction solar cells (e.g. GaInP/GaAs/GaInAsP/GaInAs) can utilise more wavelengths of the suns radiation but are also much more expensive [9]. The main types of solar cell technologies can be categorised as monocrystalline (e.g. Silicon, GaAs, CdTe), multicrystalline/polycrystalline (e.g. Silicon, GaAs), thin-film (e.g. CIGS, CdTe and Amorphous Si:H) and multi-junction (e.g. up to 4 junctions so far, involving various combinations of Gallium, Arsenide, Indium, Phosphorous, Sodium, and others). There are also a number of emerging photovoltaics which include dye-sensitized, perovskite, quantum dot, organic and inorganic cells as shown in Figure 4.

The main single and multi-crystal semiconductors at present are Gallium Arsenide (GaAs) and Silicon (Si) with wafer-based crystalline-silicon materials dominating the commercial market at present. Their efficiencies are as high as ~25% depending on the quality of the module and as expected linked to the cost [10]. The best initial efficiencies of thin film amorphous-silicon were 13.7% and 9.8% with triple-junction cells and modules in the early 1990's [10]. Stabilised efficiencies for commercial modules are however ~10% for these materials. As expected there is always a drop between laboratory record cell efficiencies and commercialised modules available in the market. This is due to the changes in accuracy from lab conditions to full scale production which of course must be done in a cost, time and resource efficient manner. Manufacturing and material flaws as well as practical environments

(varying temperatures and exposures over time) also reduce the efficiency of commercialised modules in comparison to their lab cell counterparts.

Currently the record efficiency for a single and multijucntion solar cell without concentrated light (1 sun) is 28.8% with a thin film GaAs and 38.8% with a… AlGaInP/ AlGaInAs/ GaInAs/ GaInNAsSb/ Ge combination respectively, as shown in Figure 4. The multijunction solar cell is a 5-junction Spectrolab cell [11]. The number of junctions of a solar cell increases the theoretical maximum conversion efficiency possible of that cell as it is able to accept more of the suns spectrum [10]. According to Razykov et. al. [10] the thermodynamic limit of a 2 junction solar cell is 55.6%, of 3 junctions 63.6% and for 4 junctions 68.5% under un-concentrated sunlight conditions. Doeleman [12] takes this further and calculated more realistic efficiencies of ~46% for double junctions, ~50% for triple and ~53.5% for 4-junction solar cells. Doeleman also suggests that an 8 junction solar cell can achieve around 60% efficiency and compares these efficiencies to those found in the literature where possible. Multi junction solar cells are however very expensive. Concentrating light onto single and multi-junction solar cells can increase their efficiencies and is a good solution to also reduce the cost of the system by reducing the amount of PV material required.

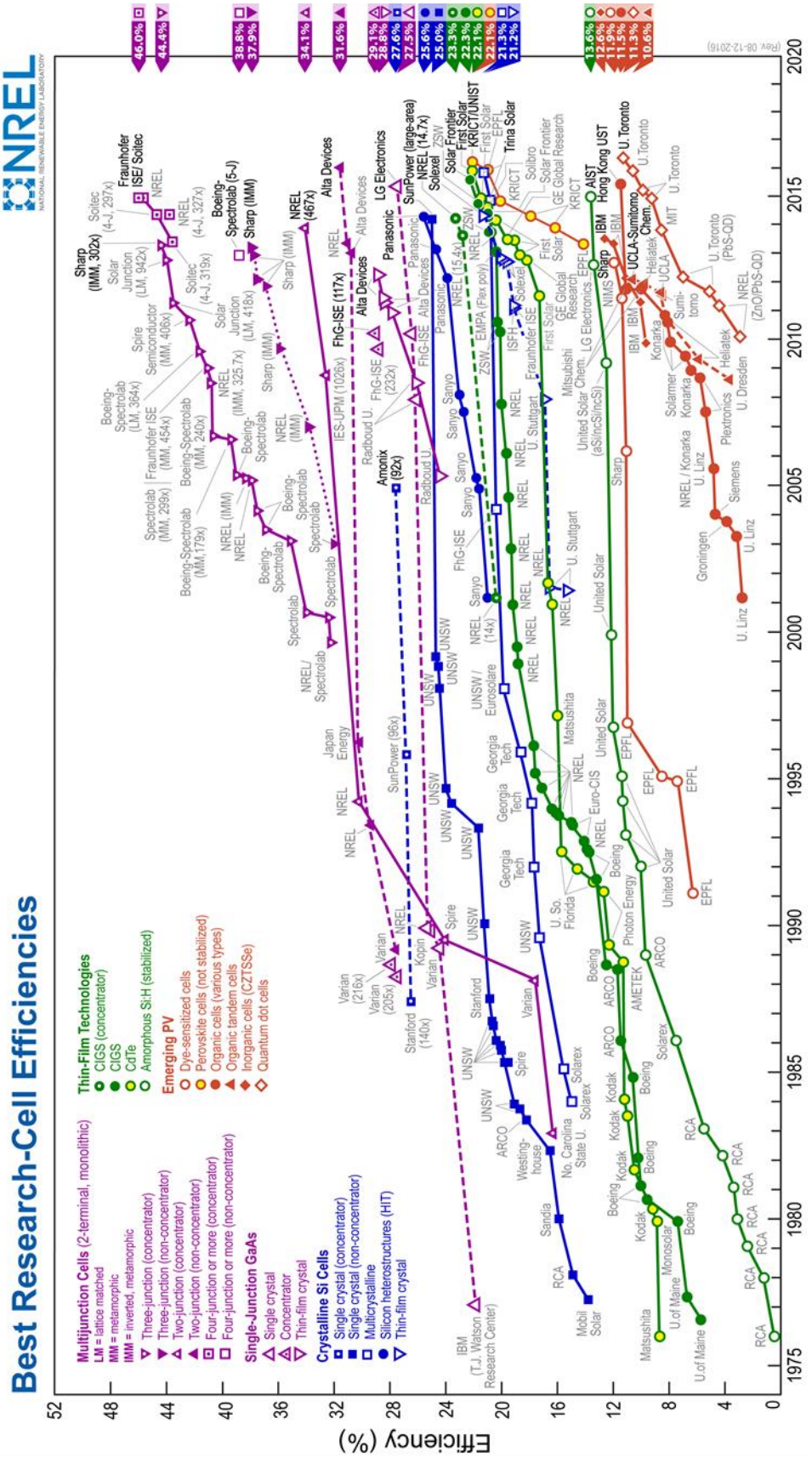

Figure 4: Record Cell Efficiencies chart [11].

1.4.3. The Benefits of Concentrator Photovoltaics

Concentrator photovoltaic (CPV) technologies are systems made up of optical devices that focus light towards decreased areas of photovoltaic (PV) material. There are many different concentrator designs still being developed, some which are illustrated in Table 1. The efficiency boundaries of solar cells can be increased by concentrating the amount of light incident on their surfaces using optical components such as lenses and mirrors. On earth the maximum concentration level possible is 46200 suns due to the law of etendue concerning the suns diameter (Figure 2) and its divergence of light (±0.27°) [Article 6] [6], [7]. Article 6 gives further detail in the maximum concentration ratio equations for different types of CPVs due to etendue. Assuming this maximum concentration ratio, the optimum theoretical efficiency of a single junction solar cell is extended to 45.1% [12]. For multijunction solar cells there are a number of suggested theoretical maximum efficiencies such as the Carnot limit (95%) and the Landsberg limit (93.3%) [12]. The realistically achievable efficiencies will however be lower but this shows the potential for solar concentrator technology in comparison to wind turbines for example which have the Betz's limit of 59.3% [13].

Table 1: Concentrator Characterisation Table [Article 1].

Type	Characterisation by mechanism				Concentration			Shape
	Refractive	Reflective (Coating)	Reflective (TIR)	Luminescent	Low	Medium	High	Key: Receiver/Cell, Reflector, TIR surface, Lens, Light Ray, Luminescent
Flat Reflector [5], [14]		X			X	X		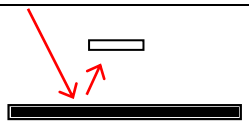
V-trough [15]		X			X	X	X	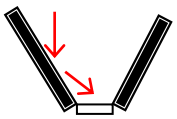
Light Funnel/ Homogeniser [15]–[21].	X		X		X			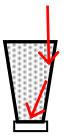
Linear Fresnel Reflector [22]–[24]		X				X	X	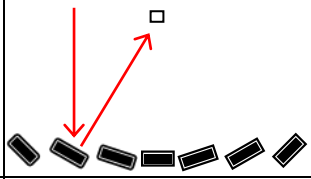
Parabolic Dish/ Trough [18], [25]–[29]		X				X	X	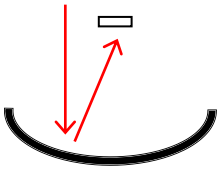
Fresnel Lens [30], [31]	X		X			X	X	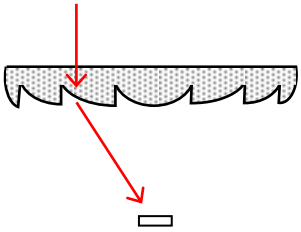
Compound Parabolic Concentrator [32]	X				X			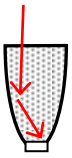
Wedge Prism [33]	X	X	X		X			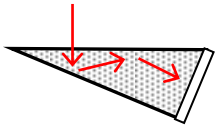
luminescent/ Quantum Dot [34]	X	X	X	X	X			

CPV technology can not only be more efficient but can also be more cost effective and environmentally friendly than standard flat plate photovoltaics. This is due to their reduced use of expensive, rare and toxic PV material [article 1]. One important factor which has only recently started gaining acknowledgement, is the effect of photovoltaic devices on the albedo, vegetation and terrain [35]. Photovoltaic panels are after all dark absorbing materials which radiate thermal energy to their surroundings. When a PV installation differs from the former background albedo, the radiative balance at the land-atmosphere interface can lead to local temperature increases [36]. This effect is however highly dependent on location. In urban cities covering a lot of area in cheap inefficient solar panels can contribute to the heat islanding effect [35], [37]. In hot countries this leads to a higher energy demand for cooling and air conditioning but perhaps can be useful in cooler countries during winter to reduce heating demand [38].

Burg et al. [37], [38] discuss this further and also emphasis that high efficiency photovoltaic devices, such as CPV, are less damaging to the albedo and more environmentally friendly. This is due to two reasons. The less efficient a photovoltaic is at converting light to electricity, the more heat it dissipates and also the more area required to generate a given demand. High efficiency technologies can cover less area, hence less albedo alteration and waste less energy as heat. In particular CPV (and the higher the concentration the better) has even smaller areas of radiative PV and higher conversion efficiencies [37]. The optical and structural parts of a CPV, which make up most of the system in the case of high and ultrahigh concentrations, are more established

than PV manufacturing and require less energy to make. When taking this and the albedo effect into account, the energy payback time for PV technologies changes and high concentrator photovoltaic (HCPV) technologies have the lowest payback period [37]. This gives a very important reason for high efficiency CPV technology development as opposed to trying to make less efficient technology cheaper.

Producing cost competitive CPV systems which can overtake flat plate photovoltaics is however still a challenge [39], [40]. A brief history of CPV research is given next and then an introduction to the different types of designs. A very thorough and comprehensive literature review has been done in article 1 and so the next sections aim to recap on what is presented there whilst including updates on recent publications.

1.4.4. A Brief History of Solar Concentrators

Although the concept of concentrating optics has been around since 1721 when John Hadley used parabolic mirrors to build a telescope with little spherical aberration [41], concentrator optics and solar cells are still in a stage of development, with growing interest. The first reported use of an external flat reflector in a solar thermal concentrator was in 1911 by Shuman for a water-pumping system powered by a flat-plate reflector assembly [42]. Lighthouses also commonly used parabolic mirrors to collimate a point of light from a lantern into a beam before being replaced by more efficient Fresnel lenses in the Nineteenth century [43]. Augustin Jean Fresnel was the first to discover the use of Fresnel lenses in 1822 as glass collimators in lighthouses [44], [45]. Only when less costly materials such as poly(methylmethacrylate) (PMMA) were discovered were Fresnel lenses implemented as solar energy collectors in the 1950s. In the late 1970s, the first modern Fresnel lens CPV system was built at Sandia National Laboratories [5]. Interest in Fresnel lens solar concentrators and CPV technology in general increased in the second half of the twentieth century [46] as shown in Figure 5.

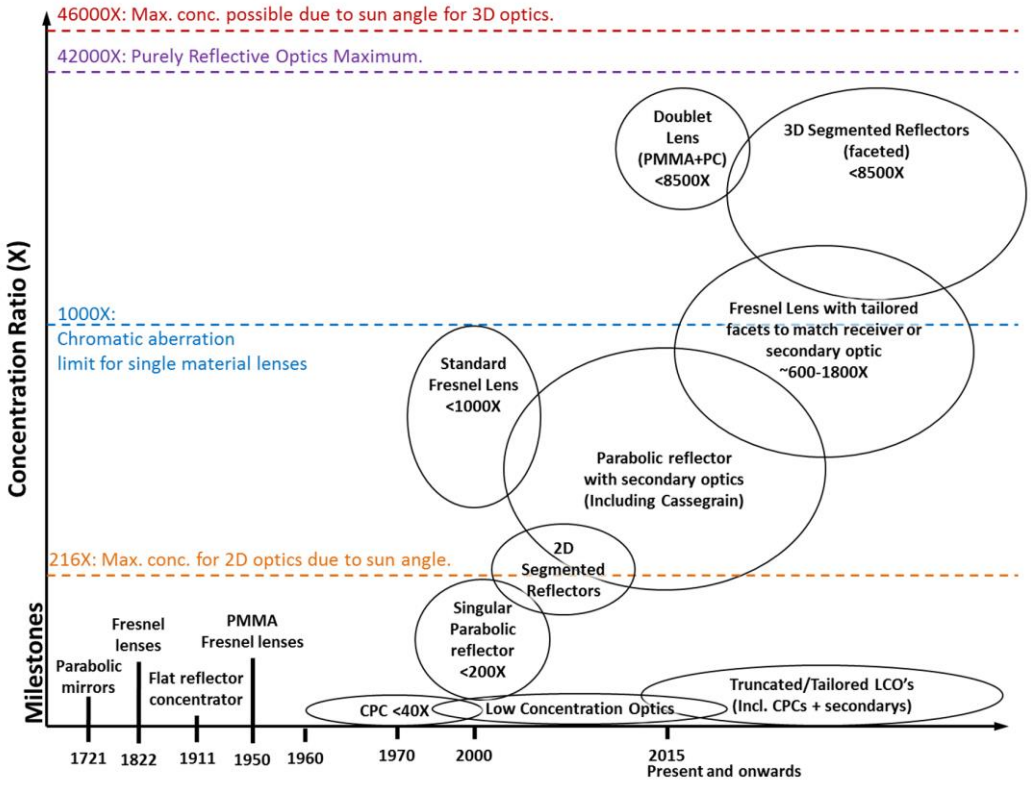

Figure 5: Solar concentrator timeline and trends in research up until 2015 with greater detail given upon theoretical concentration limits increasing.

In the 1960s, Giovanni Francia was the first person to apply the Fresnel reflector concentrator concept for industrial thermal processes in Italy [47]. The compound parabolic concentrator (CPC) was the first 2D concentrator ever designed, also in the 1960s, but the theory was not explicitly explained until the 1970s when the generalized relationship of etendue was derived [18]. Third-generation organic PVs have begun to be tested under concentrated sunlight. Organic PVs are a potentially low-cost, lightweight, and flexible alternative to inorganic PVs, but they have poor durability. At present only low-concentration optics—such as light funnels, wedges, luminescent concentrators, and small reflective dishes—are being used with organic PVs.

To add to the trends represented in Figure 5 and detailed in article 1, micro-concentrators are an emerging type of CPV design which actually take advantage of the older full sized lenses instead of faceted Fresnel lenses. Micro-concentrators are discussed further in section 1.4.13. Even from this brief history it can be seen that concentrator technology is branching further and further out, incorporating various scales of optical design, materials and mechanisms. So we will provide a simple grouping of these different designs in order to aid the comparison of different research areas and literature (this has also been done in more detail in article 1).

1.4.5. CPV Concepts, Characterisation and Solar Tracking

Concentrating photovoltaic systems can be categorised in a variety of ways as shown in Table 1 and Figure 6. The concentration of a system or optic can be classed as low (<10 suns), medium (10–100 suns), high (100–2000 suns) and ultrahigh (>2000 suns) due to the different solar tracking requirements outlined by Chemisana et al. [48]. A low concentration system can accept not only direct but a wide range of diffuse solar radiation enabling it to be stationary (no solar tracking system installed). Medium concentration designs accept less diffuse light and have smaller acceptance angles for incident light following the law of etendue and hence requiring at least single axis tracking (single axis trackers rotate from east to west following the sun) [5], [49], [50]. Higher concentration ratios then require dual axis tracker systems (adjustments east-west and south-north can be made) and ultrahigh concentration requires extremely accurate continuous (as opposed to stepped) tracking and alignment to perform at maximum power. All systems

will of course benefit from a highly accurate dual axis sun tracker system but these systems are also very expensive. Unless the power gained from installing one outweighs the cost, then cheaper means of tracking are used; hence the different concentration bands and tracking recommendations.

Designing high and ultrahigh concentrators with good acceptance angles can mean a less expensive solar tracker can be installed without a loss to performance and output. Overall, a good optical tolerance gives room for small misalignments during manufacturing which again can save costs. As shown in Figure 7, the optical performance is dependent on the optical efficiency, optical tolerance and irradiance distribution upon the cell. If any one of these factors was extremely low (due to poor design or manufacturing), the system would likely not function properly at all. As concentration levels increase, maintaining all three properties becomes exceedingly difficult.

The main methods of concentration are; reflective, refractive, luminescent, and total internal reflection (TIR) although the latter is included within the refractive and luminescent types.

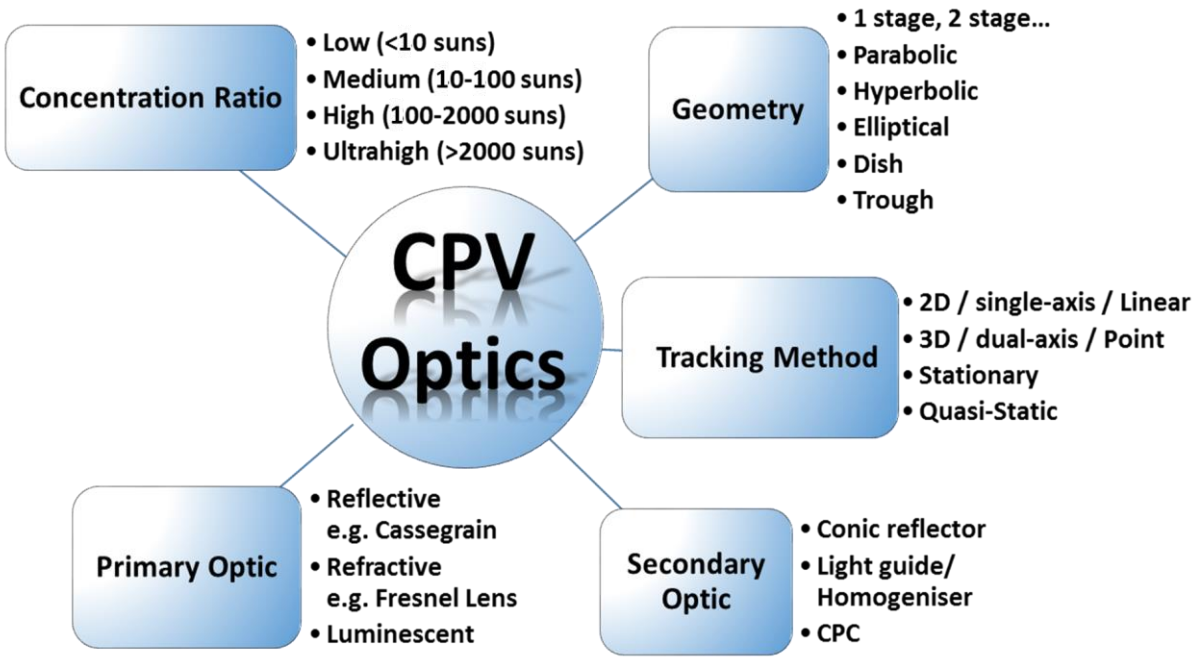

Figure 6: Concentrator dissemination chart [Article 1].

A concentrator photovoltaic system can be made up of one or more optics which themselves may involve a number of optical stages such as refraction into a lens, total internal reflections within the lens and refraction out of that lens. It is important to think of the number of stages, or medium interfaces, which the incident light will encounter in order to understand more clearly the sources of loss and alignment deviations. At present the preferred outline of a high concentration optical system is of one primary and one secondary optic [Article 1] [Article 7]. The primary optics initially collect incident light, and typical examples include the Fresnel lens and the parabolic reflector. The secondary optics are of medium to low concentration and can be referred to as “receiver optics” when in optical contact with the PV. These secondary optics can increase the concentration of the system but are used more often with the aim of improving the system’s acceptance angle and the irradiance

distribution on the PV. Receiver optics introduced to a concentrator design which improve the irradiance distribution are also suitably referred to as homogenisers [Article 7].

CPV systems can be categorised by concentration ratio, primary optic type, tracking method, geometry and number of stages, as shown in Table 1 and Figure 6. The ways in which CPV systems are judged mainly focus on their optical efficiency, irradiance distribution upon the photovoltaic(s) and their acceptance angle (or optical tolerance) as shown in Figure 7. It is also preferable to create designs which are cheap to manufacture, lightweight and easy to install and repair. Various designs and applications in the literature compromise in one area or the other as discussed next.

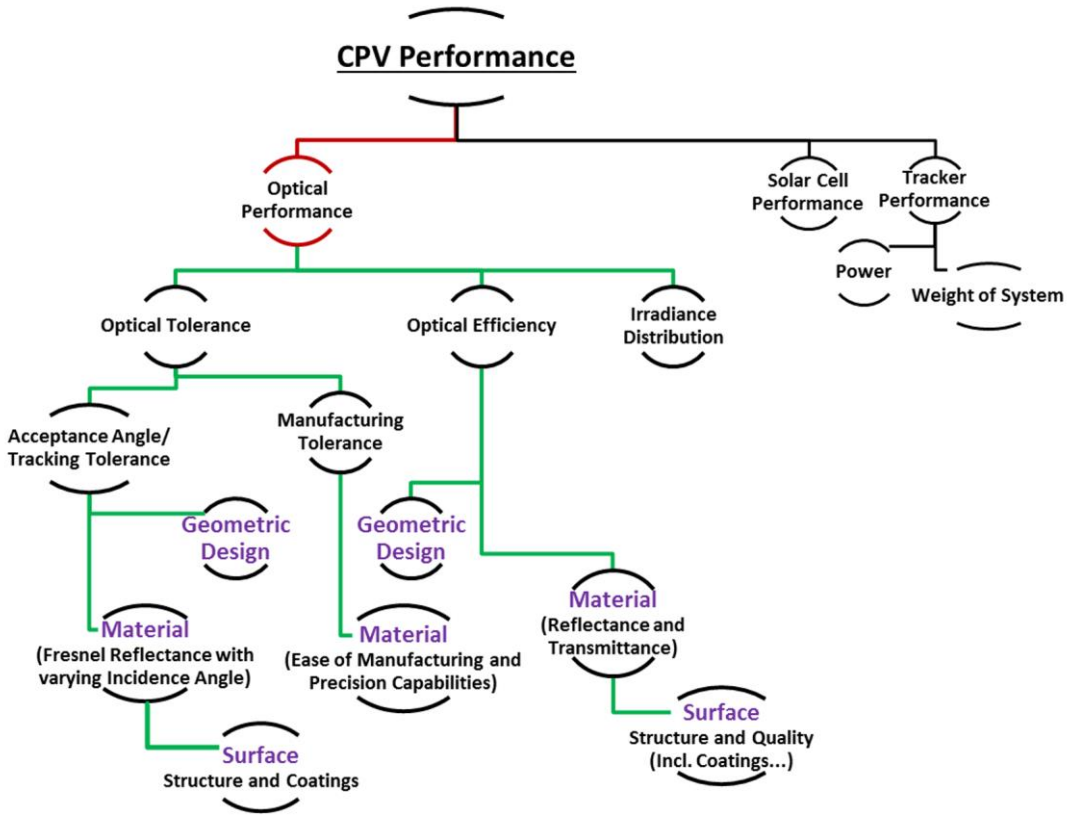

Figure 7: Factors affecting CPV performance [Article 1].

1.4.6. CPV Primary Optics

The most common and widely researched primary design concepts are the Fresnel lens and the parabolic mirror (Table 1). These two concentrators differ in a number of ways, allowing them to suit different applications.

1.4.7. Fresnel lens

One important characteristic is the range of concentration. Languy et al. [30] investigated the concentration limits of Fresnel lenses and found the concentration limit to be around 1000X due to chromatic aberration. Akisawa et al. [51] and Araki et. al. [52] have researched and developed dome shaped Fresnel lenses which can overcome the chromatic aberration limitation. Languy et. al. [53] also proposed increasing the concentration limit of Fresnel lenses but by combining a diverging polycarbonate (PC) lens and a converging poly (methyl methacrylate) (PMMA) lens to achieve up to ~8500X concentration. A recent study by Vallerotto et. Al. [54] has begun investigating a cost effective method of manufacturing such an achromatic lens starting with concentration ratios of ~ 722X. This lens is made up of PMMA, PC, ethylene-vinyl acetate (EVA) and silicone (polydimethylsiloxane) and can reach higher geometric concentration ratios and acceptance angles than the classic Silicon on Glass (SOG) Fresnel lens.

Fresnel lenses can be manufactured out of PMMA, PC or poly (dimethyl siloxane) (PDMS). The manufacturing processes can include hot-embossing,

casting, extruding, laminating, compression-moulding, crosslinking or injection-moulding thermoplastics [55], [56]. Polycarbonate (PC) is an alternative to PMMA due to its significantly greater toughness which prevents mechanical fracture and fatigue. PC is however less scratch resistant [57], has a smaller spectral bandwidth, optical transmittance [58] and suffers more from optical dispersion, chromatic aberration and solar-induced photo oxidation [59]–[62]. However, high temperature treatments such as calcination, which is a preparation method of antireflective and antifogging coatings, cannot be used on PMMA material. To achieve an anti-reflective property on PMMA (refractive index = 1.49) one method is to layer coatings of lower refractive indexes. Finding suitable sources of high transmitting but low refractive index materials however is also challenging. Zhou et al. [63] overcame both these difficulties and successfully fabricated antifogging and antireflective coatings on Fresnel lenses while achieving a transmittance of 98.5%. By spin-assembling solid and mesoporous silica nanoparticles, which have voids and result in a lower refractive index, Zhou et al. avoided high temperature treatments and produced coatings with a refractive index between 1.32 and 1.40.

These material effects on concentration ratio, optical efficiency, ease of manufacturing (including anti-reflection and anti-fogging requirements) reinforces the importance of researching new materials and surface structures to progress CPV technology further. It can be seen from the brief history in section 1.4.4 and Figure 5 that solar concentrator research expanded rapidly after the discovery of PMMA for Fresnel lenses, making them much cheaper

to manufacture and easier in general to handle and install. It is therefore not an unusual theory to suggest further leaps forward for CPV technology can be made with further advances in materials for CPV technology.

Fresnel lens designs seemingly can cope better without the aid of a secondary optic in comparison to parabolic mirrors. This however could be due to the broader interest in Fresnel lenses (which in turn is due to the cost effectiveness and lightness of Fresnel lenses), accompanied by more ongoing research and ingenuity in designs. Gonzalez et al [64] proposed a curved cylindrical Fresnel lens with good uniform irradiance but with significant manufacturing problems. J. Pan et al. [65] designed a Fresnel lens where each pitch focused to a different area upon the receiver, improving uniformity without the aid of a secondary optic. The design however lacked a good acceptance angle (only ~0.3 degrees) [65]. Benitez et al. [31] and Jing et al. [66] have also both designed their own unique Fresnel lenses to focus the light rays to different ‘entry’ areas of the secondary which has also been tailor designed. Both systems had an improved irradiance distribution, an optical efficiency of >80% and an acceptance angle of ~1.3 degrees. Zhenfeng Shuang et al. [67] more recently also redesigned the ring structure of a Fresnel lens; rearrangement of the rings resulted in a significantly improved irradiance uniformity.

This attention to surface structure is a strong method to improve concentrator performance. By tailoring the macro- or micro- structure (rings in these scenarios) and avoiding continuous surfaces on reflectors, high optical

efficiencies and improved irradiance distributions are achievable. Fitting secondarys and primarys to complement each other through their surface structures and materials also seems to improve performance as discussed further in article 1. From this, CPV technologies would benefit more from many unique designs, than a few ‘standards’. To make CPV technologies expand further out however requires more research into the prototyping methods as well as material options (see chapter 4).

1.4.8. Parabolic mirror and Cassegrain set ups

Canavarro et al. [29] suggest a singular parabolic trough (with no secondary optics) is suited to concentrations of only ~70X, above which the optical efficiency, acceptance angle and irradiance distribution begin to compromise each other. Various research in this field has extended the concentration of parabolic troughs to ~200X [18], [25]–[28] but as canavarro et al. [29] suggested these systems were unreliable in optical efficiency and acceptance angle. The use of a second concentrator element is needed to bring the concentration value as close to the limit as possible and relax the demand on the system accuracy [68]. For reflective type concentrators this results in a cassegrain set up (Table 1).

Brunotte et al. investigated the design of a primary parabolic trough with a secondary crossed standard CPC, reaching 214X concentration and concluded ratios exceeding 250X were possible [69]. More recently Canavarro et al. [26] have proposed a number of potential parabolic trough concentrator

designs with larger aperture areas but still of only medium concentration levels to maintain suitable acceptance angles. The cassegrain typically has a lower acceptance angle due to the 2 reflective stages in comparison to the 1 refraction stage of the Fresnel lens [Article 1], [Article 6]. There has been much research into the cassegrain type concentrator [70]–[78] for its greater compactness [76], [79] and higher concentration ratios over the Fresnel Lens (as it does not suffer from chromatic aberration). SolFocus has commercialised ~500X systems with an acceptance angle of ±1.4° [18] [7], [75] and Benitez et al. [80] designed a cassegrain reflector capable of 800x concentration ratio and an acceptance angle of ±0.86°. More recently the concentration ratios have pushed even higher with Ferrer-Rodriguez et al. [81] designing a cassegrain system of multiple primary reflectors focusing towards a central solar cell of effective concentration ratio 1682X and acceptance angle 0.61°. This and more systems however still need to be experimentally tested.

Zanganeh et al. [82] developed a solar dish concentrator based on ellipsoidal polyester membrane facets which could reach an optical efficiency of 90% while maintaining a good optical tolerance, and V-groove reflectors have shown optical efficiencies of >80% within systems [14] and helped surpass 2D concentration limits [83]. Nilsson et al. [84] proposed a stationary asymmetric parabolic solar concentrator with a micro-structured reflector surface. Three different micro-structures were tested, the highest optical efficiency obtained was 88% and all distributions had reduced irradiance peaks in comparison to the non-micro-structured counterpart. The optical surface, and hence material,

structure and quality evidently plays a key role in concentrator design and performance but expands extensively into the areas of materials science.

Options for reflectors include mirrored (silvered) glass, aluminized or polished metals or plastics, including silvered polymers, aluminized polymers and anodized aluminium. Examples of polymer films used include polymethlmethacrylate (PMMA) researched by Schissel et al. [85] and polyethylene terephthalate (PET) film researched by Kennedy et al. [86]. Schissel et al. [85] demonstrated the environmental durability of silvered-PMMA reflectors which have an un-weathered solar reflectance as high as glass reflectors at 97%. The reflectance of freshly deposited silver is roughly 97% (fig. 6) dropping to 84% after 3 years due to weathering. Fend et al. [87] then later compared various samples of reflectors for optical durability in outdoor weather conditions. SolarBrite 95, a silvered UV-stabilized polyester film, had an un-weathered reflectance of ~92% which dropped below 90% after 2 years. Thin glass mirrors have better durability but are more costly and difficult to handle. Their un-weathered reflectance was 93% to 96% and can last as long as 5 years with 5% reflectance loss. A graph of the standard reflectance spectra of the most common metals is given in Figure 8 however reflectance spectra will depend on specific manufacturing process, composition of metal and any coatings applied. Reflectance Measurements for a hand polished aluminium dish and a vapour metalized acrylonitrile butadiene styrene (ABS) semi-sphere are also shown in Figure 8 to show example reflectance spectra for these materials and methods of manufacturing.

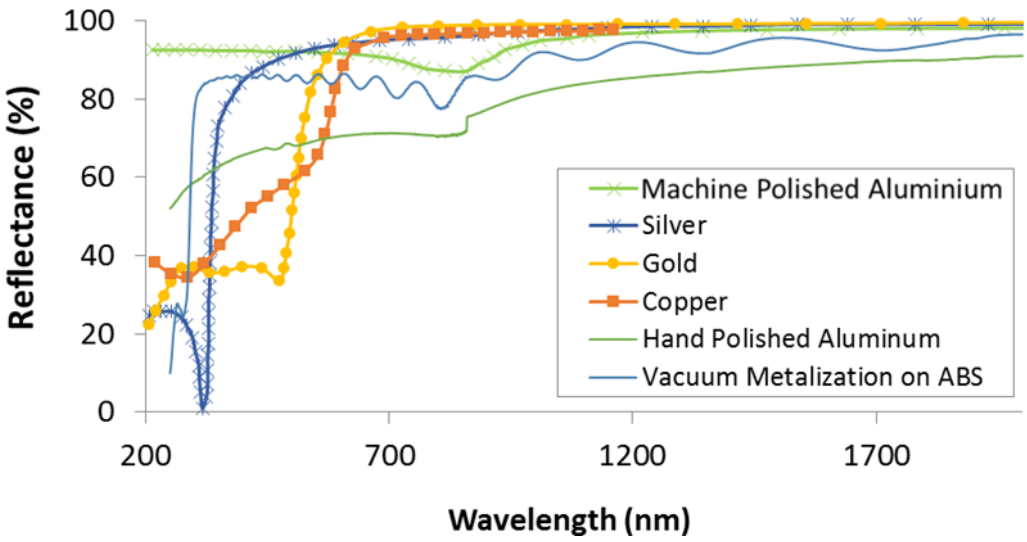

Figure 8: Reflectance spectra of various selected metals from literature and measured spectra for hand polished and vacuum metalized methods [article 1].

The simple polishing of metal can result in a reflective mirror finish but such polished surfaces are very heavy and specific curved shapes are difficult and therefore expensive to manufacture [50], [88]. Reflective film mirrors is a second option but this setup often has low reflectivity when also applied to complex surfaces [50] (discussed further in chapter 4). Polymer mirror films are a more recent third method to gain reflectance values of >90% but require specially designed structures to gain the appropriate shapes for a given application [82], [89]. Vacuum metalizing is therefore the current best option but this process is highly dependent on the material and surface quality it is bonded with in order to ensure a high quality mirror finish [88], [90].

L. Yin et al. [91] studied the surface qualities of different brittle materials used for the nano-abrasive fabrication of optical mirrors. They found that surface roughness in ultra-precision grinding increased with brittleness and hence brittle materials gave a lower reflectance after processing. The principal means of shaping and finishing ceramic optics is abrasive machining with abrasive tools involved with grinding, lapping and polishing. Laser-assisted machining is also an option [91]–[95]. In general, material responses to machining depend strongly on microstructure and mechanical properties [91].

Given the limitations of all existing systems, materials and manufacturing processes, further study into possible reflective materials and structures is important.

1.4.9. CPV Secondary Optics

The compound parabolic concentrator (CPC) (Table 1 and Figure 9) is the most studied stationary secondary optic and is said to be an ideal concentrator in that it works perfectly for all rays within the designed acceptance angle (in 2D geometry) [18], [51]. The 3D CPC is also very close to ideal [18]. CPC's can theoretically be used for higher concentration ratios than Fresnel lenses and match the theoretical concentration limit of purely reflective optics at 42000X [2], [96] but their very high aspect-ratio makes them impractical for implementation at >40X [96]. There have been variations in the CPC design to improve different aspects such as concentration ratio and irradiance distribution. Some of these designs include the crossed CPC (CCPC) [97] and similarly the 3D CPC [98], as well as the polygonal CPC

designs [99] and the lens walled CPC [100]–[102] (Figure 9). The CPC and its various developments are discussed further in articles 1 and 7.

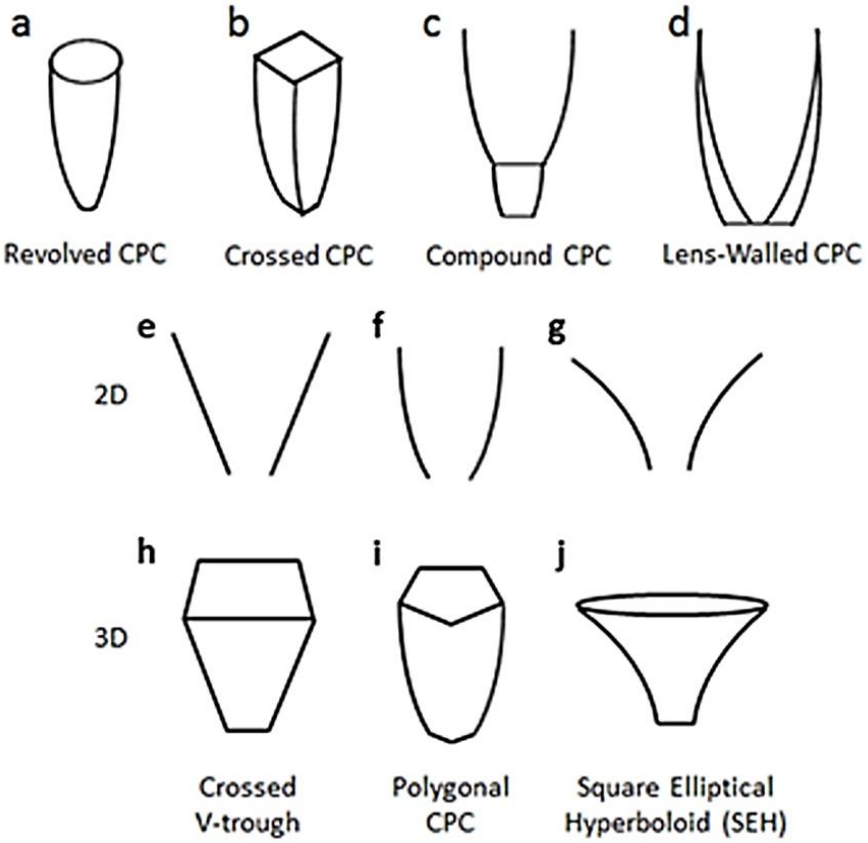

Figure 9: Variations of CPC: a) The revolved CPC, b) the crossed CPC, c) the compound CPC, d) the lens-walled cpc. Examples of 2D profiles and possible 3D transformations: e) V-trough, f) CPC, g) compound hyperbolic concentrator, h) 3D square aperture V-trough, i) polygonal aperture CPC, j) hyperboloid with an elliptical entry aperture and square exit aperture [article 1].

The significance of the differing characteristics of CPC designs however reinforces the idea that no one design will be absolutely better than another and specific adaptation, although not the easiest, is likely to be the most beneficial procedure in concentrator development. The irradiance distribution

uniformity of the CPC seems to be an inherent flaw which again suggests more novel optics need to be investigated. It is however recognised that for many systems this inhomogeneous light and heat distribution has either little effect or is manageable depending on concentration ratio, solar cell specifications and cooling methods.

Light funnels and homogenisers (Figure 9) have been utilised by many to improve the acceptance angle and irradiance distribution of a system [15]–[21]. Refractive secondarys optically coupled to the solar cell can also increase the maximum acceptance angle possible of the system according to etendue. Typical light funnels take on the shape of an inverted cone or pyramid but there are also elliptical and hyperbolic shapes possible [103]–[106] such as the square elliptical hyperboloid (SEH) designed by Nazmi et al. [107]–[109]. Some examples of geometries are shown in Figure 9 and described further in article 1 and article 7. The dome lens typically uses less material than a filled dielectric CPC and can be easier to manufacture [110]. The dome lens and ball lens have proven to have higher acceptance angle values than even the CPC and with improved irradiance distributions [110], [111]. Recently Askins et. al. [112] has investigated a hybrid dome secondary optical element which has increased acceptance angles than standard domes or reflexive secondarys. Other aspects of secondarys such as their material [article 4 and 11] [113] and the effect of antireflective coatings on them [114] have begun being researched in a broader sense.

1.4.10. Optical Tolerance and Acceptance Angle

The acceptance angle for high concentration devices such as parabolic dishes and Fresnel lenses, without additional optics is very low [7], [51], [115]. Akisawa et al. [51] proposed a dome-shaped non-imaging Fresnel lens. The tracking tolerance of the proposed lens held efficiencies of ~90% up to an incident angle of 0.4 degrees, then dropped to 80% at 0.6 degrees and then to 10% at 1 degree. Recently, more focus is given to the acceptance angle and overall tolerance of a CPV system and higher acceptance angles are being achieved. Dreger et al. [70] obtained an acceptance angle of 0.75 degrees without the need of a tertiary optic such as a homogeniser but by instead reducing the path length. ISFOC and GreenMountain studies have HCPV modules with acceptance values of 1.2 degrees and 1.4 degrees respectively [116]. Opsun Technologies claim to have a HCPV system of 380X with an acceptance angle of 3.2 degrees and an optical efficiency of 87% [116]. They also propose they can design a CPV system of 1000X with an acceptance angle 1.9 degrees [116]. This would be a significant achievement in CPV technology if the system has a similarly high optical efficiency and acceptable irradiance distribution as well.

Low concentration optics (LCO's) are not as dependent on solar tracking as high concentration systems due to the principle of etendue [19], [115]. LCO's can be static or quasi-static and due to their typical high acceptance angle they can often gather direct and diffuse radiation [107], [117]–[119]. This eliminates the need for continuous sun tracking systems and reduces the overall system cost [15], [120]–[122]. For a V-trough concentrator, Tang et al.

[15] suggests a concentration less than 2 for a fixed position but for concentrations >2 several tilt adjustments should be made to significantly increase annual solar gain and take full advantage of the systems capabilities. Similarly X. Li et al. [32] compared a 3X and 6X truncated mirror CPC where the 6X CPC needed adjusted five times a day but the 3X did not. For higher concentrations, the frequency and accuracy of the tracking must increase which tends to lead to very expensive solar trackers for HCPV technologies. New concentrator optics with improved optical tolerance could thus be vastly beneficial to developing high and ultra-high concentrator photovoltaics. There is always an inevitable trade-off required between acceptance angle, optical efficiency and irradiance distribution but recent novel designs are extending when this compromise is required. Truncation can increase the acceptance angle of a mirror CPC but it also reduces the geometrical concentration ratio [29]. This could be the condition for most optics [17], [83], [117], [123]–[125] and explains why Fresnel lenses, truncated convex lenses, typically have a higher acceptance angle than parabolic concentrators of a similar concentration ratio. Truncation can also be thought of as a method to reduce the light ray path length within an optical system which has already been said to increase the acceptance angle [70], [Article 7].

Larger opening angles are another option to improve the optical tolerance and reduce the effect of wind induced deviations, manufacturing errors and sagging as reported by Canavarro et al. [29]. This method however can also reduce the optical efficiency and concentration ratio of a system. The acceptance angle, optical efficiency and irradiance uniformity are interlinked

and hence systems usually prioritise optical efficiency. As mentioned earlier the lens walled CPC has an improved acceptance angle in comparison to the refractive CPC but a lower optical efficiency. There are studies however that suggest a decrease in optical efficiency, to gain higher acceptance angles will still produce more yearly energy output [116], [126], [127] but this will be depend on the specific application and location.

1.4.11. Novel Optical Designs

Due to the developing state of CPV technology, a variety of novel designs are still being created and tested. Laine et al. [128] investigated a transmissive non-imaging Fresnel type reflector concentrator made of a continuous reflective spiral (see article 7). Stefancich et al. [129] proposed a spectral splitting primary optic which dispersed different wavelengths to different single junction solar cells arranged along the focus plane. This was an alternative to focusing the light to one multijunction solar cell but still obtaining similar overall conversion efficiencies. This has also been proposed elsewhere [130], [131].

Jing et al. [66] coupled the design of a novel Fresnel lens with a novel secondary optic with specific ‘entry’ points. This attention to detailed design and matching primaries with secondarys can yield simultaneous benefits in concentration ratio, optical efficiency, acceptance angle and uniform distribution which is otherwise very difficult to do effectively. Y. Liu et al. [132] use a novel channel waveguide as a secondary which collects focused light rays from a Fresnel lens array primary. At each focal point there is a

microstructure which couples the light into the waveguide. This structure can reach 800X concentration at 89.1% optical efficiency and a 0.7 degrees acceptance angle. Similar designs have been tried and tested by many other researchers [122], [133]–[136]. Y. Jung et al. [125] designed a novel metal slit array Fresnel lens for wavelength scale coupling into a nano-photonic waveguide. Although aimed at a different application, this paper demonstrates the flexibility of concentrator optics. T. Waritanant et al. [33] was able to obtain a maximum collection efficiency of 54% for a wedge prism concentrator coupled with a diffraction grating. M. D. Huges et al. [137] found that a wedge shaped Luminescent Solar Concentrator (LSC) is able to produce a larger average power density year round under direct illumination than a planar LSC but unusually its optimum orientation was when tilted away from the sun and for this reason may be more suited to latitudes further from the equator. These are just some examples of the novel designs being explored within CPV technologies and how they can vary.

1.4.12. Novel Materials and Biomimicry

Some applicable concepts for solar concentrators include: spectrally selective coatings [49], [138], [139]; switchable optics which can change from transparent to reflective; anti-reflective and reflective enhancing coatings [49], [138]; water filled optics; nanocrystal materials, graphene layers [140], [141] as well as other organic and inorganic materials. Much of this technology is researched extensively in the glazing and window industry but less so in the application of CPV's due to the associated high costs of such materials. These materials however hold a lot of potential for advancing solar

concentrator technologies, some more than others for specific applications such as building integrated concentrator photovoltaics (BICPV).

Hybrid organic-inorganic (O-I) materials are nano-composite materials with both an inorganic and organic (bio-organic) component. These O-I materials often have impressive characteristics. For example, the Maya Blue pigment is the incorporation of a natural organic dye within the channels of micro-fibrous clay. This hybrid material is of a strong blue colouring which lasts against weathering and bio-degradation to the extent that 12 century old vestiges are still appreciable today [142]. The hybrid materials processed by D. Avnir et al. [143]–[146] provided many advances in many diverse fields including optics. There are now many industrially developed hybrid materials including films, membranes, fibres, powders, monoliths and micro (and nano) patterns [147]–[151]. Graphene has found many uses in a variety of applications due to its tenability and unique properties. It has a very promising optical transparency of 97.7% but more research is required into its use in solar concentrator materials [152].

Nature has a vast range of advanced complex structures which have been studied by many to be replicated and adapted for our own use [153]–[158]. A clear example is the application of light trapping microstructures, inspired by moth eye facets and other natural light trapping structures, imprinted upon solar cells to enhance light collection and conversion efficiencies [158]–[160]. Nature has created these structures over billions of years and optimised their functions through evolution. A process which will forever exceed any ‘trial and

error' optimisation routine carried out by ourselves. Structures within nature often must fulfil multiple functions and hence are usually a complex hierarchal multi-scale system. Such structures may hence appear random to us but are in fact a controlled balance of compositions [161]–[170]. Smith et al. [170] discuss the importance of quasi-random nanostructures found in nature and more recently now also in engineering applications such as blue-ray disks due to their ability to manage photons efficiently. This reinforces the importance of surface structures on optical components and why microstructures significantly effect: reflectance, distribution and acceptance angle [31], [63], [65]–[67], [84], [120], [160], [171]–[173]. Siddique et al. [174] has discovered butterfly wings which have a reflectance of only 2-5% over a range of viewing angles. This high transparency at multiple incidence angles could be very useful for solar concentrator optics, in terms of the cover glass encasing and for lens surfaces to increase the optical efficiency and acceptance angle. The Cabbage White (of the family Pieridae) butterfly achieves the opposite; it has an interesting grooved tiling upon its white wings with an underlying nipple pattern of pterin beads as shown in fig. 9. These wings have a surprisingly high reflectance of 78.9% over the 400-950nm range and are used to concentrate light onto the butterflies' body to help it heat its flight muscles faster [Article 5]. Shanks et al. [Article 5] suggest these wing structures (Figure 21) can be the basis of a new lightweight, highly reflective materials for concentrator photovoltaics to greatly improve the power to weight ratio of solar concentrator technologies as demonstrated in article 5. In both cases, the wing structures have a very interesting 'random' or 'chaotic' structure but

as mentioned earlier, this may have some underlying complex coherence to it that we have yet to understand.

There are numerous studies into how natural structures, especially insect membranes, can affect light [156], [157], [175]–[181]. There are also various bio-replication reviews covering a range of applications [182]–[185]. However, at present it is an untapped area of research for CPV applications.

1.4.13. Micro-Concentrators

In the pursuit of matching CPV technology to flat panels in terms of aesthetics, micro-concentrators are an emerging form of concentrator design which essentially scales everything down so that CPV panels are a similar thickness to standard flat PV panels. This also results in much smaller optics which although requiring a different degree of manufacturing should in theory benefit from smoother surfaces, higher resolution and ultimately less errors. Hayashi et al. [186] constructed a compact micro-concentrator of 20mm thickness using an array of small full thickness PMMA lenses and solar cells less than 1mm in diameter. Due to the very small scale of micro-concentrators, absorption losses within lenses are much lower. In fact it is easier to manufacture the small full thickness lenses instead of Fresnel lenses and this also results in avoiding the losses associated with the facets of the Fresnel lens [187]. Hayashi et. al. [186] achieved 37.1% energy conversion efficiency and an optical loss of only 9.6% for their design of 150X geometric concentration. Ritou et. al. [188] designed a micro-concentrator of 275x concentration with an efficiency of 29.7% and an acceptance angle of ±0.7°

which could be assembled in 3 relatively simple steps including simultaneously molding the primary and secondary lenses in the same high accuracy mold.

Micro-concentrators require a different set of equipment for measuring and assembling the components accurately [189]. The solar cells themselves are sub-millimetre in size and precise placement is again increasingly important as concentration ratio is increased. However there is equipment that can place such small devices with excellent accuracy. It is much harder (and expensive in terms of the equipment) to place a very large optic with the same level of accuracy than a very small optic due to equipment and measurement scaling.

1.5. Conclusions

For concentrator photovoltaic technologies to continue to develop there are some key factors that should and likely will be focused upon in ongoing research. One of these is increasing the concentration ratio. High and ultrahigh concentration ratio systems have a vast potential for increasing efficiencies and reducing cost. From the literature reviewed in article 1, other methods to be highlighted which improve CPV performance include: (1) The use of secondary/homogenising optics; (2) Reducing the path length of light rays; and (3) Tailored surfaces structures. Out of these, the attention to optical surface structure (3) is the most promising with the resulting systems being able to simultaneously achieve improved optical efficiency, tolerance and irradiance uniformity. Most CPV systems have to make compromises in one

area or another when trying to attain higher concentration ratios but the segmented reflectors described here are able to challenge or at least extend this trade-off which is inevitably encountered. The most noteworthy designs are those with ingenuity and careful geometric design.

Ultimately, future CPV optical systems will get larger in concentration ratio but may get smaller in scale with the use of micro-concentrators. This will also increase the research into possible materials which are easy to manufacture accurately on such small scales and if they have unique properties. It can be seen from Figure 5 even in the brief milestones section that one of the breakthroughs for solar concentrator technology was the discovery of PMMA and its application for Fresnel lenses. Fresnel lenses were available before this but only became popular in CPV technology when they became affordable and practical due to PMMA [39], [46], [190] [Article 6]. Hence, as previously stated, further breakthroughs in the optics for concentrator photovoltaic applications could again be largely due to the development of new materials for its purpose. The combined balance between reducing path length, utilising secondary optics and tailoring surface structures will see the way to ultrahigh concentrator photovoltaics.

An extensive review of solar concentrator research and technologies has been carried out, comparing different materials and the optical performance of different designs. There is not enough consideration into the durability of designs and their performance over years of use, especially for concentrators

utilising refractive optics. Recurring challenges and trends in the designs of CPVS have been highlighted.

The above review gives examples of how solar concentrators can be designed in a variety of unique ways boasting different characteristics for different applications. In order to make the necessary leaps in solar concentrator optics to efficient cost effective PV technologies, future novel designs should consider not only novel geometries but also the effect of different materials and surface structures. Trends towards higher performance solar concentrator designs include the use of micro-patterned structures and attention to surface quality and how these can be achieved. There is still a vast potential for what materials and hence surface structures could be utilised for solar concentrator designs especially if inspiration is taken from biological structures already proven to manipulate light.

CHAPTER 2: Limitations of Cassegrain Optics

When predicting the behaviour of light rays through an optic, either generally through mathematical formulae or with ray trace simulation software, optics are often assumed ideal. When initially designing a concentrator system or any design of optics, exact focal point distances are supposed along with 100% reflectance or transmittance. More crucially, the incoming light from the sunlight may be represented by parallel rays, instead of with the divergence of ±0.27°. All of these assumptions, although perhaps necessary as initial steps to simplify new design ideas, can lead to very poor optical design and performance if not amended early in the design process [Articles 2, 7-10].

How much the theoretical performance will differ from the experimental performance due to inaccuracies is dependent however on the concentration level and intended application. The different levels of accuracy required relate again to the different bands of low, medium, high and ultrahigh concentration [48] given in chapter 1 and articles 1 and 7. The higher the concentration, the higher the accuracy required. As previously stated, the law of etendue dictates the maximum acceptance angle of a concentrating optic. However, this acceptance angle is unachievable due to material flaws, manufacturing limitations and alignment uncertainties. The different materials and manufacturing options currently dominant in CPV technology are described in most of the articles but in detail in articles 1, as well as in chapter 1.

2.1. Optical Surface Structure

The surface structure of an optic is fundamentally one of the most influential parts of a solar concentrator. At this interface light will reflect and/or refract with various degrees of scattering [191] as shown in Figure 10. There are many ways to measure optical surface quality [94], [192], [193] and characterise or model its light scattering effects [95], [191]. For many years up until 1985, there were no practical alternatives to the cosmetic parameter of scratch and dig to describe visual imperfections of optics. The scratch and dig measurement takes the form of two numbers such as “60-40” where the first is the scratch number and the second the dig number. There are a set of calibrated samples with scratch standards which are used to compare scratches to and pick the best match and hence the scratch number. The dig number is the diameter in hundredths of a millimetre of the biggest dig on the surface. However for solar concentrators requiring high accuracy (high and ultrahigh concentrators) this type of measurement is almost useless. Aikens [192] suggests never using an optic of scratch and dig 40-20 or lower (lower numbers are higher quality indicators) since such optics will be more expensive, and since it is a cosmetic measurement, may not actually have the accuracy required depending on the application.

For solar concentrators, surface texture specifications are the preferred method of classifying the surface quality of optics but there are still many parameters to use such as route mean square (RMS), slope, skew, kurtosis and power spectral density (PSD) [192]. There are also many modelling methods which use these measurements and others to then determine the

amount of light refracted, reflected and scattered as discussed by Schroder et al. [191].

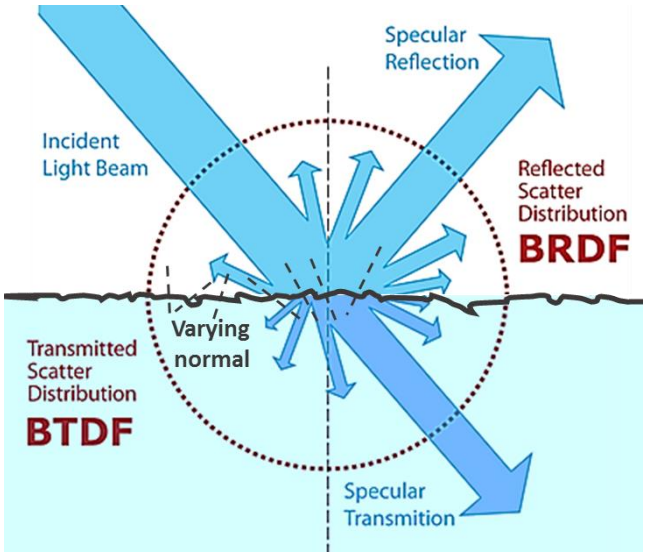

Figure 10: Representation of possible scattering when light rays are incident on a medium interface. This scattering can be referred to as the bidirectional scatter distribution function, which is made up of the reflection and transmission distributions as shown.

2.2. The Bi-Directional Scatter Distribution Function

The Bi-Directional Scatter Distribution Function (BSDF) is a characteristic function which describes the angular distribution of radiation scattered from an interface such as represented in Figure 10. The BSDF is made up of the Bi-directional Reflection Distribution Function (BRDF) and the Bi-directional Transmitted Distribution Function (BTDF). The BSDF takes different forms depending on the type of scattering model being used which should be chosen appropriately for the type of surface being simulated. For example in the Advanced Systems Analysis Program (ASAP) developed by Breault, there are various models to choose from such as the Lambertian model, for a

lambertian reflector. The Lambertian model has a constant as the BSDF and is the only scatter model whose Total Integrated Scatter (TIS) is independent of incident angle [194]. The TIS is defined as the power scattered into the hemisphere above a surface (Figure 10) divided by the power incident upon the surface. It can be calculated by taking the integral of the BSDF over the hemisphere multiplied by a cosine obliquity factor [194]. The TIS also relates to the RMS surface roughness through equation 11 below.

$$TIS \approx \left(\frac{2\pi\sigma\Delta n}{\lambda} \right)^2 \qquad (11)[194]$$

For optically polished/smooth surfaces (RMS roughness σ << wavelength λ) the Harvey model can be used to predict scattering characteristics and is dependent not only on the wavelength and incidence angle but on the angular difference between the scattered and specular rays also [194]. It assumes an isotropic surface roughness, which means the scattering is independent of the object rotation about the normal and is acceptable for ground, polished and coated surfaces [191]; the minimum quality expected for solar concentrator optics. As expected, the Harvey model dictates that the TIS will fall with increasing incidence angle for relatively smooth surfaces and will increase with incidence angle for relatively rough surfaces [194].

2.3. Simulation software

Breaults ray tracing software ASAP was used for all the simulations carried out in the accompanying articles (appendices 1-13) but there are other softwares available. Optisworks is an add-on to solidworks and has the

advantage of being easy to use and design any geometry due to the solidworks base platform. It however is not as powerful as some other modelling software and can take a very long time to run simulations. Tracepro is a very good ray tracing software that is designed more for CPV optics but lacks some flexibility as many things are ‘built in’. ASAP is one of the more powerful, flexible and fast simulation tools but is not as user friendly. Simply drawing complex geometry is best done in another software such as Solidworks and imported though this can produce errors. Complex designs can be drawn in ASAP but some time does need to be spent training before understanding how to do complex designs and modelling.

2.4. Developing a Cassegrain Concentrator Design

The following summarises the results from articles 2 and 8-10 which describes a method of simulation which takes advantage of the BSDF’s and Harvey scatter modelling for non-ideal optical surface structures.

The cassegrain concentrator can reach higher concentration ratios than standard Fresnel lens set ups but typically has a lower optical tolerance and hence a lower acceptance angle. The reasons for this are explained in chapter 1 and in articles 1 and 7. Optical tolerance and acceptance angle is very important, especially for high and ultrahigh concentration optics. For this reason a cassegrain concentrator of 500X geometric concentration ratio was designed and optimised for high optical efficiency and optical tolerance. The simulation method presented in article 2 addresses realistic errors, such as surface roughness, which can occur in manufacturing. Despite the variety and

accuracy of modelling theories outlined previously, it appears to still be uncommon practice to account for these uncertainties during the simulation stage. As CPV research tends towards achieving higher concentration ratios and its benefits, the effect of uncertainties become also increasingly important. Below is the design method used for the cassegrain concentrator.

Design Steps:

i) Calculated minimum dimensions required for entry aperture and receiver (solar cell) to gain desired geometric concentration ratio (as done in Figure 11).

- This should include shadowing losses such as the secondary reflector in a cassegrain concentrator.
- The shape of the concentrator and how it will be arrayed in multiplies side by side should also be considered here.

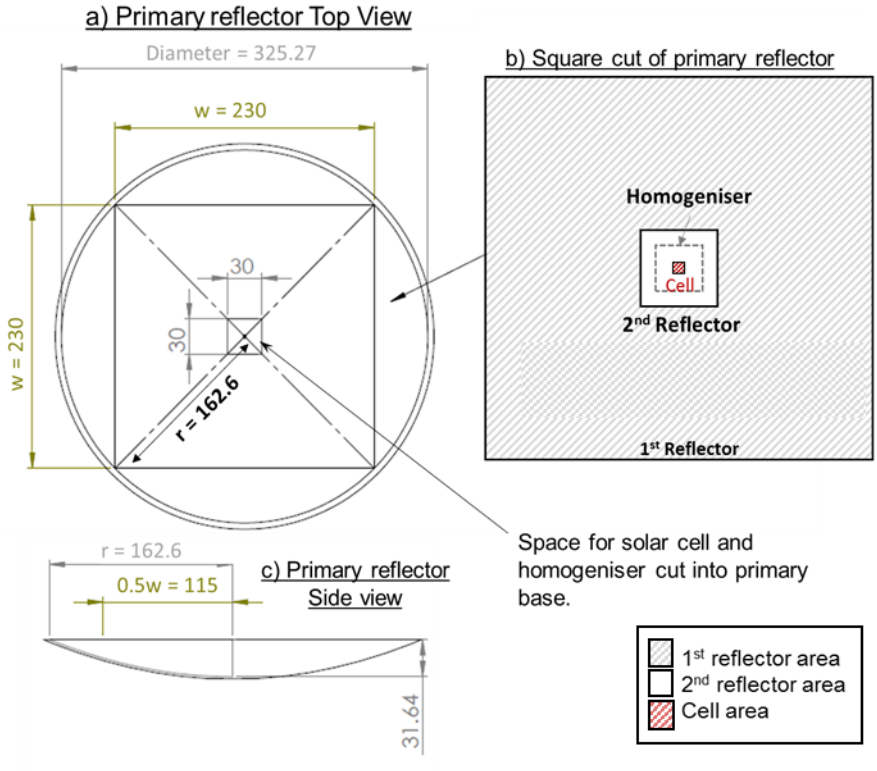

Figure 11: Schematic of square cutting and shape matching of reflectors, homogeniser and solar cell. All dimensions are given in mm. a) Top view of square cut of original circular primary reflector dish. b) Top view of all square components in central alignment with the solar cell. c) Side view of original circular primary reflector from a) showing depth, radius and resulting half width after square cut.

ii) Simulate geometries with a light source of 1000W/m^2 or a normalised power of 1 or 100 for easy analysis. Ensure a divergence of ±0.27° is included from the beginning and that the wavelengths at least include the minimum and maximum which the PV receiver will accept. (If more extensive simulations including the heat produced by the solar cell due

to unconverted wavelengths is being carried out then the full spectrum is necessary).

iii) Choose focal lengths depending on optical tolerance, device size limits and manufacturing capabilities and cost.

- This can be done by investigating the ray displacement at 1° incidence angle (or similar) as done in articles 2, 9 and shown in Figure 12 .
- A shortlist range of focal lengths should then be chosen.
- In the case of the cassegrain concentrator, two focal lengths needed to be chosen and related to each other. This was done by forming equation 12 for the separation distance [article 2 and 9].

iv) The receiver/homogeniser optic is then included along with reflection and absorption losses in the various materials of the components. The parameters of the homogeniser, along with the shortlisted focal lengths, are investigated to find an optimum combination [article 2 and 10].

- This should include considerations of optical efficiency, optical tolerance and irradiance distribution even though the irradiance distribution should change once surface roughness is included. It is still a good idea to find out if there are any serious hot spot issues at this stage before proceeding.

v) The introduction of surface roughness and manufacturing errors is next [article 2].

- This includes dimensional errors in parameters and in this study, the use of material BSDF's and the Harvey model to simulate realistic surface scattering.

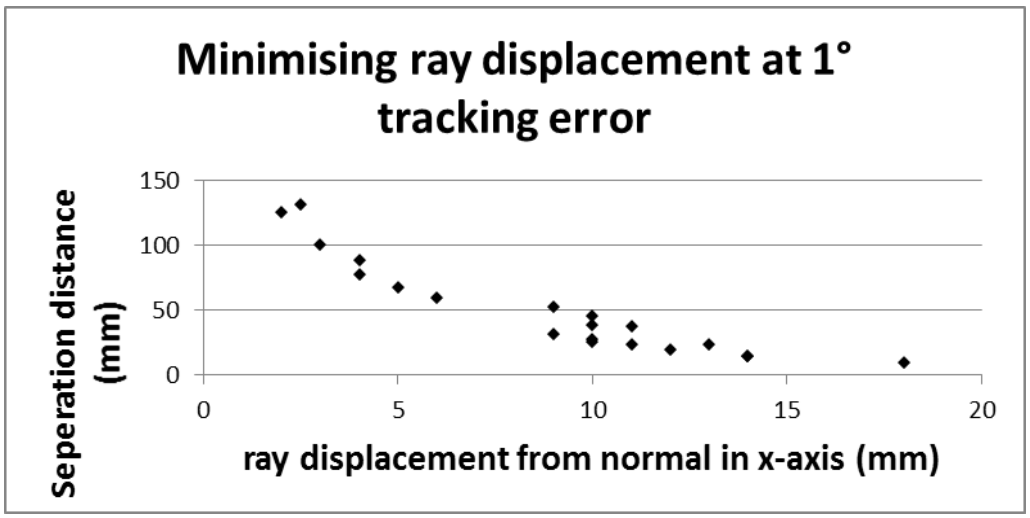

Figure 12: Graph of separation distance against ray displacement from position of normal alignment with the sun. Displacement is due to a misalignment of 1 degree. Displacement measurements only taken in x-axis but due to the symmetry of the system represent the displacement incurred in y-axis as well [article 2 and 9].

Equation 12 was used to simplify the optimisation procedure for the focal lengths of the two reflector dishes in the cassegrain concentrator.

$$SD = f_1 - \left(\frac{0.5w}{\tan\left(2\tan^{-1}\left(\frac{r_1}{2f_1} \right) \right)} \right) \tag{12}$$

Where f_1, r_1 and w are the focal length, radius and cut square width of the primary dish respectively as shown in Figure 11. SD is the separation distance between the primary and secondary dish when both dishes have the same

focal point. This equation ensures no light rays reflected from the primary dish miss the secondary dish. The second dish parameters are entirely dependent on that of the primary dishes as shown in equation 12. This relationship between the primary and secondary allowed a simplified method of obtaining the optimum focal lengths for optical tolerance. However, with the addition of the final homogenising optic, the shortlist of focal lengths as well as slight variations in all the parameters were then re-investigated [article 2 and 10], not only to ensure optimisation but also to find the effect of manufacturing errors. This is discussed in more detail in articles 2 and 3.

Upon revision and from the results of article 3 and 4, the absorption of the homogeniser material should be chosen more carefully and the surface roughness should be considered at the same time when choosing a homogeniser design. Ultimately, these sources of optical loss can affect which parameters of the homogeniser are optimum.

2.5. Results

The results are presented with more detail in articles 2 and 10 however some have been expanded on here.

The optimum homogeniser parameters were chosen to be that of a height 75mm and entry aperture area of 30mm x 30mm as shown in Figure 13 b). However, for optical tolerance, any of the conditions presented in Figure 13 a) apart from that of height 70mm and separation distance 163mm, would have

an acceptance angle of at least 1 which would be unaffected from slight changes in the separation distance or homogeniser height. This can be seen in Figure 13 a) because the 3 upper lines are very close together. So perhaps for optical tolerance, considering manufacturing and assembly errors, this should have been the optimum. However it would depend on the tracking accuracy available. High accuracy solar trackers are expensive, the 75mm height, 30 mm wide homogeniser was chosen originally as the optimum because it had the highest acceptance angle and could even produce >50% efficiency at 1.5° misalignment.

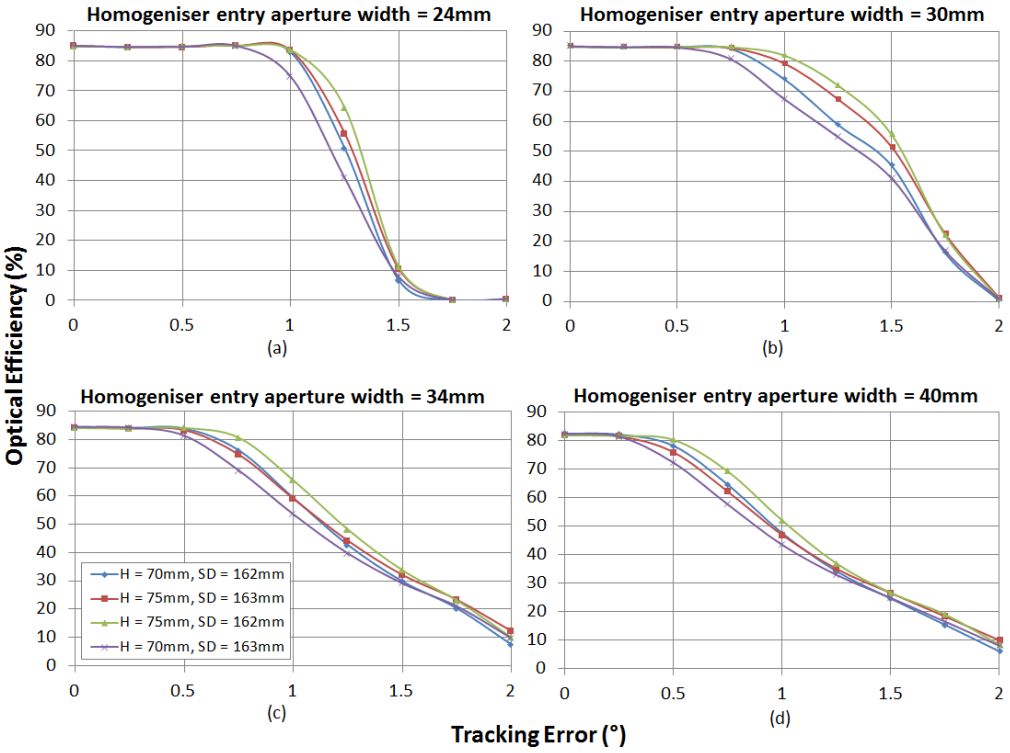

Figure 13: Graph of resulting optical tolerance from different combinations of homogeniser parameters and separation distance where H represents Homogeniser height in mm, W represents the input face width in mm and the separation distance, SD, is either 163mm or 162mm.

The surface quality of the homogeniser proved to be a very important factor when considering TIR and the full system optical efficiency [article 3]. As described in article 2 the surface structure of polished aluminium was used for the two reflector dishes and dropped the efficiency down to 80%. The refractive homogeniser then reduced the optical efficiency to ~67% or ~35% depending on the BSDF simulated [articles 2, 3 and 11].

To emphasis further the importance of surface structure, which is dependent on the substrate material, a prototype was built of the cassegrain concentrator using plastic mirrors. This is discussed in chapter 4.

2.6. Conclusions

The optical tolerance and efficiency of a cassegrain type solar concentrator was optimized through the use of ray trace analysis to achieve high optical efficiencies of 84.82% at normal incidence, 81.89% at ±1° misalignment error and 55.49% at ±1.5° tracking error for ideal optics. The optimized design was found to be with a primary parabolic reflector of focal length 200mm and a secondary inverse parabolic reflector of focal length 70mm placed 162mm from the primary collector. The optimized system required a solid transparent homogeniser of height 75mm with an entry aperture of 30mm x 30mm and exit aperture of 10mm x 10mm. The use of the homogeniser not only improves the optical tolerance and the irradiance distribution but also allows more flexibility in the manufacturing and assembly of the design. The detailed characterisation of the proposed system, as well as the separation distance

equation, may be beneficial in the design of parabolic reflector systems. It may also benefit single stage lens systems (that focus onto a homogeniser), as a guideline to help improve an aspect of the system dependent on alignment, focusing area or uncertainties.

Manufacturing uncertainties were considered and the material and surface structures in particular proved to be the biggest source of loss. The consideration of non-ideal optics and manufacturing limitations are proved to be very important during theoretical design steps and ray trace simulations. With such high powered modelling software there is scope to include as much of the realistic conditions as possible. A design method was presented which suggests when to switch from ideal conditions (for ease of initial design ideas) to realistic conditions. This is crucial for solar concentrators to develop as reliable efficient sources of renewable energy, expand in applications, and reach higher concentration ratios with even greater benefits.

CHAPTER 3: Design and Optimisation of the Conjugate Refractive Reflective Homogeniser

Following on from chapter 2, the effects of different surface structures on refractive optics and their TIR efficiency were investigated further. A simple but effective solution was also proposed to compensate for the inefficient TIR and capture the scattered rays that would otherwise be lost. In this way the Conjugate Refractive-Reflective Homogeniser (CRRH) is presented in articles 3 and 11. The CRRH is a dielectric filled crossed v-trough lined with a reflective film but maintaining an air gap between them (see Figure 14). This air gap ensures both total internal reflection (TIR) and standard reflection (for those rays which fail the TIR critical angle) take place. As shown in Figure 14 b and c, when there is a misalignment, rays can be more likely to fail TIR. Failed TIR could occur anywhere but is more likely after 2 or more reflections. Figure 14 b) shows one such scenario.

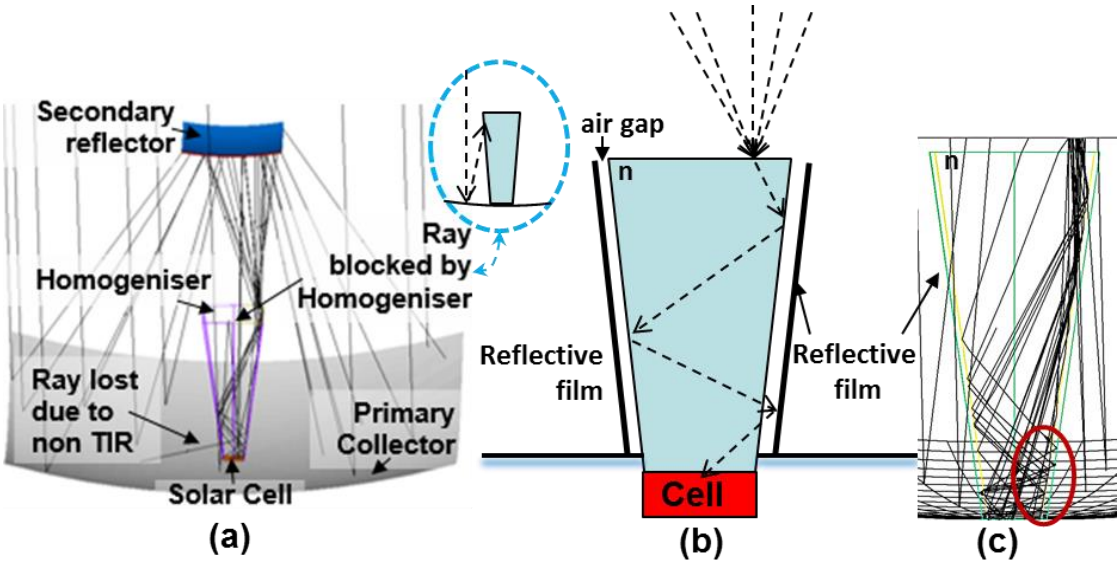

Figure 14: (a) Ray Trace Simulation of Cassegrain concentrator at a tracking error of ±1.75°. Lost rays are shown including an inlet diagram of how a light

ray can be blocked by the homogeniser on route to the secondary reflector. (b) Theoretical performance of CRRH with air gap and reflective film when there is a misalignment. (c) Ray trace diagram confirming that refracted rays can be caught by the reflective film (red circle) [Article 3].

As discussed in chapter 2, the surface quality of a refractive optic can significantly reduce its accuracy and performance, especially if TIR is intended to take place. TIR is assumed to be 100% efficient in reflection and hence superior to standard metal reflectance. However, depending on the material and surface quality, which may be inherent to the material and/or to the manufacturing method, the surface smoothness might be inadequate for sufficient TIR.

3.1. The Physics of TIR and Refractive Optics

When a refractive lens or light funnel/homogeniser is used in a concentrator system, the light will undergo a number of different processes. When light is incident on the refractive optic such as the homogeniser, a portion of the light will refract into the optic and a portion will reflect away, counting as lost light in most cases. How much light is lost on this initial refraction step depends on the angle of incidence, the refractive index of the homogeniser material and the surface structure of the material. The refracted light will also have its own scattering distribution as represented in Figure 10 where the majority of the light will be reflected at the angle predicted by snells law (equation 13), and the rest will be scattered in decreasing intensities away from this angle (α_2) unless the surface structure is designed to do differently. Once inside the

refractive medium the light rays begin to be absorbed by the medium. The longer the path length within the medium the more absorption takes place and hence the reason for truncating refractive optics as discussed in chapter 1. When the light rays come into contact with another interface, again reflection or refraction can take place as before.

$$n_1 \sin \alpha_1 = n_2 \sin \alpha_2 \tag{13}$$

In the above equation n_1 is the refractive index the light ray is initially present in (typically air at n= 1) and n_2 is the refractive index of the medium the light ray is about to enter. Angles α_1 and α_1 are the angles the ray makes with the normal surface before and after refraction. For the case of reflection $n_1=n_2$ resulting in $\alpha_1= \alpha_2$ which is the angle of specular reflectance, where the highest portion of reflected light should be directed.

Total internal reflection (TIR) occurs when a light ray comes into contact with a less optically dense medium (lower refractive index) than the medium it is currently travelling in ($n_2<n_1$) and if the angle of incidence is greater than the critical angle for TIR ($\alpha_1>\theta_c$). The critical angle for TIR can be calculated from Snell's law by letting $\alpha_2=\pi/2$ and rearranging for α_1 which now represents the critical angle θ_c in equation 14.

$$\sin \theta_c = \frac{n_2}{n_1} \tag{14}$$

Snells law and the critical angle requirements for TIR become slightly more complex when considering the refractive index's dependence on wavelength. The dispersion functions of PMMA and SCHOTT BK7 are shown in Figure 15 and are used in articles 3 and 11 simulations.

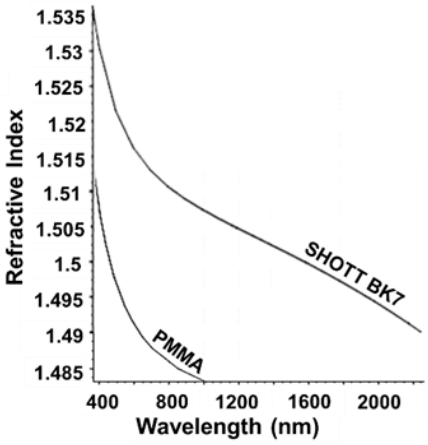

Figure 15: Refractive index relationship with wavelength (dispersion function) for PMMA and SCHOTT BK7 [article 3].

From Figure 15 it can be seen that for each wavelength of light there will be a slightly different refractive index, hence a different angle of refraction and a different critical angle. It can also be determined that a material with an overall higher refractive index will have a lower critical angle and hence more TIR. From this, and Figure 15, SCHOTT BK7 should be more efficient as a light funnel optic than PMMA. This is one example where material choice becomes important in solar concentrator design, simulation and prototyping. However, the properties and performance of a material will also depend on the absorption, cost and surface quality of the materials. Of which so far in literature it seems cost often dominates as discussed in chapter 1 and article 2.

It might be assumed that such a slight difference in refractive index between materials is negligible in solar concentrators but not when we consider the process of optimisation and combine it with surface roughness. The optimum conditions for a homogeniser for example will be that it accepts the most rays

(highest geometrical concentration ratio and acceptance angle) while having as high an optical efficiency as possible (before TIR decreases). Between these criteria there is a balance but in theory the parameters which will fulfil these conditions lie on the border of TIR attainment (just fulfilling TIR, or possibly just after optimum TIR fulfilment). Beyond those parameters the optical efficiency will drop even if, depending on the set up, the input of light increases. In this way optimisation of most refractive concentrator optics may actually be positioning them in a very poor or unreliable position for experimental performance. This is partially shown in article 3 where depending on the material and resulting surface roughness of the homogeniser, the optical efficiency could drop to <40% (Figure 16).

3.2. Sources of optical loss within a refractive light funnel

However another reason for loss of rays is too many reflections within the homogeniser [99], [195] which also leads to increased path lengths (more absorption). Even if 100% reflective material was utilised for a V-trough concentrator, eventually the repeated reflection would cause the light rays to start reflecting back upwards and out of the concentrator. Irshid et al. [195] calculate the maximum number of reflections within a V-trough concentrator of specific dimensions and give detailed relationships between the average number of reflections, concentration ratio and optical efficiency. They hypothesis that the maximum concentration ratio for a v-trough concentrator occurs at the maximum number of reflections and hence also the maximum height. As already mentioned, with non-ideal optics this criteria would actually result in very high absorption, reflection losses or failed TIR. The number of

reflections within a light funnel show the dependency of that optic on the reflection efficiency (whether standard mirror reflection or TIR). Coughenour et al. [111] chose a reflective type light funnel over a refractive one due to the Fresnel reflections when the light entered the optic which reduced the optical efficiency at normal incidence. This was justified as a greater overall loss in comparison to the increased acceptance angle from using the refractive type optic.

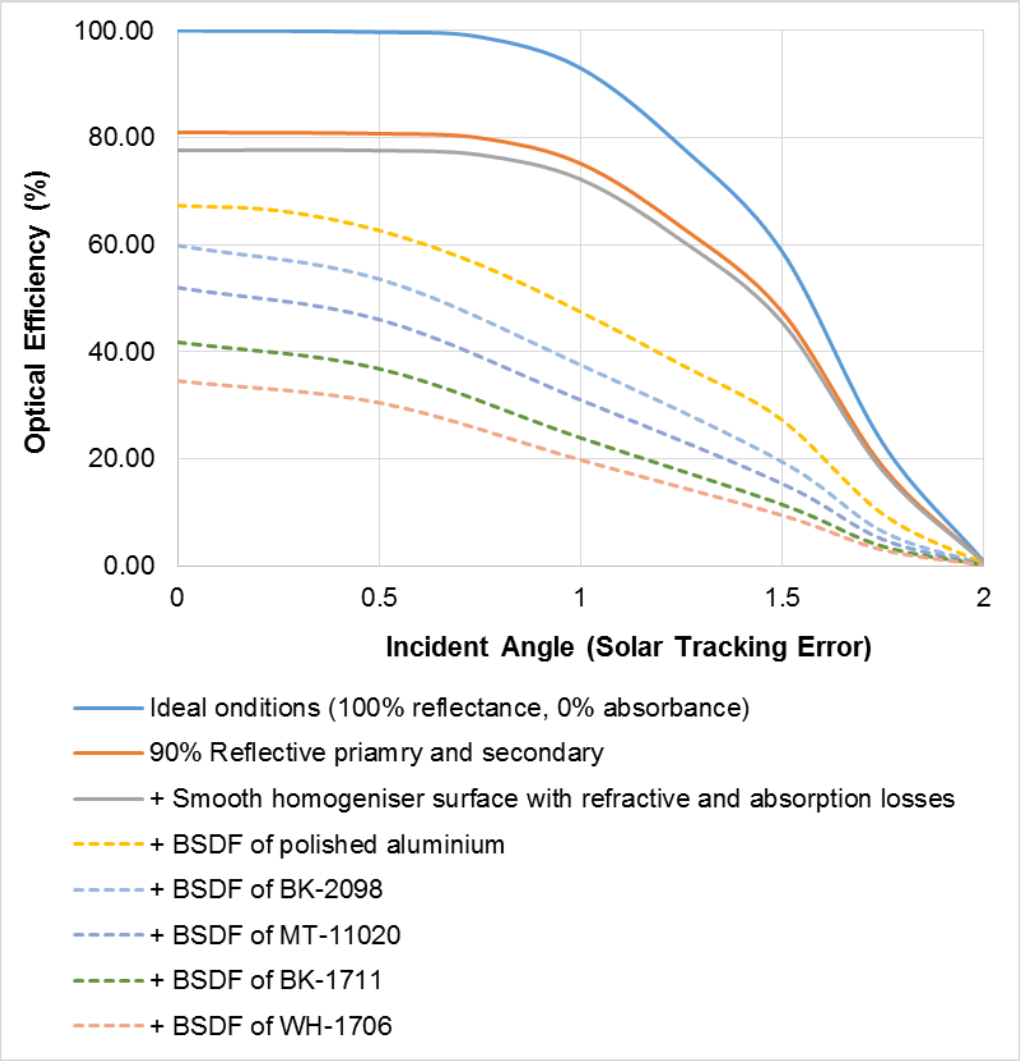

Figure 16: Practical losses summary. Optical efficiency decreases as surface losses are added in stages. The dashed lines represent possible surface scattering profiles of the homogeniser based.

Figure 16 shows how non-ideal optical losses can affect the optical efficiency differently at normal incidence and increased misalignment angles. The optical efficiency decreases are discussed further in article 3 and 4. The BSDF's used for the results displayed in Figure 16 are shown in Figure 17. These graphs basically show an idea of the distributed scattered light after reflecting from that surface. The majority of light is specularly reflected at an angle equal to the angle of incidence, the amount of light scattered around this angle and further then differs. For some distributions, such as Figure 17a), a larger angle of incidence strengthens the proportion of light reflected at the specular angle, which is expected of smooth optics but less predictable for rough ones. The wider, or less gradual the distributions decrease from the specular maximum, the more scattering is taking place and hence the more rough the material it represents.

Gaussian shaped scattering can also be and has been used to simulate the propagation of rays through optical systems and their resulting distributions upon photovoltaic receivers [110]. Ideally, the exact scattering behaviour of an optic would be directly measured and utilised to give correct performance predictions but then this requires designing, making and paying for an optic which may or may not be optimised. Instead optical designers need to rely on the accuracy of material scatter profiles supplied by companies and various software databases. The BSDF's presented in article 3 were chosen only to give a good range of results. Most concentrator optics should perform in the upper band of these scattering profiles but as of yet there has not been an

extensive categorising and matching of materials or manufacturing processes to scatter profiles, surface roughness or similar simulative parameter.

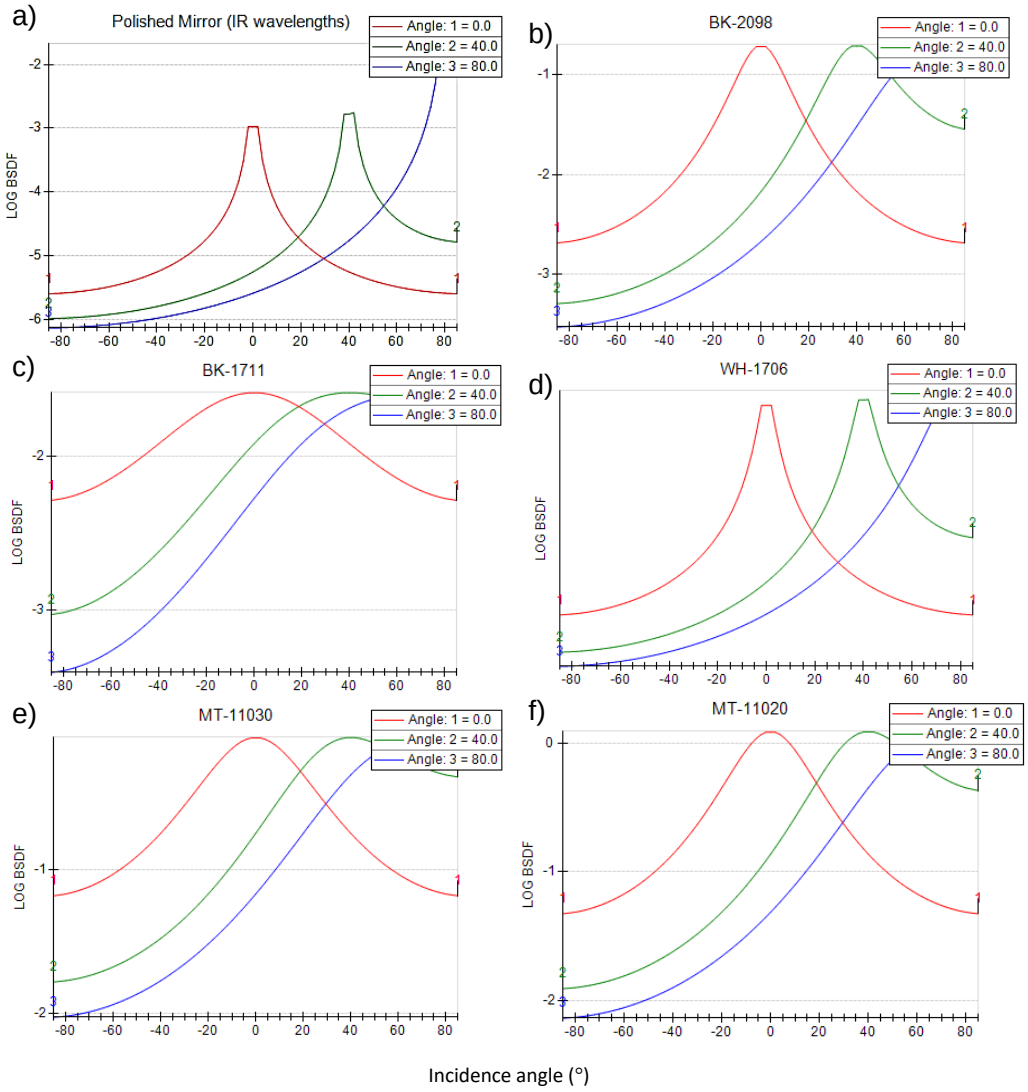

Figure 17: LOG BSDF vs. scatter angle from specular of a) polished mirror; b) BK-2098, c) BK-1711, d) WH-1706, e) MT-11030, f) MT-11020. 3 plots are shown in each graph for an incidence angle of 0°, 40° and 80°. The BSDFs beginning with MT are representative of moulded optics surface profiles and those beginning with BK and WH are associated with specific materials available from lens providers. All plots were taken from the breault ASAP scattering library [194].

3.3. The effect of the CRRH

In article 2 we propose the use of a refractive filled homogeniser optic with a reflective outer optic which acts as a catchment for rays which fail TIR (Figure 14). The cassegrain concentrator was used for the investigations in article 3 as an easy starting design which was already fully understood from the investigations of chapter 2 and articles 2, 8-10. A refractive medium takes advantage of total internal reflection (TIR) but again, surface roughness, scratches or any form of soiling enhances refraction losses. This includes when the rays initially refract into the homogeniser and a small portion of energy is reflected instead of refracted. A simple but effective method to recover rays which fail TIR at the homogeniser walls is to use a reflective sleeve with an air gap [196] as shown in Figure 14. Baig et al. [197], [198] discuss the optical loss caused by the encapsulation medium used in connecting low concentration optics to solar cells. Light rays incident in this overlap region do not reflect towards the solar cell but continue through the encapsulation medium until lost. Baig et al. overcame the encapsulation issue by adding a strip of reflective film to the bottom edge of the 3D cross compound parabolic concentrator designed for building integration [197], [198]. We expand on this method by applying reflective film with an air gap to all of the TIR active walls of a homogeniser in a high concentration Cassegrain concentrator. Hence, the conjugate refractive reflective homogeniser (CRRH) is presented. The following summarises the findings from article 3.

The CRRH was proven to increase the optical efficiency in comparison to its purely reflective counterpart (no refractive material) for a selection of simulated scattering profiles as shown in Figure 18.

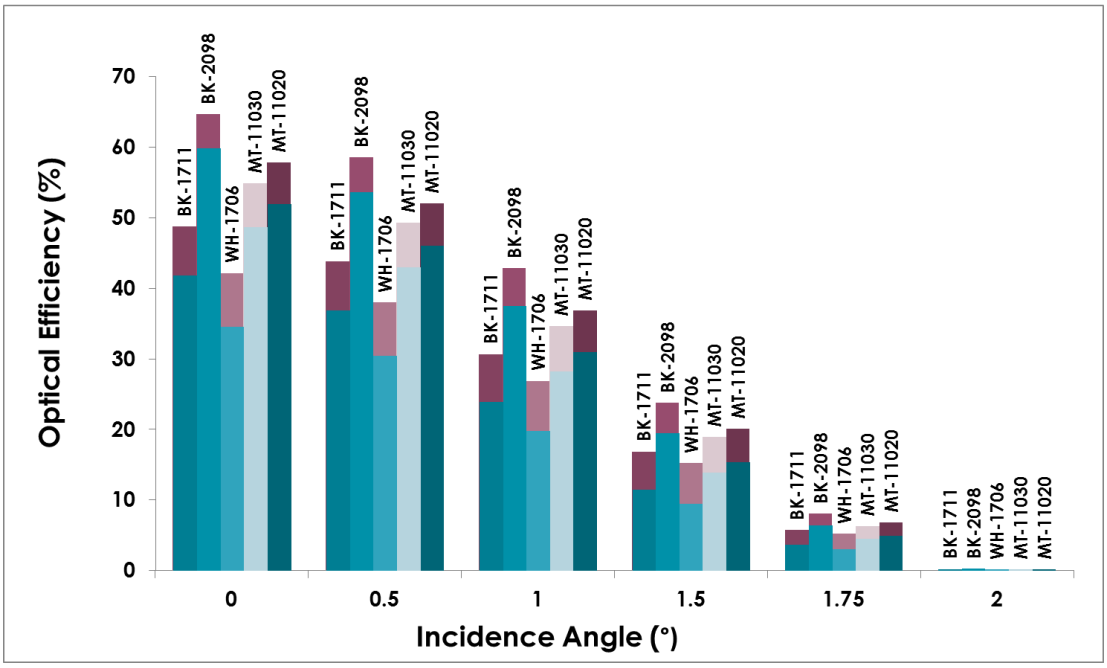

Figure 18: Increase in optical efficiency (purple shades) due to the addition of the reflective sleeve to the refractive homogeniser with an air gap of 0.01mm for increasing BSDF's. The incidence angle of the light is also increased up to 2 degrees to show the effect misalignment has on the benefit of the CRRH in comparison to the performance of a refractive homogeniser (blue shades).

The thickness of the airgap between the refractive material and reflective outer casing (reflective sleeve) was also investigated and found to have very little effect. As small an air gap as possible would give slightly improved results as shown in article 3 but most importantly an air gap must be present to ensure TIR occurs where possible. It is also hypothesised that the more

light going into a TIR optic, and so the more light possibly being lost due to surface imperfections, the greater the benefit of the CRRH. This suggests that high and ultrahigh concentration ratios will benefit even more from optics such as the CRRH.

A simple prototype of the CRRH was made using the careful positioning of reflective film around the refractive homogeniser and tested with a Fresnel lens under a solar simulator (WACOMS continuous solar simulator at 1000W/m2). A 3.5% current increase and 6.7% power increase were measured with the addition of the reflective film. This is slightly lower than the optical efficiency increase predicted from theory (a maximum of 7.75% absolute optical efficiency) but there could be many reasons for this. First of all the set-up is not the same as the cassegrain concentrator simulated, a full prototype was however built and is explained in the next chapter and in article 4. The Fresnel lens set up was a proof of concept experiment before full scale prototyping was undertaken. Other reasons for the difference in theoretical and experimental predictions include: solar divergence of the solar simulator, slight variations in the set up due to alignment errors as already discussed, different angle of incidence rays upon the homogeniser due to the Fresnel lens and simulators divergence angle. The relationship between optical efficiency and power efficiency is also not direct and is effected by the internal resistance within the cell and the temperature of the cell but this effect should only contribute a very small difference [199].

3.4. Conclusions

Overall the CRRH was proven to be a simple but effective method to increase the optical efficiency of a solar concentrator where a TIR optic is utilised. The CRRH compensates for incomplete TIR whether due to surface imperfections, too many internal reflections or the combination of both. In the investigations outlined in this chapter and in articles 4 and 11, the CRRH can in theory improve the optical efficiency by as much as 7.75% for the cassegrain concentrator set up of 500X geometric concentration. This is likely to be less in a built system and is proven so in the following chapter.

CHAPTER 4: Manufacturing and Fabrication of Optics for CPV Prototypes

At present, manufacturing processes for optics include precise grinding, milling, polishing, and a variety of coating methods for a smooth finish [200]. Most current manufacturing processes struggle to produce acceptable priced prototype optics of new specific shapes and reliable accuracy [201], [202]. Here, we have tested plastic mirrors for their advantages in cost, weight and smooth surface quality. We have also utilised 3D printing and tested a structure for its heat tolerance within a CPV system. 3D printing is a very powerful prototyping tool which needs further testing for use within CPV research. The 3D printed support structure also compensates for the possibly weaker coupling joint of the 1 step moulding which is proposed to reduce manufacturing time and improve alignment accuracy. This study, though specific in design and material, highlights a general issue in optics and prototyping and suggests simple but effective methods of compensating for losses due to surface roughness. One of the challenges of CPV technology is its increased initial investment in comparison to flat plate PV due to the added optics and tracking required [203]. Simple but effective prototyping techniques are needed to help develop CPV designs and establish their performance and cost benefits. This depends greatly on the quality of the optics utilised for the prototype, which are normally dictated by budget.

Once optics are manufactured, whether of a specific novel design or bought as a standard shape from a company, checking the accuracy of the manufacturing is also an area requiring further focus. Kiefel et. al. [56] suggest a method to measure slope-deviation in Fresnel lenses using their mould surfaces. Lenses and mirrors can suffer from warping and bending produced during their manufacturing process, during assembly and even after prolonged use due to heating and cooling cycles. There is very little knowledge on how to measure these shape errors in a cost-effective way or on how significant their effect is. Herrero et. al. [204] discuss the ‘checkerboarad method’ to evaluate the errors within an optic and hence the alteration to ray paths. This method is similar to others specifically for mirror concentrators. The material type and manufacturing process will effect what kind of deformations occur and to what degree but further research is required [204].

The cassegrain concentrator designed in chapter 2 with the standard refractive homogeniser and the CRRH described in chapter 3 was manufactured. Various methods were attempted before the final prototypes presented in articles 2 and 4. A singular module and two 3 by 3 arrays were made in total. The parabolic dishes of the cassegrain, with focal length 200mm and 70mm for the large and small dishes respectively, were particularly hard to obtain at a reasonable cost. Prototyping only requires a small number of optics or components, this makes paying for expensive moulds, casts or special machines impractical. High quality optics available from manufactures are cost effective as they have already invested in the initial machinery and moulds to mass produce the specifically shaped optics.

Novel optics of specific shape, size and design are hence typically expensive to manufacture in small batches. The smaller the optic however usually indicates a reduction in cost but there are limitations to the resolution of different manufacturing methods.

4.1. Manufacturing and assembly steps

The first prototype of the cassegrain module was made from a metal spun primary which was then polished and vacuum metalized. The secondary reflector was made from a computer numerical control machine (CNC) to achieve its specific shape, and then polished. Both reflector dishes were made from aluminium and the primary was cut to its square shape using water jet cutting. The singular module prototype was then assembled with a low iron glass cover and a sylgaurd 184 refractive homogeniser as shown in Figure 19b). As can be seen the primary reflector was designed with corners for assembly purposes. Rods were used to initially achieve the separation distance required for optimum performance [article 2] and the solar cell was thermally attached to a thick aluminium base plate which acted as a heat sink.

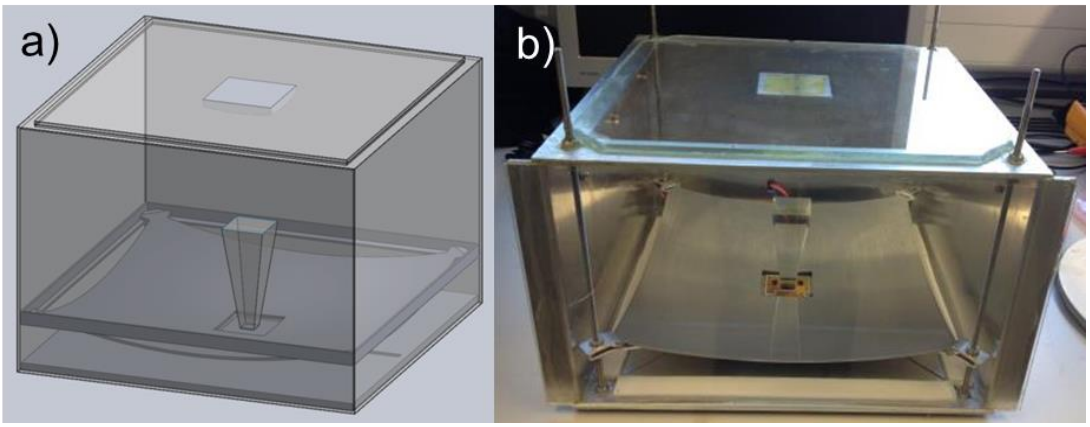

Figure 19: Singular module prototype. a) Solidworks cad drawing and b) built prototype.

The method of assembly and structure of a prototype is also important, especially when accurate alignment could be the difference between a good result and no result (no concentrated light reaching the cell). This can be the case for high and ultrahigh concentrators. The first prototype was very difficult to align using the small clamps to grip the primary reflector in place without bending or tilting it to one side. The metal spun dishes had also a very poor reflectance of only ~ 67%. Second stage prototyping hence investigated the use of plastic mirrors with reflective coating. The plastic base material resulted in a much smoother finish with a clearer and higher reflectance as can be seen by comparing Figure 20 a) and b). The reflectance spectra are given in articles 2 and 4.

The plastic secondary's however could not cope with the concentrated light and accumulated heat and started to deform under exposure Figure 20 d). Reflective film, although measured to have a higher reflectance than the polished solid aluminium, could not be attached in a way that maintained the curve of the secondary reflector (Figure 20 c) and would have also begun to peel due to the heat.

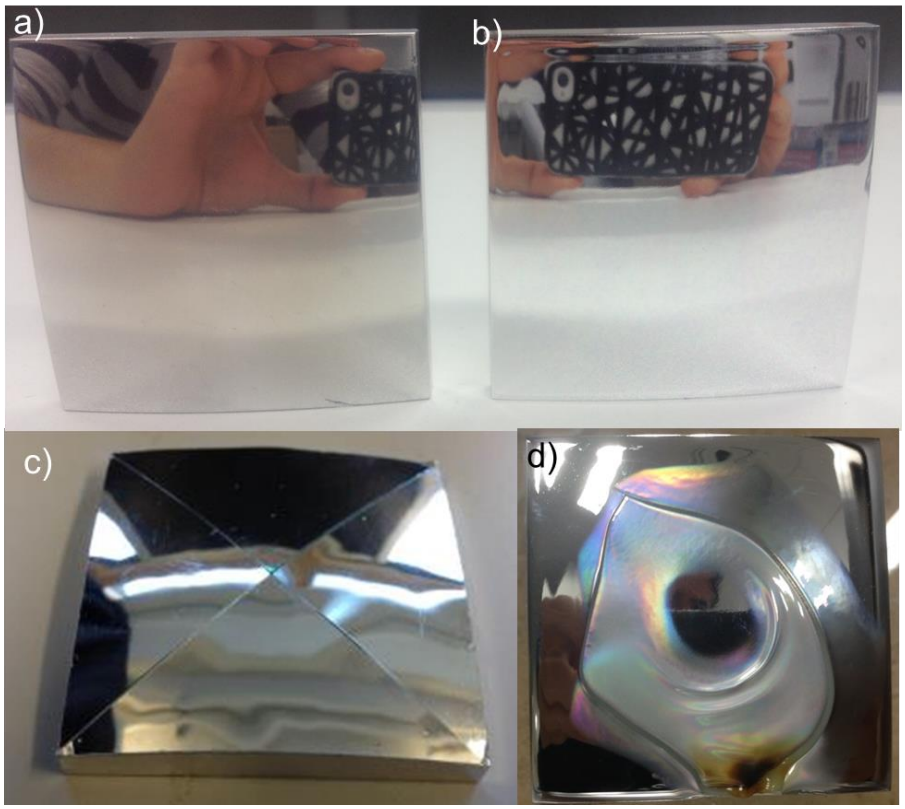

Figure 20: a) Polished aluminium secondary. b) Vacuum metalized plastic CNC'd and post polished secondary. c) Aluminium secondary with reflective film. d) Melting of plastic secondary after concentrated light exposure.

The plastic primary reflector did not deform while in use since it had no concentrated light incident on it and reduced the weight of the 3 x 3 module array prototype significantly in comparison to if metal primarys were installed. Further research into using plastics for primary optical components is required to understand their long term stability but from the results in articles 2 and 4 plastic reflectors can be more efficient, lighter and cost effective but only used for primary or low concentrator optics.

The first 3 x 3 module array (9 modules) was tested in the Helios3198 solar simulator at the Centre for Advanced Studies in Energy and Environment (CEAMA) at the University of Jaen in Southern Spain [article 2]. This is a very powerful flash solar simulator with a divergence angle of only ±0.4°. The purely refractive homogeniser however appeared to be of very low optical efficiency and stability as it would lean to one side when the prototype was mounted as described further in article 2. This was another reason for the CRRH designed in article 4 and discussed in the previous chapter.

4.2. 3D Printed CRRH

3D printing is a fast and accurate prototyping solution that could be very useful for the development of CPV designs. Investigations of its practical use and reliability in high temperature conditions are however needed. This has been done in article 5. The ABSplus-P430 material which the 3D printed CRRH outer structure was made of did not show any signs of deformation at temperatures up to 80°C when preliminary heat testing was done in a vacuum oven. Experimental measurements on the other hand showed temperatures as high as 226°C were possible at the focal spot on top of the CRRH when the system was installed at the Indian Institue of Technology Madras in Chennai, India. This is discussed in more detail in article 4 but ultimately the melting of the 3D printed structure only occurred when the focal spot was incident on the material itself due to misalignment in tracking. When the focused light was central on the homogeniser refractive material, no melting occurred. In this way 3D printed structures, similarly to the plastic mirrors, could be used for primary concentrators or low concentration optics. 3D

printed structures at present have a prominent ribbed texture to them unsuitable for mirrors or optics unless this surface structure can actually be incorporated into the design. For example, Nilsson et. al. [84] investigated grooved reflector surfaces which reduced irradiance peaks. If reflective film or a very thick reflective coating is being applied to the 3D printed structure then the surface pattern may not be an issue, though this seems impossible for the case of high and ultrahigh concentrators that require the highest accuracy in their optics. 3D printing as shown in article 4 is however very useful as a structural part of a CPV module as long as the structure is either separate from the focused light or protected in some way to handle the increased temperatures.

Advances in the resolution of 3D printing or smooth surface post procedures would also help expand and rapidly develop CPV concentrator prototyping and hence commercialisation but in both cases the surface structure again is a feature of optics worth understanding further.

4.3. Conclusions

The Conjugate Refractive Reflective Homogeniser has been experimentally tested within a 500x geometric concentration cassegrain design. A prototype of the complete system was built and experimentally tested. Measurements showed a 4.5% increase in power. This was ~40% of the theoretical improvement calculated by simulations (7.76%) in article 3 and presented in chapter 3. Temperature testing was also carried out on the components and the 3D printed support structure for the CRRH was

found to be inadequate at coping with the direct focused sunlight similar to the plastic secondary reflectors which were tested in the first array prototype. However the resulting deformation in the structure only occurs when there is a misalignment of 2-3 degrees in the system. Improving the design by using a protective layer on the 3D printed support structure should easily solve this issue. The experimental tests confirmed the CRRH can improve the power output of a cassegrain concentrator of this design and 500x geometric concentration ratio. The use of plastic as a substrate for mirrors or support structure has been proven here with the advantage of smoother surface finishes for vacuum metalized mirrors. Plastic mirrors can however only be used for primary or low concentration optics. This is an important step towards the development of CPV technology as plastic prototyping can be done more cost effectively with good performance results and accuracy due to the improved surface smoothness. There is still however many material options available to be explored for CPV technology.

CHAPTER 5: Development of Novel Bio-inspired Materials for CPV Optics

Nature has a vast range of advanced complex structures which have been studied by many to be replicated and adapted for our own use [153]–[158]. A clear example is the application of light trapping microstructures, inspired by moth eye facets and other natural light trapping structures, imprinted upon solar cells to enhance light collection and conversion efficiencies [158]–[160].

V-grooved, U-grooved, honeycomb and randomly dispersed pyramid textured silicon substrates are some surface structures utilised to improve the light coupling efficiency of solar cells. Chiadini et. al. [205] designed a prismatic lens inspired by the compound cylindrical facets arrayed on the curved surface of flys (specifically the common house fly and blow fly) which enhanced the light harvesting capabilities of the silicon cells it was mounted upon. This bioinspired compound lens (named the bioinspired hillock texture) surface structure made from silicon dioxide was found to enhance the acceptance angle of the silicon solar cells better than expensive nanofabrication techniques or antireflection layers. Chiadini et al. [206] also investigated the inverse of this hillock structure where instead of ‘bumps’ and hills there were grooves and pits. This topology was found to improve the light coupling efficiency even more but experimental validation for both structures is still required. From simulations light-coupling efficiency was enhanced by a maximum of 20% and 24% in comparison to an untextured silicon cell when

decorated with the bioinspired hillock texture and the bioinspired pit texture, respectively [205].

Articles 1 and 5 gives more examples of natural structures, typically insect wings and eyes, which have optical properties of interest for CPV research. Article 5 investigates the specific use of the cabbage white butterfly wings as lightweight reflectors for solar concentration. This article also experimentally proves that the V-shaped basking inhibited by the butterflies is concentrating light and so experimentally proves how these insects are heating their flight muscles faster than other species (Figure 21).

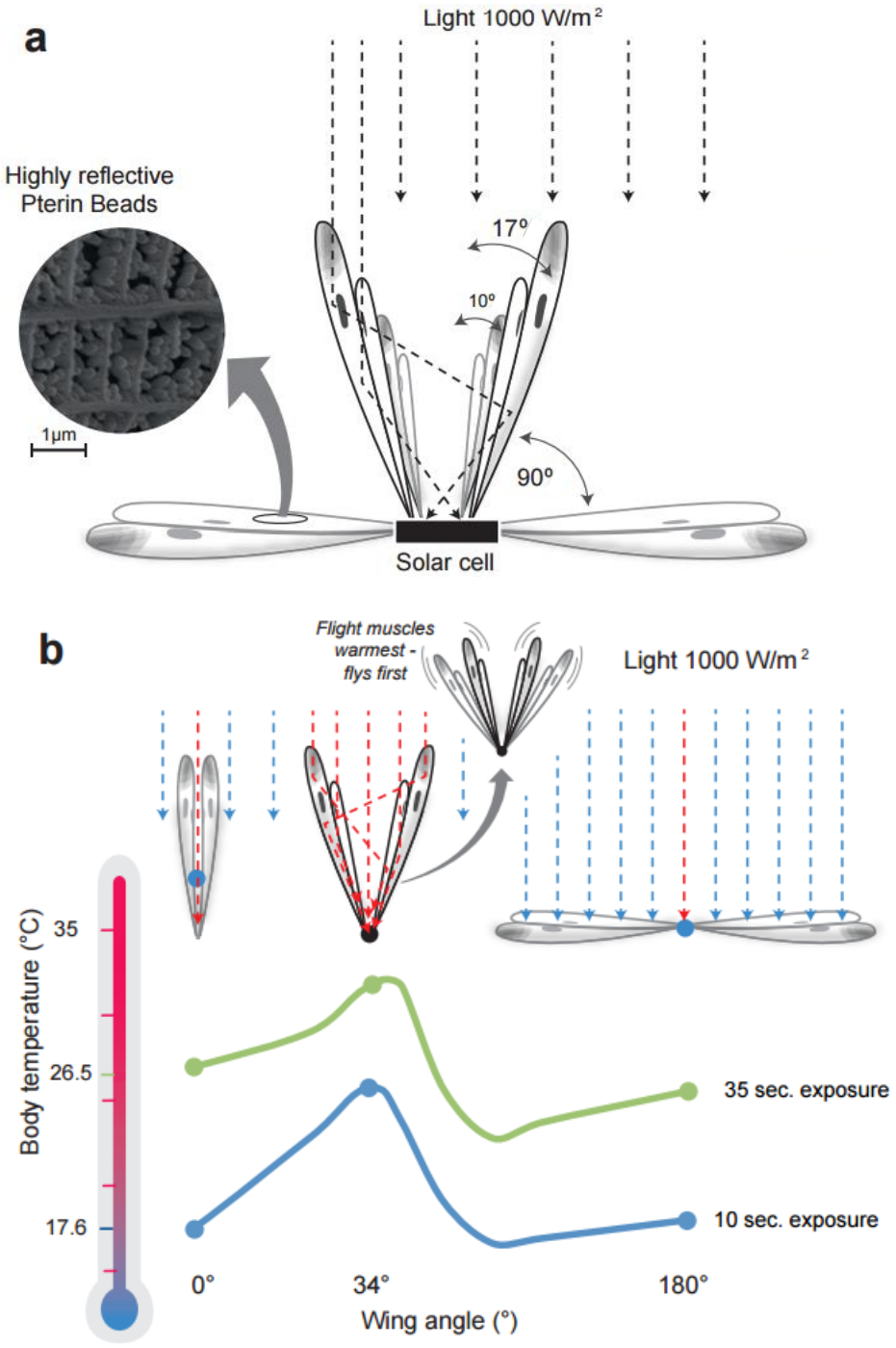

Figure 21: a) V-shaped CPV using wings as reflectors where their unique structure of pterin beads in chitin ladders is leightweight, strong and highly eflective. b) Concentration effects of different wing angles and the temperature increase as a result.

The cabbage white butterfly was investigated for its unique concentration basking behaviour. Specifically it is the butterfly's wing scale nanostructure of ellipsoidal pterin beads [176], [207]–[211] which is of particular interest to achieve the combination of lightweight and reflective properties in a new material of similar nanostructure design. Novel macro- and micro- structures have been analyzed elsewhere [84], [159], [160], [170], [212] for their effect on light manipulation. In particular it can be the height, density and curvature of nanoparticles in a coating or material surface that pertains the reflective properties [213]–[217]. The large cabbage white butterfly wings were found to have reflectance values as high as 78.9% over the input range of the silicon solar cell used in the study (400-950nm). Furthermore the power to weight ratio of the butterfly wing CPV was 17 times lighter than that utilizing standard reflective film. Although these results are impressive and hold great potential for reducing the weight of CPV technology and hence enhancing its application range and cost effectiveness, manufacturing of such a material is yet to be done. Future research will be undertaken which investigates the use of nano-carbon ladder structures and TiO2 beads or similar to try to mimic the butterfly wing structures. Further understanding of how the wing structure contributes to light reflection, low weight and strength is however required. Hence, we expand on the work presented in article 5 and begin the theoretical development of the new lightweight reflective material envisaged.

5.1. Lightweight material surface structure theory

The reflecting component of a material is typically metallic and heavy. No matter what the material however, the density and thickness will have an effect on the reflectance. We propose reducing the density and thickness of a materials structure such that the heavy reflective particles are spaced further apart (Figure 22A and B), reducing the weight of the material. This reduced density will also reduce the reflectance at normal incidence (Figure 22B), but in the case of solar concentrators, reflectors are rarely positioned to reflect normal incident light. In this way, the less dense and lighter material may still have a high reflectance at a range of angles with respect to the incident light as shown in Figure 22C and D.

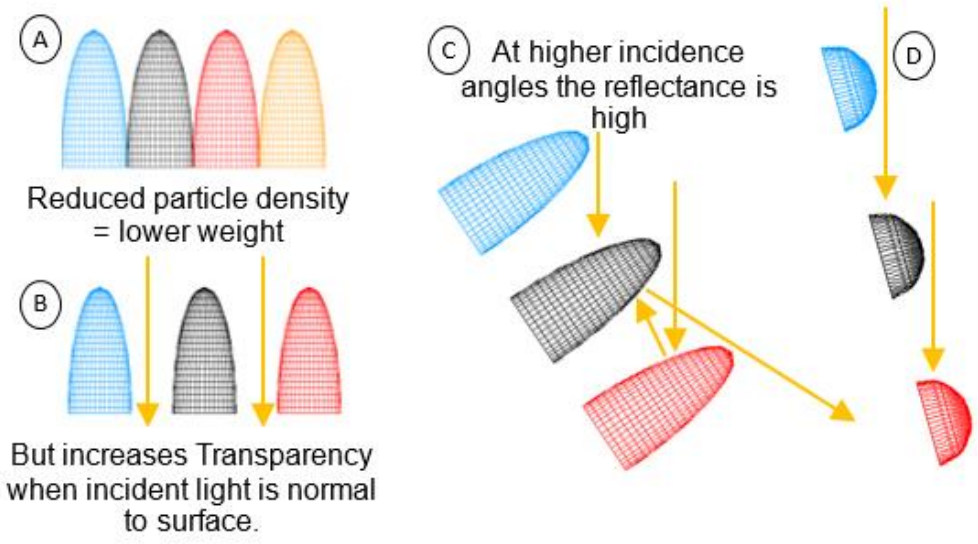

Figure 22: Theoretical example of less dense particle structure for lighter reflective material. 1) Example of ellipsoidal surface structure of material which can be reduced to 2) where less particles are required for the same area. This configuration has a higher transparency at normal light incidence as shown by the arrows. 3) Same spaced structure at an angle so incident light no longer passes through. 4) Example of spherical particle surface

structure which requires a sharper angle against incident light to increase reflectance.

To test this theory we employ the simple geometry of the V-trough concentrator which is also the shape adopted by the cabbage white butterflies [Article 5]. Initial simple ray trace simulations were carried out for this design where each reflector was simulated out of a number of particles in a line and the receiver at the base. The particles were either reflecting spherical particles or reflecting ellipsoidal particles. No specific refractive index or material was assigned to the particles for these initial investigations. We use this design to validate this new method of weight reduction in reflective materials by varying the shape and number of reflective particles along each reflector plane.

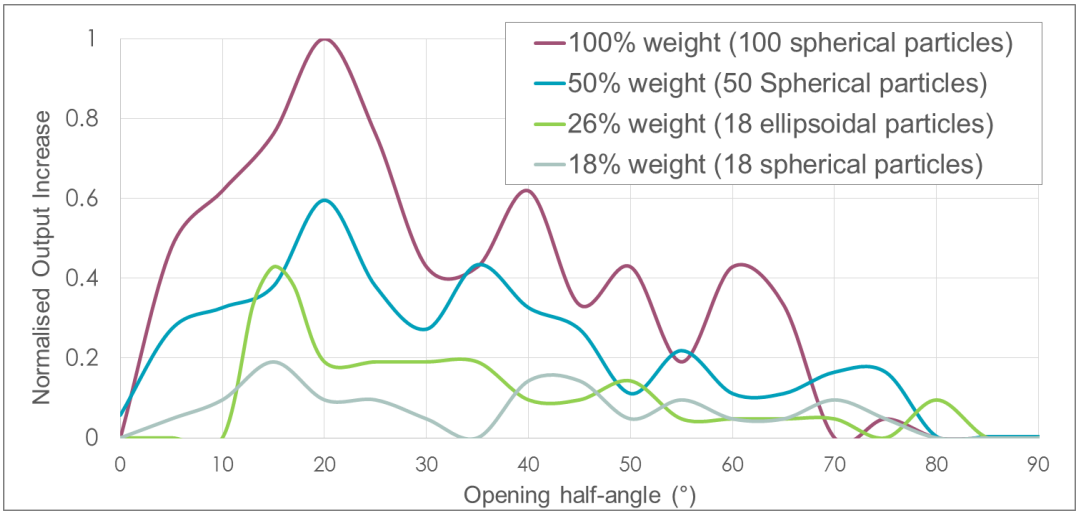

Figure 23: Normalised output power with respects to the maximum with 100% weight (which is taken as 100 spherical particles for comparison purposes) vs. opening half angle of the reflectors.

As can be seen from Figure 23 the output oscillates as the curved particles allow for light to be mostly reflected towards the receiver or away, depending

on the orientation and number of reflections. Straight away it can be seen that the weight can be halfed but achieve 60% of the maximum output power (shown from the 50% weight line). One of the most impressive results from Figure 23 however is the 26% weight - 18 ellipsoidal beads structure. This structure is 26% the weight of the original compact structure but can achieve the same output power as the 50% weighted structure of 50 spherical beads at 15° open half angle. So the same power output has been achieved with almost half of the weight. The fact that this occurs at 15° open half angle of the reflectors also reinforces that a similar effect is occurring with the butterfly wings whose maximum wing open half angle was found to be 17°. The optimum angle for the spherical particles seems to be 20° in these simulations so it could be possible that the beads of the cabbage white butterfly are of a shape between the straight forward ellipsoidal and spherical particles used here. The ellipsoidal dimensions here were taken from SEM measurements of the peterin beads of the butterfly wings [article 5]. An average width and height was taken and scaled for the simulations so maybe the error is in the averaging. More thorough and detailed simulations and experimental work are planned. Figure 23 is interesting even though based on simple geometry, especially if future optics are optimized for specific angles of incidence which will no doubt consider surface structure.

The wing structure and structure of reflectors is far more complicated than these simulations so there is much more to investigate before solid conclusions can be drawn. The findings from article 5 and from these preliminary experiments presented here for the next stage of leightweight

reflective material fabrication are highly promising. This type of research encourages the need for more research into the materials and surface structure of optics for CPV technology and the vast potential novel surface structures have, whether based on nature or otherwise.

5.2. Results of Cabbage White butterfly Wings as Concentrators

The V-shaped reflectance basking of the family Pieridae is easily comparable to V-trough solar concentrators and even more so when considering studies into the segmented surface structure of solar concentrators as carried out by Zanganeh et al. [82], Nilsson et al. [84] and more broadly by Sangster et al. [218]. Further investigation into the acceptance angle of these basking butterfly wings is however required. In our study (article 5) the optimum wing angle for light concentration by the butterfly wings was found to be 17° for both the thermal and photovoltaic receiver conditions. In the case of the pierids, the surface structure of their wings as well as the shape and size of their target area (flight muscles) will predominantly decide the angle with which their wings are held. Other factors however could include: the desired energy/temperature upon flight muscles [219]; the time of year (sun's location, ambient temperature, thorax size [220]); and location (global horizontal irradiance values) [221], [222]. This optimum angle does however prove that other receiver dimensions and applications are possible with these wings and that they are not solely optimised for the characteristics of the thorax reciever.

The overlap match between the reflectance spectra of the large white butterfly and the working range of a monocrystalline silicon solar cell (see article 5)

ensures that useful light rays are incident upon the solar cell [article 5]. There is however significant unwanted wavelengths which would also be reflected towards the receiver. These results indicate that if used in larger concentration systems (500 fold concentration) that receiver cooling would be required to avoid damage to the photovoltaic receiver. This is a common necessity for current concentrator technology at high concentration ratios [223], [224].

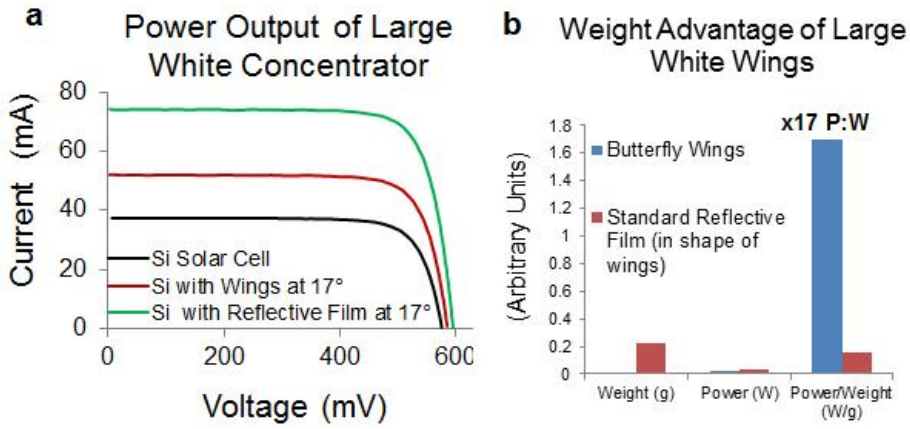

Figure 24: a) Power output of a mono-crystalline silicon (Si) solar cell either alone, or with large white wings versus reflective film held at the optimal angle of 17°. b) Histogram representing the relative changes in both power, weight and the subsequent power to weight ratio of large white butterfly wings versus reflective film.

The I-V output curves in Figure 24 show a 42.3% increase in power from the solar cell with attached large white butterfly wings. In terms of increased solar input (solar concentration) this works out as a concentrating effect of 1.3x, compared to the 2x concentration achieved by the reflective film. However in terms of weight, the butterfly wings have 17x the power to weight ratio of the reflective film structure. In theory, the maximum concentration ratio possible using the angle of the wings and receiver size with no light loss, would be 7.5

x concentrations. The miss-match in values however is due to the configuration of the wings where most light can be lost to the front and rear where there is no wing coverage. The 2x concentration result from the reflective film wings prove the majority of the loss is due to the wing configuration and not the wings themselves. A different configuration of the wings, with a smaller receiver similar to the butterflies' thorax should result in even higher I-V values with less loss.

5.3. Conclusion

In conclusion, the results obtained from the various investigations carried out in article 5, and expanded upon here, have several implications both for the biology of butterflies and for the design of more lightweight but efficient solar concentrator systems. First, the infra-red measurements of butterfly body temperature given in article 5 confirm the assumption that the thermal basking exhibited by pierid butterflies really does provide an increase in thorax temperature proving that their V-shaped posture is an effective thermal basking method. Second, butterfly wings are both highly reflective and much lighter than any current reflective material. Mimicking reflective pterin bead structures with similar power to weight properties will be extremely useful in the design of new reflective materials for use in applications where weight is a limiting issue, such as flight. Third, and perhaps most obviously, this suggests that butterflies have evolved to concentrate light effectively for their needs and supports the idea that any given problem may first have been solved by nature [155], [159], [160]. Finally, despite the apparent complexity of the multi-layered array of butterfly scales on the wing, we have shown that a

simple mono-layer of scale cells removed onto adhesive tape is also highly reflective. We hence speculate that nano-fabrication of a layer of ovoid pigment containing beads will also form a reflective and light weight mimic of a pierid scale cell, provided that the nano-beads are presented in their correct orientation. Not only could this potentially enhance the properties and application of reflective materials but it could also expand the application of technologies such as solar concentrators which are currently limited by power to weight issues.

CHAPTER 6: Ultra-high Concentrator Optical Design and Modelling

As already discussed in chapter 1 and article 1, higher concentration ratios are being reached, although not as rapidly as the efficiency of concentrator multi-junction solar cells are increasing. The challenges against ultrahigh concentration range across the main areas of CPV technology as outlined in Figure 7. In order to achieve reliable ultrahigh concentrator photovoltaic (UHCPV) systems materials, surface structure and geometrical design needs to be carefully chosen. Considerations of cost, manufacturing and assembly must also be taken to ensure the full benefits of UHCPV technology can be realised. As a first step, article 6 proposes an ultra-high concentration set up which should be relatively easy to manufacture due to the use of multiple primary Fresnel lenses (instead of a large single primary) and the use of flat mirrors instead of curved.

6.1. The advantage of Flat mirrors

With each addition of an optical component or stage within a CPV design, there is added error to the light rays intended paths. This is discussed in article 6 and represented in Figure 25.

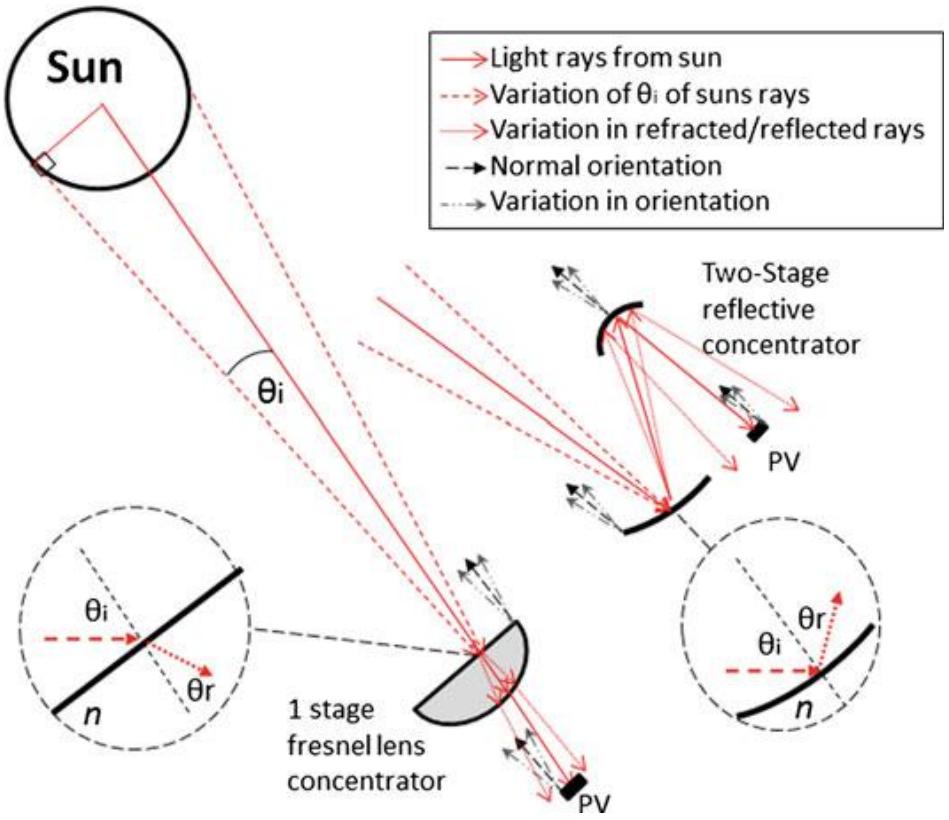

Figure 25: Representation of the uncertainty in rays from the sun and how this uncertainty increases through different optics and onto the photovoltaic receiver which will also have its own alignment errors [article 6].

As previously mentioned, higher concentration ratio optics have reduced acceptance angles due to etendue. Another way of visualising the effect of higher concentration ratios on light path error is to think of the curvatures required for higher concentration ratios. To achieve higher concentration ratios light rays must pass through a curved interface (or faceted curved interface such as a Fresnel lens) with a higher degree of curvature (faster rate of gradient change). This means that a displaced light ray from normal will undergo a more altered angle of reflection or refraction than an optic of lower concentration would dictate. Following this description, flat mirrors have a

reduced uncertainty to them in comparison to curved mirrors. In theory, a high quality flat mirror (which is not very difficult to manufacture) should mostly maintain the uncertainty of the previous stage. In the case of this ultrahigh design this means the acceptance angle of the Fresnel lens primaries should be mostly maintained through the first and second flat mirrors, assuming their positioning is also accurate along with the surface smoothness. In this way the two flat mirrors are better or equal in optical tolerance than if a conic reflector was used instead and the 4 optics in the ultrahigh design should not be thought of being particularly worse than a 3 stage design of purely curved optics.

One quantifiable method to compare how good a design is at achieving its optimum performance given the limitations of etendue is the concentration acceptance product (CAP). This is used in article 6.

6.2. Antireflective coatings and incidence angle

One influential measurement not simulated or experimentally investigated for this ultrahigh design is the acceptance angle of the solar cell. The light rays incident on the solar cell in this design are coming from 4 different directions and are hitting the receiver at large angles of incidence. As discussed in chapter CHAPTER 5: the surface structure of a solar cell effects its acceptance angle for various wavelengths and hence its light coupling efficiency. Anti-reflective coatings can increase the efficiency of light harvesting at normal incidence but may reduce it at larger angles of incidence or vice versa [213], [225]. This needs to be investigated further. The solar cell

intended to be used can come with or without AR coatings and so these must be tested first. The secondary and primary lenses can also be coated with anti-reflective coatings which similarly should improve the optical efficiency although more experimental investigation is required to ensure these coatings would not decrease the acceptance angle. Vahanian et. al. recently showed that applying antireflective coatings consisting of silica nanoparticles could substantially improve the optical efficiency and hence output of a CPV system [114]. To demonstrate the full advantages of CPV technology, all considerations should be taken to produce the best performing prototype. However depending on the application, aims and limitations (cost, space..) compromises are often made.

6.3. Design objectives – cost vs efficiency vs area required

As discussed in chapter CHAPTER 4:, the performance of a CPV system will depend on the quality of the optics and PV cells used. The highest quality of optics and photovoltaics will of course be very expensive but they should also outperform other systems and in theory require the smallest area. The most efficient system should also require the least amount of material (optical, structural and photovoltaic) and be the most environmentally friendly although due to the many contributing factors this can get very complex. Solar concentrators, although able to increase the efficiency of solar cells, overall may not have the highest module efficiency due to optical efficiency and heat management. CPV however requires far less PV material and as already discussed (chapter 1) is better for the environment due to its reduced effect on the albedo of an area. So overall solar concentrators are a good solution to

helping fight global warming and high cost high efficiency systems have the greatest potential to do it.

Another option is available. As presented in article 6, an overly ambitious geometric concentration ratio with relatively cheap optics and a resultantly low optical efficiency could result in a cost effective CPV module still capable and reliable of producing at least >2000X (even at 1° incidence angle). Such a system would of course not be space efficient, but depending on the application and location, space may be the lowest factor.

6.4. Ultrahigh Concentrator Design Results

An ultrahigh solar concentrator photovoltaic design of >5800x geometrical concentration ratio was designed utilizing multiple primary Fresnel lenses. The final stage optic is of a novel design to accept light from four different directions and reflect the light towards the solar cell. The high geometrical concentration of 5800x was chosen in anticipation of the losses incurred in such a system. An optical efficiency of ~75% is achieved in simulations which gives an effective concentration ratio of >4300x (Figure 26a)). Standard optical constraints were also considered (Figure 26b)) and if less accurate optics are used to build a prototype then this should result in an optical efficiency of >55% which translates to an effective concentration ratio of >3000x. The optical efficiency of each component is simulated as well as experimentally measured to ensure the accuracy of the simulations. An acceptance angle of 0.4° was achieved for this design which is considered good for such a high concentration level. The need for achromatic Fresnel

lenses is apparent from this study to reach optimum performance and concentration. The solar cells irradiance distribution of the design is also presented.

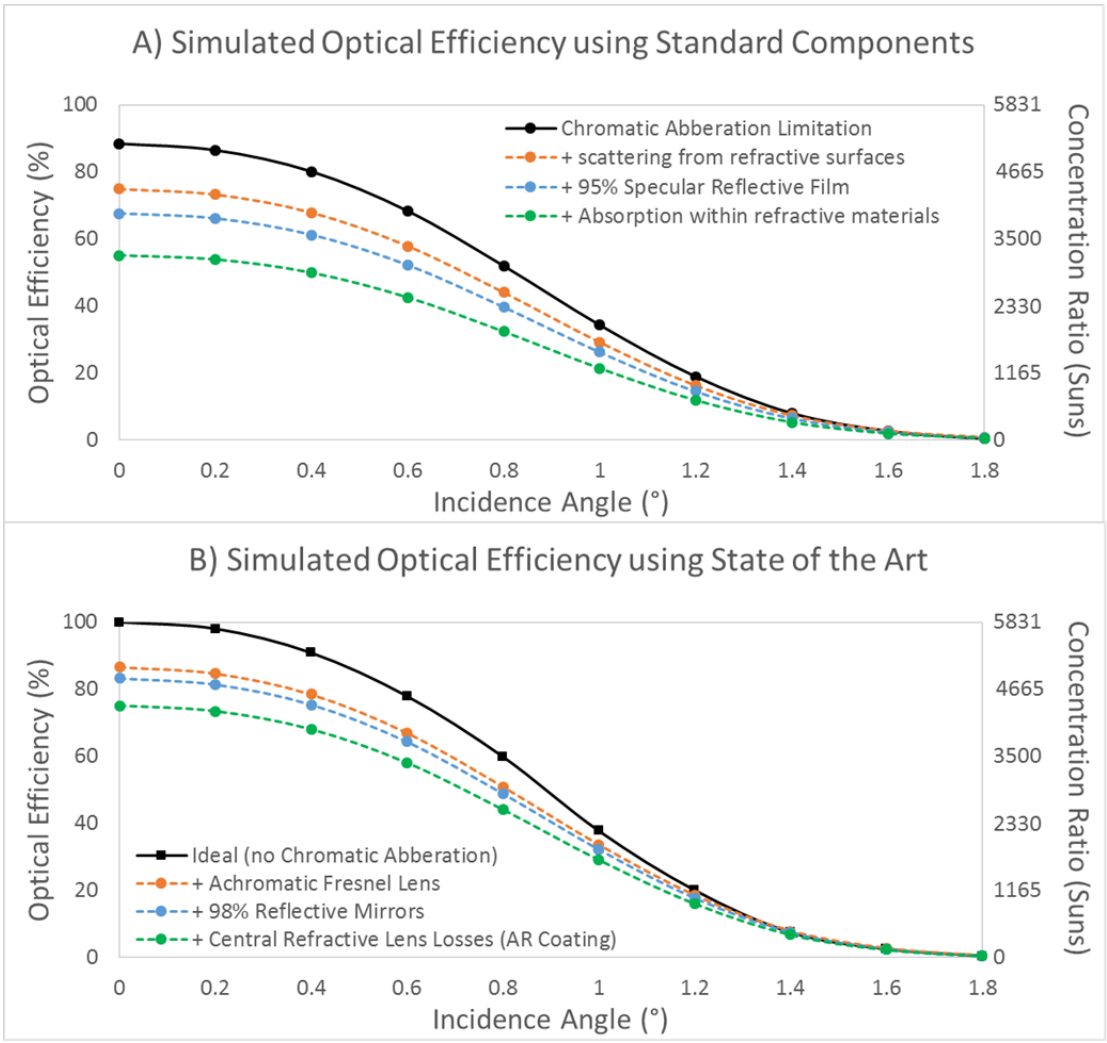

Figure 26: A) Simulated optical efficiency of the concentrator using standard components including a silicon on glass Fresnel lens, flat 95% reflective mirrors and an uncoated sapphire centre optic. B) The simulated optical efficiency of the system if top of the range components are utilised including an achromatic Fresnel lens made of two refractive index materials on glass, 98% silver mirrors and a high quality sapphire centre optic with an antireflective coating.

The design takes advantage of flat mirrors and easy manufacturing methods in line with current and state of the art optical capabilities (Figure 26). The system is anticipated to achieve an optical efficiency of >70% which is >4000x or if poorer quality optics are utilized then an optical efficiency of ~55% should be obtained which translates to ~3000x. The system has an acceptance angle of 0.4° which is very good for such levels of ultrahigh concentration and of a relatively simple design. The design should be easy to manufacture and will be very useful in pushing CPV technology to higher concentration ratios. Experimental prototyping is required next but from the simulations results presented here and in article 6, the optical efficiency should fall between the two scenarios given in Figure 26. The effect of the surface roughness of the high refractive index receiver optic will be of most importance in the manufacturing but at present there has not been enough investigations into sapphire optics for solar concentration. Both optical quality scenarios given will produce ultrahigh-concentration ratios which can be investigated further in terms of solar cell performance, temperature and reliability.

6.5. Conclusion

Overall the design presented for ultrahigh concentration has a number of advantages and points of interest for the field of CPV. Mainly it achieves an ultrahigh concentration of ~3000x even if a low optical efficiency of ~55% is achieved, which would not be unusual as manufacturing and alignment issues for ultrahigh concentration are severe. Second most importantly is the ‘assembly friendly’ design with the use of multiple smaller primarys and flat

optics within this design. The Fresnel lenses and flat mirrors are relatively easy to make and align in comparison to other larger or curved optics. Even the receiver optic uses dome curves to focus the light further. The simple circular curve is relatively easy and inexpensive to acquire as opposed to custom curves.

A built prototype of this design will be very interesting to investigate the temperature effects of the optics and solar cell under such a high concentration. Concentrator solar cells of different recommended concentrations can be investigated with the system to compare the cost effectiveness to efficiency balance as proposed by article 13. Future work would compare the reliabilities of using an ultrahigh concentrator at low optical efficiency and a high concentrator at high optical efficiency.

CHAPTER 7: Conclusions and Future Work

7.1. Conclusions

Concentrator photovoltaics have been investigated through a comprehensive literature review as well as various theoretical and experimental studies. The subject of surface structure and its implications on concentrator optics has been discussed in detail while highlighting the need for enhanced considerations towards material and the surface quality of optics. A simulation method has been presented which gives attention to surface scattering of refractive optics and shows that the optical efficiency of a refractive optic utilising TIR can decrease by 10-40% (absolute value) depending on the material and manufacturing method. New plastic optics and support structures have been proposed and experimentally tested including the use of a conjugate refractive-reflective homogeniser (CRRH). The CRRH uses a reflective outer casing to capture any light rays which have failed TIR due to non-ideal surface topography. The CRRH was theoretically simulated to improve the optical efficiency of a cassegrain concentrator by a maximum of 7.75%. A prototype was built and tested and the power output increase when utilising the CRRH was a promising 4.5%. The 3D printed support structure however melted under focused light which reached temperatures of 226.3°C when tested at the Indian Institute of Technology Madras in Chennai India.

The need for further research into prototyping methods and optical materials for novel optics was also demonstrated as well as the advantages of

broadening CPV technology into the fields of biomimicry. The cabbage white butterfly was proven to concentrate light onto its thorax using its highly reflective and lightweight wings in a basking V-shape not unlike V-trough concentrators. These wings were measured to have a unique structure consisting of ellipsoidal pterin beads aligned in ladder like structures on each wing scale which itself is then tiled in a roof like pattern on the wing. Such structures of a reflective material may be the answer to lightweight materials capable of increasing the power to weight ratio of CPV technology greatly. Experimental testing of the large cabbage white wings with a silicon solar cell confirmed a 17x greater power to weight ratio in comparison to the same set up with reflective film instead of the wings. Further work is however required to fully understand the properties of the wing structure; how to achieve similar power to weight ratios and perhaps some of the other advantages of the wings (strength, extreme durability with time, water resistance).

All of the findings presented contribute to the development of higher performance CPV technologies. Specifically high and ultrahigh concentrator designs and the accompanied need for high accuracy high quality optics has been supported. An ultrahigh design was proposed taking into account manufacturing considerations and material options. The geometrical design was of 5800x of which an optical efficiency of either ~75% with state of the art optics should produce an effective concentration of >4300x while relatively standard quality optics should give an optical efficiency of ~55% and concentration ratio ~3000x. A prototype of the system is hypothesised to fall between these two predictions. Ultrahigh designs can be realised if the design

process is as comprehensive as possible, considering materials, surface structure, component combinations, anti-reflective coatings, manufacturing processing and alignment methods. Most of which have been addressed in this work and the accompanied articles. Higher concentration designs have been discussed to have greater advantages in terms of the environmental impact, efficiency and cost effectiveness. But these benefits can only be realised if designs take into account the aforementioned factors. Most importantly surface structure plays a big role in the performance of ultrahigh concentrator photovoltaics.

Most CPV systems have to make compromises in one area or another when trying to attain higher concentration ratios but segmented primary optics are able to challenge or at least extend this trade-off which is inevitably encountered [article 1 and 11]. Ultimately, future CPV optical systems will get larger in concentration ratio but require the use of modular surfaces, facets, truncation and more acute design. This will also increase the dependency on the materials available and their properties. One of the breakthroughs for solar concentrator technology was the discovery of PMMA and its application for Fresnel lenses. It is hence not an unusual notion that further breakthroughs in the optics for concentrator photovoltaic applications will be largely due to the development of new materials for its purpose.

This work gives examples of how solar concentrators can be designed in a variety of unique ways boasting different characteristics for different applications. In order to make the necessary leaps in solar concentrator optics

to efficient cost effective PV technologies, future novel designs should consider not only novel geometries but also the effect of different materials and surface structures. Trends towards higher performance solar concentrator designs include the use of micro-patterned structures and attention to detailed design such as tailoring secondary optics to primary optics and vice-versa. There is still a vast potential for what materials and hence surface structures could be utilised for solar concentrator designs especially if inspiration is taken from biological structures already proven to manipulate light.

This work, its findings and the attached articles contribute significantly to the research field of CPV technology in the following ways. (1) Proves the importance of surface structure and amterial choice in the design and manufacturing stages of CPV production. (2) Provides effective methods and solutions to the accounting and capturing of the lsot energy due to surface scattering. This includes the development of the CRRH which is a simple optic that can increase the optical efficiency. (3) The effect and practicality of using plastic optics has also been investigated as another option to combat conventional material and surface flaws. Lightweight plastic optics or support structures can be used as long as no more than low concentration light is incident on them. (4) Pioneering work into biomimicry, specifically of the cabbage white butterfly’s reflective wings, for developing lightweight reflective materials has been presented. (5) A novel ultrahigh concentrator design is given which accounts for optical losses and gives realistic minimum and maximum performance predictions depending on the quality of optics employed.

7.2. Recommendations for future work

- Further investigations into the cabbage white butterfly wing structure and its contributions to light manipulations. A full 3D simulated model would be benifitial as well as synthetic materials utilising nanocarbon rods and beads to achieve similar structures and power to weight ratios.
- Differently shaped optics could be tested for use as conjugate refractive reflective optics and their associated benefits.
- The reflectance spectra of solar cells and optics used could be measured at increasing angles of incidence.
- Prototypes of the ultrahigh concentrator design can be built with different quality optics and the performance weighed against the costs saved.

Bibliography

[1] G. R. Timilsina, L. Kurdgelashvili, and P. a. Narbel, “Solar energy: Markets, economics and policies,” *Renew. Sustain. Energy Rev.*, vol. 16, no. 1, pp. 449–465, Jan. 2012.

[2] P. Perez-Higueras and E. F. Fernandez, *High Concentrator Photovoltaics: Fundamentals, Engineering and Power Plants*, 1st ed. Jaen: Springer International Publishing, 2015.

[3] A. Rabl and P. Bendt, “Effect of Circumsolar Radiation on Performance of Focusing Collectors,” *Journal of Solar Energy Engineering*, vol. 104. p. 237, 1982.

[4] L. L. Vant-Hull, “Concentrator Optics,” in *Solar Power Plants: Fundamentals, Technology, Systems, Economics*, C.-J. Winter, R. L. Sizmann, and L. L. Vant-Hull, Eds. Berlin, Heidelberg: Springer-Verlag Berlin Heidelberg, 1991, pp. 84–133.

[5] A. Luque and S. Hegedus, *Handbook of Photovoltaic Science*. England: John Wiley & Sons Ltd, 2003.

[6] R. Winston, J. Miñano, and P. Benitez, *Nonimaging optics*. London: Elsevier, 2005.

[7] J. Chaves, *Introduction to nonimaging optics*. CRC Press, 2008.

[8] W. Shockley and H. J. Queisser, “Detailed balance limit of efficiency of p-n junction solar cells,” *J. Appl. Phys.*, vol. 32, pp. 510–519, 1961.

[9] E. Cartlidge, “Bright Outlook for Solar Cells,” *Physics World*, 2007.

[10] T. M. Razykov, C. S. Ferekides, D. Morel, E. Stefanakos, H. S. Ullal, and H. M. Upadhyaya, “Solar photovoltaic electricity: Current status and future prospects,” *Sol. Energy*, vol. 85, no. 8, pp. 1580–1608, 2011.

[11] National Renewable Energy Laboratory (NREL) - National Center for Photovoltaics, “Research Cell Record Efficiency Chart,” 2016. [Online]. Available: http://www.nrel.gov/pv/assets/images/efficiency_chart.jpg. [Accessed: 22-Nov-2016].

[12] H. Doeleman, “Limiting and realistic efficiencies of multi-junction solar cells,” *Photonic Mater.*, 2012.

[13] A. Betz, “Introduction to the Theory of Flow Machines,” *Introd. to Theory Flow Mach.*, pp. 167–174, 1966.

[14] K. J. Weber, V. Everett, P. N. K. Deenapanray, E. Franklin, and a. W. Blakers, “Modeling of static concentrator modules incorporating lambertian or v-groove rear reflectors,” *Sol. Energy Mater. Sol. Cells*, vol. 90, no. 12, pp. 1741–1749, Jul. 2006.

[15] R. Tang and X. Liu, “Optical performance and design optimization of V-trough concentrators for photovoltaic applications,” *Sol. Energy*, vol. 85, no. 9, pp. 2154–2166, Sep. 2011.

[16] K. Araki, M. Kondo, H. Uommi, and M. Yamaguchi, “Experimental proof and theoretical analysis on effectiveness,” in *3rd World Conference on Photovoltaic Energy Conversion*, 2003, pp. 853–856.

[17] K. Araki, R. Leutz, M. Kondo, A. Akisawa, T. Kashiwagi, M. Yamaguchi, and M. Germany, “Development of a metal homogenizer for concentrator

monolithic multi-junction-cells," in *Conference Record of the Twenty-Ninth IEEE Photovoltaic Specialists Conference, 2002.*, 2002, pp. 1572–1575.

[18] R. Winston, J. C. Miñano, P. Benítez, N. Shatz, and J. C. Bortz, *Nonimaging Optics*. Elsevier, 2005.

[19] J. M. Gordon, D. Feuermann, and P. Young, "Unfolded aplanats for high-concentration photovoltaics," *Opt. Lett.*, vol. 33, no. 10, p. 1114, May 2008.

[20] L. Fu, R. Leutz, and H. P. Annen, "Secondary optics for Fresnel lens solar concentrators," in *SPIE 7785, Nonimaging Optics: Efficient Design for Illumination and Solar Concentration VII*, 2010, p. 778509.

[21] R. Tang and J. Wang, "A note on multiple reflections of radiation within CPCs and its effect on calculations of energy collection," *Renew. Energy*, vol. 57, pp. 490–496, Sep. 2013.

[22] N. El Gharbi, H. Derbal, S. Bouaichaoui, and N. Said, "A comparative study between parabolic trough collector and linear Fresnel reflector technologies," *Energy Procedia*, vol. 6, pp. 565–572, Jan. 2011.

[23] R. Abbas, M. J. Montes, M. Piera, and J. M. Martínez-Val, "Solar radiation concentration features in Linear Fresnel Reflector arrays," *Energy Convers. Manag.*, vol. 54, no. 1, pp. 133–144, Feb. 2012.

[24] R. Abbas, J. Muñoz-Antón, M. Valdés, and J. M. Martínez-Val, "High concentration linear Fresnel reflectors," *Energy Convers. Manag.*, vol. 72, pp. 60–68, Aug. 2013.

[25] Q. C. Murphree, "A point focusing double parabolic trough concentrator," *Sol. Energy*, vol. 70, no. 2, pp. 85–94, Jan. 2001.

[26] D. Canavarro, J. Chaves, and M. Collares-Pereira, "New Optical Designs for Large Parabolic Troughs," *Energy Procedia*, vol. 49, pp. 1279–1287, 2014.

[27] M. Collares-Pereira, J. M. Gordon, A. Rabl, and R. Winston, "High concentration two-stage optics for parabolic trough solar collectors with tubular absorber and large rim angle," *Solar Energy*, vol. 47. pp. 457–466, 1991.

[28] K. Riffelmann, T. Richert, P. Nava, and A. Schweitzer, "Ultimate Trough® – A Significant Step towards Cost-competitive CSP," *Energy Procedia*, vol. 49, pp. 1831–1839, 2014.

[29] D. Canavarro, J. Chaves, and M. Collares-Pereira, "New second-stage concentrators (XX SMS) for parabolic primaries; Comparison with conventional parabolic trough concentrators," *Sol. Energy*, vol. 92, pp. 98–105, Jun. 2013.

[30] F. Languy, K. Fleury, C. Lenaerts, J. Loicq, D. Regaert, T. Thibert, and S. Habraken, "Flat Fresnel doublets made of PMMA and PC: combining low cost production and very high concentration ratio for CPV.," *Opt. Express*, vol. 19 Suppl 3, no. May, pp. A280-94, May 2011.

[31] P. Benítez, J. C. Miñano, P. Zamora, R. Mohedano, A. Cvetkovic, M. Buljan, J. Chaves, and M. Hernández, "High performance Fresnel-based photovoltaic concentrator.," *Opt. Express*, vol. 18, pp. A25–A40, 2010.

[32] X. Li, Y. J. Dai, Y. Li, and R. Z. Wang, "Comparative study on two novel intermediate temperature CPC solar collectors with the U-shape evacuated tubular absorber," *Sol. Energy*, vol. 93, pp. 220–234, Jul. 2013.

[33] T. Waritanant, S. Boonruang, and T.-Y. Chung, "High angular tolerance thin profile solar concentrators designed using a wedge prism and diffraction

grating," *Sol. Energy*, vol. 87, pp. 35–41, Jan. 2013.

[34] W. G. J. H. M. van Sark, K. W. J. Barnham, L. H. Slooff, A. J. Chatten, A. Büchtemann, A. Meyer, S. J. McCormack, R. Koole, D. J. Farrell, R. Bose, E. E. Bende, A. R. Burgers, T. Budel, J. Quilitz, M. Kennedy, T. Meyer, C. D. M. Donegá, A. Meijerink, and D. Vanmaekelbergh, "Luminescent Solar Concentrators--a review of recent results.," *Opt. Express*, vol. 16, pp. 21773–21792, 2008.

[35] G. A. Barron-Gafford, R. L. Minor, N. A. Allen, A. D. Cronin, A. E. Brooks, and M. A. Pavao-Zuckerman, "The Photovoltaic Heat Island Effect: Larger solar power plants increase local temperatures," *Sci. Rep.*, vol. 6, no. October, p. 35070, 2016.

[36] R. R. Hernandez, S. B. Easter, M. L. Murphy-Mariscal, F. T. Maestre, M. Tavassoli, E. B. Allen, C. W. Barrows, J. Belnap, R. Ochoa-Hueso, S. Ravi, and M. F. Allen, "Environmental impacts of utility-scale solar energy," *Renew. Sustain. Energy Rev.*, vol. 29, pp. 766–779, 2014.

[37] B. R. Burg, P. Ruch, S. Paredes, and B. Michel, "Placement and efficiency effects on radiative forcing of solar installations," 2015, p. 90001.

[38] B. R. Burg, A. Selviaridis, S. Paredes, and B. Michel, "Ecological and Economical Advantages of Efficient Solar Systems," in *CPV-10*, 2014, no. 2, pp. 317–320.

[39] D. A. Baharoon, H. A. Rahman, W. Z. W. Omar, and S. O. Fadhl, "Historical development of concentrating solar power technologies to generate clean electricity efficiently – A review," *Renew. Sustain. Energy Rev.*, vol. 41, pp. 996–1027, 2015.

[40] K. Branker, M. J. M. Pathak, and J. M. Pearce, "A review of solar photovoltaic levelized cost of electricity," *Renew. Sustain. Energy Rev.*, vol. 15, no. 9, pp. 4470–4482, Dec. 2011.

[41] R. N. Wilson, *Reflecting Telescope Optics I*. 2004.

[42] B. Norton, *Harnessing Solar Heat*, vol. 18. Dordrecht: Springer Netherlands, 2014.

[43] D. C. Miller and S. R. Kurtz, "Durability of Fresnel lenses: A review specific to the concentrating photovoltaic application," *Sol. Energy Mater. Sol. Cells*, vol. 95, no. 8, pp. 2037–2068, Aug. 2011.

[44] R. Leutz and A. Suzuki, *Nonimaging Fresnel Lenses: Design and Performance of Solar Concentrators*. Springer Science & Business Media, 2001.

[45] N. Yeh, "Analysis of spectrum distribution and optical losses under Fresnel lenses," *Renew. Sustain. Energy Rev.*, vol. 14, no. 9, pp. 2926–2935, 2010.

[46] W. T. Xie, Y. J. Dai, R. Z. Wang, and K. Sumathy, "Concentrated solar energy applications using Fresnel lenses: A review," *Renewable and Sustainable Energy Reviews*, vol. 15. pp. 2588–2606, 2011.

[47] C. Silvi, "The Pioneering Work on Linear Fresnel Reflector Concentrators (LFC's) in Italy," 2009.

[48] D. Chemisana and T. Mallick, "Building Integrated Concentrated Solar Systems," in *Solar Energy Sciences and Engineering Applications*, 1st ed., N. Enteria and A. Akbarzadeh, Eds. CRC Press, 2014, pp. 545–788.

[49] S. Suman, M. K. Khan, and M. Pathak, "Performance enhancement of solar

collectors—A review," *Renew. Sustain. Energy Rev.*, vol. 49, pp. 192–210, 2015.

[50] Z. Jagoo, *Tracking Solar Concentrators*, 1st ed. Springer Nether, 2013.

[51] A. Akisawa, M. Hiramatsu, and K. Ozaki, "Design of dome-shaped non-imaging Fresnel lenses taking chromatic aberration into account," *Sol. Energy*, vol. 86, no. 3, pp. 877–885, Mar. 2012.

[52] K. Araki, H. Nagai, K.-H. Lee, K. Ikeda, and M. Yamaguchi, "Design and Development of Dome-Shaped Fresnel Lens," *IEEE J. Photovoltaics*, vol. 6, no. 5, pp. 1339–1344, Sep. 2016.

[53] F. Languy and S. Habraken, "Nonimaging achromatic shaped Fresnel lenses for ultrahigh solar concentration.," *Opt. Lett.*, vol. 38, no. 10, pp. 1730–2, May 2013.

[54] G. Vallerotto, Victoria, Marta, S. Askins, R. Herrero, C. Dominguez, I. Anton, and G. Sala, "Design and modeling of a cost-effective achromatic Fresnel lens for concentrating photovoltaics," *Opt. Express*, vol. 24, no. 18, pp. 89–92, 2016.

[55] R. Leutz, L. Fu, and H. P. Annen, "Stress in large-area optics for solar concentrators," in *SPIE Solar Energy + Technology*, 2009, pp. 741206-741206–7.

[56] P. Kiefel, T. Hornung, P. Nitz, and H. Reinecke, "Slope-deviation measurement of Fresnel-shaped mold surfaces," *Appl. Opt.*, vol. 55, no. 8, p. 2091, Mar. 2016.

[57] Z. Mathys and P. J. Burchill, "Influence of location on the weathering of acrylic sheet materials," *Polym. Degrad. Stab.*, vol. 55, no. 1, pp. 45–54, Jan. 1997.

[58] D. C. Miller, "Analysis of transmitted optical spectrum enabling accelerated testing of multijunction concentrating photovoltaic designs," *Opt. Eng.*, vol. 50, no. 1, p. 13003, Jan. 2011.

[59] J. E. Greivenkamp, *Field Guide to Geometrical Optics*. 2004.

[60] S. N. Kasarova, N. G. Sultanova, C. D. Ivanov, and I. D. Nikolov, "Analysis of the dispersion of optical plastic materials," *Opt. Mater. (Amst).*, vol. 29, no. 11, pp. 1481–1490, Jul. 2007.

[61] A. Andrady, "Wavelength Sensitivity in Polymer Photodegradation," *Polymer (Guildf).*, vol. 128, pp. 47–94, 1997.

[62] A. L. Andrady, S. H. Hamid, X. Hu, and A. Torikai, "Effects of increased solar ultraviolet radiation on materials," *J. Photochem. Photobiol. B Biol.*, vol. 46, pp. 96–103, 1998.

[63] G. Zhou, J. He, and L. Xu, "Antifogging antireflective coatings on Fresnel lenses by integrating solid and mesoporous silica nanoparticles," *Microporous Mesoporous Mater.*, vol. 176, pp. 41–47, Aug. 2013.

[64] J. C. González, "Design and analysis of a curved cylindrical Fresnel lens that produces high irradiance uniformity on the solar cell," vol. 48, no. 11, pp. 2127–2132, 2009.

[65] J. W. Pan, J. Y. Huang, C. M. Wang, H. F. Hong, and Y. P. Liang, "High concentration and homogenized Fresnel lens without secondary optics element," *Opt. Commun.*, vol. 284, no. 19, pp. 4283–4288, 2011.

[66] L. Jing, H. Liu, H. Zhao, Z. Lu, H. Wu, H. Wang, and J. Xu, "Design of novel

compound fresnel lens for high-performance photovoltaic concentrator," *Int. J. Photoenergy*, vol. 2012, 2012.

[67] Z. Zhuang and F. Yu, "Optimization design of hybrid Fresnel-based concentrator for generating uniformity irradiance with the broad solar spectrum," *Opt. Laser Technol.*, vol. 60, pp. 27–33, Aug. 2014.

[68] I. Palavras and G. C. Bakos, "Development of a low-cost dish solar concentrator and its application in zeolite desorption," *Renew. Energy*, vol. 31, no. 15, pp. 2422–2431, Dec. 2006.

[69] M. Brunotte, A. Goetzberger, and U. Blieske, "Two-stage concentrator permitting concentration factors up to 300x with one-axis tracking," *Sol. Energy*, vol. 56, no. 3, pp. 285–300, Mar. 1996.

[70] M. Dreger, M. Wiesenfarth, A. Kisser, T. Schmid, and A. W. Bett, "Development And Investigation Of A CPV Module With Cassegrain Mirror Optics," in *CPV-10*, 2014.

[71] N. Yehezkel, J. Appelbaum, a. Yogev, and M. Oron, "Losses in a three-dimensional compound parabolic concentrator as a second stage of a solar concentrator," *Sol. Energy*, vol. 51, no. 1, pp. 45–51, Jul. 1993.

[72] K. K. Chong, S. L. Lau, T. K. Yew, and P. C. L. Tan, "Design and development in optics of concentrator photovoltaic system," *Renewable and Sustainable Energy Reviews*, vol. 19. pp. 598–612, 2013.

[73] Y. T. Chen and T. H. Ho, "Design method of non-imaging secondary (NIS) for CPV usage," *Sol. Energy*, vol. 93, pp. 32–42, Jul. 2013.

[74] M. Victoria, C. Dominguez, S. Askins, I. Anton, and G. Sala, "Experimental analysis of a photovoltaic concentrator based on a single reflective stage immersed in an optical fluid," *Prog. Photovoltaics Res. Appl.*, 2013.

[75] M. McDonald, S. Horne, and G. Conley, "Concentrator design to minimize LCOE," vol. 6649, p. 66490B–66490B–11, Sep. 2007.

[76] R. J. Roman, J. E. Peterson, and D. Y. Goswami, "An Off-Axis Cassegrain Optimal Design for Short Focal Length Parabolic Solar Concentrators," *J. Sol. Energy Eng.*, vol. 117, no. 1, p. 51, Feb. 1995.

[77] C. K. Terry, J. E. Peterson, and D. Y. Goswami, "Feasibility of an Iodine Gas Laser Pumped by Concentrated Terrestrial Solar Radiation," *J. Sol. Energy Eng.*, vol. 118, no. 2, p. 136, May 1996.

[78] C. K. Terry, J. E. Peterson, and D. Y. Goswami, "Terrestrial solar-pumped iodine gas laser with minimum threshold concentration requirements," *J. Thermophys. Heat Transf.*, May 2012.

[79] J. C. Miñano, J. C. Gonźlez, and P. Benítez, "A high-gain, compact, nonimaging concentrator: RXI.," *Appl. Opt.*, vol. 34, no. 34, pp. 7850–7856, 1995.

[80] P. Benitez, A. Cvetkovic, R. Winston, and L. Reed, "New High-Concentration Mirror-Based Kohler Integrating Optical Design for Multijunction Solar Cells," in *International Optical Design*, 2006, p. TuD3.

[81] J. P. Ferrer-Rodriguez, E. F. Fernandez, F. Almonacid, and P. Perez-Higueras, "Optical Design of a 4-Off-Axis-Unit Cassegrain Ultra- High CPV Module with Central Receiver," *Opt. Lett.*, vol. 41, no. 0, pp. 3–6, 2016.

[82] G. Zanganeh, R. Bader, a. Pedretti, M. Pedretti, and a. Steinfeld, "A solar

dish concentrator based on ellipsoidal polyester membrane facets," *Sol. Energy*, vol. 86, no. 1, pp. 40–47, Jan. 2012.

[83] R. Leutz and H. Ries, "Microstructured light guides overcoming the two-dimensional concentration limit.," *Appl. Opt.*, vol. 44, pp. 6885–6889, 2005.

[84] J. Nilsson, R. Leutz, and B. Karlsson, "Micro-structured reflector surfaces for a stationary asymmetric parabolic solar concentrator," *Sol. Energy Mater. Sol. Cells*, vol. 91, no. 6, pp. 525–533, Mar. 2007.

[85] P. Schissel, G. Jorgensen, C. Kennedy, and R. Goggin, "Silvered-PMMA reflectors," *Sol. Energy Mater. Sol. Cells*, vol. 33, no. 2, pp. 183–197, Jun. 1994.

[86] C. E. Kennedy, R. V. Smilgys, D. A. Kirkpatrick, and J. S. Ross, "Optical performance and durability of solar reflectors protected by an alumina coating," *Thin Solid Films*, vol. 304, no. 1–2, pp. 303–309, Jul. 1997.

[87] T. Fend, B. Hoffschmidt, G. Jorgensen, H. Kuster, D. Kruger, R. Pitz-Paal, P. Rietbrock, and K. J. Riffelmann, "Comparative assessment of solar concentrator materials," *Sol. Energy*, vol. 74, pp. 149–155, 2003.

[88] G. J. Barber, a. Braem, N. H. Brook, W. Cameron, C. D'Ambrosio, N. Harnew, J. Imong, K. Lessnoff, R. N. Martin, F. C. D. Metlica, R. C. Romeo, and D. Websdale, "Development of lightweight carbon-fiber mirrors for the RICH 1 detector of LHCb," *Nucl. Instruments Methods Phys. Res. Sect. A Accel. Spectrometers, Detect. Assoc. Equip.*, vol. 593, no. 3, pp. 624–637, Aug. 2008.

[89] R. Bader, P. Haueter, a. Pedretti, and a. Steinfeld, "Optical Design of a Novel Two-Stage Solar Trough Concentrator Based on Pneumatic Polymeric Structures," *J. Sol. Energy Eng.*, vol. 131, no. 3, p. 31007, 2009.

[90] S. Guo, G. Zhang, L. Li, W. Wang, and X. Zhao, "Effect of materials and modelling on the design of the space-based lightweight mirror," *Mater. Des.*, vol. 30, no. 1, pp. 9–14, Jan. 2009.

[91] L. Yin and H. Huang, "Brittle materials in nano-abrasive fabrication of optical mirror-surfaces," *Precis. Eng.*, vol. 32, pp. 336–341, 2008.

[92] F. Z. Fang, X. D. Zhang, a. Weckenmann, G. X. Zhang, and C. Evans, "Manufacturing and measurement of freeform optics," *CIRP Ann. - Manuf. Technol.*, vol. 62, no. 2, pp. 823–846, 2013.

[93] G. S. Lodha, K. Yamashita, H. Kunieda, Y. Tawara, J. Yu, Y. Namba, and J. M. Bennett, "Effect of surface roughness and subsurface damage on grazing-incidence x-ray scattering and specular reflectance.," *Appl. Opt.*, vol. 37, no. 22, pp. 5239–5252, 1998.

[94] A. Duparré, J. Ferre-Borrull, S. Gliech, G. Notni, J. Steinert, and J. M. Bennett, "Surface characterization techniques for determining the root-mean-square roughness and power spectral densities of optical components.," *Appl. Opt.*, vol. 41, no. 1, pp. 154–171, 2002.

[95] B. P. W. Mayne and a M. Asce, "Relation Between Surface Roughness and Specular Reflectance at Normal Incidence," vol. 106, no. November 1980, 1981.

[96] F. Languy, C. Lenaerts, J. Loicq, T. Thibert, and S. Habraken, "Performance of solar concentrator made of an achromatic Fresnel doublet measured with a continuous solar simulator and comparison with a singlet," *Sol. Energy Mater.*

Sol. Cells, vol. 109, pp. 70–76, Feb. 2013.

[97] N. Sellami and T. K. Mallick, “Optical efficiency study of PV Crossed Compound Parabolic Concentrator,” *Appl. Energy*, vol. 102, pp. 868–876, Feb. 2013.

[98] G.-L. Dai, X.-L. Xia, C. Sun, and H.-C. Zhang, “Numerical investigation of the solar concentrating characteristics of 3D CPC and CPC-DC,” *Sol. Energy*, vol. 85, no. 11, pp. 2833–2842, Nov. 2011.

[99] T. Cooper, F. Dähler, G. Ambrosetti, A. Pedretti, and A. Steinfeld, “Performance of compound parabolic concentrators with polygonal apertures,” *Sol. Energy*, vol. 95, pp. 308–318, Sep. 2013.

[100] Y. Su, G. Pei, S. B. Riffat, and H. Huang, “Radiance/Pmap simulation of a novel lens-walled compound parabolic concentrator (lens-walled CPC),” *Energy Procedia*, vol. 14, pp. 572–577, Jan. 2012.

[101] Y. Su, S. B. Riffat, and G. Pei, “Comparative study on annual solar energy collection of a novel lens-walled compound parabolic concentrator (lens-walled CPC),” *Sustain. Cities Soc.*, vol. 4, pp. 35–40, Oct. 2012.

[102] L. Guiqiang, P. Gang, S. Yuehong, J. Jie, and S. B. Riffat, “Experiment and simulation study on the flux distribution of lens-walled compound parabolic concentrator compared with mirror compound parabolic concentrator,” *Energy*, vol. 58, pp. 398–403, Sep. 2013.

[103] I. M. Saleh Ali, T. S. O’Donovan, K. S. Reddy, and T. K. Mallick, “An optical analysis of a static 3-D solar concentrator,” *Sol. Energy*, vol. 88, pp. 57–70, Feb. 2013.

[104] I. Ali, K. S. Reddy, and T. K. Mallick, “Optical performance of circular and elliptical 3-D static solar concentrators,” *Natl. Sol.*, pp. 1–8, 2010.

[105] F. Muhammad-Sukki, S. H. Abu-Bakar, R. Ramirez-Iniguez, S. G. McMeekin, B. G. Stewart, N. Sarmah, T. K. Mallick, A. B. Munir, S. H. Mohd Yasin, and R. Abdul Rahim, “Mirror symmetrical dielectric totally internally reflecting concentrator for building integrated photovoltaic systems,” *Appl. Energy*, vol. 113, pp. 32–40, Jan. 2014.

[106] T. Cooper, G. Ambrosetti, A. Pedretti, and A. Steinfeld, “Surpassing the 2D limit : a 600x high-concentration PV collector based on a parabolic trough with tracking secondary optics,” *Energy Procedia*, vol. 57, pp. 285–290, 2014.

[107] N. Sellami and T. K. Mallick, “Optical characterisation and optimisation of a static Window Integrated Concentrating Photovoltaic system,” *Sol. Energy*, vol. 91, pp. 273–282, May 2013.

[108] N. Sellami, T. K. Mallick, and D. A. McNeil, “Optical characterisation of 3-D static solar concentrator,” in *Energy Conversion and Management*, 2012, vol. 64, pp. 579–586.

[109] I. Ali, “Design and Analysis of a Novel 3-D Elliptical Hyperboloid Static Solar Concentrator for Process Heat Applications Submitted by Institute of Mechanical , Process and Energy Engineering School of Engineering and Physical Sciences Edinburgh , United Kingdom,” 2013.

[110] M. Victoria, C. Domínguez, I. Antón, and G. Sala, “Comparative analysis of different secondary optical elements for aspheric primary lenses,” *Opt. Express*, vol. 17, no. 8, pp. 6487–6492, 2009.

[111] B. M. Coughenour, T. Stalcup, B. Wheelwright, A. Geary, K. Hammer, and R.

Angel, “Dish-based high concentration PV system with Köhler optics,” *Opt. Express*, vol. 22, no. S2, p. A211, Jan. 2014.

[112] S. Askins, M. Victoria, R. Herrero, C. Domínguez, I. Antón, G. Sala, S. Askins, M. Victoria, R. Herrero, C. Domínguez, I. Antón, and G. Sala, “Hybrid dome with total internal reflector as a secondary optical element for CPV Hybrid Dome with Total Internal Reflector as a Secondary Optical Element for CPV,” in *CPV-12*, 2016, vol. 1766.

[113] M. Victoria, S. Askins, C. Domínguez, I. Antón, and G. Sala, “Durability of dielectric fluids for concentrating photovoltaic systems,” *Sol. Energy Mater. Sol. Cells*, vol. 113, no. June, pp. 31–36, 2013.

[114] E. Vahanian, A. Yavrian, R. Gilbert, and T. Galstian, “Enhancement of the electrical response in high concentrating photovoltaic systems by antireflective coatings based on silica nanoparticles,” *Sol. Energy*, vol. 137, pp. 273–280, 2016.

[115] A. Goldstein and J. M. Gordon, “Tailored solar optics for maximal optical tolerance and concentration,” *Sol. Energy Mater. Sol. Cells*, vol. 95, no. 2, pp. 624–629, Feb. 2011.

[116] A. Yavrian, S. Tremblay, M. Levesque, and R. Gilbert, “How to increase the efficiency of a high concentrating PV (HCPV) by increasing the acceptance angle to ±3.2°,” in *AIP -9th International Conference on Concentrator Photovoltaic Systems (CPV-9)*, 2013, vol. 1556, pp. 197–200.

[117] N. Sarmah, B. S. Richards, and T. K. Mallick, “Evaluation and optimization of the optical performance of low-concentrating dielectric compound parabolic concentrator using ray-tracing methods.,” *Appl. Opt.*, vol. 50, no. 19, pp. 3303–10, Jul. 2011.

[118] H. Baig, N. Sellami, D. Chemisana, J. Rosell, and T. K. Mallick, “Performance analysis of a dielectric based 3D building integrated concentrating photovoltaic system,” *Sol. Energy*, vol. 103, pp. 525–540, 2014.

[119] P. Kotsidas, E. Chatzi, and V. Modi, “Stationary nonimaging lenses for solar concentration.,” *Appl. Opt.*, vol. 49, pp. 5183–5191, 2010.

[120] A. R. Peaker and V. P. Markevich, “Photovoltaic Power Generation: the Impact of Solar Energy,” in *Advances in Electronic Materials*, E. Kasper, H.-J. Mussig, and H. G. Grimmeiss, Eds. Stafa-Zuerich: Trans Tech Publications Ltd., 2009.

[121] F. Duerr, Y. Meuret, and H. Thienpont, “Tracking integration in concentrating photovoltaics using laterally moving optics.,” *Opt. Express*, vol. 19 Suppl 3, no. May, pp. A207-18, May 2011.

[122] S. Bouchard and S. Thibault, “Planar waveguide concentrator used with a seasonal tracker,” *Applied Optics*, vol. 51. p. 6848, 2012.

[123] O. Selimoglu and R. Turan, “Exploration of the horizontally staggered light guides for high concentration CPV applications.,” *Opt. Express*, vol. 20, no. 17, pp. 19137–47, Aug. 2012.

[124] I. Fujieda, K. Arizono, and Y. Okuda, “Design considerations for a concentrator photovoltaic system based on a branched planar waveguide,” *J. Photonics Energy*, vol. 2, p. 21807, 2012.

[125] Y. J. Jung, D. Park, S. Koo, S. Yu, and N. Park, “Metal slit array Fresnel lens for wavelength-scale optical coupling to nanophotonic waveguides.,” *Opt. Express*, vol. 17, pp. 18852–18857, 2009.

[126] R. Tang, M. Wu, Y. Yu, and M. Li, “Optical performance of fixed east-west aligned CPCs used in China,” *Renew. Energy*, vol. 35, pp. 1837–1841, 2010.

[127] A. A. Earp, G. B. Smith, P. D. Swift, and J. Franklin, “Maximising the light output of a Luminescent Solar Concentrator,” *Sol. Energy*, vol. 76, no. 6, pp. 655–667, Jan. 2004.

[128] D. C. Lainé, “Transmissive, non-imaging Fresnel types of reflective radiation concentrators revisited,” *Opt. Laser Technol.*, vol. 54, pp. 274–283, Dec. 2013.

[129] M. Stefancich, A. Zayan, M. Chiesa, S. Rampino, D. Roncati, L. Kimerling, and J. Michel, “Single element spectral splitting solar concentrator for multiple cells CPV system,” *Optics Express*, vol. 20. p. 9004, 2012.

[130] W. T. Welford and R. Winston, *High Collection Nonimaging Optics*. Elsevier, 1989.

[131] C. Michel, J. Loicq, F. Languy, and S. Habraken, “Optical study of a solar concentrator for space applications based on a diffractive/refractive optical combination,” *Sol. Energy Mater. Sol. Cells*, vol. 120, pp. 183–190, 2014.

[132] Y. Liu, R. Huang, and C. K. Madsen, “Design of a lens-to-channel waveguide system as a solar concentrator structure,” *Opt. Express*, vol. 22, no. March, p. A198, 2014.

[133] J. H. Karp, E. J. Tremblay, J. M. Hallas, and J. E. Ford, “Orthogonal and secondary concentration in planar micro-optic solar collectors.,” *Opt. Express*, vol. 19 Suppl 4, pp. A673–A685, 2011.

[134] W.-C. Shieh and G.-D. Su, “Compact Solar Concentrator Designed by Minilens and Slab Waveguide,” *Spie*, vol. 8108, no. 1, p. 81080H–81080H–9, 2011.

[135] S.-C. Chu, H.-Y. Wu, and H.-H. Lin, “Planar lightguide solar concentrator,” in *SPIE*, 2012, vol. 8438, no. 1, pp. 843810-843810–7.

[136] J. H. Karp and J. E. Ford, “Planar micro-optic solar concentration using multiple imaging lenses into a common slab waveguide,” *SPIE Sol. Energy+ Technol.*, vol. 7407, p. 74070D–74070D–11, 2009.

[137] M. D. Hughes, C. Maher, D.-A. Borca-Tasciuc, D. Polanco, and D. Kaminski, “Performance comparison of wedge-shaped and planar luminescent solar concentrators,” *Renew. Energy*, vol. 52, pp. 266–272, Apr. 2013.

[138] C. Atkinson, C. L. Sansom, H. J. Almond, and C. P. Shaw, “Coatings for concentrating solar systems – A review,” *Renew. Sustain. Energy Rev.*, vol. 45, pp. 113–122, May 2015.

[139] K. Valleti, D. Murali Krishna, and S. V. Joshi, “Functional multi-layer nitride coatings for high temperature solar selective applications,” *Sol. Energy Mater. Sol. Cells*, vol. 121, pp. 14–21, 2014.

[140] N. Li, M. Cao, and C. Hu, “Review on the latest design of graphene-based inorganic materials,” *Nanoscale*, vol. 4, p. 6205, 2012.

[141] D. Jariwala, V. K. Sangwan, L. J. Lauhon, T. J. Marks, and M. C. Hersam, “Carbon nanomaterials for electronics, optoelectronics, photovoltaics, and sensing.,” *Chem. Soc. Rev.*, vol. 42, pp. 2824–60, 2013.

[142] L. Nicole, C. Laberty-Robert, L. Rozes, and C. Sanchez, “Hybrid materials science: a promised land for the integrative design of multifunctional materials.,” *Nanoscale*, vol. 6, pp. 6267–92, 2014.

[143] D. Avnir, “Organic Chemistry within Ceramic Matrixes: Doped Sol-Gel

Materials," *Acc. Chem. Res.*, vol. 28, no. 8, pp. 328–334, Aug. 1995.

[144] F. Gelman, J. Blum, and D. Avnir, "One-pot sequences of reactions with sol-gel entrapped opposing reagents: an enzyme and metal-complex catalysts.," *J. Am. Chem. Soc.*, vol. 124, no. 48, pp. 14460–3, Dec. 2002.

[145] D. Levy, S. Einhorn, and D. Avnir, "Applications of the sol-gel process for the preparation of photochromic information-recording materials: synthesis, properties, mechanisms," *J. Non. Cryst. Solids*, vol. 113, pp. 137–145, 1989.

[146] D. Avnir, V. R. Kaufman, and R. Reisfeld, "Organic fluorescent dyes trapped in silica and silica-titania thin films by the sol-gel method. Photophysical, film and cage properties," *J. Non. Cryst. Solids*, vol. 74, no. 2–3, pp. 395–406, Nov. 1985.

[147] C. Sanchez, B. Julián, P. Belleville, and M. Popall, "Applications of hybrid organic–inorganic nanocomposites," *J. Mater. Chem.*, vol. 15, p. 3559, 2005.

[148] K. J. Sanchez Clément, "Hybrid materials themed issue," *Chem. Soc. Rev.*, vol. 40, no. 2, pp. 588–595, 2011.

[149] M. Faustini, L. Nicole, C. Boissière, P. Innocenzi, C. Sanchez, and D. Grosso, "Hydrophobic, antireflective, self-cleaning, and antifogging sol-gel coatings: An example of multifunctional nanostructured materials for photovoltaic cells," *Chem. Mater.*, vol. 22, pp. 4406–4413, 2010.

[150] R. Gupta, *Polymer nanocomposites : handbook*. Boca Raton: CRC Press Taylor & Francis Group, 2010.

[151] M. Faustini, C. Boissière, L. Nicole, and D. Grosso, "From chemical solutions to inorganic nanostructured materials: A journey into evaporation-driven processes," *Chem. Mater.*, vol. 26, pp. 709–723, 2014.

[152] L. Wang, X. Lu, S. Lei, and Y. Song, "Graphene-based polyaniline nanocomposites: preparation, properties and applications," *J. Mater. Chem. A*, vol. 2, p. 4491, 2014.

[153] B. Bhushan, "Biomimetics inspired surfaces for drag reduction and oleophobicity/philicity.," *Beilstein J. Nanotechnol.*, vol. 2, pp. 66–84, Jan. 2011.

[154] P. Fratzl and R. Weinkamer, "Nature's hierarchical materials," *Prog. Mater. Sci.*, vol. 52, pp. 1263–1334, 2007.

[155] R. a. Potyrailo, H. Ghiradella, A. Vertiatchikh, K. Dovidenko, J. R. Cournoyer, and E. Olson, "Morpho butterfly wing scales demonstrate highly selective vapour response," *Nat. Photonics*, vol. 1, no. 2, pp. 123–128, Feb. 2007.

[156] M. Kolle, P. M. Salgard-Cunha, M. R. J. Scherer, F. Huang, P. Vukusic, S. Mahajan, J. J. Baumberg, and U. Steiner, "Mimicking the colourful wing scale structure of the Papilio blumei butterfly.," *Nat. Nanotechnol.*, vol. 5, pp. 511–515, 2010.

[157] P. Vukusic, "Manipulating the flow of light with photonic crystals," *Phys. Today*, vol. 59, pp. 82–83, 2006.

[158] P. Vukusic and J. R. Sambles, "Photonic structures in biology.," *Nature*, vol. 424, pp. 852–855, 2003.

[159] R. Dewan, S. Fischer, V. B. Meyer-Rochow, Y. Özdemir, S. Hamraz, and D. Knipp, "Studying nanostructured nipple arrays of moth eye facets helps to design better thin film solar cells.," *Bioinspir. Biomim.*, vol. 7, no. 1, p. 16003, Mar. 2012.

[160] C. K. Huang, K. W. Sun, and W.-L. Chang, “Efficiency enhancement of silicon solar cells using a nano-scale honeycomb broadband anti-reflection structure.,” *Opt. Express*, vol. 20, no. 1, pp. A85-93, Jan. 2012.

[161] A. R. Parker, “515 million years of structural colour,” *J. Opt. A Pure Appl. Opt.*, vol. 2, no. 6, pp. R15–R28, Nov. 2000.

[162] A. L. Ingram and A. R. Parker, “A review of the diversity and evolution of photonic structures in butterflies, incorporating the work of John Huxley (The Natural History Museum, London from 1961 to 1990).,” *Philos. Trans. R. Soc. Lond. B. Biol. Sci.*, vol. 363, no. 1502, pp. 2465–80, Jul. 2008.

[163] J. Bíró, “Temporal-spatial pattern of true bug assemblies (Heteroptera: gerromorpha, nepomorpha) in lake Balaton,” *Appl. Ecol. Environ. Res.*, vol. 1, pp. 173–181, 2003.

[164] L. P. Biró and P. Lambin, “Nanopatterning of graphene with crystallographic orientation control,” *Carbon*, vol. 48. pp. 2677–2689, 2010.

[165] P. Biro, “Maya Calendar Origins: Monuments, Mythistory, and the Materialization of Time,” *Hispanic American Historical Review*, vol. 89. pp. 323–324, 2009.

[166] S. Berthier, J. Boulenguez, M. Menu, and B. Mottin, “Butterfly inclusions in Van Schrieck masterpieces. Techniques and optical properties,” *Appl. Phys. A Mater. Sci. Process.*, vol. 92, pp. 51–57, 2008.

[167] S. Berthier, E. Charron, and J. Boulenguez, “Morphological structure and optical properties of the wings of Morphidae,” *Insect Sci.*, vol. 13, pp. 145–158, 2006.

[168] J. Boulenguez, S. Berthier, and J. P. Vigneron, “Simulations tools for natural photonic structures,” *Phys. B Condens. Matter*, vol. 394, pp. 217–220, 2007.

[169] A. L. Ingram, O. Deparis, J. Boulenguez, G. Kennaway, S. Berthier, and A. R. Parker, “Structural origin of the green iridescence on the chelicerae of the red-backed jumping spider, Phidippus johnsoni (Salticidae: Araneae),” *Arthropod Struct. Dev.*, vol. 40, pp. 21–25, 2011.

[170] A. J. Smith, C. Wang, D. Guo, C. Sun, and J. Huang, “Repurposing Blu-ray movie discs as quasi-random nanoimprinting templates for photon management.,” *Nat. Commun.*, vol. 5, p. 5517, Jan. 2014.

[171] B. W. Schneider, N. N. Lal, S. Baker-Finch, and T. P. White, “Pyramidal surface textures for light trapping and antireflection in perovskite-on-silicon tandem solar cells,” *Opt. Express*, vol. 22, no. S6, p. A1422, Aug. 2014.

[172] H.-P. Wang, D.-H. Lien, M.-L. Tsai, C.-A. Lin, H.-C. Chang, K.-Y. Lai, and J.-H. He, “Photon management in nanostructured solar cells,” *J. Mater. Chem. C*, vol. 2, p. 3144, 2014.

[173] J. K. Tseng, Y. J. Chen, C. T. Pan, T. T. Wu, and M. H. Chung, “Application of optical film with micro-lens array on a solar concentrator,” *Sol. Energy*, vol. 85, no. 9, pp. 2167–2178, Sep. 2011.

[174] R. H. Siddique, G. Gomard, and H. Hölscher, “The role of random nanostructures for the omnidirectional anti-reflection properties of the glasswing butterfly,” *Nat. Commun.*, vol. 6, p. 6909, 2015.

[175] P. Vukusic, “Structural colour: Elusive iridescence strategies brought to light,” *Curr. Biol.*, vol. 21, 2011.

[176] D. G. Stavenga, H. L. Leertouwer, and B. D. Wilts, “Coloration principles of nymphaline butterflies - thin films, melanin, ommochromes and wing scale stacking.,” *J. Exp. Biol.*, vol. 217, pp. 2171–80, 2014.

[177] H. L. Leertouwer, “Colourful butterfly wings : scale stacks , iridescence and sexual dichromatism of Pieridae,” vol. 67, no. 5, pp. 158–164, 2007.

[178] D. G. Stavenga and K. Arikawa, “Evolution of color and vision of butterflies.,” *Arthropod Struct. Dev.*, vol. 35, no. 4, pp. 307–18, Dec. 2006.

[179] M. D. Shawkey, N. I. Morehouse, and P. Vukusic, “A protean palette: colour materials and mixing in birds and butterflies.,” *J. R. Soc. Interface*, vol. 6 Suppl 2, pp. S221–S231, 2009.

[180] P. Vukusic, R. Sambles, C. Lawrence, and G. Wakely, “Sculpted-multilayer optical effects in two species of Papilio butterfly.,” *Appl. Opt.*, vol. 40, pp. 1116–1125, 2001.

[181] P. Vukusic and I. Hooper, “Directionally controlled fluorescence emission in butterflies.,” *Science*, vol. 310, p. 1151, 2005.

[182] M. a Meyers, P.-Y. Chen, M. I. Lopez, Y. Seki, and A. Y. M. Lin, “Biological materials: a materials science approach.,” *J. Mech. Behav. Biomed. Mater.*, vol. 4, no. 5, pp. 626–657, 2011.

[183] K. Yu, T. Fan, S. Lou, and D. Zhang, “Biomimetic optical materials: Integration of nature’s design for manipulation of light,” *Prog. Mater. Sci.*, vol. 58, no. 6, pp. 825–873, Jul. 2013.

[184] H. Zhou, T. Fan, and D. Zhang, “Biotemplated materials for sustainable energy and environment: current status and challenges.,” *ChemSusChem*, vol. 4, no. 10, pp. 1344–87, Oct. 2011.

[185] D. P. Pulsifer and A. Lakhtakia, “Background and survey of bioreplication techniques.,” *Bioinspir. Biomim.*, vol. 6, no. 3, p. 31001, Sep. 2011.

[186] N. Hayashi, D. Inoue, M. Matsumoto, A. Matsushita, H. Higuchi, Y. Aya, and T. Nakagawa, “High-efficiency thin and compact concentrator photovoltaics with micro-solar cells directly attached to a lens array,” *Opt. Express*, vol. 23, no. 11, p. A594, 2015.

[187] M. Steiner, G. Siefer, T. Schmidt, M. Wiesenfarth, F. Dimroth, and A. W. Bett, “43% Sunlight to Electricity Conversion Efficiency Using CPV,” *IEEE J. Photovoltaics*, vol. 6, no. 4, pp. 1020–1024, 2016.

[188] A. Ritou, P. Voarino, S. Bernardis, T. Hilt, A. Aitmani, C. Dominguez, and M. Baudrit, “Micro-concentrator with a self-assembly process,” in *CPV-12*, 2016, vol. 1766, p. 80005.

[189] H. Piombini, P. Voarino, D. Breider, and F. Lemarchand, “Toward the reflectance measurement of micro components,” *J. Eur. Opt. Soc. Rapid Publ.*, vol. 5, p. 10034s, 2010.

[190] V. Kumar, R. L. Shrivastava, and S. P. Untawale, “Fresnel lens: A promising alternative of reflectors in concentrated solar power,” *Renew. Sustain. Energy Rev.*, vol. 44, pp. 376–390, 2015.

[191] S. Schröder, A. Duparré, L. Coriand, A. Tünnermann, D. H. Penalver, and J. E. Harvey, “Modeling of light scattering in different regimes of surface roughness.,” *Opt. Express*, vol. 19, no. 10, pp. 9820–9835, 2011.

[192] D. Aikens, “Meaningful surface roughness and quality tolerances,” *Int. Opt.*

Des. …, vol. 7652, pp. 765217-765217–7, 2010.

[193] K. H. Guenther, P. G. Wierer, and J. M. Bennett, “Surface roughness measurements of low-scatter mirrors and roughness standards.,” *Appl. Opt.*, vol. 23, no. 21, p. 3820, 1984.

[194] Breault Research Organization, “ASAP Technical Guide: Scattering in ASAP,” 2012. [Online]. Available: http://www.breault.com/sites/default/files/knowledge_base/brotg0922_scatter_1.pdf. [Accessed: 12-Oct-2015].

[195] M. I. Irshid, “V-troughs with High Concentration Ratios for Photovoltaic Concentrator Cells,” *Sol. Cells*, vol. 23, pp. 159–172, 1988.

[196] H. Baig, “Enhancing Performance of Building Integrated Concentrating Photovoltaic systems,” University of Exeter, 2015.

[197] H. Baig, N. Sellami, and T. K. Mallick, “Trapping light escaping from the edges of the optical element in a Concentrating Photovoltaic system,” *Energy Convers. Manag.*, vol. 90, pp. 238–246, 2015.

[198] H. Baig, N. Sarmah, D. Chemisana, J. Rosell, and T. K. Mallick, “Enhancing performance of a linear dielectric based concentrating photovoltaic system using a reflective film along the edge,” *Energy*, vol. 73, no. 14, pp. 177–191, 2014.

[199] Azure Space Solar Power GMBH, “Enhanced Fresnel Assembly - EFA Type: 3C42A – with 10x10mm^2 CPV TJ Solar Cell Application: Concentrating Photovoltaic (CPV) Modules,” 2014.

[200] Y. J. Xu, J. X. Liao, Q. W. Cai, and X. X. Yang, “Preparation of a highly-reflective TiO 2 / SiO 2 / Ag thin film with self-cleaning properties by magnetron sputtering for solar front reflectors,” *Sol. Energy Mater. Sol. Cells*, vol. 113, pp. 7–12, 2013.

[201] N. . Kaushika and K. . Reddy, “Performance of a low cost solar paraboloidal dish steam generating system,” *Energy Convers. Manag.*, vol. 41, no. 7, pp. 713–726, May 2000.

[202] C.-Y. Tsai, “Enhanced irradiance distribution on solar cell using optimized variable-focus-parabolic concentrator,” *Opt. Commun.*, vol. 305, pp. 221–227, Sep. 2013.

[203] L. M. Fraas, *Low-Cost Solar Electric Power*. Cham: Springer International Publishing, 2014.

[204] R. Herrero, C. Domínguez, S. Askins, I. Antón, and G. Sala, “Methodology of quantifying curvature of Fresnel lenses and its effect on CPV module performance,” *Opt. Express*, vol. 23, no. 19, p. A1030, Sep. 2015.

[205] F. Chiadini, V. Fiumara, A. Scaglione, and A. Lakhtakia, “Simulation and analysis of prismatic bioinspired compound lenses for solar cells.,” *Bioinspir. Biomim.*, vol. 5, no. 2, p. 26002, 2010.

[206] F. Chiadini, V. Fiumara, A. Scaglione, and A. Lakhtakia, “Bioinspired pit texturing of silicon solar cell surfaces,” *J. Photonics Energy*, vol. 3, no. 1, p. 34596, 2013.

[207] D. G. Stavenga, M. a Giraldo, and B. J. Hoenders, “Reflectance and transmittance of light scattering scales stacked on the wings of pierid butterflies.,” *Opt. Express*, vol. 14, no. 11, pp. 4880–90, May 2006.

[208] D. G. Stavenga, S. Stowe, K. Siebke, J. Zeil, and K. Arikawa, “Butterfly wing colours: scale beads make white pierid wings brighter.,” *Proc. Biol. Sci.*, vol. 271, no. 1548, pp. 1577–84, Aug. 2004.

[209] M. A. Giraldo and D. G. Stavenga, “Sexual dichroism and pigment localization in the wing scales of Pieris rapae butterflies.,” *Proc. Biol. Sci.*, vol. 274, pp. 97–102, 2007.

[210] M. A. Giraldo and D. G. Stavenga, “Wing coloration and pigment gradients in scales of pierid butterflies,” vol. 37, pp. 118–128, 2008.

[211] N. I. Morehouse, P. Vukusic, and R. Rutowski, “Pterin pigment granules are responsible for both broadband light scattering and wavelength selective absorption in the wing scales of pierid butterflies.,” *Proc. Biol. Sci.*, vol. 274, no. 1608, pp. 359–66, Feb. 2007.

[212] S. Johnsen and E. Widder, “The physical basis of transparency in biological tissue: ultrastructure and the minimization of light scattering,” *J. Theor. Biol.*, vol. 199, no. 2, pp. 181–98, Jul. 1999.

[213] J. B. Kim, C. Il Yeo, Y. H. Lee, S. Ravindran, and Y. T. Lee, “Broadband antireflective silicon nanostructures produced by spin-coated Ag nanoparticles.,” *Nanoscale Res. Lett.*, vol. 9, no. 1, p. 54, Jan. 2014.

[214] Y. M. Song, S. J. Jang, J. S. Yu, and Y. T. Lee, “Bioinspired parabola subwavelength structures for improved broadband antireflection.,” *Small*, vol. 6, no. 9, pp. 984–7, May 2010.

[215] J. W. Leem, K. S. Chung, and J. S. Yu, “Antireflective properties of disordered Si SWSs with hydrophobic surface by thermally dewetted Pt nanomask patterns for Si-based solar cells,” *Curr. Appl. Phys.*, vol. 12, no. 1, pp. 291–298, Jan. 2012.

[216] Y.-F. Huang, S. Chattopadhyay, Y.-J. Jen, C.-Y. Peng, T.-A. Liu, Y.-K. Hsu, C.-L. Pan, H.-C. Lo, C.-H. Hsu, Y.-H. Chang, C.-S. Lee, K.-H. Chen, and L.-C. Chen, “Improved broadband and quasi-omnidirectional anti-reflection properties with biomimetic silicon nanostructures.,” *Nat. Nanotechnol.*, vol. 2, no. 12, pp. 770–4, Dec. 2007.

[217] C. Fei Guo, T. Sun, F. Cao, Q. Liu, and Z. Ren, “Metallic nanostructures for light trapping in energy-harvesting devices,” *Light Sci. Appl.*, vol. 3, no. 4, p. e161, Apr. 2014.

[218] A. J. Sangster, *Electromagnetic Foundations of Solar Radiation Collection*. Cham: Springer International Publishing, 2014.

[219] M. J. Kohane, W. B. Watt, and B. Sciences, “Flight-muscle adenylate pool responses to flight demands and thermal constraints in individual Colias eurytheme (Lepidoptera, pieridae),” *J. Exp. Biol.*, vol. 3154, pp. 3145–3154, 1999.

[220] B. Karlsson and A. Johansson, “Seasonal polyphenism and developmental trade-offs between flight ability and egg laying in a pierid butterfly.,” *Proc. Biol. Sci.*, vol. 275, no. 1647, pp. 2131–6, Sep. 2008.

[221] P. Chai and R. B. Srygley, “The Predation and the Flight, Morphology, and Temperature of Neotropical Rain-Forest Butterflies,” *Am. Nat.*, vol. 135, no. 6, pp. 748–765, 2014.

[222] E. F. Fernández, F. Almonacid, J. A. Ruiz-Arias, and A. Soria-Moya, “Analysis of the spectral variations on the performance of high concentrator photovoltaic

modules operating under different real climate conditions," *Sol. Energy Mater. Sol. Cells*, vol. 127, pp. 179–187, Aug. 2014.

[223] L. Micheli, N. Sarmah, X. Luo, K. S. Reddy, and T. K. Mallick, "Design of A 16-Cell Densely-packed Receiver for High Concentrating Photovoltaic Applications," *Energy Procedia*, vol. 54, pp. 185–198, 2014.

[224] L. Micheli, N. Sarmah, X. Luo, K. S. Reddy, and T. K. Mallick, "Opportunities and challenges in micro- and nano-technologies for concentrating photovoltaic cooling : A review," *Renew. Sustain. Energy Rev.*, vol. 20, pp. 595–610, 2013.

[225] E. E. Perl, W. E. McMahon, J. E. Bowers, and D. J. Friedman, "Design of antireflective nanostructures and optical coatings for next-generation multijunction photovoltaic devices," *Opt. Express*, vol. 22, no. S5, pp. A1243–A1256, 2014.

Appendix

[Article 1]

K. Shanks, S. Senthilarasu, and T. K. Mallick, “Optics for concentrating photovoltaics: Trends, limits and opportunities for materials and design,” *Renew. Sustain. Energy Rev.*, vol. 60, pp. 394–407, Jul. 2016.

Appendix

[Article 1]

K. Shanks, S. Senthilarasu, and T. K. Mallick, “Optics for concentrating photovoltaics: Trends, limits and opportunities for materials and design,” *Renew. Sustain. Energy Rev.*, vol. 60, pp. 394–407, Jul. 2016.

Renewable and Sustainable Energy Reviews 60 (2016) 394–407

Contents lists available at ScienceDirect

Renewable and Sustainable Energy Reviews

journal homepage: www.elsevier.com/locate/rser

Optics for concentrating photovoltaics: Trends, limits and opportunities for materials and design

Katie Shanks *, S. Senthilarasu, Tapas K. Mallick

Environment and Sustainability Institute, University of Exeter Penryn Campus, Penryn TR10 9FE, UK

ARTICLE INFO

Article history:
Received 23 April 2015
Received in revised form
17 August 2015
Accepted 14 January 2016
Available online 6 February 2016

Keywords:
Renewable energy
Solar
Concentrating photovoltaic
Materials
Biomimicry

ABSTRACT

Concentrating photovoltaic (CPV) systems are a key step in expanding the use of solar energy. Solar cells can operate at increased efficiencies under higher solar concentration and replacing solar cells with optical devices to capture light is an effective method of decreasing the cost of a system without compromising the amount of solar energy absorbed. However, CPV systems are still in a stage of development where new designs, methods and materials are still being created in order to reach a low levelled cost of energy comparable to standard silicon based PV systems. This article outlines the different types of concentration photovoltaic systems, their various design advantages and limitations, and noticeable trends. This will include comparisons on materials used, optical efficiency and optical tolerance (acceptance angle). As well as reviewing the recent development in the most commonly used and most established designs such as the Fresnel lens and parabolic trough/dish, novel optics and materials are also suggested. The aim of this review is to provide the reader with an understanding of the many types of solar concentrators and their reported advantages and disadvantages. This review should aid the development of solar concentrator optics by highlighting the successful trends and emphasising the importance of novel designs and materials in need of further research. There is a vast opportunity for solar concentrator designs to expand into other scientific fields and take advantage of these developed resources. Solar concentrator technologies have many layers and factors to be considered when designing. This review attempts to simplify and categorise these layers and stresses the significance of comparing as many of the applicable factors as possible when choosing the right design for an application.

From this review, it has been ascertained that higher concentration levels are being achieved and will likely continue to increase as high performance high concentration designs are developed. Fresnel lenses have been identified as having a greater optical tolerance than reflective parabolic concentrators but more complex homogenisers are being developed for both system types which improve multiple performance factors. Trends towards higher performance solar concentrator designs include the use of micro-patterned structures and attention to detailed design such as tailoring secondary optics to primary optics and vice-versa. There is still a vast potential for what materials and surface structures could be utilised for solar concentrator designs especially if inspiration is taken from biological structures already proven to manipulate light in nature.

Contents

* Corresponding author.
E-mail addresses: kmas201@exeter.ac.uk (K. Shanks), S.Sundaram@exeter.ac.uk (S. Senthilarasu), T.K.Mallick@exeter.ac.uk (T.K. Mallick).

http://dx.doi.org/10.1016/j.rser.2016.01.089

1. Introduction

1.1. The benefits of concentrator photovoltaics and review objectives

The sun delivers 120 petajoules of energy per second to the Earth. In 1 h the sun delivers more energy to Earth than humanity consumes over the course of a year. The ability to harvest this solar energy efficiently and cost effectively however is challenging. For this reason, there is a growing interest in concentrating photovoltaic (CPV) technologies which are systems made up of optical devices that focus light towards decreased areas of photovoltaic (PV) material. In this way the expensive PV material is replaced by more affordable mirrors and/or lenses, reducing the overall cost of the system but maintaining the area of energy captured and the efficiency at which it is converted. Not only can CPV systems be the answer to reducing the cost of solar power but they are more environmentally friendly than regular flat plate PV panels. This is due to two reasons; CPV technology uses less semiconductor components which are made from heavily mined and relatively rare metals, and CPV technology has a smaller impact on the albedo change in an area than flat plate PV panels [1,2]. Burg et al. [1] and Akbari et al. [2] explain this further. Aside from this, the two main advantages of concentrating photovoltaics (CPV) are their ability to reduce system costs and to increase the efficiency limits of solar cells [3].

However, at present it is difficult to produce cost competitive CPV systems in comparison to those of flat plate photovoltaic (PV) [4–6]. More reliable optics of higher concentration levels and lower dependencies on expensive tracking and cooling systems need to be designed. This requires novel structures and materials to be investigated. Secondary optics in particular hold a vast potential for improving the acceptance angle and optical tolerance of a CPV system and there are many more designs and materials yet to be tested.

This literature review aims to identify new routes to developing high performance and reliable optics for solar concentrator applications. To do this, the subject of solar concentrators must first be explained as it stands, and then broadened to justify novel design opportunities. One objective of this review is to give a basis of the most established methods of solar photovoltaic concentrating and group them where possible. By categorising designs effectively, development trends can be seen more clearly and routes for improved devices substantiated. This also requires presenting the advantages and disadvantages of each group of devices which can become very complicated as a solar concentrator's performance depends on multiple factors (Fig. 1). We also aim to outline the design considerations and in particular emphasis the importance of surface structure and material on a concentrator optics performance as shown in Fig. 1. This area of research hence requires us to branch into the materials science where inspiration can often be taken by structures found in nature. Overall, this results in a rather extensive review but one which is necessary to fully appreciate the potential for solar concentrator designs and guide them towards a more comprehensive capacity.

1.2. Concentrator design categorisation

Concentrating photovoltaic systems can be categorised in a variety of ways as shown in Fig. 2. We will provide a simple grouping of these different designs in order to aid the comparison of different research areas and literature. The concentration of a system or optic can be classed as low (<10 suns), medium (10–100 suns), high (100–2000 suns) and ultrahigh (>2000 suns) due to the different solar tracking requirements outlined by Chemisana et al. [7]. The main methods of concentration are; reflective, refractive, luminescent, and total internal reflection (TIR) although the latter is included within the refractive and luminescent types. This paper focuses on reflective and refractive photovoltaic systems. Each type of concentrating photovoltaic system has advantages and disadvantages and it is important to know the application and location to choose the most appropriate design. A concentrator characterisation table is given in Table 1 to help visualise the different basic systems and the many combinations possible.

2. Primary optics

The most common and widely adopted primary design concepts are the Fresnel lens and parabolic mirror (Table 1). These two concentrators differ in a number of ways, allowing them to suit different applications. One important characteristic is their range of concentration. Under normal incidence the maximum concentration ratio achievable on earth is 46,000× [8]. Languy et al. [9] investigated the concentration limits of Fresnel lenses and found the concentration limit to be around 1000× due to

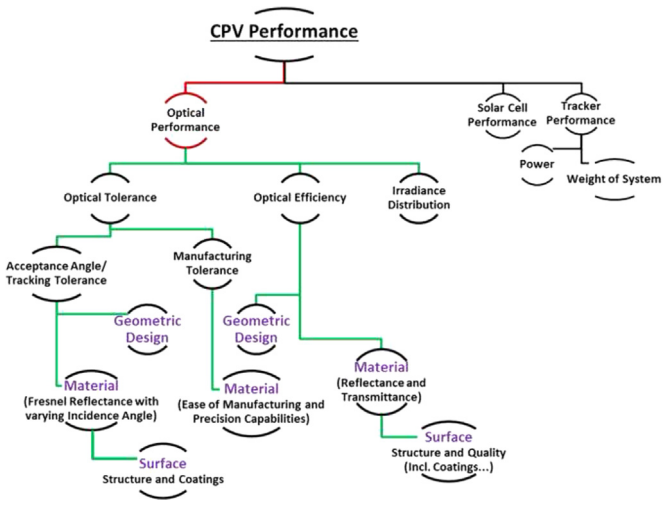

Fig. 1. Factors affecting CPV performance.

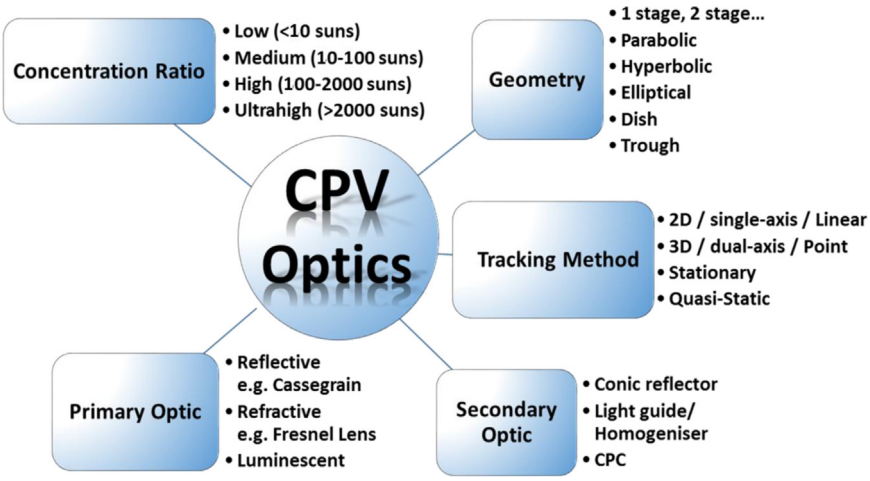

Fig. 2. Concentrator dissemination chart.

chromatic aberration but this could be increased by combining a diverging polycarbonate (PC) lens and a converging PMMA lens to achieve up to ~8500× concentration [8]. Canavarro et al. [10] suggest a singular parabolic trough (with no secondary optics) is suited to concentrations of only ~70×, above which the optical efficiency, acceptance angle and irradiance distribution begin to compromise each other. Various research in this field has extended the concentration of parabolic troughs to ~200× [11–15]. These singular optic designs however still have a severe dependency on optical tolerance, which includes: acceptance angle, solar tracking, manufacturing accuracy, wind load effects and the optical finish quality (see Fig. 1). By matching receiver size to concentrated beam radius, the optical tolerance can be increased for high concentration optics, but not without lowering the topical efficiency due to the Gaussian shape of solar light [16,17]. The use of a second concentrator element is needed to bring the concentration value as close to the limit as possible and relax the demand on the system accuracy. This is the case for both point focus and line focus systems [18]. Due to the increasing importance and complexity of the optical tolerance and acceptance angle of CPV systems, this area is reviewed on its own in section 2.3.

Brunotte et al. investigated the design of a primary parabolic trough with a secondary crossed standard CPC, reaching 214× concentration and concluded ratios exceeding 250× were possible [19]. Canavarro et al. [10] similarly later proposed the use of a new ZZ SMS secondary optic to increase the 70× limit to 213× and achieve an increased acceptance angle. More recently Canavarro et al. [12] have proposed a number of potential parabolic trough concentrator designs with larger aperture areas but still of only medium concentration levels to maintain acceptable acceptance angles.

Fresnel lens designs seemingly can cope better without the aid of a secondary optic in comparison to parabolic mirrors. There are a number of reports describing Fresnel lens systems with somewhat enhanced irradiance uniformity, optical tolerance, efficiency and concentration. This however could be due to the broader interest in Fresnel lenses, accompanied by more ongoing research and ingenuity in designs. Gonzalez et al. [20] proposed a curved cylindrical Fresnel lens with good uniform irradiance but with significant manufacturing problems. Pan et al. [21] designed a Fresnel lens where each pitch focused to a different area upon the receiver, improving uniformity without the aid of a secondary optic. The design however lacked a good acceptance angle (only ~0.3°) [21]. Benitez et al. [22] and Jing et al. [23] have also both designed their own unique Fresnel lenses to focus the light rays to different 'entry' areas of the secondary which has also been tailor designed. Both systems had an improved irradiance distribution, an optical efficiency of >80% and an acceptance angle of ~1.3°. This suggests fitting secondaries and primaries to complement each other is important and that CPV technologies would benefit more from many unique designs, than a few 'standards'. Although moving towards new designs, solar concentrators, especially in a commercial sense, are currently largely in the standards phase. This is however understandable as the technology is still relatively new and the conventional Fresnel lens and parabolic concentrators are the most tested and proven.

Zhenfeng Zhuang et al. [24] more recently also redesigned the ring structure of a Fresnel lens; rearrangement of the rings resulted in a significantly improved irradiance uniformity as shown in Fig. 3. This attention to surface structure again protrudes, this time for a singular optic, as a strong method to improve concentrator performance. By tailoring the macro- or micro-structure (rings in these scenarios) and avoiding continuous surfaces on reflectors, high optical efficiencies and improved irradiance distributions are achievable. Zanganeh et al. [25] developed a solar dish concentrator based on ellipsoidal polyester membrane facets which could reach an optical efficiency of 90% while maintaining a good optical tolerance, and V-groove reflectors have shown optical efficiencies of >80% within systems [26] and helped surpass 2D concentration limits [27]. Nilsson et al. [28] proposed a stationary asymmetric parabolic solar concentrator with a micro-structured reflector surface. Three different micro-structures were tested, the highest optical efficiency obtained was 88% and all distributions had reduced irradiance peaks in comparison to the non-micro-structured counterpart. The optical surface, and hence material, structure and quality evidently plays a key role in concentrator design and performance but expands extensively into the areas of materials science. The subject is hence discussed later in Sections 5 and 6.

3. Secondary optics

The compound parabolic concentrator (CPC) (Fig. 4) is the most studied stationary and secondary optic and is said to be an ideal concentrator in that it works perfectly for all rays within the designed acceptance angle (in 2D geometry) [13,29]. The 3D CPC is also very close to ideal [13]. CPC's can theoretically be used for higher concentration ratios than Fresnel lenses and match the theoretical concentration limit of purely reflective optics at 42,000× [30,31] but their very high aspect-ratio makes them impractical for implementation at >40× [30]. There have been

Table 1
Concentrator characterisation table.

Type	Characterisation by mechanism				Concentration			Shape
	Refractive	Reflective (Coating)	Reflective (TIR)	Luminescent	Low	Medium	High	
Flat reflector [26,164]		X			X	X		
V-trough [42]		X			X	X	X	
Light funnel/homogeniser [13,39-44]	X		X		X			
Linear Fresnel reflector [165-167]		X				X	X	
Parabolic dish/trough [10-15]		X				X	X	
Fresnel lens [9,22]	X		X			X	X	
Compound parabolic concentrator [67]	X				X			
Wedge prism [109]	X	X	X		X			
luminescent/quantum dot [168]	X	X	X	X	X			

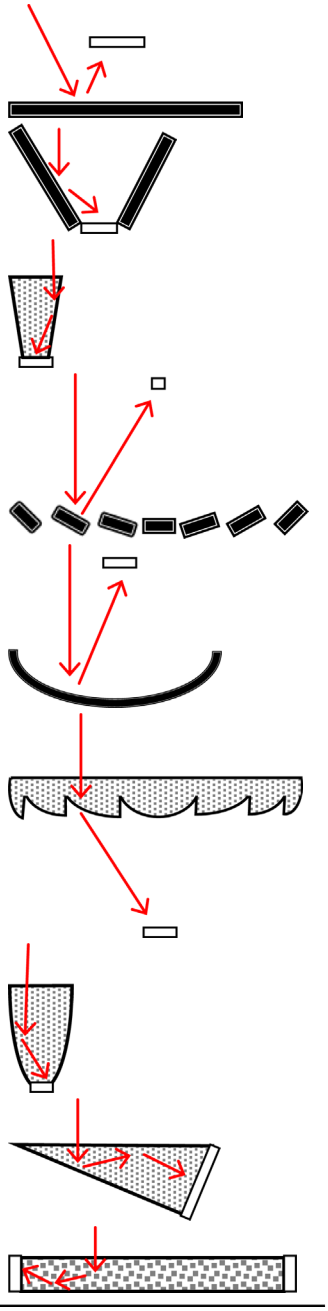

variations in the CPC design to improve different aspects such as concentration ratio and irradiance distribution. Some of these designs include the crossed CPC (CCPC) [32] and similarly the 3D CPC [33], as well as the polygonal CPC designs [34] and the lens walled CPC [35–37] (all shown in Fig. 4). The CPC and many of its variations commonly lack a good irradiance distribution as described by Victoria et al. [38] who compared different secondaries for a primary lens, and by Sellami et al. [32] for the CCPC.

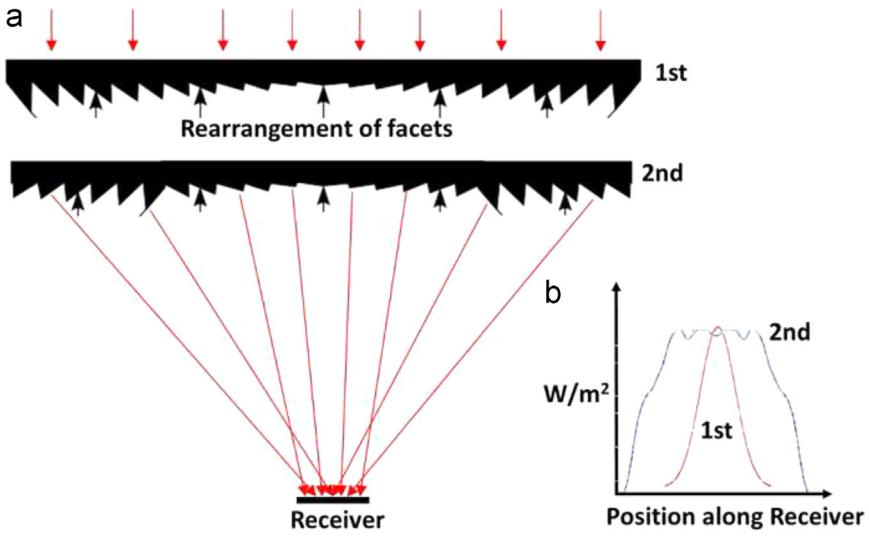

Fig. 3. Improved irradiance distribution of Fresnel lens. By rearranging, or horizontally 'flipping' the Fresnel lens rings (a) an improved, more uniform irradiance distribution is obtained as shown in (b) [4,24].

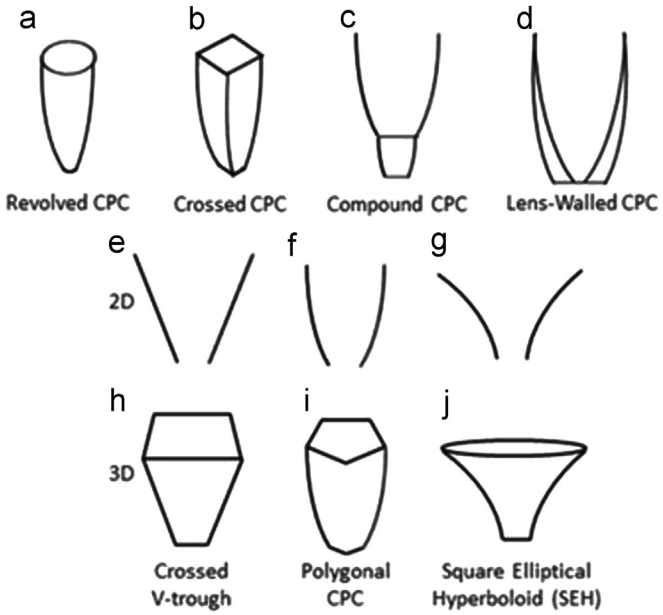

Fig. 4. Variations of CPC: (a) The revolved CPC. (b) The Crossed CPC. (c) The Compound CPC. (d) The Lens-Walled CPC. Examples of 2D profiles and possible 3D transformations: (e) V-trough. (f) CPC. (g) Compound Hyperbolic Concentrator. (h) 3D square aperture V-trough. (i) Polygonal aperture CPC. (j) Hyperboloid with an elliptical entry aperture and square exit aperture [4].

Cooper et al. [34] investigated polygonal CPCs with a varying number of sides and concluded that the cubic CPC was best suited when low reflectance materials are being utilised. This is one example of when the true optimum concentrator design will be an amalgamation of multiple factors, in this case of the efficiency and available resources. The lens-walled CPC reduces the amount of material required and hence has a lower weight than the filled dielectric CPC. It has been proven to have an improved acceptance angle and irradiance distribution than the mirror CPC but has a lower maximum optical efficiency [35–37].

The significance of these differing characteristics is that the location, incident sunlight conditions and tracker options would decide which CPC type suited best. Again, this reinforces the idea that no one design will be absolutely better than another and specific adaptation, although not the easiest, is likely to be the most beneficial procedure in concentrator development. The irradiance distribution uniformity of the CPC seems to be an inherent flaw which again suggests more novel optics need to be investigated. It is however recognised that for many systems this inhomogeneous light and heat distribution has either little effect or is manageable depending on concentration ratio, solar cell specifications and cooling methods. Solar cell structures and cooling technologies are beyond the scope of this review but can influence optic design as significantly as any other factor already discussed.

Light funnels and homogenisers (Fig. 4) have been utilised by many to improve the acceptance angle and irradiance distribution of a system [13,39–44]. These typically take on the shape of an inverted cone or pyramid but there are also elliptical and hyperbolic shapes possible [45–48] such as the square elliptical hyperboloid (SEH) designed by Nazmi et al. [49–51]. Some examples of geometries are shown in Fig. 4. The square elliptical hyperboloid (SEH) based on the ideal trumpet concentrator has an elliptical entry aperture connected to a square exit aperture

via hyperbolic curves [49]. Nazmi et al. concluded a concentration ratio of 6× for the SEH is the optimum for use as a stationary solar concentrator despite its low optical efficiency of 55% but the main use of this type of concentrator is for building integrated photovoltaic applications and its performance as a final stage light funnel has still to be tested. The 4× concentration ratio SEH design has however a higher optical efficiency of 68% [49] and may be more suited in HCPV optical systems if it can improve optical tolerance significantly.

The dome lens typically uses less material than a filled dielectric CPC and can be easier to manufacture [38]. The dome lens and ball lens have proven to have higher acceptance angle values than even the CPC and with improved irradiance distributions [38,52]. Due to the ball lens 3D symmetry, any expansion due to heat should not affect the performance of the ball lens to redirect the light rays to the intended destination. However the weight and support of the ball lens is more difficult to accommodate and may need another optic at the receiver [52]. More research is needed to find the full potential of the ball and dome lenses as secondary optics but there is growing interest in similar geometries for secondary optics [22,23].

Simple plane mirrors can be used to homogenise the distribution of solar flux on to the receiver as discussed by Chong et al. [53] but it has been shown that V-groove reflectors are more effective as mentioned earlier and investigated by Uematsu et al. [54–56] and Weber et al. [26].

4. Overall optical tolerance and acceptance angle

The acceptance angle for high concentration devices such as parabolic dishes and Fresnel lenses, without additional optics is very low [29,57,58] as depicted in Fig. 5. Akisawa et al. [29] proposed a dome-shaped non-imaging Fresnel lens. The tracking tolerance of the proposed lens held efficiencies of ~90% up to an incident angle of 0.4°, then dropped to 80% at 0.6° and then to 10% at 1°. Recently, more focus is given to the acceptance angle and overall tolerance of a CPV system and higher acceptance angles are being achieved. Dreger et al. [59] obtained an acceptance angle of 0.75° without the need of a tertiary optic such as a homogeniser but by instead reducing the path length. ISFOC and GreenMountain studies have HCPV modules with acceptance values of 1.2 degrees and 1.4° respectively [60]. Opsun Technologies claim to have a HCPV system of 380× with an acceptance angle of 3.2° and an optical efficiency of 87% [60]. They also propose they can design a CPV system of 1000× with an acceptance angle 1.9° [60]. This would be a significant achievement in CPV technology if the system has a similarly high optical efficiency and acceptable irradiance distribution as well.

Low concentration optics (LCO) are not as dependent on solar tracking as high concentration systems due to the principle of etendue [41,58]. LCO's can be static or quasi-static and due to their typical high acceptance angle they can often gather direct and diffuse radiation [49,61–63]. This eliminates the need for continuous sun tracking systems and reduces the overall system cost [42,64–66]. For a V-trough concentrator, Tang et al. [42] suggests a concentration less than 2 for a fixed position but for concentrations >2 several tilt adjustments should be made to significantly increase annual solar gain and take full advantage of the systems capabilities. Similarly Li et al. [67] compared a 3× and 6× truncated mirror CPC where the 6× CPC needed adjusted five times a day but the 3× did not. For higher concentrations, the frequency and accuracy of the tracking must increase which tends to lead to very expensive solar trackers for HCPV technologies. New concentrator optics with improved optical tolerance could thus be vastly beneficial to developing high and ultra-high concentrator photovoltaics. There is always an inevitable trade-off required between acceptance angle, optical efficiency and irradiance distribution but recent novel designs are extending when this compromise is required (Fig. 5). Truncation can increase the acceptance angle of a mirror CPC but it also reduces the geometrical concentration ratio [10]. This could be the condition for most optics [27,40,61,68–70] and explains why Fresnel lenses, truncated convex lenses, typically have a higher acceptance angle than parabolic concentrators of a similar concentration ratio. Truncation can also be thought of as a method to reduce the light ray path length within an optical system which has already been said to increase the acceptance angle [4,59]

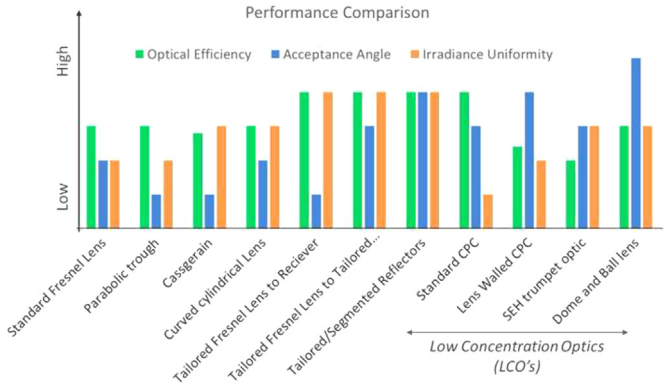

Fig. 5. Performance comparison of various CPV designs on optical efficiency, acceptance angle and irradiance uniformity upon receiver.

Larger opening angles are another option to improve the optical tolerance and reduce the effect of wind induced deviations, manufacturing errors and sagging as reported by Canavarro et al. [10]. This method however can also reduce the optical efficiency and concentration ratio of a system. The acceptance angle, optical efficiency and irradiance uniformity are interlinked and hence systems usually prioritise optical efficiency as shown in Fig. 5. As mentioned earlier the lens walled CPC has an improved acceptance angle in comparison to the refractive CPC but a lower optical efficiency (Fig. 5). There are studies however that suggest a decrease in optical efficiency, to gain higher acceptance angles will still produce more yearly energy output [60,71,72] but this will depend on the specific application and location.

5. Materials

5.1. Reflective

The optical performance of a CPV system is equally dependent on chosen material and surface structure as well as geometrical design. Reflective concentrators for example do not suffer from selective wavelength absorption and dispersion associated with dielectric lenses [73–75]. In terms of the overall desired criteria of a CPV system and its individual components, reflectors technically use less material than conventional lenses as they are not "filled". They are however said to be more prone to manufacturing errors and are less tolerant to slope error than lenses [30]. The advantage of reflective secondary optics is they tend to have increased flux uniformity and colour mixing effects. Dielectric secondaries utilise TIR and can withstand more internal reflections without much loss [76]. For both reflective and refractive optics fewer reflections and stages are always preferred.

The simple polishing of metal can result in a reflective mirror finish but such polished surfaces are very heavy and specific

curved shapes are difficult and therefore expensive to manufacture [77,78]. Reflective film mirrors is a second option but this setup often has low reflectivity when also applied to complex surfaces [78]. Polymer mirror films are a more recent third method to gain reflectance values of >90% but require specially designed structures to gain the appropriate shapes for a given application [25,79]. Vacuum metalizing is therefore the current best option but this process is highly dependent on the material and surface quality it is bonded with in order to ensure a high quality mirror finish [77,80]. Due to the limitations of all these materials and processes it can be concluded that further research into effective reflective materials for CPV applications is required.

Yin et al. [81] studied the surface qualities of different brittle materials used for the nano-abrasive fabrication of optical mirrors. They found that surface roughness in ultra-precision grinding increased with brittleness and hence brittle materials gave a lower reflectance after processing. The principal means of shaping and finishing ceramic optics is abrasive machining with abrasive tools involved with grinding, lapping and polishing. Laser-assisted machining is also an option [81–85]. The high hardness of these materials as well as the inherent brittleness and associated susceptibility to fracture, makes abrasive machining response an important issue in the fabrication of optical mirrors. In general, material responses to machining depend strongly on microstructure and mechanical properties [81].

Options for reflectors include mirrored (silvered) glass, aluminized or polished metals or plastics, including silvered polymers, aluminized polymers and anodised aluminium. Examples of polymer films used include polymethlmethacrylate (PMMA) researched by Schissel et al. [86] and polyethylene terephthalate (PET) film researched by Kennedy et al. [87]. Schissel et al. [86] demonstrated the environmental durability of silvered-PMMA reflectors which have an un-weathered solar reflectance as high as glass reflectors at 97%. The reflectance of freshly deposited silver is roughly 97% (Fig. 6) dropping to 84% after 3 years due to weathering. Soiling appears not to be a major issue affecting the long-term performance of silvered-PMMA reflectors but regular contact (abrasive) cleaning is required to retain efficiencies up to about 93%. Fend et al. [88] researched cheaper lighter high reflectance aluminized sheets which also had good mechanical properties. Fend et al. [89] then later compared various samples of reflectors for optical durability in outdoor weather conditions. SolarBrite 95, a silvered UV-stabilized polyester film, had an un-weathered reflectance of ~92% which dropped below 90% after 2 years. Thin glass mirrors have better durability but are more costly and difficult to handle. Their un-weathered reflectance was 93% to 96% and can last as long as 5 years with 5% reflectance loss. A graph of the standard reflectance spectra of the most common metals is given in Fig. 6 however reflectance spectra will depend on specific manufacturing process, composition of metal and any coatings applied. Reflectance Measurements for a hand polished aluminium dish and a vapour metalized acrylonitrile butadiene styrene (ABS) semi-sphere are also shown in Fig. 6 to show example reflectance spectra for these materials and methods of manufacturing.

Fend et al. [89] also confirmed that different locations and environments affect durability by as much as 2 years difference. Front surfaced aluminized reflectors exhibit adequate optical durability in non-industrial/urban environments but corrode rapidly in atmospheric pollutants. Their un-weathered reflectance was ~90% and dropped by ~4% in 4 years depending on location [89]. Flabeg thick glass mirrors have excellent durability to scratches and surface damage but are still fragile if strained and heavy. Curvature is also difficult and requires slumped glass that is expensive and in some cases can break due to high winds. The un-

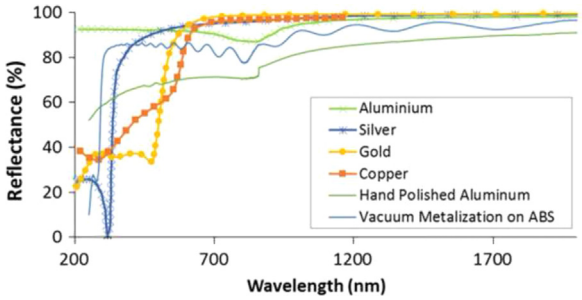

Fig. 6. Standard reflectance spectra for aluminium, silver, gold and copper metal [169]. Graph also shows measured reflectance spectra for a hand polished aluminium dish and a vacuum metalized acrylonitrile butadiene styrene (ABS) semi-sphere.

weathered reflectance was reported as 88–92% and dropped by ~2% depending on location for up to 4–5 years [89].

Mallick et al. [90] designed and experimentally tested a non-imaging asymmetric compound parabolic concentrator with a self-adhesive multi-layer polymer film, which had a quoted specular reflectance of 98% in the visible region. The material was also non-corroding and non-conductive due to it being metal free and also thermally stable up to a continuous temperature of 150° with low levels of shrinkage. The designed system was of 2 × concentration however and its performance under higher concentrations and temperatures needs to be tested. Higher concentration optics as mentioned have a reduced optical tolerance and hence require higher accuracy of optical shape and surface smoothness. Given the limitations of all existing systems, materials and manufacturing processes, further study into possible reflective materials and structures is important.

5.2. Refractive

Fresnel lenses have traditionally been manufactured out of poly (methyl methacrylate) (PMMA) which due to the dispersion curve causes longitudinal chromatic aberration (LCA). The manufacturing processes can include hot-embossing, casting, extruding, laminating, compression-moulding, or injection-moulding thermoplastic PMMA [91]. Sources for refractive lenses and materials are abundant but not all have been tested for CPV applications. Optical or mirror-grade PMMA material may come from the automotive, lighting or skylight industries. Optical-grade poly (dimethyl siloxane) (PDMS), another material increasingly being used, has applicable formulations shared with the aerospace, electronics, and light-emitting diode industries. A heavier lens technology consists of acrylic or silicone facets patterned onto glass as researched in the late 1970s by Egger [92] and Lorenzo et al. [93] in 1979. PMMA and PDMS are at present the preferred medium to be adhered to glass and patterned as a Fresnel lens. Polycarbonate (PC) is sometimes suggested as an alternative to PMMA due to its significantly greater toughness which prevents mechanical fracture and fatigue. However PC is less scratch resistant [94] and has a smaller spectral bandwidth, optical transmittance [95] and suffers more from optical dispersion, chromatic aberration and solar-induced photo oxidation [96–99].

One of the advantages of Fresnel lens designs is that they double as the top cover encasing of the system. In reflective systems a cover glass of high transmittance is used to seal and protect the optics inside but still adds loss to the system. Refractive lens systems effectively eliminate this stage and save around 5–10% light loss. Using the primary lens as the boundary to the outside weather however, adds other demands. PMMA has a transmittance of ~95% (Fig. 7) but high temperature treatments such as calcination, which is a preparation method of antireflective and antifogging coatings, cannot be used on PMMA material. To achieve an anti-reflective

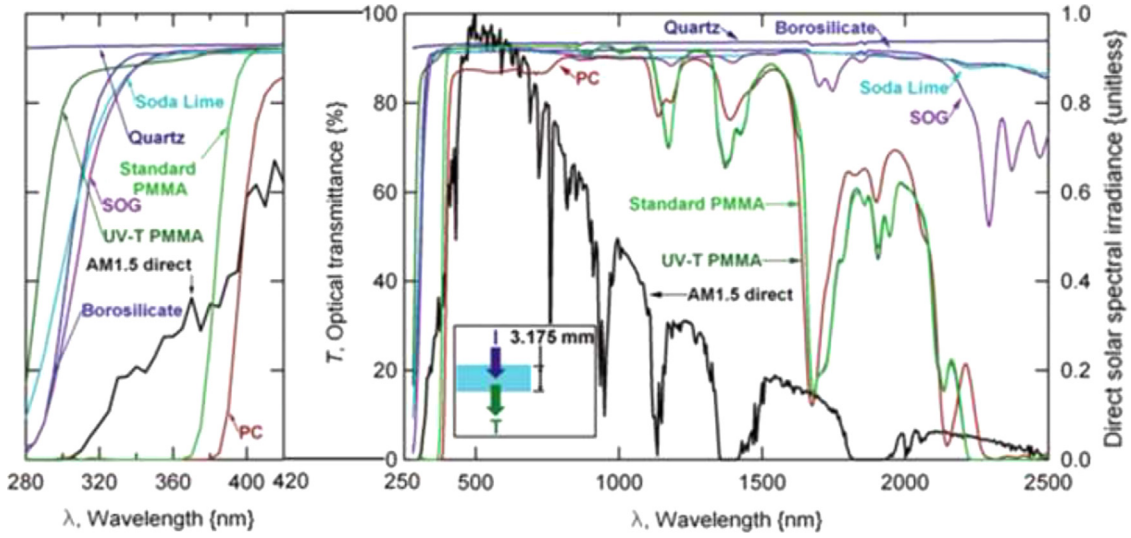

Fig. 7. Optical transmittance spectra of various refractive materials for CPV as measured by Miller et al. [95]. The results for flat-panel PV (soda lime glass) as well as the normalised direct solar spectral irradiance (AM1.5 in ASTM G173) are provided for reference [95].
Reprinted from Ref [80] Copyright 2014 American Chemical Society.

property on PMMA (refractive index = 1.49) one method is to layer coatings of lower refractive indexes. Finding suitable sources of high transmitting but low refractive index materials however is also challenging. Zhou et al. [100] overcame both these difficulties and successfully fabricated antifogging and antireflective coatings on Fresnel lenses while achieving a transmittance of 98.5%. By spin-assembling solid and mesoporous silica nanoparticles, which have voids and result in a lower refractive index, Zhou et al avoided high temperature treatments and produced coatings with a refractive index between 1.32 and 1.40. This reinforces the importance of researching new materials and structures to overcome current CPV challenges and limitations.

Chromatic aberration is a common problem in refractive lenses. Chromatic aberration can be reduced if a domed Fresnel lens geometry is used as carried out by Akisawa et al. [29]. As discussed earlier, Languy et al. [9,30] designed and manufactured an achromatic Fresnel doublet which combines the advantages of plastic lenses without being affected by chromatic aberrations. The achromatic Fresnel doublet is tolerant of manufacturing errors and the dispersion uncertainty of the refractive index, making it suitable in conditions where the temperature can alter the refractive index and shape of the lens. However, a redesign was required to avoid soiling of the outward patterned lens [8]. In the latter study, PMMA and PC were suitable materials at minimising the longitudinal chromatic aberration (LCA) down to 0.1% with a wavelength range of 380–1680 nm along the visible and near-infrared regions [8].

For refractive materials under concentrated light conditions there can be significant temperature and ultraviolet (UV) exposure effects. Miller et al. [95] investigated the photo degradation of CPV modules via accelerated UV testing and analysed the optical transmittance spectra of various CPV refractive materials as shown in Fig. 7. There is however still a great need for research into material durability and performance with time in different environments.

6. Novel optics and materials

6.1. Novel optics

Due to the developing state of CPV technology, a variety of novel designs are still being created and tested. Laine et al. [73] investigated a transmissive non-imaging Fresnel type reflector concentrator made of a continuous reflective spiral (shown in Fig. 8). Stefancich et al. [101] proposed a spectral splitting primary optic which dispersed different wavelengths to different single junction solar cells arranged along the focus plane. This was an alternative to focusing the light to one multijunction solar cell but still obtaining similar overall conversion efficiencies. This has also been proposed elsewhere [102,103].

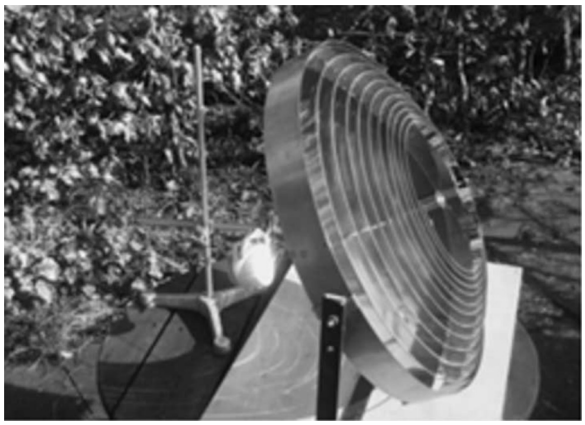

Fig. 8. Photograph of transmissive solar concentrator designed and tested by Laine et al. [73].
Reprinted from Ref. [68] Copyright 2014 American Chemical Society.

Jing et al. [23] coupled the design of a novel Fresnel lens with a novel secondary optic with specific 'entry' points. This attention to detailed design and matching primaries with secondaries can yield simultaneous benefits in concentration ratio, optical efficiency, acceptance angle and uniform distribution which is otherwise very difficult to do effectively. Liu et al. [104] use a novel channel waveguide as a secondary which collects focused light rays from a Fresnel lens array primary. At each focal point there is a microstructure which couples the light into the waveguide. This structure can reach 800× concentration at 89.1% optical efficiency and a 0.7° acceptance angle. Similar designs have been tried and tested by many other researchers [66,105–108]. Jung et al. [70] designed a novel metal slit array Fresnel lens for wavelength scale coupling into a nano-photonic waveguide. Although aimed at a different

application, this paper demonstrates the flexibility of concentrator optics. Waritanant et al. [109] was able to obtain a maximum collection efficiency of 54% for a wedge prism concentrator coupled with a diffraction grating. Huges et al. [110] found that a wedge shaped Luminescent Solar Concentrator (LSC) is able to produce a larger average power density year round under direct illumination than a planar LSC but unusually its optimum orientation was when tilted away from the sun and for this reason may be more suited to latitudes further from the equator. These are just some examples of the novel designs being explored within CPV technologies and how they can vary.

6.2. Novel materials

Some applicable concepts for solar concentrators include: spectrally selective coatings [111–113]; switchable optics which can change from transparent to reflective; anti-reflective and reflective enhancing coatings [111,113]; water filled optics; nanocrystal materials, graphene layers [114,115] as well as other organic and inorganic materials. Much of this technology is researched extensively in the glazing and window industry but less so in the application of CPV's due to the associated high costs of such materials. These materials however hold a lot of potential for advancing solar concentrator technologies, some more than others for specific applications such as building integrated concentrator photovoltaics (BICPV).

Hybrid organic–inorganic (O–I) materials are nano-composite materials with both an inorganic and organic (bio-organic) component. These O–I materials often have impressive characteristics. For example, the Maya Blue pigment is the incorporation of a natural organic dye within the channels of micro-fibrous clay. This hybrid material is of a strong blue colouring which lasts against weathering and bio-degradation to the extent that 12 century old vestiges are still appreciable today [116]. The hybrid materials processed by Avnir et al. [117–120] provided many advances in many diverse fields including optics. There are now many industrially developed hybrid materials including films, membranes, fibres, powders, monoliths and micro (and nano) patterns [121–125]. Graphene has found many uses in a variety of applications due to its tenability and unique properties. It has a very promising optical transparency of 97.7% but more research is required into its use in solar concentrator materials [126].

Nature has a vast range of advanced complex structures which have been studied by many to be replicated and adapted for our own use [127–132]. A clear example is the application of light trapping microstructures, inspired by moth eye facets and other natural light trapping structures, imprinted upon solar cells to enhance light collection and conversion efficiencies [132–134]. Nature has created these structures over billions of years and optimised their functions through evolution. A process which will forever exceed any 'trial and error' optimisation routine carried out by ourselves. Structures within nature often must fulfil multiple functions and hence are usually a complex hierarchal multiscale system. Such structures may hence appear random to us but are in fact a controlled balance of compositions [135–144]. Smith et al. [144] discuss the importance of quasi-random nanostructures found in nature and more recently now also in engineering applications such as blue-ray discs due to their ability to manage photons efficiently. This reinforces the importance of surface structures on optical components and why microstructures significantly effect: reflectance, distribution and acceptance angle [21–24,28,64,100,134,145–147]. Siddique et al. [148] has discovered butterfly wings which have a reflectance of only 2–5% over a range of viewing angles. This high transparency at multiple incidence angles could be very useful for solar concentrator optics, in terms of the cover glass encasing and for lens surfaces to increase the optical efficiency and acceptance angle. The Pieridae butterfly achieves the opposite; it has an interesting grooved tiling upon its white wings with an underlying nipple pattern of pterin beads as shown in Fig. 9. These wings have a surprisingly high reflectance of 78.9% over the 400–950 nm range and are used to concentrate light onto the butterflies' body to help it heat its flight muscles faster [149]. Shanks et al. [149] suggest these wing structures (Fig. 9) can be the basis of a new lightweight, highly reflective materials for concentrator photovoltaics to greatly improve the power to weight ratio of solar concentrator technologies as demonstrated in Fig. 10 [149]. In both cases, the wing structures have a very interesting 'random' or 'chaotic' structure but as mentioned earlier, this may have some underlying complex coherence to it that we have yet to understand.

There are numerous studies into how natural structures, especially insect membranes, can affect light [130,131,150–156]. There are also various bio-replication reviews covering a range of applications [157–160]. However, at present it is an untapped area of research for CPV applications.

6.3. Future outlook and discussion

For concentrator photovoltaic technologies to continue to develop there are some key factors that should and likely will be focused upon in ongoing research. One of these is increasing the concentration ratio. High and ultrahigh concentration ratio systems have a vast potential for increasing efficiencies and reducing cost. This is relatively well known and discussed elsewhere [8,60,161]. From the literature reviewed here, other methods to be highlighted which improve CPV performance include: (1) The use of secondary/homogenising optics; (2) Reducing the path length of light rays; and (3) Tailored surfaces structures. Out of these, the attention to optical surface structure (3) is the most promising with the resulting systems being able to simultaneously achieve improved optical efficiency, tolerance and irradiance uniformity (Figs. 5 and 11). Most CPV systems have to make compromises in one area or another when trying to attain higher concentration ratios but the segmented reflectors described here are able to challenge or at least extend this trade-off which is inevitably encountered. The most noteworthy designs are those with ingenuity and careful geometric design (Fig. 5). Matching the primary output light to input sections of the secondary optic or to illuminate the receiver in a more effective and reliable manner. Ultimately, future CPV optical systems will become larger in concentration ratio but require the use of modular surfaces, facets, truncation and more acute design. This will also increase the dependency on the materials available and their properties. It can be seen from Fig. 5 even in the brief milestones section that one of the breakthroughs for solar concentrator technology was the discovery of PMMA and its application for Fresnel lenses. Fresnel lenses were available before this but only became popular in CPV technology when they became affordable and practical due to PMMA [4,5,162,163]. It is hence not an unusual notion that further breakthroughs in the optics for concentrator photovoltaic applications will be largely due to the development of new materials for its purpose. The combined balance between reducing path length, utilising secondary optics and tailoring surface structures will see the way to ultrahigh concentrator photovoltaics (Fig. 11).

7. Conclusion

An extensive review of solar concentrator research and technologies has been carried out, comparing different materials and the optical performance of different designs. There is not enough consideration into the durability of designs and their performance

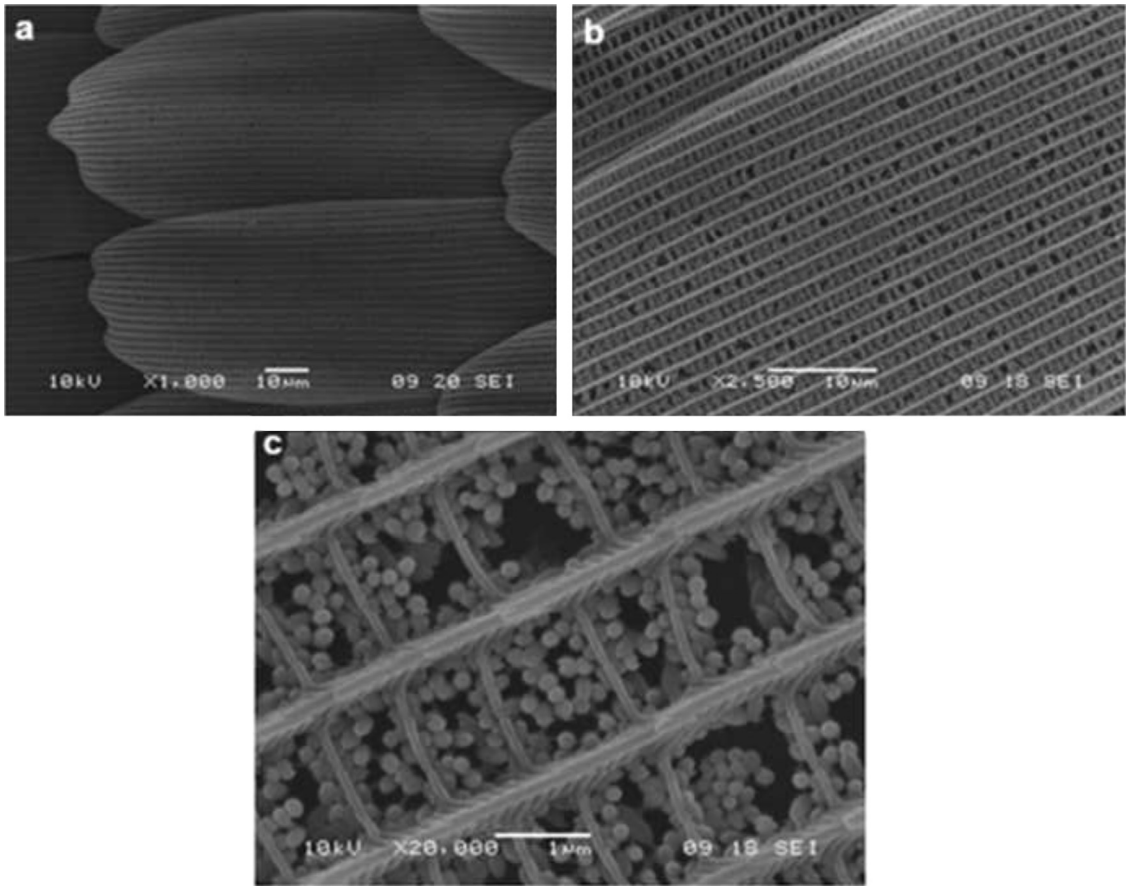

Fig. 9. Large white Pieridae wing structures at increased magnification.

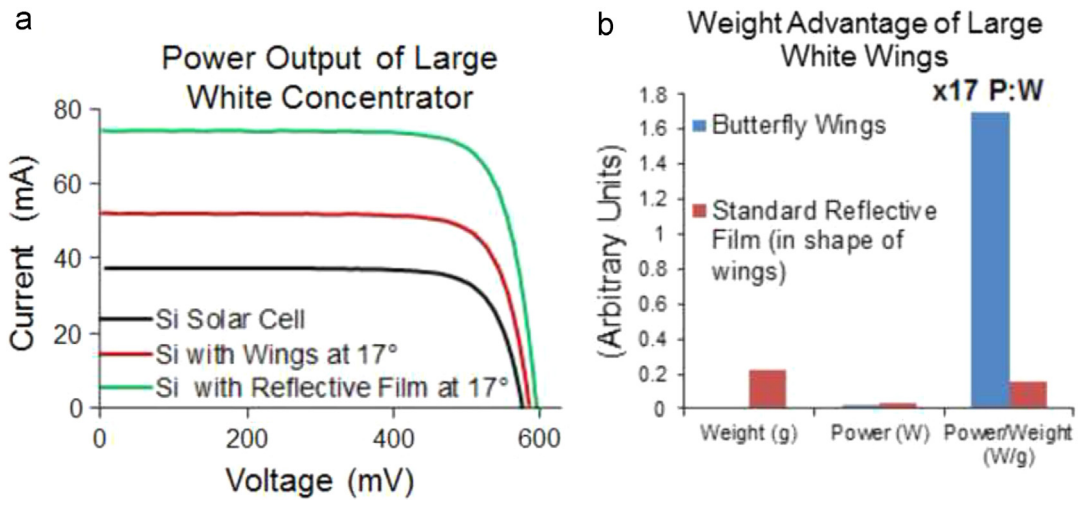

Fig. 10. Butterfly wings increase both the output power and the final power to weight ratio of solar cells. (a) Power output of a mono-crystalline silicon (Si) solar cell either alone, or with large white wings versus reflective film held at the optimal angle of 17°. (b) Histogram representing the relative changes in power, weight and the subsequent power to weight ratio of large white butterfly wings versus reflective film [149].

over years of use, especially for concentrators utilising refractive optics. Recurring challenges and trends in the designs of CPVS have been highlighted.

The above review gives examples of how solar concentrators can be designed in a variety of unique ways boasting different characteristics for different applications. In order to make the necessary leaps in solar concentrator optics to efficient cost effective PV technologies, future novel designs should consider not only novel geometries but also the effect of different materials and surface structures. Trends towards higher performance solar concentrator designs include the use of micro-patterned structures and attention to detailed design such as tailoring secondary optics to primary optics and vice-versa. There is still a vast potential for what materials and hence surface structures could be utilised for

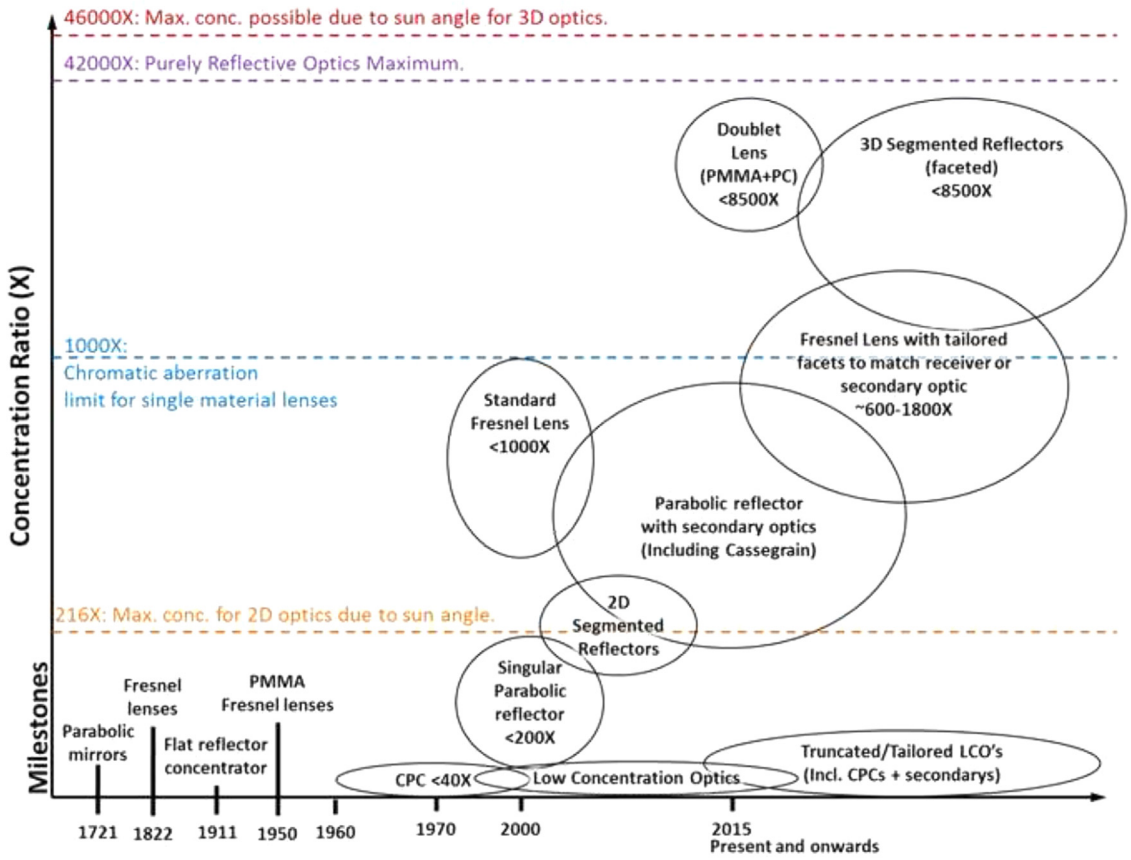

Fig. 11. Timeline of CPV designs and predicted future trends towards high and ultrahigh concentration ratios. Within each CPV types range, the most reliable versions will be in the bottom half of the circles whereas the upper half designs will require high accuracy manufacturing and quality materials.

solar concentrator designs especially if inspiration is taken from biological structures already proven to manipulate light.

Acknowledgements

This work has been carried out in the aid of the BioCPV project jointly funded by DST, India (Ref No: DST/SEED/INDO-UK/002/2011) and EPSRC, UK, (Ref No: EP/J000345/1). Authors acknowledge the funding agencies for the support.

References

[1] Burg BR, Selviaridis A, Paredes S, Michel B. Ecological and Economical Advantages of efficient solar systems CPV-10. AIP conference proceedings; 2014 p. 317–320. doi:10.1063/1.4897086.
[2] Akbari H, Damon Matthews H, Seto D. The long-term effect of increasing the albedo of urban areas. Environ Res Lett 2012;7:024004. http://dx.doi.org/10.1088/1748-9326/7/2/024004.
[3] Doeleman H. Limiting and realistic efficiencies of multi-junction solar cells. Photonic Mater 2012.
[4] Shanks K, Senthilarasu S, Mallick TK. High-concentration optics for photovoltaic applications. In: Pérez-Higueras P, Fernández EF, editors. High concentrator photovoltaics fundamentals, engineering and power plants. 1st ed.. Cham: Springer International Publishing; 2015. p. 85–113. http://dx.doi.org/10.1007/978-3-319-15039-0.
[5] Baharoon DA, Rahman HA, Omar WZW, Fadhl SO. Historical development of concentrating solar power technologies to generate clean electricity efficiently – a review. Renew Sustain Energy Rev 2015;41:996–1027. http://dx.doi.org/10.1016/j.rser.2014.09.008.
[6] Branker K, Pathak MJM, Pearce JM. A review of solar photovoltaic levelized cost of electricity. Renew Sustain Energy Rev 2011;15:4470–82. http://dx.doi.org/10.1016/j.rser.2011.07.104.
[7] Chemisana D, Mallick T. Building Integrated Concentrated Solar Systems. In: Enteria N, Akbarzadeh A, editors. Solar energy sciences and engineering applications. 1st ed.. CRC Press; 2014. p. 545–788.
[8] Languy F, Habraken S. Nonimaging achromatic shaped Fresnel lenses for ultrahigh solar concentration. Opt Lett 2013;38:1730–2.
[9] Languy F, Fleury K, Lenaerts C, Loicq J, Regaert D, Thibert T, et al. Flat Fresnel doublets made of PMMA and PC: combining low cost production and very high concentration ratio for CPV. Opt Express 2011;19(Suppl. 3):A280–94.
[10] Canavarro D, Chaves J, Collares-Pereira M. New second-stage concentrators (XX SMS) for parabolic primaries; comparison with conventional parabolic trough concentrators. Sol Energy 2013;92:98–105. http://dx.doi.org/10.1016/j.solener.2013.02.011.
[11] Murphree QC. A point focusing double parabolic trough concentrator. Sol Energy 2001;70:85–94. http://dx.doi.org/10.1016/S0038-092X(00)00138-9.
[12] Canavarro D, Chaves J, Collares-Pereira M. New optical designs for large parabolic troughs. Energy Procedia 2014;49:1279–87. http://dx.doi.org/10.1016/j.egypro.2014.03.137.
[13] Winston R, Miñano JC, Benítez P, Shatz N, Bortz JC. Nonimaging Optics. Elsevier; http://dx.doi.org/10.1016/B978-012759751-5/50013-0.
[14] Collares-Pereira M, Gordon JM, Rabl A, Winston R. High concentration two-stage optics for parabolic trough solar collectors with tubular absorber and large rim angle. Sol Energy 1991;47:457–66. http://dx.doi.org/10.1016/0038-092X(91)90114-C.
[15] Riffelmann K, Richert T, Nava P, Schweitzer A. Ultimate Trough® – a significant step towards cost-competitive CSP. Energy Procedia 2014;49:1831–9. http://dx.doi.org/10.1016/j.egypro.2014.03.194.
[16] Baig H, Heasman KC, Mallick TK. Non-uniform illumination in concentrating solar cells. Renew Sustain Energy Rev 2012;16:5890–909. http://dx.doi.org/10.1016/j.rser.2012.06.020.
[17] Shanks K, Sarmah N, Mallick TK. The design and optical optimisation of a two stage reflecting high concentrating photovoltaic module using ray trace modelling. PVSAT 2013;9.
[18] Palavras I, Bakos GC. Development of a low-cost dish solar concentrator and its application in zeolite desorption. Renew Energy 2006;31:2422–31. http://dx.doi.org/10.1016/j.renene.2005.11.007.
[19] Brunotte M, Goetzberger A, Blieske U. Two-stage concentrator permitting concentration factors up to 300× with one-axis tracking. Sol Energy 1996;56:285–300. http://dx.doi.org/10.1016/0038-092X(95)00107-3.

[20] González JC. Design and analysis of a curved cylindrical Fresnel lens that produces high irradiance uniformity on the solar cell. Appl Opt 2009;48:2127–32.

[21] Pan JW, Huang JY, Wang CM, Hong HF, Liang YP. High concentration and homogenized Fresnel lens without secondary optics element. Opt Commun 2011;284:4283–8. http://dx.doi.org/10.1016/j.optcom.2011.06.019.

[22] Benítez P, Miñano JC, Zamora P, Mohedano R, Cvetkovic A, Buljan M, et al. High performance Fresnel-based photovoltaic concentrator. Opt Express 2010;18:A25–40. http://dx.doi.org/10.1364/OE.18.000A25.

[23] Jing L, Liu H, Zhao H, Lu Z, Wu H, Wang H, et al. Design of novel compound fresnel lens for high-performance photovoltaic concentrator. Int J Photoenergy 2012. http://dx.doi.org/10.1155/2012/630692.

[24] Zhuang Z, Yu F. Optimization design of hybrid Fresnel-based concentrator for generating uniformity irradiance with the broad solar spectrum. Opt Laser Technol 2014;60:27–33. http://dx.doi.org/10.1016/j.optlastec.2013.12.021.

[25] Zanganeh G, Bader R, Pedretti a, Pedretti M, Steinfeld a. A solar dish concentrator based on ellipsoidal polyester membrane facets. Sol Energy 2012;86:40–7. http://dx.doi.org/10.1016/j.solener.2011.09.001.

[26] Weber KJ, Everett V KJ, PNK Deenapanray, Franklin E, Blakers a. W. Modeling of static concentrator modules incorporating lambertian or v-groove rear reflectors. Sol Energy Mater Sol Cells 2006;90:1741–9. http://dx.doi.org/10.1016/j.solmat.2005.09.012.

[27] Leutz R, Ries H. Microstructured light guides overcoming the two-dimensional concentration limit. Appl Opt 2005;44:6885–9. http://dx.doi.org/10.1364/AO.44.006885.

[28] Nilsson J, Leutz R, Karlsson B. Micro-structured reflector surfaces for a stationary asymmetric parabolic solar concentrator. Sol Energy Mater Sol Cells 2007;91:525–33. http://dx.doi.org/10.1016/j.solmat.2006.11.003.

[29] Akisawa A, Hiramatsu M, Ozaki K. Design of dome-shaped non-imaging Fresnel lenses taking chromatic aberration into account. Sol Energy 2012;86:877–85. http://dx.doi.org/10.1016/j.solener.2011.12.017.

[30] Languy F, Lenaerts C, Loicq J, Thibert T, Habraken S. Performance of solar concentrator made of an achromatic Fresnel doublet measured with a continuous solar simulator and comparison with a singlet. Sol Energy Mater Sol Cells 2013;109:70–6. http://dx.doi.org/10.1016/j.solmat.2012.10.008.

[31] Perez-Higueras P, Fernandez EF. High concentrator photovoltaics: fundamentals, engineering and power plants. 1st ed.SpringerInternational Publishing; http://dx.doi.org/10.1007/978-3-319-15039-0.

[32] Sellami N, Mallick TK. Optical efficiency study of PV crossed compound parabolic concentrator. Appl Energy 2013;102:868–76. http://dx.doi.org/10.1016/j.apenergy.2012.08.052.

[33] Dai G-L, Xia X-L, Sun C, Zhang H-C. Numerical investigation of the solar concentrating characteristics of 3D CPC and CPC-DC. Sol Energy 2011;85:2833–42. http://dx.doi.org/10.1016/j.solener.2011.08.022.

[34] Cooper T, Dähler F, Ambrosetti G, Pedretti A, Steinfeld A. Performance of compound parabolic concentrators with polygonal apertures. Sol Energy 2013;95:308–18. http://dx.doi.org/10.1016/j.solener.2013.06.023.

[35] Su Y, Pei G, Riffat SB, Huang H. Radiance/Pmap simulation of a novel lens-walled compound parabolic concentrator (lens-walled CPC). Energy Procedia 2012;14:572–7. http://dx.doi.org/10.1016/j.egypro.2011.12.977.

[36] Su Y, Riffat SB, Pei G. Comparative study on annual solar energy collection of a novel lens-walled compound parabolic concentrator (lens-walled CPC). Sustain Cities Soc 2012;4:35–40. http://dx.doi.org/10.1016/j.scs.2012.05.001.

[37] Guiqiang L, Gang P, Yuehong S, Jie J, Riffat SB. Experiment and simulation study on the flux distribution of lens-walled compound parabolic concentrator compared with mirror compound parabolic concentrator. Energy 2013;58:398–403. http://dx.doi.org/10.1016/j.energy.2013.06.027.

[38] Victoria M, Domínguez C, Antón I, Sala G. Comparative analysis of different secondary optical elements for aspheric primary lenses. Opt Express 2009;17:6487–92.

[39] Araki K, Kondo M, Uommi H, Yamaguchi M. Experimental proof and theoretical analysis on effectiveness. In: Proceedings of the 3rd world conference on photovoltaic energy conversion; 2003. p. 853–6.

[40] Araki K, Leutz R, Kondo M, Akisawa A, Kashiwagi T, Yamaguchi M, et al. Development of a metal homogenizer for concentrator monolithic multi-junction-cells. Conference Record. In: Proceedings of the twenty-ninth IEEE photovoltaic specialists conference 2002. IEEE; 2002, p. 1572–5. doi:10.1109/PVSC.2002.1190914.

[41] Gordon JM, Feuermann D, Young P. Unfolded aplanats for high-concentration photovoltaics. Opt Lett 2008;33:1114. http://dx.doi.org/10.1364/OL.33.001114.

[42] Tang R, Liu X. Optical performance and design optimization of V-trough concentrators for photovoltaic applications. Sol Energy 2011;85:2154–66. http://dx.doi.org/10.1016/j.solener.2011.06.001.

[43] Fu L, Leutz R, Annen HP. Secondary optics for Fresnel lens solar concentrators. In: Winston R, Gordon JM, editors. Nonimaging optics: efficient design for illumination and solar concentration VII. San Diego: International Society for Optics and Photonics; 2010http://dx.doi.org/10.1117/12.860438.

[44] Tang R, Wang J. A note on multiple reflections of radiation within CPCs and its effect on calculations of energy collection. Renew Energy 2013;57:490–6. http://dx.doi.org/10.1016/j.renene.2013.02.010.

[45] Saleh Ali IM, O'Donovan TS, Reddy KS, Mallick TK. An optical analysis of a static 3-D solar concentrator. Sol Energy 2013;88:57–70. http://dx.doi.org/10.1016/j.solener.2012.11.004.

[46] Ali I, Reddy KS, Mallick TK. Optical performance of circular and elliptical 3-D static solar concentrators. Natl Sol 2010:1–8.

[47] Muhammad-Sukki F, Abu-Bakar SH, Ramirez-Iniguez R, McMeekin SG, Stewart BG, Sarmah N, et al. Mirror symmetrical dielectric totally internally reflecting concentrator for building integrated photovoltaic systems. Appl Energy 2014;113:32–40. http://dx.doi.org/10.1016/j.apenergy.2013.07.010.

[48] Cooper T, Ambrosetti G, Pedretti A, Steinfeld A. Surpassing the 2D limit : a 600× high-concentration PV collector based on a parabolic trough with tracking secondary optics. Energy Procedia 2014;57:285–90. http://dx.doi.org/10.1016/j.egypro.2014.10.033.

[49] Sellami N, Mallick TK. Optical characterisation and optimisation of a static window integrated concentrating photovoltaic system. Sol Energy 2013;91:273–82. http://dx.doi.org/10.1016/j.solener.2013.02.012.

[50] Sellami N, Mallick TK, McNeil DA. Optical characterisation of 3-D static solar concentrator. Energy Convers. Manag. 2012;64:579–86. http://dx.doi.org/10.1016/j.enconman.2012.05.028.

[51] Ali I. Design and analysis of a novel 3-D elliptical hyperboloid static solar concentrator for process heat applications submitted by institute of mechanical. United Kingdom: Process and Energy Engineering School of Engineering and Physical Sciences Edinburgh; 2013.

[52] Coughenour BM, Stalcup T, Wheelwright B, Geary A, Hammer K, Angel R. Dish-based high concentration PV system with Köhler optics. Opt Express 2014;22:A211. http://dx.doi.org/10.1364/OE.22.00A211.

[53] Chong KK, Lau SL, Yew TK, Tan PCL. Design and development in optics of concentrator photovoltaic system. Renew Sustain Energy Rev 2013;19:598–612. http://dx.doi.org/10.1016/j.rser.2012.11.005.

[54] Uematsu T, Yazawa Y, Miyamura Y, Muramatsu S, Ohtsuka H, Tsutsui K, et al. Static concentrator photovoltaic module with prism array. Sol Energy Mater Sol Cells 2001;67:415–23.

[55] Uematsu T, Yazawa Y, Joge T, Kokunai S. Fabrication and characterization of a flat-plate static-concentrator photovoltaic module. Sol Energy Mater Sol Cells 2001;67:425–34.

[56] Uematsu T, Yazawa Y, Tsutsui K, Miyamura Y, Ohtsuka H, Warabisako T, et al. Design and characterization of flat-plate static-concentrator photovoltaic modules. Sol Energy Mater Sol Cells 2001;67:441–8.

[57] Chaves J. Introduction to nonimaging optics. CRC Press; 2008.

[58] Goldstein A, Gordon JM. Tailored solar optics for maximal optical tolerance and concentration. Sol Energy Mater Sol Cells 2011;95:624–9. http://dx.doi.org/10.1016/j.solmat.2010.09.029.

[59] Dreger M, Wiesenfarth M, Kisser A, Schmid T, Bett AW. Development And Investigation Of A CPV Module With Cassegrain Mirror Optics. CPV-10 2014.

[60] Yavrian A, Tremblay S, Levesque M, Gilbert R. How to increase the efficiency of a high concentrating PV (HCPV) by increasing the acceptance angle to ± 3.2°. In: Proceedings of the 9th international conference on concentrator photovoltaic systems. CPV-9. AIP Conference proceedings, vol. 1556; 2013. p. 197–200. doi:10.1063/1.4822230.

[61] Sarmah N, Richards BS, Mallick TK. Evaluation and optimization of the optical performance of low-concentrating dielectric compound parabolic concentrator using ray-tracing methods. Appl Opt 2011;50:3303–10.

[62] Baig H, Sellami N, Chemisana D, Rosell J, Mallick TK. Performance analysis of a dielectric based 3D building integrated concentrating photovoltaic system. Sol Energy 2014;103:525–40. http://dx.doi.org/10.1016/j.solener.2014.03.002.

[63] Kotsidas P, Chatzi E, Modi V. Stationary nonimaging lenses for solar concentration. Appl Opt 2010;49:5183–91. http://dx.doi.org/10.1364/AO.49.005183.

[64] Peaker AR, Markevich VP. Photovoltaic Power Generation: the impact of solar energy. In: Kasper E, Mussig H-J, Grimmeiss HG, editors. Advanced energy materials. Stafa-Zuerich: Trans Tech Publications Ltd.; 2009.

[65] Duerr F, Meuret Y, Thienpont H. Tracking integration in concentrating photovoltaics using laterally moving optics. Opt Express 2011;19(Suppl. 3):A207–18.

[66] Bouchard S, Thibault S. Planar waveguide concentrator used with a seasonal tracker. Appl Opt 2012;51:6848. http://dx.doi.org/10.1364/AO.51.006848.

[67] Li X, Dai YJ, Li Y, Wang RZ. Comparative study on two novel intermediate temperature CPC solar collectors with the U-shape evacuated tubular absorber. Sol Energy 2013;93:220–34. http://dx.doi.org/10.1016/j.solener.2013.04.002.

[68] Selimoglu O, Turan R. Exploration of the horizontally staggered light guides for high concentration CPV applications. Opt Express 2012;20:19137–47.

[69] Fujieda I, Arizono K, Okuda Y. Design considerations for a concentrator photovoltaic system based on a branched planar waveguide. J Photonics Energy 2012;2:021807. http://dx.doi.org/10.1117/1.JPE.2.021807.

[70] Jung YJ, Park D, Koo S, Yu S, Park N. Metal slit array Fresnel lens for wavelength-scale optical coupling to nanophotonic waveguides. Opt Express 2009;17:18852–7. http://dx.doi.org/10.1364/OE.17.018852.

[71] Tang R, Wu M, Yu Y, Li M. Optical performance of fixed east–west aligned CPCs used in China. Renew Energy 2010;35:1837–41. http://dx.doi.org/10.1016/j.renene.2009.12.006.

[72] Earp AA, Smith GB, Swift PD, Franklin J. Maximising the light output of a luminescent solar concentrator. Sol Energy 2004;76:655–67. http://dx.doi.org/10.1016/j.solener.2004.02.001.

[73] Lainé DC. Transmissive, non-imaging Fresnel types of reflective radiation concentrators revisited. Opt Laser Technol 2013;54:274–83. http://dx.doi.org/10.1016/j.optlastec.2013.05.013.

[74] Xu YJ, Liao JX, Cai QW, Yang XX. Solar Energy Materials Solar Cells Preparation of a highly-reflective TiO_2/SiO_2/Ag thin film with self-cleaning properties by magnetron sputtering for solar front reflectors. Solar Energy

Mater. Solar Cells 2013;113:7–12. http://dx.doi.org/10.1016/j.solmat.2013.01.034.
[75] Alcock SG, Sutter JP, Sawhney KJS, Hall DR, McAuley K, Sorensen T. Bimorph mirrors: the good, the bad, and the ugly. Nucl Instrum Methods Phys Res Sect A Accel Spectrom, Detect Assoc Equip 2013;710:87–92. http://dx.doi.org/10.1016/j.nima.2012.10.135.
[76] Jaus J, Peharz G, Gombert A, Pablo J, Rodriguez F, Dimroth F, et al. Development of flatcon modules using secondary optics. IEEE 2009:1931–6.
[77] Barber GJ, Braem a, Brook NH, Cameron W, D'Ambrosio C, Harnew N, et al. Development of lightweight carbon-fiber mirrors for the RICH 1 detector of LHCb. Nucl Instrum Methods Phys Res Sect A Accel Spectrom, Detect Assoc Equip 2008;593:624–37. http://dx.doi.org/10.1016/j.nima.2008.05.050.
[78] Jagoo Z. Tracking solar concentrators. 1st ed.Springer Nether; 2013.
[79] Bader R, Haueter P, Pedretti a, Steinfeld a. Optical design of a novel two-stage solar trough concentrator based on pneumatic polymeric structures. J Sol Energy Eng 2009;131:031007. http://dx.doi.org/10.1115/1.3142824.
[80] Guo S, Zhang G, Li L, Wang W, Zhao X. Effect of materials and modelling on the design of the space-based lightweight mirror. Mater Des 2009;30:9–14. http://dx.doi.org/10.1016/j.matdes.2008.04.056.
[81] Yin L, Huang H. Brittle materials in nano-abrasive fabrication of optical mirror-surfaces. Precis Eng 2008;32:336–41. http://dx.doi.org/10.1016/j.precisioneng.2007.09.001.
[82] Fang FZ, Zhang XD, Weckenmann a, Zhang GX, Evans C. Manufacturing and measurement of freeform optics. CIRP Ann - Manuf Technol 2013;62:823–46. http://dx.doi.org/10.1016/j.cirp.2013.05.003.
[83] Lodha GS, Yamashita K, Kunieda H, Tawara Y, Yu J, Namba Y, et al. Effect of surface roughness and subsurface damage on grazing-incidence x-ray scattering and specular reflectance. Appl Opt 1998;37:5239–52. http://dx.doi.org/10.1364/AO.37.005239.
[84] Duparré A, Ferre-Borrull J, Gliech S, Notni G, Steinert J, Bennett JM. Surface characterization techniques for determining the root-mean-square roughness and power spectral densities of optical components. Appl Opt 2002;41:154–71. http://dx.doi.org/10.1364/AO.41.000154.
[85] BPW Mayne, Asce a M. Relation between surface roughness and specular reflectance at normal incidence. 1981. p. 106.
[86] Schissel P, Jorgensen G, Kennedy C, Goggin R. Silvered-PMMA reflectors. Sol Energy Mater Sol Cells 1994;33:183–97. http://dx.doi.org/10.1016/0927-0248(94)90207-0.
[87] Kennedy CE, Smilgys RV, Kirkpatrick DA, Ross JS. Optical performance and durability of solar reflectors protected by an alumina coating. Thin Solid Films 1997;304:303–9. http://dx.doi.org/10.1016/S0040-6090(97)00198-3.
[88] Fend T, Jorgensen G, Kuster H. Applicability of highly reflective aluminium coil for solar concentrators. Sol Energy 2000;68:361–70.
[89] Fend T, Hoffschmidt B, Jorgensen G, Kuster H, Kruger D, Pitz-Paal R, et al. Comparative assessment of solar concentrator materials. Sol Energy 2003;74:149–55. http://dx.doi.org/10.1016/S0038-092X(03)00116-6.
[90] Mallick TKK, Eames PCC, Hyde TJJ, Norton B. The design and experimental characterisation of an asymmetric compound parabolic photovoltaic concentrator for building facade integration in the UK. Sol Energy 2004;77:319–27. http://dx.doi.org/10.1016/j.solener.2004.05.015.
[91] Leutz R, Fu L, Annen HP. Stress in large-area optics for solar concentrators. In: Dhere NG, Wohlgemuth JH, Ton DT, editors. SPIE solar energy+technology. International Society for Optics and Photonics; 2009http://dx.doi.org/10.1117/12.827357.
[92] Egger JR. Manufacturing Fresnel lens master tooling for solar photovoltiac concentrators; 1979. p. 149–54.
[93] Lorenzo E, Sala G. Hybrid silicone-glass Fresnel lens as concentrator for photovoltaic applications. Sun II; Proc Silver Jubil Congr 1979;1:536–9.
[94] Mathys Z, Burchill PJ. Influence of location on the weathering of acrylic sheet materials. Polym Degrad Stab 1997;55:45–54. http://dx.doi.org/10.1016/S0141-3910(96)00131-0.
[95] Miller DC. Analysis of transmitted optical spectrum enabling accelerated testing of multijunction concentrating photovoltaic designs. Opt Eng 2011;50:013003. http://dx.doi.org/10.1117/1.3530092.
[96] Greivenkamp JE. Field guide to geometrical optics. http://dx.doi.org/10.1117/3.547461.
[97] Kasarova SN, Sultanova NG, Ivanov CD, Nikolov ID. Analysis of the dispersion of optical plastic materials. Opt Mater 2007;29:1481–90. http://dx.doi.org/10.1016/j.optmat.2006.07.010.
[98] Andrady A. Wavelength sensitivity in polymer photodegradation. Polymer 1997;128:47–94.
[99] Andrady AL, Hamid SH, Hu X, Torikai A. Effects of increased solar ultraviolet radiation on materials. J Photochem Photobiol B Biol 1998;46:96–103. http://dx.doi.org/10.1016/S1011-1344(98)00188-2.
[100] Zhou G, He J, Xu L. Antifogging antireflective coatings on Fresnel lenses by integrating solid and mesoporous silica nanoparticles. Microporous Mesoporous Mater 2013;176:41–7. http://dx.doi.org/10.1016/j.micromeso.2013.03.038.
[101] Stefancich M, Zayan A, Chiesa M, Rampino S, Roncati D, Kimerling L, et al. Single element spectral splitting solar concentrator for multiple cells CPV system. Opt Express 2012;20:9004. http://dx.doi.org/10.1364/OE.20.009004.
[102] Welford WT, Winston R. High collection nonimaging optics. Elsevier; http://dx.doi.org/10.1016/B978-0-12-742885-7.50021-8.
[103] Michel C, Loicq J, Languy F, Habraken S. Optical study of a solar concentrator for space applications based on a diffractive/refractive optical combination. Sol Energy Mater Sol Cells 2014;120:183–90. http://dx.doi.org/10.1016/j.solmat.2013.08.042.
[104] Liu Y, Huang R, Madsen CK. Design of a lens-to-channel waveguide system as a solar concentrator structure. Opt Express 2014;22:A198. http://dx.doi.org/10.1364/OE.22.00A198.
[105] Karp JH, Tremblay EJ, Hallas JM, Ford JE. Orthogonal and secondary concentration in planar micro-optic solar collectors. Opt Express 2011;19(Suppl. 4). http://dx.doi.org/10.1364/OE.19.00A673.
[106] Shieh W-C, Su G-D. Compact solar concentrator designed by minilens and slab waveguide, 8108. Spie; http://dx.doi.org/10.1117/12.892980.
[107] Chu S-C, Wu H-Y, Lin H-H. Planar lightguide solar concentrator, vol. 8438. SPIE; http://dx.doi.org/10.1117/12.922185.
[108] Karp JH, Ford JE. Planar micro-optic solar concentration using multiple imaging lenses into a common slab waveguide. SPIE Sol Energy++ Technol 2009. http://dx.doi.org/10.1117/12.826531.
[109] Waritanant T, Boonruang S, Chung T-Y. High angular tolerance thin profile solar concentrators designed using a wedge prism and diffraction grating. Sol Energy 2013;87:35–41. http://dx.doi.org/10.1016/j.solener.2012.10.009.
[110] Hughes MD, Maher C, Borca-Tasciuc D-A, Polanco D, Kaminski D. Performance comparison of wedge-shaped and planar luminescent solar concentrators. Renew Energy 2013;52:266–72. http://dx.doi.org/10.1016/j.renene.2012.10.034.
[111] Atkinson C, Sansom CL, Almond HJ, Shaw CP. Coatings for concentrating solar systems – a review. Renew Sustain Energy Rev 2015;45:113–22. http://dx.doi.org/10.1016/j.rser.2015.01.015.
[112] Valleti K, Murali Krishna D, Joshi SV. Functional multi-layer nitride coatings for high temperature solar selective applications. Sol Energy Mater Sol Cells 2014;121:14–21. http://dx.doi.org/10.1016/j.solmat.2013.10.024.
[113] Suman S, Khan MK, Pathak M. Performance enhancement of solar collectors—A review. Renew Sustain Energy Rev 2015;49:192–210. http://dx.doi.org/10.1016/j.rser.2015.04.087.
[114] Li N, Cao M, Hu C. Review on the latest design of graphene-based inorganic materials. Nanoscale 2012;4:6205. http://dx.doi.org/10.1039/c2nr31750h.
[115] Jariwala D, Sangwan VK, Lauhon LJ, Marks TJ, Hersam MC. Carbon nanomaterials for electronics, optoelectronics, photovoltaics, and sensing. Chem Soc Rev 2013;42:2824–60. http://dx.doi.org/10.1039/c2cs35335k.
[116] Nicole L, Laberty-Robert C, Rozes L, Sanchez C. Hybrid materials science: a promised land for the integrative design of multifunctional materials. Nanoscale 2014;6:6267–92. http://dx.doi.org/10.1039/c4nr01788a.
[117] Avnir D. Organic chemistry within ceramic matrixes: doped sol–gel materials. Acc Chem Res 1995;28:328–34. http://dx.doi.org/10.1021/ar00056a002.
[118] Gelman F, Blum J, Avnir D. One-pot sequences of reactions with sol–gel entrapped opposing reagents: an enzyme and metal-complex catalysts. J Am Chem Soc 2002;124:14460–3.
[119] Levy D, Einhorn S, Avnir D. Applications of the sol–gel process for the preparation of photochromic information-recording materials: synthesis, properties, mechanisms. J Non Cryst Solids 1989;113:137–45. http://dx.doi.org/10.1016/0022-3093(89)90004-5.
[120] Avnir D, Kaufman VR, Reisfeld R. Organic fluorescent dyes trapped in silica and silica–titania thin films by the sol-gel method. Photophysical, film and cage properties. J Non Cryst Solids 1985;74:395–406. http://dx.doi.org/10.1016/0022-3093(85)90081-X.
[121] Sanchez C, Julián B, Belleville P, Popall M. Applications of hybrid organic–inorganic nanocomposites. J Mater Chem 2005;15:3559. http://dx.doi.org/10.1039/b509097k.
[122] Sanchez Clément KJ. Hybrid materials themed issue. Chem Soc Rev 2011;40:588–95. http://dx.doi.org/10.1039/c0cs00076k.
[123] Faustini M, Nicole L, Boissière C, Innocenzi P, Sanchez C, Grosso D. Hydrophobic, antireflective, self-cleaning, and antifogging sol-gel coatings: An example of multifunctional nanostructured materials for photovoltaic cells. Chem Mater 2010;22:4406–13. http://dx.doi.org/10.1021/cm100937e.
[124] Gupta R. Polymer nanocomposites: handbook. Boca Raton: CRC Press Taylor & Francis Group; 2010.
[125] Faustini M, Boissière C, Nicole L, Grosso D. From chemical solutions to inorganic nanostructured materials: a journey into evaporation-driven processes. Chem Mater 2014;26:709–23. http://dx.doi.org/10.1021/cm402132y.
[126] Wang L, Lu X, Lei S, Song Y. Graphene-based polyaniline nanocomposites: preparation, properties and applications. J Mater Chem A 2014;2:4491. http://dx.doi.org/10.1039/c3ta13462h.
[127] Bhushan B. Biomimetics inspired surfaces for drag reduction and oleophobicity/philicity. Beilstein J Nanotechnol 2011;2:66–84. http://dx.doi.org/10.3762/bjnano.2.9.
[128] Fratzl P, Weinkamer R. Nature's hierarchical materials. Prog Mater Sci 2007;52:1263–334. http://dx.doi.org/10.1016/j.pmatsci.2007.06.001.
[129] Potyrailo R a, Ghiradella H, Vertiatchikh A, Dovidenko K, Cournoyer JR, Olson E. Morpho butterfly wing scales demonstrate highly selective vapour response. Nat Photonics 2007;1:123–8. http://dx.doi.org/10.1038/nphoton.2007.2.
[130] Kolle M, Salgard-Cunha PM, Scherer MRJ, Huang F, Vukusic P, Mahajan S, et al. Mimicking the colourful wing scale structure of the *Papilio blumei* butterfly. Nat Nanotechnol 2010;5:511–5. http://dx.doi.org/10.1038/nnano.2010.101.
[131] Vukusic P. Manipulating the flow of light with photonic crystals. Phys Today 2006;59:82–3. http://dx.doi.org/10.1063/1.2387101.
[132] Vukusic P, Sambles JR. Photonic structures in biology. Nature 2003;424:852–5. http://dx.doi.org/10.1038/nature01941.

[133] Dewan R, Fischer S, Meyer-Rochow VB, Özdemir Y, Hamraz S, Knipp D. Studying nanostructured nipple arrays of moth eye facets helps to design better thin film solar cells. Bioinspir Biomim 2012;7:016003. http://dx.doi.org/10.1088/1748-3182/7/1/016003.
[134] Huang CK, Sun KW, Chang W-L. Efficiency enhancement of silicon solar cells using a nano-scale honeycomb broadband anti-reflection structure. Opt Express 2012;20:A85–93.
[135] Parker AR. 515 Million years of structural colour. J Opt A Pure Appl Opt 2000;2:R15–28. http://dx.doi.org/10.1088/1464-4258/2/6/201.
[136] Ingram AL, Parker AR. A review of the diversity and evolution of photonic structures in butterflies, incorporating the work of John Huxley (The Natural History Museum, London from 1961 to 1990). Philos Trans R Soc Lond B Biol Sci 2008;363:2465–80. http://dx.doi.org/10.1098/rstb.2007.2258.
[137] Bíró J. Temporal-spatial pattern of true bug assemblies (Heteroptera: gerromorpha, nepomorpha) in lake Balaton. Appl Ecol Environ Res 2003;1:173–81.
[138] Biró LP, Lambin P. Nanopatterning of graphene with crystallographic orientation control. Carbon N Y 2010;48:2677–89. http://dx.doi.org/10.1016/j.carbon.2010.04.013.
[139] Biro P. Maya Calendar Origins: monuments, mythistory, and the materialization of time. Hisp Am Hist Rev 2009;89:323–4. http://dx.doi.org/10.1215/00182168-2008-086.
[140] Berthier S, Boulenguez J, Menu M, Mottin B. Butterfly inclusions in Van Schrieck masterpieces. Techniques and optical properties. Appl Phys A Mater Sci Process 2008;92:51–7. http://dx.doi.org/10.1007/s00339-008-4480-8.
[141] Berthier S, Charron E, Boulenguez J. Morphological structure and optical properties of the wings of Morphidae. Insect Sci 2006;13:145–58. http://dx.doi.org/10.1111/j.1744-7917.2006.00077.x.
[142] Boulenguez J, Berthier S, Vigneron JP. Simulations tools for natural photonic structures. Phys B Condens Matter 2007;394:217–20. http://dx.doi.org/10.1016/j.physb.2006.12.023.
[143] Ingram AL, Deparis O, Boulenguez J, Kennaway G, Berthier S, Parker AR. Structural origin of the green iridescence on the chelicerae of the red-backed jumping spider, *Phidippus johnsoni* (Salticidae: Araneae). Arthropod Struct Dev 2011;40:21–5. http://dx.doi.org/10.1016/j.asd.2010.07.006.
[144] Smith AJ, Wang C, Guo D, Sun C, Huang J. Repurposing Blu-ray movie discs as quasi-random nanoimprinting templates for photon management. Nat Commun 2014;5:5517. http://dx.doi.org/10.1038/ncomms6517.
[145] Schneider BW, Lal NN, Baker-Finch S, White TP. Pyramidal surface textures for light trapping and antireflection in perovskite-on-silicon tandem solar cells. Opt Express 2014;22:A1422. http://dx.doi.org/10.1364/OE.22.0A1422.
[146] Wang H-P, Lien D-H, Tsai M-L, Lin C-A, Chang H-C, Lai K-Y, et al. Photon management in nanostructured solar cells. J Mater Chem C 2014;2:3144. http://dx.doi.org/10.1039/c3tc32067g.
[147] Tseng JK, Chen YJ, Pan CT, Wu TT, Chung MH. Application of optical film with micro-lens array on a solar concentrator. Sol Energy 2011;85:2167–78. http://dx.doi.org/10.1016/j.solener.2011.06.004.
[148] Siddique RH, Gomard G, Hölscher H. The role of random nanostructures for the omnidirectional anti-reflection properties of the glasswing butterfly. Nat Commun 2015;6:6909. http://dx.doi.org/10.1038/ncomms7909.
[149] Shanks K, Senthilarasu S, Ffrench-Constant RH, Mallick TK. White butterflies as solar photovoltaic concentrators. Sci Rep 2015;5:12267. http://dx.doi.org/10.1038/srep12267.
[150] Vukusic P. Structural colour: elusive iridescence strategies brought to light. Curr Biol 2011:21. http://dx.doi.org/10.1016/j.cub.2011.01.049.
[151] Stavenga DG, Leertouwer HL, Wilts BD. Coloration principles of nymphaline butterflies – thin films, melanin, ommochromes and wing scale stacking. J Exp Biol 2014;217:2171–80. http://dx.doi.org/10.1242/jeb.098673.
[152] Leertouwer HL, Colourful butterfly wings : scale stacks , iridescence and sexual dichromatism of Pieridae, vol. 67; 2007. p. 158–64.
[153] Stavenga DG, Arikawa K. Evolution of color and vision of butterflies. Arthropod Struct Dev 2006;35:307–18. http://dx.doi.org/10.1016/j.asd.2006.08.011.
[154] Shawkey MD, Morehouse NI, Vukusic P. A protean palette: colour materials and mixing in birds and butterflies. J R Soc Interface 2009;6(Suppl 2). http://dx.doi.org/10.1098/rsif.2008.0459.focus.
[155] Vukusic P, Sambles R, Lawrence C, Wakely G. Sculpted-multilayer optical effects in two species of Papilio butterfly. Appl Opt 2001;40:1116–25. http://dx.doi.org/10.1364/AO.40.001116.
[156] Vukusic P, Hooper I. Directionally controlled fluorescence emission in butterflies. Science 2005;310:1151. http://dx.doi.org/10.1126/science.1116612.
[157] Meyers M a, Chen P-Y, Lopez MI, Seki Y, Lin AYM. Biological materials: a materials science approach. J Mech Behav Biomed Mater 2011;4:626–57. http://dx.doi.org/10.1016/j.jmbbm.2010.08.005.
[158] Yu K, Fan T, Lou S, Zhang D. Biomimetic optical materials: Integration of nature's design for manipulation of light. Prog Mater Sci 2013;58:825–73. http://dx.doi.org/10.1016/j.pmatsci.2013.03.003.
[159] Zhou H, Fan T, Zhang D. Biotemplated materials for sustainable energy and environment: current status and challenges. ChemSusChem 2011;4:1344–87. http://dx.doi.org/10.1002/cssc.201100048.
[160] Pulsifer DP, Lakhtakia A. Background and survey of bioreplication techniques. Bioinspir Biomim 2011;6:031001. http://dx.doi.org/10.1088/1748-3182/6/3/031001.
[161] Gordon JM, Katz E a, Feuermann D, Huleihil M. Toward ultrahigh-flux photovoltaic concentration. Appl Phys Lett 2004;84:3642. http://dx.doi.org/10.1063/1.1723690.
[162] Xie WT, Dai YJ, Wang RZ, Sumathy K. Concentrated solar energy applications using Fresnel lenses: a review. Renew Sustain Energy Rev 2011;15:2588–606. http://dx.doi.org/10.1016/j.rser.2011.03.031.
[163] Kumar V, Shrivastava RL, Untawale SP. Fresnel lens: a promising alternative of reflectors in concentrated solar power. Renew Sustain Energy Rev 2015;44:376–90. http://dx.doi.org/10.1016/j.rser.2014.12.006.
[164] Luque A, Hegedus S. Handbook of photovoltaic science. England: John Wiley & Sons Ltd.; 2003.
[165] Gharbi N, El, Derbal H, Bouaichaoui S, Said N. A comparative study between parabolic trough collector and linear Fresnel reflector technologies. Energy Procedia 2011;6:565–72. http://dx.doi.org/10.1016/j.egypro.2011.05.065.
[166] Abbas R, Montes MJ, Piera M, Martínez-Val JM. Solar radiation concentration features in Linear Fresnel reflector arrays. Energy Convers Manag 2012;54:133–44. http://dx.doi.org/10.1016/j.enconman.2011.10.010.
[167] Abbas R, Muñoz-Antón J, Valdés M, Martínez-Val JM. High concentration linear Fresnel reflectors. Energy Convers Manag 2013;72:60–8. http://dx.doi.org/10.1016/j.enconman.2013.01.039.
[168] WGJHM Van Sark, KWJ Barnham, Slooff LH, Chatten AJ, Büchtemann A, Meyer A, et al. Luminescent solar concentrators—a review of recent results. Opt Express 2008;16:21773–92. http://dx.doi.org/10.1364/OE.16.021773.
[169] Bass M, Enoch JM, Stryland EW, Wolfe WL. Handbook of optics 2000. http://dx.doi.org/10.3109/15360288.2011.620691.

[Article 2]

K. Shanks, N. Sarmah, J. P. Ferrer-Rodriguez, S. Senthilarasu, K. S. Reddy, E. F. Fernández, and T. Mallick, “Theoretical investigation considering manufacturing errors of a high concentrating photovoltaic of cassegrain design and its experimental validation,” *Sol. Energy*, vol. 131, pp. 235–245, Jun. 2016.

Available online at www.sciencedirect.com

ScienceDirect

Solar Energy 131 (2016) 235–245

SOLAR ENERGY

www.elsevier.com/locate/solener

Theoretical investigation considering manufacturing errors of a high concentrating photovoltaic of cassegrain design and its experimental validation

Katie Shanks [a,*], Nabin Sarmah [b], Juan P. Ferrer-Rodriguez [c], S. Senthilarasu [a], K.S. Reddy [d], Eduardo F. Fernández [c], Tapas Mallick [a,*]

[a] Environmental and Sustainability Institute, University of Exeter Penryn Campus, Penryn TR10 9FE, UK
[b] Department of Energy, Tezpur University, Tezpur, Assam 784 028, India
[c] Centre for Advanced Studies in Energy and Environment, University of Jaen, Campus las Lagunillas, Jaen 23071, Spain
[d] Heat Transfer and Thermal Power Laboratory, Department of Mechanical Engineering, Indian Institute of Technology Madras, Chennai 600 036, India

Received 13 November 2015; received in revised form 4 February 2016; accepted 24 February 2016
Available online 9 March 2016

Communicated by: Associate Editor Igor Tyukhov

Abstract

A compact high concentrating photovoltaic module based on cassegrain optics is presented; consisting of a primary parabolic reflector, secondary inverse parabolic reflector and a third stage homogeniser. The effect of parabolic curvatures, reflector separation distance and the homogeniser's height and width on the acceptance angle has been investigated for optimisation. Simulated optical efficiencies of 84.82–81.89% over a range of ±1° tracking error and 55.49% at a tracking error of ±1.5° were obtained. The final singular module measures 169 mm in height and 230 mm in width (not including structural components such as cover glass). The primary reflector dish has a focal length of 200 mm and is a focal with the secondary inverse reflector which has a focal length of 70 mm. The transparent homogenising optic has a height of 70 mm, an entry aperture of 30 × 30 mm and an output aperture of 10 × 10 mm to match the solar cell. This study includes an analysis of the optical efficiency, acceptance angle, irradiance distribution and component errors for this type of concentrator. In particular material stability and the surface error of the homogeniser proved to be detrimental in theoretical and experimental testing – reducing the optical efficiency to ~40%. This study proves the importance of material choice and simulating optical surface quality, not simply assuming ideal conditions. In the experimental testing, the acceptance angle followed simulation results as did the optical efficiency of the primary and secondary reflectors. The optical efficiency of the system against increasing solar misalignment angles is given for the theoretical and experimental work carried out.

Keywords: Concentrator photovoltaics; Optics; Ray trace simulation; Experimental testing

1. Introduction

Solar concentrator systems are an expanding research topic with various applications and benefits. Concentrator photovoltaic (CPV) designs have been pushing higher concentration ratios to achieve higher conversion efficiencies and cost effectiveness (Gordon et al., 2004; Languy and

* Corresponding authors.
E-mail addresses: Kmas201@exeter.ac.uk (K. Shanks), nabin@tezu.ernet.in (N. Sarmah), jferrer@ujaen.es (J.P. Ferrer-Rodriguez), S.Sundaram@exeter.ac.uk (S. Senthilarasu), KSReddy@iitm.ac.in (K.S. Reddy), fenandez@ujaen.es (E.F. Fernández), T.K.Mallick@exeter.ac.uk (T. Mallick).

http://dx.doi.org/10.1016/j.solener.2016.02.050
0038-092X/

Habraken, 2013; Yavrian et al., 2013). However, the higher the concentration ratio of a solar concentrator system, the more dependent upon accuracy it becomes. This includes manufacturing accuracy and solar tracking accuracy. The relationship between concentration ratio and acceptance angle directly follows from etendue and is explained further by Gordon et al. (2008), Goldstein and Gordon (2011), Welford and Winston (1989). When comparing the types of solar concentrator photovoltaics, the Fresnel lens and cassegrain designs can both achieve high concentration ratios but the reflective cassegrain is not limited by chromatic aberration (<1000X limit) Shanks et al., 2015, 2016a; Languy et al., 2013. The cassegrain however typically has a lower acceptance angle due to the 2 reflective stages in comparison to the 1 refraction stage of the Fresnel lens (Shanks et al., 2015, 2016a). There has been much research into the cassegrain type concentrator (Dreger et al., 2014; Yehezkel et al., 1993; Chong et al., 2013; Chen and Ho, 2013; Victoria et al., 2013; McDonald et al., 2007; Roman et al., 1995; Terry et al., 1996, 2012) for its greater compactness (Roman et al., 1995; Miñano et al., 1995) and higher concentration ratios over the Fresnel Lens. Roman et al. (1995) and Yavrian et al. (2013) highlight the importance of optimising concentrator designs not only for optical efficiency but optical tolerance also.

Acceptance angles for high concentration systems are low (McDonald et al., 2007; Luque and Andreev, 2007; Akisawa et al., 2012; Chaves, 2008; Winston et al., 2005). However, research and careful design have been increasing the acceptance angle of high concentration photovoltaics (HCPV's) Dreger et al., 2014; Benitez et al., 2006. Benitez et al. (2006) designed a cassegrain reflector capable of 800× concentration ratio and an acceptance angle of ±0.86° but this and more systems still need to be experimentally tested. SolFocus has commercialised systems with an acceptance angle of ±1.4° (Winston et al., 2005) (McDonald et al., 2007; Chaves, 2008). OpSun have also performed outdoor measurements of three high concentration photovoltaics of geometrical concentration ratios 380X, 900X and 2250X, which gave acceptance angle valued of ±3.2°, ±1.9° and ±1.2° respectively (Yavrian et al., 2013). These commercial systems are however expensive and require highly accurate optics. In this paper ray trace simulations are carried out to optimise a cassegrain CPV design with respects to optical efficiency and acceptance angle. The simulation method also addresses realistic errors (such as surface roughness) which can occur in manufacturing. These uncertainties are not normally simulated despite the variety of modelling theory's and accuracy with which they can predict light behaviour (Schröder et al., 2011). As CPV research focuses towards achieving higher concentration ratios, the effect of these uncertainties will become increasingly important.

Untrue optimised designs can also occur depending on the simulation method and order of parameter determination. In a cassegrain concentrator many of the dimensions are linked and require to and fro optimisation of multiple variables together. This can become very complex if aiming for a specific geometric concentration, optical efficiency, irradiance distribution and overall size limit. In most cases there are a number of simplifying yet unrealistic assumptions made when performing ray trace simulations which can lead to significant losses within the built version of the system. The material, manufacturing method and location of the CPV device can significantly alter how it performs in comparison to the predicted simulations (Brogren et al., 2004; Fang et al., 2006; Guo et al., 2009; Han et al., 2008; Fernández et al., 2012).

2. Design method

The following study details the ray trace optimisation of a 500× cassegrain concentrator which was then built and tested to compare theoretical and experimental results. Parameters are optimised is stages with consideration to realistic conditions. This means the radius and width of the primary and secondary reflector dishes are determined first due to the 500× geometrical concentration requirement and shadowing effects of the secondary reflector. The focal lengths and separation distance of the two reflectors are then optimised but first with a reflective type homogenizer and then with a transparent homogenizer. The dimensions of the homogenizer are then refined further.

The optimisation criteria during simulations is to obtain a high optical efficiency and a well distributed irradiance upon the receiver over a range of at least ±1° tracking error. The effect of different attributes in the cassegrain design on the acceptance angle are characterised and an equation given for the minimum separation distance required to ensure all light from the primary reflector is intercepted by the secondary reflector. Typically, large focal lengths are required for good acceptance angles to be realised, however in this design we have obtained an acceptance angle of 1.2° for a primary reflector with focal length 200 mm. This in depth optimisation also allows for an optical efficiency of >55% to be maintained up to ±1.5° tracking error.

More importantly, the simulation method presented in this paper considers the surface quality of the optical components, the surface structure of the reflective and refractive optics are modelled using their material bidirectional scattering distribution function (BSDF). The BSDF is associated with the surface roughness through the total integrated scatter (TIS) of optical interfaces and dictates how light is transmitted or reflected from it. The BSDF is the combined function of the bidirectional reflectance distribution function (BRDF) and the bidirectional transmittance distribution function (BTDF). The BSDF is generally in the form of a mathematical formula, often encompassing discrete samples of measured data, which approximately models the actual surface behaviour. The bidirectional scattering distribution function radiometrically characterizes the scatter of light from a surface as a function of

the angular positions of the incident and scattered rays (Asmail, 1991; Breault Research Organization, 2012). A range of BSDF's are used in these simulations for the reflective and refractive components to represent the possible optical finishes they may have depending on material and manufacturing process. The BSDF's used are company provided models which are available in the ray tracing software ASAP's library of materials and associated light scattering profiles.

During the experimental testing, the dielectric material of the homogenising optic was found to be the source of significant loss due to poor stability and surface finish. The acceptance angle of the design was however proved and measurements excluding the homogeniser loss validated the performance of the primary and secondary reflectors. Of which, the primary reflector was manufactured out of plastic for an improved surface finish, weight and reduced cost. The experimental testing confirmed the materials use as a primary optical component in CPV technology.

3. Design Concept and geometric concentration ratio

A two-stage reflector type concentrator was explored due to the advantages of compactness and having an upward facing receiver (Welford and Winston, 1989). With the receiver situated in the base of the primary reflector (See Fig. 1), passive cooling methods are easier employed and the cell temperature is more manageable. The basic design for this solar concentrator employs a cassegrain set up of two parabolas (McDonald et al., 2007) as shown in Fig. 1. For this study we will be aiming for a geometric concentration ratio of 500× which requires, for a solar cell of 1 cm^2, an input area of at least 500 cm^2. This must also take into account the shadowing effect of the secondary reflector.

In ideal conditions this set up should produce a concentrated uniform irradiance distribution upon a solar cell placed in the base of the 1st reflector. Light rays from the sun however are not parallel and have a small divergence of ±0.27°, resulting in a diffused focusing point. This can be compensated for by adjusting the reflective dishes to be afocal, so they are no longer coincident, and finding the optimum position of the secondary reflector with respects to the primary reflector and receiver.

The focal point, f, radius, r, and depth, y, of a parabola are related through Eq. (1) (McDonald et al., 2007).

$$r^2 = 4fy \tag{1}$$

where the focal length can be related to the Radius of Curvature (ROC), through Eq. (2), which should be noted is not the same as the curvature, k, which can be defined as the rate of change of the angle θ with respect to the distance, s, travelled along the curve (Victoria et al., 2013).

$$2f = ROC = \frac{1}{k} = \frac{1}{|\partial\theta/\partial s|} \tag{2}$$

From Eq. (2) it can be assumed a lower curvature produces a better tolerance to error. Wither the error is in incident light angle or curve manufacturing. A larger focal length is hence desired for a better acceptance angle, however the secondary reflector focal length and curvature will also have an effect.

From Fig. 1, the reflector dimensions can be related through angle A, the maximum value of θ which light rays can make with the vertical and still pass through the focal point. It determines the utmost limit that light can strike the inside curve of the primary reflector and is related to the reflector's parabolic parameters via Eq. (3) (Roman et al., 1995).

$$\frac{f_1}{2r_1} = \frac{1}{4\tan(A/2)} = \frac{f_2}{2r_2} \tag{3}$$

Angle A links both reflectors dimensions to each other when they are coincident. When they are not coincident Eq. (3) no longer holds and care must be taken to ensure the secondary reflector still accommodates all rays being reflected with angle A. It should also be noted that square cut parabolic reflectors were chosen for the primary collector and secondary reflector in order to increase the packing factor when the primary reflectors are arranged side by side in an array system. The width, w, of a reflector is related to

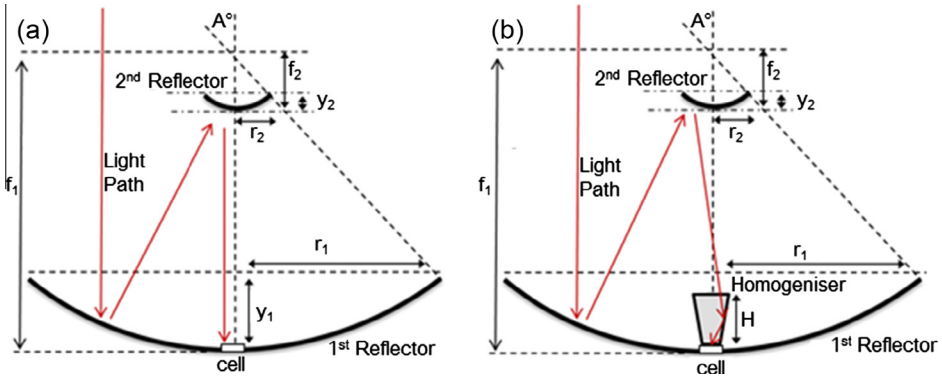

Fig. 1. Diagrams of the theoretical path for parallel light incident on a parabolic reflector, reflecting towards the focal point and then reflecting from the 2nd parabolic reflector to (a) become parallel again or (b) focus on the surface of a homogeniser.

the radius, r, through Pythagoras as shown in Fig. 2 and is now the one of the main factors determining how much light with angle A is captured.

To efficiently capture the light from reflected from the primary dish, the secondary dish should be as large as possible with a large focal length to improve acceptance angle, according to Eq. (2). However, to large a secondary component will cause significant shadowing, increasing the primary reflectors width to maintain 500× geometric concentration and increase strain on the cover glass to which the secondary is attached. The width of the secondary reflector was hence chosen to be a maximum of 50 mm as a suitable size and weight that will not incur excessive shadowing or difficulties in manufacturing and assembly. The following relationship was then formed to calculate the separation distance (SD) between the two reflectors required to collect all rays given the secondary reflector width and primary collector focal length and radius:

$$SD = f_1 - \left(\frac{0.5w}{\tan\left(2\tan^{-1}\left(\frac{r_1}{2f_1}\right)\right)} \right) \quad (4)$$

The radius of the primary reflector, r_1, is also dependent on the width, w, to ensure a geometric concentration ratio of 500× is reachable. In this way, taking w as 50 mm, results in a r_2 of 35.4 mm and r_1 of 162.6 mm as illustrated in Fig. 2.

4. Effect of separation distance on optical tolerance

Combinations of varying primary and secondary reflector focal lengths were carried out next, investigating the displacement of the final ray positions due to a 1° tracking error. The secondary reflector width, w was taken as 50 mm, r_1 as 162.6 mm, f_1 was varied between 150 and 220 mm and f_2 varied between 50 and 80 mm The separation distance was also changed as discussed earlier, calculated using Eq. (4) above, to accommodate all rays from the primary reflector.

Larger separation distances result in lower ray displacement and hence a higher tracking tolerance as shown in Fig. 3. There is a cluster of results situated at a ray displacement of ~10 mm, this is due to the light rays focusing before the receiver and diverging out in all directions including towards the receiver and the normal. The separation distance is linked to the primary reflector focal length which counter intuitively (Eq. (2)) must be decreased to gain a better optical tolerance by increasing the separation distance (Eq. (4) and Fig. 3). Next, the homogeniser is introduced to allow for a larger separation distance and improve the irradiance uniformity upon the cell. The homogeniser is of a square pyramid shape, positioned upside down without a point as shown in Fig. 1 and later in Fig. 5. It can be made of either metal with reflective inside walls or can be a solid transparent homogeniser so

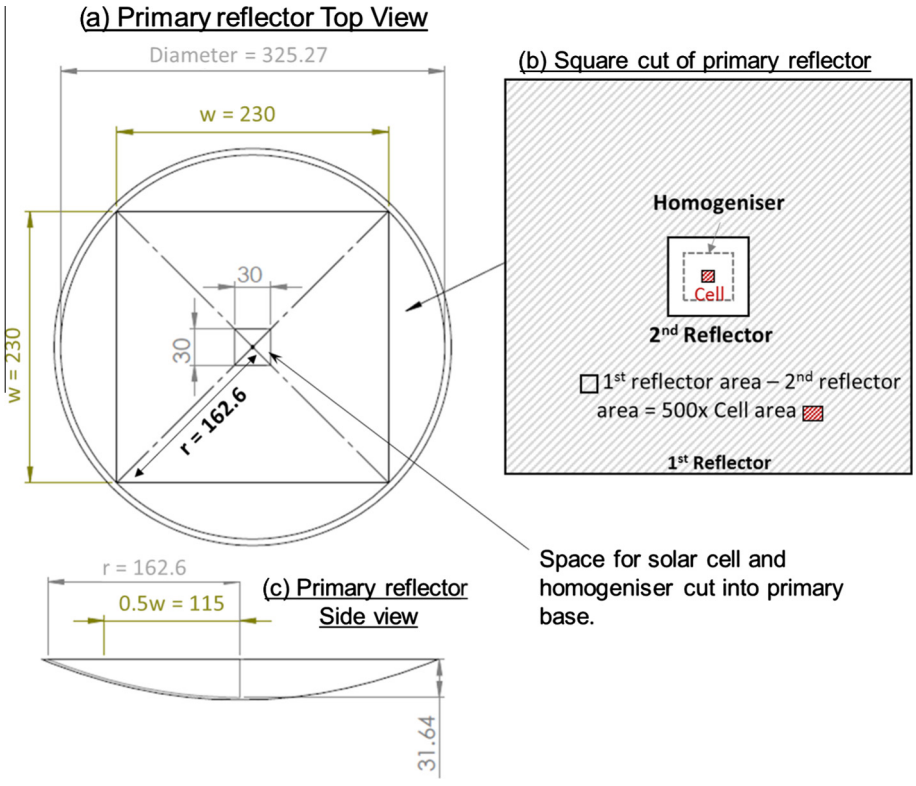

Fig. 2. Schematic of square cutting and shape matching of reflectors, homogeniser and solar cell. All dimensions are given in mm. (a) Top view of inside square cut of original circular primary reflector dish with a square hole in the base for the receiver assembly and homogeniser. (b) Top view of all square components in central alignment with the solar cell. (c) Side view of original circular primary reflector from (a) showing depth, radius and resulting half width after square cut.

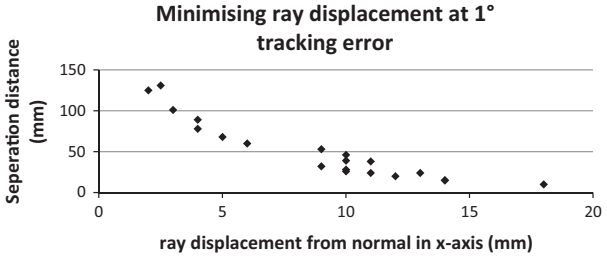

Fig. 3. Graph of separation distance against ray displacement from position of normal alignment with the sun due to a tracking error of 1°. Displacement measurements only taken in *x*-axis but due to the symmetry of the system represent the displacement incurred in *y*-axis as well.

as to take advantage of total internal reflection (TIR) at the sloped sides of the homogeniser.

5. Effect of homogeniser

Taking the same range of focal lengths as used before for the separation distance investigation but focusing simulations to the ~200 mm and ~70 mm focal length combination, rough dimensions of the homogeniser were next determined. The focal lengths of the primary concentrator and secondary reflector were investigated with a metal homogeniser (mirrored sides), aiming for high optical efficiencies. The reflectivity of the homogeniser walls were initially taken to be 95% for the optimisation procedure and a shortlist of parameter combinations were found from various simulation testing and shown in Fig. 4(a) below.

The initial optical efficiency at normal incidence in Fig. 4 (a) is due to the reflection loss at the primary reflector, secondary reflector, and third stage homogeniser. The sharp decline in optical efficiency from 1° to 1.5° seen is due to an increase in the number of reflections within the homogeniser, each costing 5% of optical efficiency (reflective losses), and because of light passing by the homogeniser (diverging by >10 mm). The acceptance angle can hence be increased by using a transparent solid homogeniser, which utilises total internal reflection to direct the rays towards the receiver and optimising the width. For this, the parameters obtaining the highest optical efficiency at normal incidence (f1 = 200 mm, f2 = 70 mm and H = 70 mm from Fig. 4(a)) were investigated further for optimisation as shown in Figs. 4(b) and 6. The optimum parameters from Fig. 4(b) were found to be that of f1 = 200 mm, f2 = 70 mm, H = 75 mm and SD = 162 mm.

Ideally the output face of the homogeniser, where the receiver is placed, is the exact size of the receiver to avoid loss. An output face of 10.1 mm × 10.1 mm was taken, instead of 10 mm × 10 mm as a tolerance measure and the homogenisers height and entry aperture width were optimised further (Figs. 5 and 6).

For maximum acceptance angle, the light rays reflected from the secondary reflector should come to a focus upon entering the homogenisers input surface and the input surface width should be large enough to collect offset rays due to tracking errors (Fig. 5). Increasing the width however also decreases the gradient of the sloped sides, resulting in more rays not meeting the criteria for TIR and passing through the walls of the homogeniser (Fig. 5b). This can be balanced by expanding the height of the homogeniser, but again this tends to an increasing number of rays being lost due to more incurred reflections. Various parameter combinations were investigated in an attempt to find the optimum scenario (Fig. 6).

The most promising system parameter combination for tracking tolerance was chosen to be that with a homogeniser height of 75 mm, an input width of 30 mm and a separation distance between the two reflectors of 162 mm. This configuration maintains an optical efficiency of 84.82–81.89% over ±1° tracking error and 55.49% optical efficiency at a tracking error of 1.5°. This is assuming a reflection loss of 5% at the primary and secondary and hence could be higher or lower depending on the mirror quality. The surface quality of the reflective dishes and the refractive homogeniser will both have an effect on the final optical efficiency of the system and is discussed further in the practical considerations and error analysis section.

The irradiance distribution of each set of parameter configurations was also recorded, all of which followed a

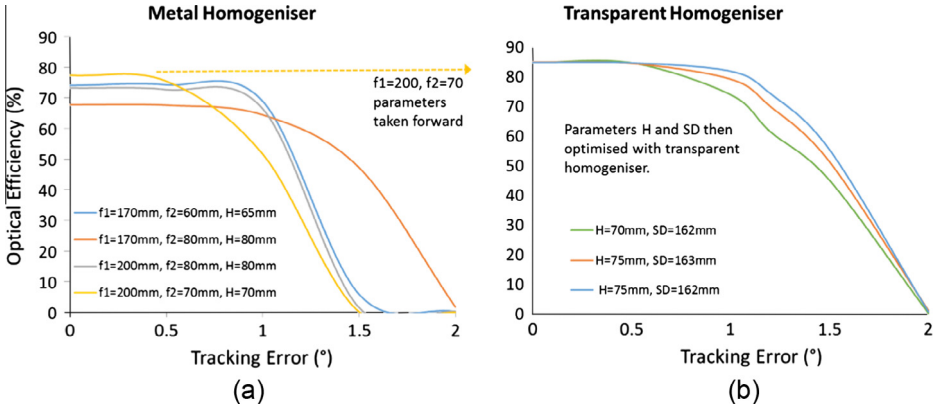

Fig. 4. Graph of optical efficiency as tracking error is increased in the horizontal axes whilst using (a) a metal homogeniser and (b) a solid transparent homogeniser. Where f1 and f2 are the focal lengths of the primary and secondary reflectors, H represents the height of the homogeniser and SD represents the Separation Distance between the two reflectors. In (b) f1 and f2 are 200 mm and 70 mm for all 4 results with varying H and SD.

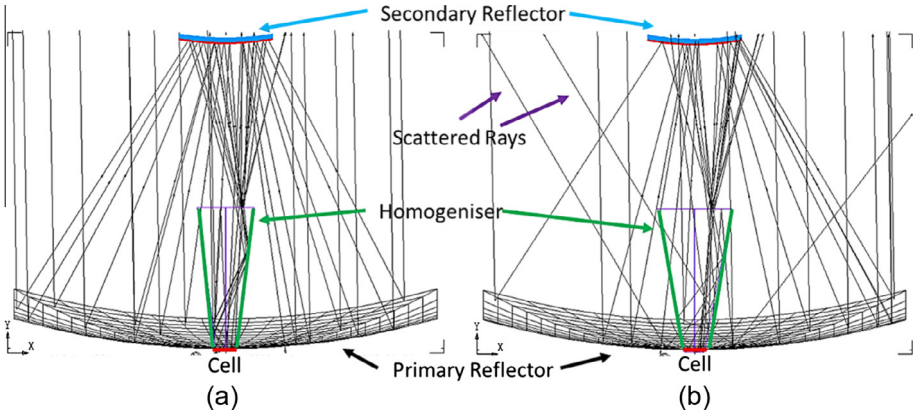

Fig. 5. 3D ray trace diagrams of rays with an incidence angle of 1° and a solid transparent homogeniser with (a) the optimised homogeniser dimensions and (b) showing an increased homogeniser input width (which results in more rays refracting out of the homogeniser instead of undergoing TIR).

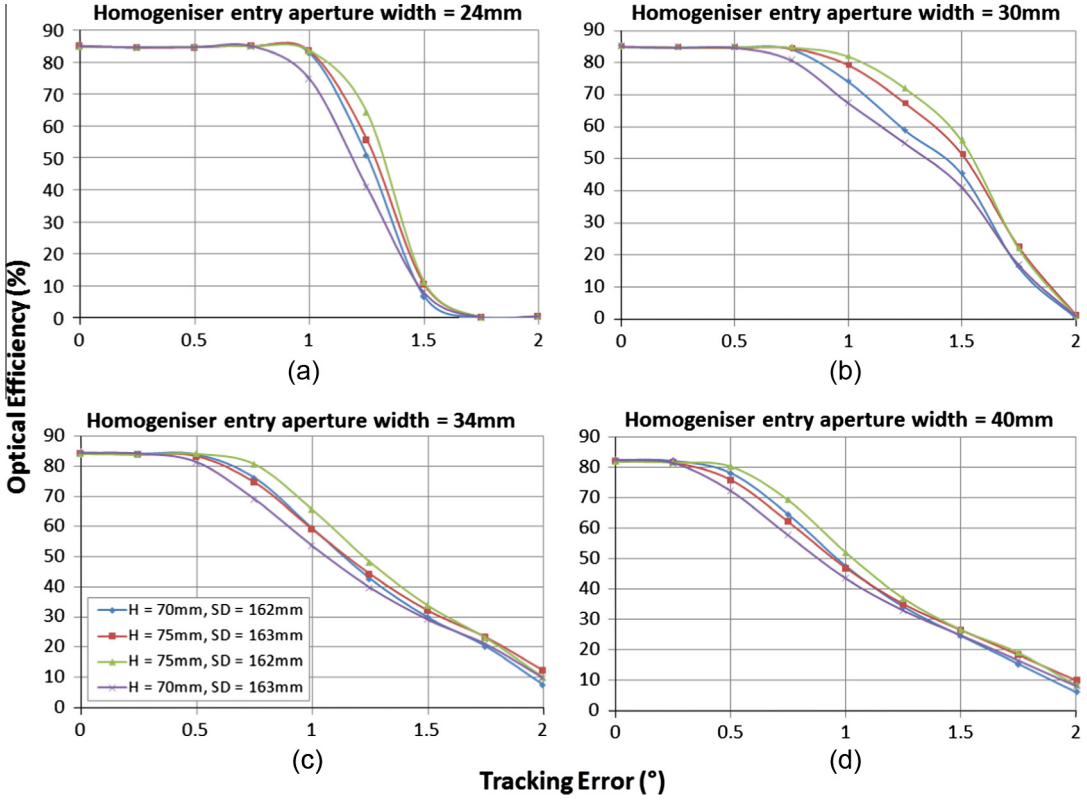

Fig. 6. Graph of resulting tracking tolerance from different combinations of homogeniser parameters and separation distance where H represents Homogeniser height in mm, W represents the input face width in mm and the separation distance, SD, is either 163 mm or 162 mm.

similar trend with increasing tracking error as shown below in Fig. 7.

The crossed pattern observed in Fig. 7(a), is due to less light reflecting directly from the corners of the homogeniser walls. The flux distribution at normal incidence is relatively well distributed and although this declines with increasing tracking error as expected, the change in irradiance across the cell is gradual, there are no sharp peaks of high irradiance. From Fig. 7 above it can be seen the maximum flux increases with tracking error, from 0.585 W/sq-mm in (a) to 0.723 W/sq-mm in (b) and 1.1 W/sq-mm in Fig. 7(c), before returning down to 0.441 W/sq-mm in (c). The *x*-axis and *z*-axis flux profiles however remain at a gradual incline. As the tacking error increases the light rays are reflected first by one of the side walls of the homogeniser then by both, shifting the irradiance distribution from one corner of the cell through to the other side, depending on the direction the tracking error is incurred. At 1.5° tracking error, Fig. 7(d), roughly half of the light rays are lost by not being captured by the homogeniser at the entry aperture, or reflecting at an angle greater than that for TIR.

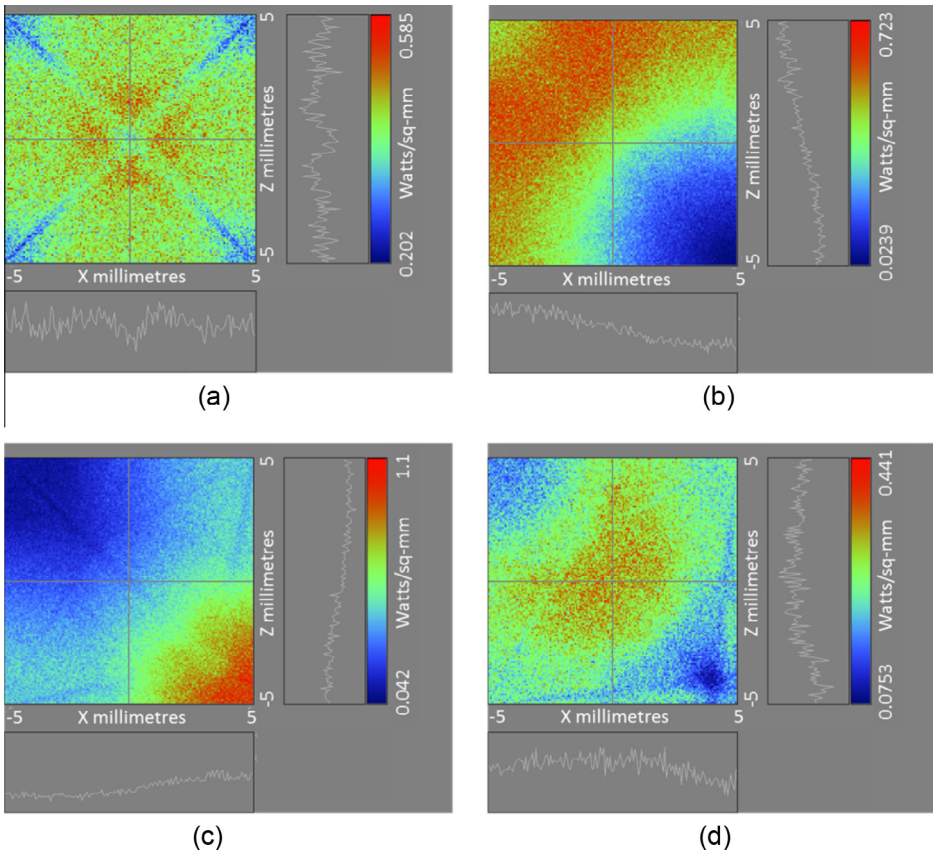

Fig. 7. The irradiance distribution upon the receiver with increasing tracking error for the chosen system parameter configuration with: (a) No tracking error; (b) 0.5° tracking error; (c) 1° tracking error and (d) 1.5° tracking error.

6. Practical considerations and error analysis

6.1. Dimensional and alignment errors due to manufacturing

Possible errors in the dimensions of the individual components have been considered in the design process of the proposed system. Errors in the width of the primary collector and secondary reflector will affect the geometrical concentration ratio and possibly the tracking tolerance range if large enough. Errors in the horizontal alignment of the two parabolic reflectors will have a similar effect to tracking error so are not as detrimental due to the use of the homogeniser but would offset the optical efficiency shown in Fig. 6 by the horizontal error incurred. The vertical error in the separation distance between the primary collector and secondary reflector can decrease the optical efficiency but the effect is only noticeable at tracking errors >0.5° and is still relatively small at ±1° error as shown in Fig. 6. The optical efficiency can drop from 81.89% to 79.21% due to a ±1 mm vertical error at a tracking error of ±1°. The accuracy of the homogenisers' exit aperture dimensions (Fig. 8) and its alignment with the cell are the main sources of loss when considering dimensional and alignment errors for this design.

Perfect alignment with the cell and a homogeniser exit aperture of 10 × 10 mm obtains a maximum of 86.46% optical efficiency. With a 0.1 mm alignment tolerance, the exit aperture dimensions, 10.1 mm × 10.1 mm, produces a maximum of 84.82% optical efficiency and decreases by ~1.7% (absolute value) for every 0.1 mm increase in the area dimensions as shown in Fig. 8. At present time, moulds of the homogeniser are achieving an accuracy of ±0.2 mm, resulting in an uncertainty of ±3.3% optical efficiency (absolute value).

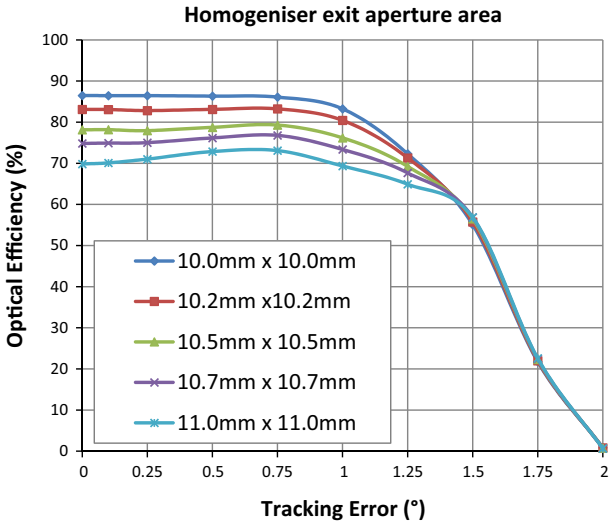

Fig. 8. Varying homogeniser output face area and the effect on optical efficiency with increasing tracking error.

6.2. Material and surface imperfections

Fig. 9 confirms that no light rays are lost within the system at normal incidence as shown by the 'ideal' scenario results. Although a reflectance loss of 5% was assumed for finding the optimum design requirements, manufacturing limitations in the prototyping stage may result in a lower reflectance. When simulating the primary and secondary reflectors with a BSDF of polished aluminium there is around 10% reflectance loss at both surfaces. The focus of the rays also widens due to the increase in scattering from these two surfaces. This reflection loss on both dishes causes a significant drop in optical efficiency as shown in Fig. 9. There are materials and coatings with improved reflectance (Shanks et al., 2015) such as silver (~97% reflectance) but degradation and/or expense are common problems with such high quality optics. On entering the homogeniser, there is a small amount of energy loss where some light is reflected away instead of refracting into the dielectric material. This can be improved with antireflection coatings and special textures of the homogeniser surface but again this is expensive (Huang et al., 2012; Zhou et al., 2013). The surface roughness of the homogeniser is a main factor causing a drop in optical efficiency and lowering the acceptance angle depending on the material used in manufacturing. There is a severe drop especially for the BSDF's related to poorer surface finishes as shown in Fig. 9. These BSDF's were selected from a database of expected BSDF's of optical finishes available from companies. The BSDF's were chosen simply to give a good range. Typical surface quality would be expected to be in the upper region of these samples. More accurate solar trackers and accurately built systems would not suffer as significantly if within ±0.5° accuracy but these incur further expense as well.

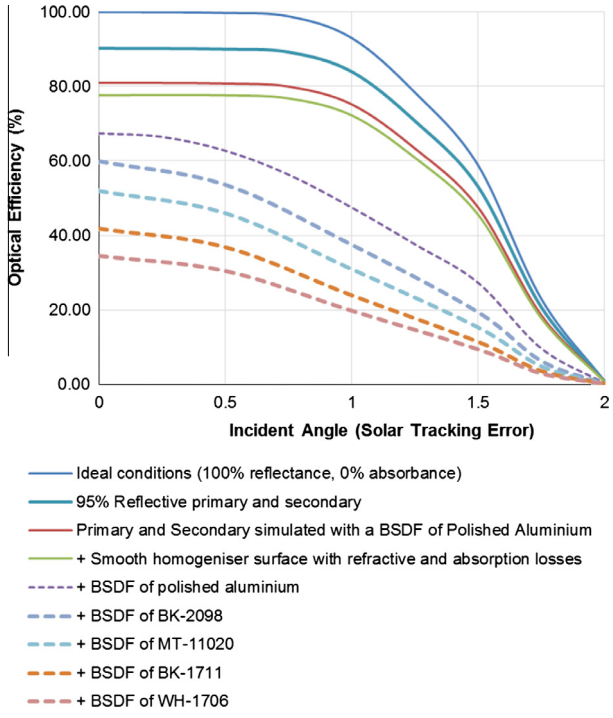

Fig. 9. Practical losses summary. Optical efficiency decreases as realistic surface losses are added in stages. The dashed lines represent possible surface finishes of the homogeniser depending on which material and manufacturing process is employed (Shanks et al., 2016b).

7. Manufacturing of prototype

In this study, a primary reflector dish was computer numerical control (CNC) machined out of a high temperature form of ABS plastic to take advantage of the lightweight and surface smoothness of the material. The dish was then vacuum metallised and a reflectance of ~90% measured. The secondary reflector was made of solid aluminium due to the high concentration of light and temperature it would be subject to. Similarly this was CNC'd but then polished. The homogeniser was moulded using sylgaurd which had a measured absorbance of ~6% over the working wavelength range of the solar cell to be used but the overall optical efficiency depends on the surface structure and angle of incident light when entering the homogenizer (some reflection loss and scattering). A prototype of the optimum design was manufactured as a 3 by 3 module as shown in Fig. 10 below.

8. Experimental investigation

The module was tested by the Helios 3198 solar simulator (Fig. 11) Domínguez et al., 2008 at the Centre for

Fig. 10. Photo of 3 by 3 cassegrain concentrator prototype from (a) top view and (b) side view. (a) Shows the concentration of sunlight onto the homogenisers and solar cells.

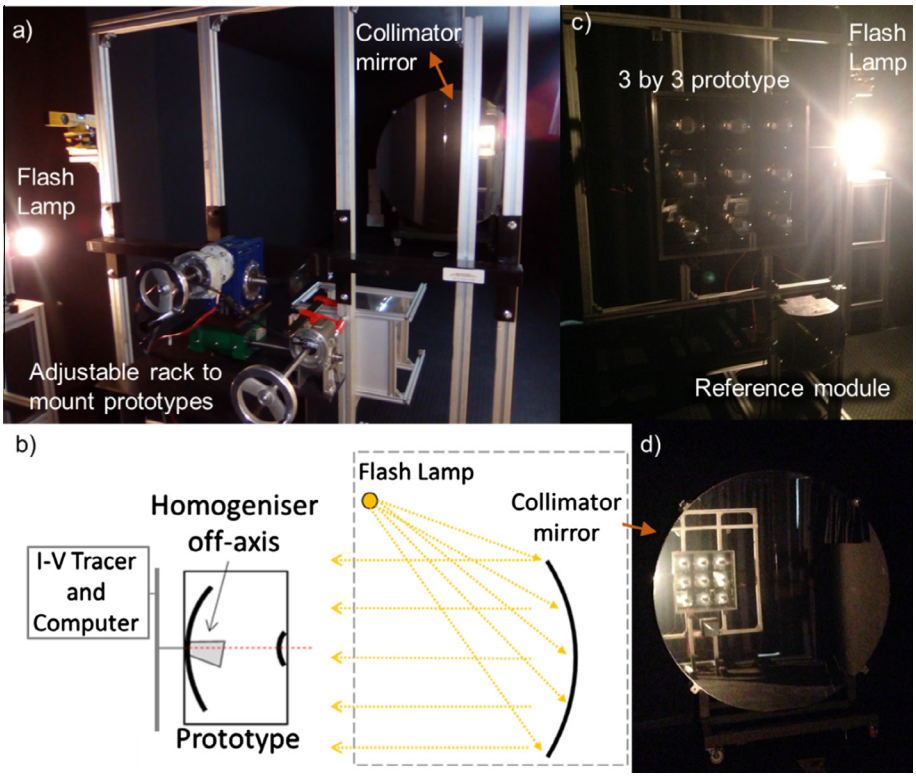

Fig. 11. (a) Photo of Helios 3198 solar simulator taken from behind adjustable mounting rack showing flash lamp and collimator mirror. (b) Schematic diagram showing set up of solar simulator and the tilting homogeniser within the prototype when mounted. (c) Photo of 3 by 3 prototype mounted on rack for testing. (d) Photo of collimator mirror on opposite of the room with reflection of prototype.

Advanced Studies in Energy and Environment (CEAEMA) at the University of Jaen in Southern Spain (Fernández et al., 2012) under 850 W/m^2. The Helios has a collimation angle of ±0.4° and matches the spectrum of AM1.5D. It is a very powerful flash simulator for measuring the performance of concentrator photovoltaic modules and allows accurate analysis of the acceptance angle of such modules (Domínguez et al., 2008).

Initial measurements showed challenges with the stability of the Homogeniser optic. Due to the small contact area of the homogeniser with the solar cell and base (10 × 10 mm contact area), and the flexibility of the material used (sylgaurd), when the full system was rotated towards the solar simulator (Fig. 11) the homogeniser also leaned out of alignment with the primary and secondary reflectors (shown in Fig. 11). Further investigation with the homogeniser optic proved it has an increased optical loss resulting in the full system only performing at ~40% optical efficiency instead of the anticipated ~65% at normal incidence (Fig. 12). The output of the measured system as the misalignment angle was increased did not drop as sharply as expected from the results suggested in Fig. 9. This suggests that the homogeniser has a surface scattering profile close to that of BK-1711 in Fig. 9 but the tilting issue and perhaps the connecting medium to the solar cell reduces the normal incidence maximum. The experimental measurements shown in Fig. 12 however confirm the acceptance angle of the designed system.

Equivalent measurements were taken without the homogeniser and instead a solar cell of increased size used at the position of the homogenisers entry aperture (where the light focuses). This test proves the efficiency of the primary and secondary reflectors follows simulation predictions and only the homogenising optic needs replacement. The acceptance angle without the homogeniser however is much smaller as expected and the maximum optical efficiency at normal incidence is slightly increased due to the removal of the homogenisers refractive losses (Fresnel reflection upon entry, absorption, scattering). A higher optical grade glass homogeniser would increase the acceptance angle of these practical results which would then lead to an expected performance similar to the uppermost curve in Fig. 12. This will be the next step of experimental testing as well as increasing the geometric concentration ratio to 1500× with use of a smaller solar cell and redesigned homogenising optic.

9. Conclusion

The tracking tolerance and optical efficiency of a cassegrain type solar concentrator was optimised through the use of ray trace analysis to achieve high optical efficiencies of 84.82% at normal incidence, 81.89% at ±1° tacking error and 55.49% at ±1.5° tracking error for high optical grade components. The optimised design was found to be with a primary parabolic reflector of focal length 200 mm and

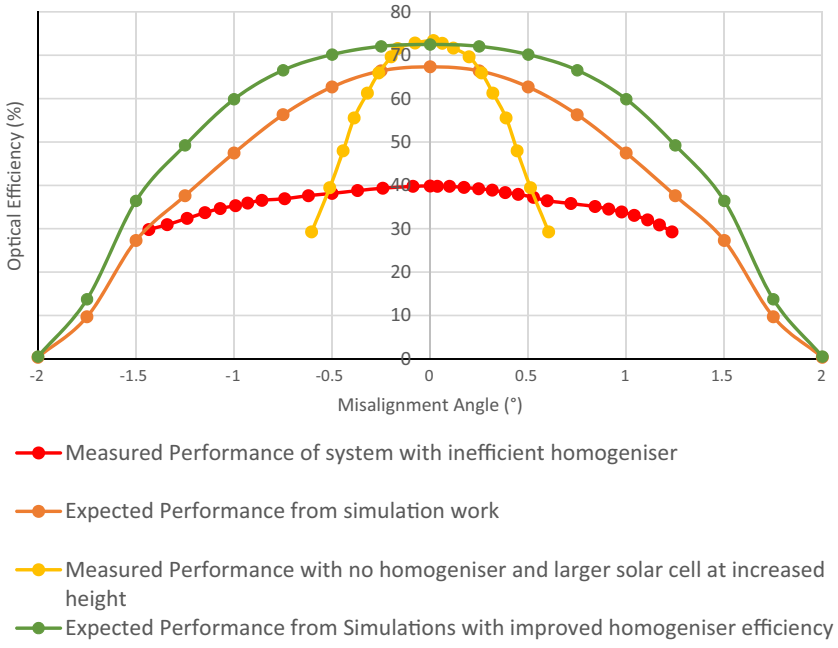

Fig. 12. Comparison of Expected performance from simulation and real case measured performance.

a secondary inverse parabolic reflector of focal length 70 mm placed 162 mm from the primary collector. The optimised system required a solid transparent homogeniser of height 75 mm with an entry aperture of 30 mm × 30 mm and exit aperture of 10 mm by 10 mm. The use of the homogeniser not only improves the tracking tolerance and the irradiance distribution but also allows more flexibility in the manufacturing and assembly of the design. The detailed characterisation of the proposed system, as well as the separation distance equation, may be beneficial in the design of parabolic reflector systems. It may also benefit single stage lens systems (that focus onto a homogeniser), as a guideline to help improve an aspect of the system dependent on alignment, focusing area or uncertainties. Manufacturing uncertainties were considered and the material and surface structure of the homogeniser in particular proved to be the biggest source of loss. This was confirmed in experimental tests of the prototype where the module produced 40% of the ideal 500× power output from the cell instead of the anticipated ~65% from simulation work. However, the designed acceptance angle of ~1° appears to be confirmed. The primary and secondary reflectors follow simulation predictions in performance and redirect the light to the desired focusing area with ~90% reflectance efficiency. This is a key result as reflective optics of a specific 3D shape are not always manufactured accurately at the prototype stage for an acceptable cost. This result also validates the ABS plastic material for use as a CPV primary optic and reinforces the benefit of investigating more materials for CPV applications. Further outdoor testing is required over prolonged periods and a remodel of the homogeniser with a 5.5 × 5.5 mm solar cell will be carried out to increase the geometric concentration ratio to 1500×.

Acknowledgments

This work has been carried out as a part of BioCPV project jointly funded by DST, India (Ref No: DST/SEED/INDO-UK/002/2011) and EPSRC, UK, (Ref No: EP/J000345/1). J.P. Ferrer-Rodriguez is supported by the Spanish Economy Ministry and the European Regional Development Fund/Fondo Europeo de Desarrollo Regional (ERDF/FEDER) under the project ENE2013-45242-R. Authors acknowledge the funding agencies for the support. In support of open access research all underlying article materials (such as data, samples or models) can be accessed upon request via email to the corresponding author.

References

Akisawa, A., Hiramatsu, M., Ozaki, K., 2012. Design of dome-shaped non-imaging Fresnel lenses taking chromatic aberration into account. Sol. Energy 86, 877–885. http://dx.doi.org/10.1016/j.solener.2011.12.017.

Asmail, C., 1991. Bidirectional scattering distribution function (BSDF): a systematized bibliography. J. Res. Natl. Inst. Stand. Technol. 96, 215. http://dx.doi.org/10.6028/jres.096.010.

Benitez, P., Cvetkovic, A., Winston, R., Reed, L., 2006. New High-Concentration Mirror-Based Kohler Integrating Optical Design for Multijunction Solar Cells. Int. Opt. Des., Washington, D.C.: OSA; p. TuD3. http://dx.doi.org/10.1364/IODC.2006.TuD3.

Breault Research Organization. ASAP Technical Guide: Scattering in ASAP 2012:17–21. http://www.breault.com/sites/default/files/knowledge_base/brotg0922_scatter_1.pdf (accessed October 12, 2015).

Brogren, M., Helgesson, A., Karlsson, B., Nilsson, J., Roos, A., 2004. Optical properties, durability, and system aspects of a new aluminium-polymer-laminated steel reflector for solar concentrators. Sol. Energy Mater. Sol. Cells 82, 387–412. http://dx.doi.org/10.1016/j.solmat.2004.01.029.

Chaves, J., 2008. Introduction to Nonimaging Optics. CRC Press.

Chen, Y.T., Ho, T.H., 2013. Design method of non-imaging secondary (NIS) for CPV usage. Sol. Energy 93, 32–42. http://dx.doi.org/10.1016/j.solener.2013.03.013.

Chong, K.K., Lau, S.L., Yew, T.K., Tan, P.C.L., 2013. Design and development in optics of concentrator photovoltaic system. Renew. Sustain. Energy Rev. 19, 598–612. http://dx.doi.org/10.1016/j.rser.2012.11.005.

Domínguez, C., Antón, I., Sala, G., 2008. Solar simulator for concentrator photovoltaic systems. Opt. Express 16, 14894–14901. http://dx.doi.org/10.1364/OE.16.014894.

Dreger, M., Wiesenfarth, M., Kisser, A., Schmid, T., Bett, A.W., 2014. Development and investigation of a CPV module with cassegrain mirror optics. CPV-10.

Fang, H., Guo, P., Yu, J., 2006. Surface roughness and material removal in fluid jet polishing. Appl. Opt. 45, 4012–4019. http://dx.doi.org/10.1364/AO.45.004012.

Fernández, E.F., Pérez-Higueras, P., Garcia Loureiro, A.J., Vidal, P.G., 2012. Outdoor evaluation of concentrator photovoltaic systems modules from different manufacturers: first results and steps. Prog. Photovoltaics Res. Appl. http://dx.doi.org/10.1002/pip.1262, n/a – n/a.

Goldstein, A., Gordon, J.M., 2011. Tailored solar optics for maximal optical tolerance and concentration. Sol. Energy Mater. Sol. Cells 95, 624–629. http://dx.doi.org/10.1016/j.solmat.2010.09.029.

Gordon, J.M., Katz, E.a., Feuermann, D., Huleihil, M., 2004. Toward ultrahigh-flux photovoltaic concentration. Appl. Phys. Lett. 84, 3642. http://dx.doi.org/10.1063/1.172369.

Gordon, J.M., Feuermann, D., Young, P., 2008. Unfolded aplanats for high-concentration photovoltaics. Opt. Lett. 33, 1114–1116.

Guo, S., Zhang, G., Li, L., Wang, W., Zhao, X., 2009. Effect of materials and modelling on the design of the space-based lightweight mirror. Mater. Des. 30, 9–14. http://dx.doi.org/10.1016/j.matdes.2008.04.056.

Han, J.-Y., Kim, S.-W., Han, I., Kim, G.-H., 2008. Evolutionary grinding model for nanometric control of surface roughness for aspheric optical surfaces. Opt. Express 16, 3786–3797. http://dx.doi.org/10.1364/OE.16.003786.

Huang, C.K., Sun, K.W., Chang, W.-L., 2012. Efficiency enhancement of silicon solar cells using a nano-scale honeycomb broadband antireflection structure. Opt. Express 20, A85–A93.

Languy, F., Habraken, S., 2013. Nonimaging achromatic shaped Fresnel lenses for ultrahigh solar concentration. Opt. Lett. 38, 1730–1732.

Languy, F., Lenaerts, C., Loicq, J., Thibert, T., Habraken, S., 2013. Performance of solar concentrator made of an achromatic Fresnel doublet measured with a continuous solar simulator and comparison with a singlet. Sol. Energy Mater. Sol. Cells 109, 70–76. http://dx.doi.org/10.1016/j.solmat.2012.10.008.

Luque, A., Andreev, V.M., 2007. Concentrator photovoltaics. http://dx.doi.org/10.1007/978-3-540-68798-6.

McDonald, M., Horne, S., Conley, G., 2007. Concentrator design to minimize LCOE; 6649:66490B – 66490B – 11. http://dx.doi.org/10.1117/12.735738.

Miñano, J.C., Gonźlez, J.C., Benítez, P., 1995. A high-gain, compact, nonimaging concentrator: RXI. Appl. Opt. 34, 7850–7856. http://dx.doi.org/10.1364/AO.34.007850.

Roman, R.J., Peterson, J.E., Goswami, D.Y., 1995. An off-axis cassegrain optimal design for short focal length parabolic solar concentrators. J. Sol. Energy Eng. 117, 51. http://dx.doi.org/10.1115/1.2847742.

Schröder, S., Duparré, A., Coriand, L., Tünnermann, A., Penalver, D.H., Harvey, J.E., 2011. Modeling of light scattering in different regimes of surface roughness. Opt. Express 19, 9820–9835. http://dx.doi.org/10.1364/OE.19.009820.

Shanks, K., Senthilarasu, S., Mallick, T.K., 2015. High-Concentration Optics for Photovoltaic Applications. In: Pérez-Higueras, P., Fernández, E.F. (Eds.), High Conc. Photovoltaics Fundam. Eng. Power Plants, 1st ed. Springer International Publishing, Cham, pp. 85–113. http://dx.doi.org/10.1007/978-3-319-15039-0.

Shanks, K., Senthilarasu, S., Mallick, T.K., 2016a. Optics for Concentrating Photovoltaics: trends, limits and opportunities for materials and design. Renew. Sustain. Energy Rev. 60, 394–407.

Shanks, K., Baig, H., Senthilarasu, S., Reddy, K.S., Mallick, T.K., Baig, H., et al., 2016b. Conjugate refractive–reflective homogeniser in a 500× cassegrain concentrator: design and limits. IET Renew. Power Gener., 1–8 http://dx.doi.org/10.1049/iet-rpg.2015.0371.

Terry, C.K., Peterson, J.E., Goswami, D.Y., 1996. Feasibility of an iodine gas laser pumped by concentrated terrestrial solar radiation. J. Sol. Energy Eng. 118, 136. http://dx.doi.org/10.1115/1.2848006.

Terry, C.K., Peterson, J.E., Goswami, D.Y., 2012. Terrestrial solar-pumped iodine gas laser with minimum threshold concentration requirements. J. Thermophys. Heat Transf.

Victoria, M., Dominguez, C., Askins, S., Anton, I., Sala, G., 2013. Experimental analysis of a photovoltaic concentrator based on a single reflective stage immersed in an optical fluid. Prog. Photovoltaics Res. Appl. http://dx.doi.org/10.1002/pip.2381.

Welford, W.T., Winston, R., 1989. High Collection Nonimaging Optics. Elsevier. http://dx.doi.org/10.1016/B978-0-12-742885-7.50002-4.

Winston, R., Miñano, J.C., Benítez, P., Shatz, N., Bortz, J.C., 2005. Nonimaging Optics. Elsevier. http://dx.doi.org/10.1016/B978-012759751-5/50013-0.

Yavrian, A., Tremblay, S., Levesque, M., Gilbert, R., 2013. How to increase the efficiency of a high concentrating PV (HCPV) by increasing the acceptance angle to ±3.2°. 9TH Int. Conf. Conc. Photovolt. Syst. CPV-9. AIP Conf. Proc., vol. 1556, p. 197–200. http://dx.doi.org/10.1063/1.4822230.

Yehezkel, N., Appelbaum, J., Yogev, a., Oron, M., 1993. Losses in a three-dimensional compound parabolic concentrator as a second stage of a solar concentrator. Sol. Energy 51, 45–51. http://dx.doi.org/10.1016/0038-092X(93)90041-L.

Zhou, G., He, J., Xu, L., 2013. Antifogging antireflective coatings on Fresnel lenses by integrating solid and mesoporous silica nanoparticles. Microporous Mesoporous Mater. 176, 41–47. http://dx.doi.org/10.1016/j.micromeso.2013.03.038.

[Article 3]

K. Shanks, H. Baig, S. Senthilarasu, K. S. Reddy, and T. K. Mallick, “Conjugate refractive–reflective homogeniser in a 500× Cassegrain concentrator: design and limits,” *IET Renew. Power Gener.*, vol. 10, no. 4 (Special Issue - Invited from PVSAT-11), pp. 440–447, Apr. 2016.

IET Renewable Power Generation

Special Issue: 11th Photovoltaic Science, Application and Technology Conference (PVSAT-11)

IET Journals
The Institution of Engineering and Technology

Conjugate refractive–reflective homogeniser in a 500× Cassegrain concentrator: design and limits

ISSN 1752-1416
Received on 11th August 2015
Revised on 10th November 2015
Accepted on 20th November 2015
doi: 10.1049/iet-rpg.2015.0371
www.ietdl.org

Katie Shanks[1] ✉, *Hasan Baig*[1], *Sundaram Senthilarasu*[1], *K.S. Reddy*[2], *Tapas K. Mallick*[1]

[1]*Environmental and Sustainability Institute, University of Exeter Penryn Campus, Penryn TR10 9FE, UK*
[2]*Heat Transfer and Thermal Power Laboratory, Department of Mechanical Engineering, Indian Institute of Technology Madras, Chennai 600 036, India*
✉ *E-mail: kmas201@exeter.ac.uk*

Abstract: In this study, we present the conjugate refractive reflective homogeniser (CRRH) to be used in a 500× Cassegrain photovoltaic concentrator. The CRRH is a dielectric crossed v-trough lined with a reflective film whilst maintaining an air gap between them. This air gap between the two surfaces helps in trapping the scattered light from the refractive geometry and ensures both total internal reflection and standard reflection of the escaped rays. A 10–42% drop in optical efficiency has been shown to occur due to varying the surface roughness of the homogeniser in these ray trace simulations for the Cassegrain setup. The CRRH increased the overall optical efficiency by a maximum of 7.75% in comparison with that of a standard refractive homogeniser simulated within the same concentrator system. The acceptance angle and flux distribution of these homogenisers was also investigated. The simple shape of the CRRH ensures easy manufacturing and produces a relatively uniform irradiance distribution on the receiver. The theoretical benefit of the CRRH is also validated via practical measurements. Further research is required but a 6.7% power increase was measured under a 1000 W/m^2 solar simulator at normal incidence for the experimental test.

1 Introduction

There is a growing interest in concentration photovoltaic (CPV) technologies due to their reduced need for photovoltaic (PV) material and higher potential efficiencies. Not only can CPV systems be the answer to reducing the cost of solar power but they are also more environmentally friendly than regular flat plate PV panels. Two reasons for this are: first, CPV technologies use less semiconductor material and second they have a smaller effect on the albedo change in an area than that of flat plate PV panels [1–3]. The Albedo is the percentage of incoming radiation reflected off a surface. Covering surfaces with dark coloured flat plate PV panels results in absorbing and emitting more thermal energy if the original surface was not initially of a similar dark colour (e.g. fields). Owing to the relatively low efficiency of flat plate PV panels in comparison with CPV, they convert more of the incoming radiation into heat rather than electricity. This method of PV can change the overall albedo of an area, and contribute to the effect of 'urban heat islanding' [1–3]. Higher-efficiency technologies transfer less of the absorbed energy into heat and do not affect the albedo of an area as significantly as that of flat PV panels [3].

As the concentration ratio of an optic is increased, it becomes more difficult to maintain a high optical efficiency, uniform irradiance distribution, and an acceptable optical tolerance for the system simultaneously [4]. Matching the output irradiance size and shape to the receiver size and shape affects all of these factors and non-uniform illumination has a detrimental impact on the solar cell performance [5]. A secondary optic or homogeniser element improves this and is needed to relax the demand on the system's accuracy [6, 7]. Some secondary concentrator optics include the compound parabolic concentrator (CPC) [8], the dome lens [9], the ball lens [10] and various homogenising light funnel geometries [11–13]. These typically take on the shape of an inverted cone or pyramid but there are also elliptical and hyperbolic optics possible [8, 14, 15].

One key consideration in all of the above named designs is the material to be used and the resulting surface quality. The surface roughness of total internal reflection (TIR) optics causes scattering of incoming light, reducing its performance from the ideal design.

Glass is typically the best choice for high-quality accurate optics but the strength, flexibility and light weight of plastics make polymers such as Polymethylmethacrylate (PMMA) the more economic option. PMMA is the most popular polymer used in CPVs and polyethylene is used widely in other areas but has a short lifetime. Polyamide, polystyrene, acrylics and polycarbonate have been investigated but more research is required [16]. Lenses may be manufactured by hot-embossing, casting, extruding, laminating, compression-moulding or injection-moulding thermoplastic PMMA [17]. Reflective optics also depend greatly on their surface quality. A silvered mirror using smooth glass produces a common mirror with reflectivity >85% but complex shapes are difficult and expensive. Reflective films are an alternative simple and effective option for reflective-based optics. They are lightweight, typically cheaper than solid polished metals and films with >90% reflectivity are available. Their application to surfaces, especially three-dimensional (3D) curves, can be difficult however [18]. Polymer mirror films are a more recent low-cost, low-weight option to gain >90% reflective surfaces but require specially designed structures to gain the correct shape [19, 20]. In terms of mirrors, vacuum metallising is the current best option but this process, such as refractive lenses, is again highly dependent on the material and surface quality [21, 22].

The surface structure of an optical element or the interface between two optical mediums, has a strong influence on the final direction of the reflected or refracted light. During design simulations, these optical surfaces are sometimes assumed ideally smooth with no scattered light losses. There is however no ideally smooth optical surface for lenses or mirrors and an inherent roughness is always present. The degree of this surface inhomogeneity depends on the manufacturing process and material used with higher-quality optical finishes and coatings costing more [23]. Manufacturing processes for optics include precise grinding, milling, polishing and a variety of coating methods for a smooth finish. Computer-controlled diamond turning machines, as well as

other modern materials and moulding techniques, have significantly improved the design and accuracy of refractive optics such as Fresnel lenses [24]. Similarly, computer-aided design and machining has improved the quality of reflective optics but in both cases good-quality prototyping can be expensive when requiring smooth and accurate geometries. Simple cost effective methods to improve the optical efficiency of optics are needed, whether the design is in a prototyping or final installation stage. There are several methods to measure the optical scattering of a surface, and hence various terms associated with its severity [25, 26]. Here, we will refer to the bidirectional scattering distribution function (BSDF) which is associated with the surface roughness of optical interfaces through the total integrated scatter and dictates how light is transmitted or reflected from it. The BSDF is the combined function of the bidirectional reflectance distribution function and the bidirectional transmittance distribution function. The BSDF is generally in the form of a mathematical formula, often encompassing discrete samples of measured data, which approximately models the actual surface behaviour. The BSDF radiometrically characterises the scatter of light from a surface as a function of the angular positions of the incident and scattered rays [27].

2 Design considerations

One commonly utilised and widely researched concentrator design is the Cassegrain concentrator which has the advantages of compactness and having an upward facing receiver [6]. With the receiver situated in the base of the primary reflector (see Fig. 1*a*), passive cooling methods are more easily employed and the cell temperature is more manageable. Surface imperfections however will reduce the optical efficiency at every stage. The primary and secondary dishes as shown in Fig. 1*a* will have an associated non-ideal reflectance. A reflective homogeniser optic would similarly suffer, especially if there are many reflections occurring within. A refractive medium takes advantage of TIR but again, surface roughness, scratches or any form of soiling is subject to refraction losses. This includes when the rays initially refract into the homogeniser and a small portion of energy is reflected instead of refracted. A simple but effective method to recover rays which fail TIR at the homogeniser walls is to use a reflective sleeve with an air gap [28] as shown in Figs. 1*b* and 1*c*. Baig *et al.* [29, 30] discuss the optical loss caused by the encapsulation medium used in connecting low-concentration optics to solar cells. Light rays incident in this overlap region do not reflect toward the solar cell but continue through the encapsulation medium until lost. Baig *et al.* [29, 30] overcame the encapsulation issue by adding a strip of reflective film to the bottom edge of the 3D cross CPC designed for building integration. We expand on this method by applying reflective film with an air gap to all of the TIR active walls of a homogeniser in a high-concentration Cassegrain concentrator. Hence, the conjugate refractive–reflective homogeniser (CRRH) is presented.

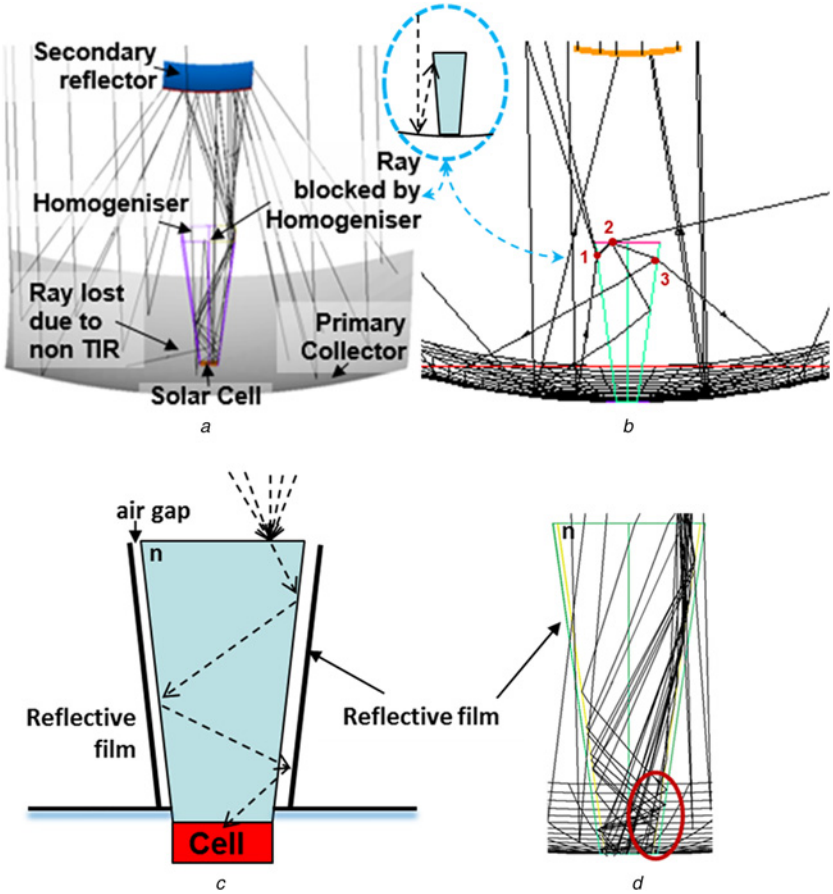

Fig. 1 *Design considerations*

a Ray trace simulation of Cassegrain concentrator at a tracking error of ±1.75°. Lost rays are shown including an inlet diagram of how a light ray can be blocked by the homogeniser on route to the secondary reflector. This 'blocked' ray can take various routes as shown in (b)

b Ray trace simulation showing possible processes of intercepted ray at homogeniser interfaces indicated by nodes 1, 2 and 3. At node 1, an intercepted ray from the primary reflector is either scattered away from the homogeniser and lost upwards or refracted into the homogeniser depending on the materials refractive index and surface structure. At node 2, the light can again either be scattered out of the homogeniser or scattered within the homogeniser. In reality, a number of rays would be dispersed in many directions at each node but only a few are shown here. Again each of these rays can either be reflected or refracted when incident on the homogenisers' walls as shown at node 3. It is possible that some of these rays find their way to the cell, though from the results obtained in these experiments their contribution is negligible

c Theoretical performance of CRRH with air gap between reflective films

d Ray trace diagram confirming that refracted rays can be caught by the reflective film (thick red circle)

2.1 Parameters and limitations

A previous study has been carried out to determine the dimensions of the primary and secondary reflectors as well as the homogeniser dimensions [31]. Overall, the design has a good acceptance angle of >1°. The homogeniser geometry is set such that a perfect surface should only loose a negligible percentage of energy due to light rays not meeting TIR (>0.01%). When increasing the misalignment with the Sun up to 2° an increase in light loss occurs in this design due to interception by the homogeniser after reflection from the large primary mirror (Figs. 1*a* and 1*b*) which increases loss. At <0.5°, misalignment of this loss is almost negligible but increases up to ∼1.7% at ±2° solar misalignment. This will limit the air gap and thickness of the reflective sleeve but would not be the case for other designs such as the Fresnel lens. In this paper, simulations with an increasing air gap between the refractive homogeniser surface and reflective film surface (Figs. 1*b* and 1*c*) were carried out. The solar cell size was 1 cm × 1 cm and the geometrical concentration ratio was 500×.

3 Simulation method

Simulations were carried out using Breault's Advanced System Analysis Program (ASAP) ray tracing software. The source was set to imitate energy from the Sun with 1000 W/m^2 and a divergence angle of ±0.27°. The homogeniser material is set as SHOTT BK7, with a dispersion curve as shown in Fig. 2. This is a commonly used medium and has a higher refractive index than others such as PMMA. The homogeniser will be made out of a material with a similarly stable and high refractive index to SHOTT BK7 (to improve TIR within).

For measurements of the air gap thickness, the BSDF of the homogeniser was chosen to be similar to that of standard polished aluminium, following the Harvey model. This model was chosen as the homogeniser will be moulded from an aluminium casing with polished inner surfaces.

Simulations were carried out assuming first the scenario of perfect surface qualities and 100% reflectance for reflectors and 0% absorbance for the homogeniser. About ∼10% reflectance loss is then assumed for the two reflective dishes assuming their surfaces follow the polished mirror BSDF (Fig. 3*a*). The losses incurred when the light rays refract into the homogenisers entry aperture and are absorbed are included next and finally a surface roughness is added to the homogeniser material. A selection of BSDFs were used in the simulations for this investigation, their plots are given in Fig. 3 and all taken from the Breault software ASAP scattering library [32]. For these simulations a modified Harvey model was used with the selected BSDFs and though the BSDF cannot fully be shown with any 2D or 3D graph the curves in Fig. 3 are given as some indication of the light scattering profile. The graphs show the log BSDF versus the scattering angle (with respect to the specular angle) for three different incidence angles. All the scatter profiles follow the rule that most of the scattered light should be equal to the angle of incidence (the peaks shown in the graphs in Fig. 3). Differences can be seen in how the remainder of the light is distributed at non-specular angles (scattered) [27, 32]. The effects and contributions of these imperfect optical elements on optical efficiency and acceptance angle are given in Figs. 4 and 5.

Simulations were then carried out with the addition of a reflective film sleeve to the homogeniser at increasing air gap widths to investigate its advantages.

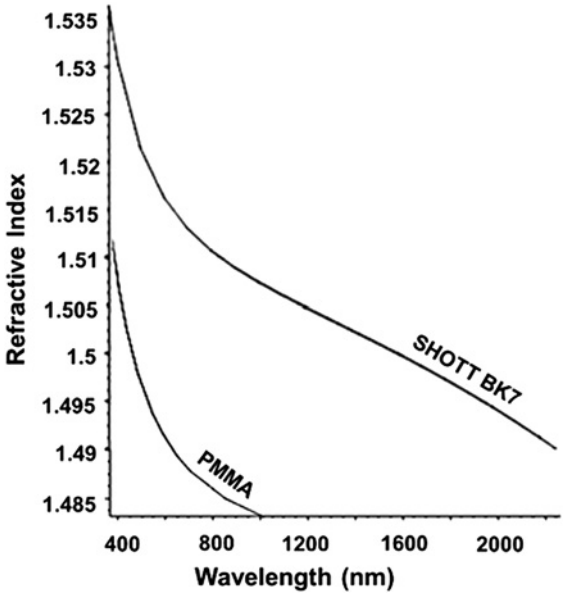

Fig. 2 *Dispersion functions of PMMA and SHOTT BK7*

4 Results and discussion

4.1 Optical efficiency decrease in realistic system

Fig. 4 confirms that no light rays are lost within the system at normal incidence as shown by the 'ideal' scenario results.

As can be seen from Figs. 4 and 5, the addition of a 10% reflection loss on both dishes causes a significant drop in optical efficiency. There are materials and coatings with improved reflectance [16] such as silver (∼97% reflectance) but degradation and/or expense are common problems with such high-quality reflective materials. All following simulations hence consider 90% reflective primary and secondary dishes so as final results are more realistic.

There is a small loss of energy due to when the light refracts into the homogeniser and some portion of the rays is reflected away. This can be improved with antireflection coatings and special textures of the homogeniser surface but again this is expensive [33, 34].

The surface roughness is a main factor causing a drop in optical efficiency and lowering the acceptance angle (Figs. 4 and 5). There is a severe drop especially for the BSDF's related to poorer surface finishes as shown in Fig. 4. These BSDF's were selected from a database of expected BSDF's of optical finishes available from companies. The BSDF's were chosen simply to give a good range. Typical surface quality would be expected to be in the upper region of these samples. Their effect is shown more clearly in Fig. 5 for the BSDF of polished aluminium, which though has the smallest drop in optical efficiency in Fig. 4, still contributes significantly to the total optical loss in Fig. 5. Owing to the increase in the solar misalignment angles, the rays reflect more within the homogeniser against the rough surfaced walls and are more likely to scatter instead of undergoing TIR. This causes the greater loss at >0.75° solar incident angles in Fig. 5. More accurate solar trackers and accurately built systems would not suffer as significantly if within ±0.5° accuracy but these incur further expense as well.

4.2 Impact of CRRH and air gap

Using first the lowest effecting BSDF (that of a standard polished aluminium) for the homogeniser surface and the added reflective film surface, an increase in optical efficiency was measured as shown in Fig. 6. The CRRH improves optical efficiency most between the 1° and 1.5° range of misalignment due to the increased incidence angle. When considering realistic conditions (90% reflectance from primary dishes and reflective film), the optical efficiency is increased by 2.8% (absolute value) at normal incidence and as high as 4.7% over the 1° and 1.5° regions as shown in Fig. 6. Though this is a significant gain, it should be noted that other manufacturing methods can result in smoother surface finishes with less light loss. The optical efficiency of any previous stage optics will also have an effect on the light saved by using the CRRH. If there is more energy going into the homogeniser, there is a greater portion of energy that can be trapped. The reflectance of the reflective film itself will alter

IET Renew. Power Gener., 2016, Vol. 10, Iss. 4, pp. 440–447

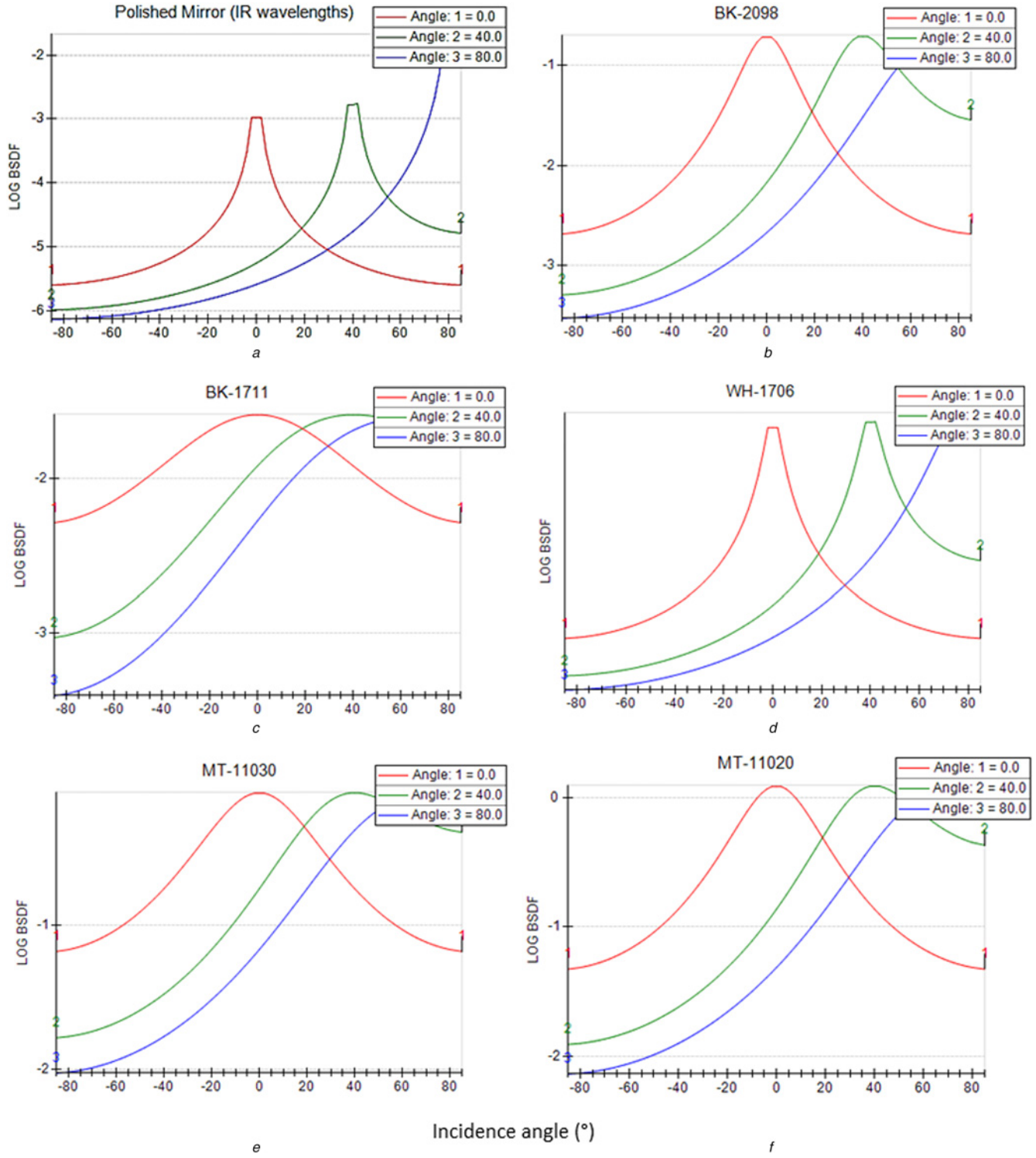

Fig. 3 *Logarithmic (LOG) BSDF against scatter angle from specular of*

a Polished mirror
b BK-2098
c BK-1711
d WH-1706
e MT-11030
f MT-11020

Three plots are shown in each graph for incidence angles of 0°, 40° and 80°. The BSDFs beginning with MT are representative of moulded optics surface profiles and those beginning with BK and WH are associated with specific materials available from lens providers. All plots were taken from the Breault ASAP scattering library [32]

results as well. If the CRRH with 0.01 mm air gap had 100% reflectance for the primary dishes and reflective film, the maximum optical efficiency gain would be ~7% for these simulations of a 500× Cassegrain system.

The thickness of the air gap was found to have very little effect on the efficiency with which refracted light rays are caught as shown in Fig. 7, though there is a significant difference without an air gap. Fig. 7 shows the optimum air gap to be 0.01 mm in these

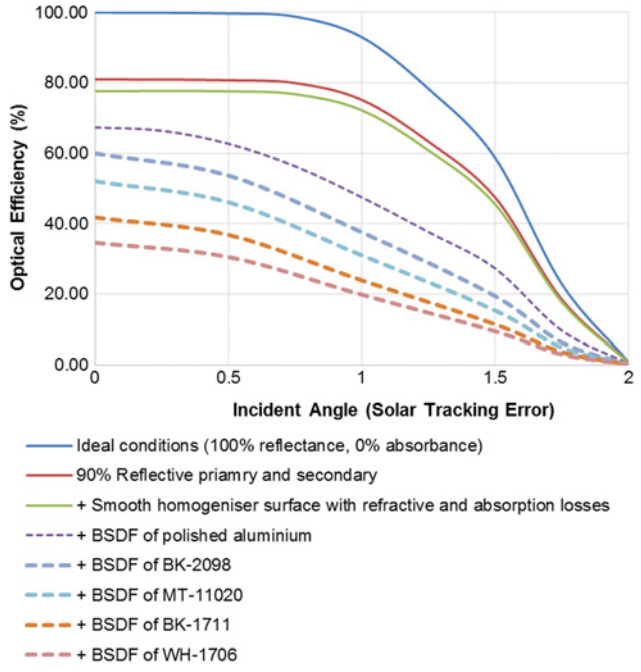

Fig. 4 *Practical losses summary. Optical efficiency decreases as surface losses are added in stages. The dashed lines represent possible surface finishes of the homogeniser depending on which material and manufacturing process is employed*

investigations. This would be nearly impossible to cost effectively implement due to manufacturing limitations but it can be assumed as small an air gap as is feasible considering manufacturing and cost would have the highest benefit.

Fig. 7 shows that with no air gap (0 mm), TIR is lost and all rays are reflected with specular losses (10%) in energy due to the 90% reflectance of the reflective film. As soon as there is an air gap, even as small as 0.01 mm in these simulations, the optical efficiency sharply increases as shown in Fig. 7. This increase in optical efficiency indicates how many reflections are experienced by the light rays, and hence the benefit TIR provides. The larger the increase in optical efficiency between the 0 and 0.01 air gap marks in Fig. 7, the more reflections occurring within the homogeniser which will benefit from TIR. This is why larger misalignment angles (except for 2° misalignment where most rays completely miss the homogeniser) have a more significant optical efficiency gain (vertical incline from 0 to 0.01 mm) in Fig. 7, because there are more reflections occurring.

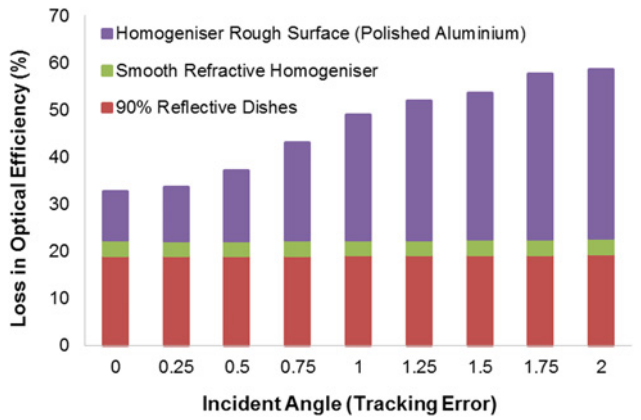

Fig. 5 *Contribution of optical losses from different imperfect surface considerations*

Thicker air gaps result in a longer path length of the non-TIR rays. This means rays will re-enter into the refractive medium at a lower position close to the solar cell and in theory possibly increase the optical efficiency of the system. However, in this Cassegrain design, a thicker air gap also blocks more rays travelling toward the secondary from the primary dish as mentioned earlier and as shown in Fig. 3. This would explain why there is a slight decrease in optical efficiency as the air gap thickness is increased in Fig. 7.

4.3 Impact of BSDF value

From the above results, it can be concluded that as small an airgap as possible is preferred. An air gap of 0.01 mm was hence used to investigate the effect of different BSDFs such as those already given in Figs. 3 and 4.

As can be seen from Fig. 8, the CRRH consistently improves the optical efficiency in comparison with a standard refractive homogeniser of this type for a range of surface scattering profiles. The maximum improvement is 7.75% with the BSDF of WH-1701 at normal incidence. Contrary to initial expectations however, this improvement did not increase with larger solar misalignment angles. At increased incident angles, the benefit of the CRRH decreased until negligible at 2° incidence angle as shown in Fig. 8 where the optical efficiency of the standard refractive homogeniser is almost zero. Misalignment with the Sun causes less light to reach the input surface of the homogeniser which can explain why the benefit of the CRRH decreases with increasing incidence angle. Also, if too many reflections occur within the homogeniser (due to the increased initial incidence angle), some light rays, despite being trapped at the CRRH walls, can still be reflected back out the entry aperture of the CRRH.

It can be drawn from these results that as long as there is some percentage (>2%) of light reaching the solar cell for the standard refractive homogeniser case, the CRRH will improve the optical efficiency by a non-negligible amount (as shown for the case of 1.75° incidence angle in Fig. 8). At normal incidence, the smallest optical efficiency improvement by the CRRH was 4.82% with a BSDF of BK-2098. These results confirm that the more efficient a purely refractive optic is to begin with (BK-2098 had the highest original optical efficiency as shown in Fig. 8), the less the addition of a reflective sleeve will improve the optical efficiency.

It should be noted that other manufacturing methods can result in smoother surface finishes with less light loss. The BSDFs beginning with MT in Figs. 3, 4 and 8 are representative of moulded optics surface profiles and those beginning with BK and WH are associated with specific materials available from lens providers.

4.4 Effect on irradiance distribution

The irradiance distribution on the solar cell is also affected by the surface roughness of the homogeniser as shown in Fig. 9.

The irradiance distribution is improved due to the slight diffusion of the rays from the rough surface of the homogeniser. In the case of the CRRH, when the reflective sleeve is added, the irradiance distribution is negligibly different to that without the reflective sleeve. The differences between the maximum and minimum irradiance values are given in Fig. 10. This shows a purely smooth and ideal optic to have the least homogeneous distribution, the addition of the rough surface modelling has the most homogeneous irradiance distribution and the CRRH has slightly less evenly distributed irradiance on the cell. As expected, with a higher misalignment angle, the distribution is less even, especially at 1°, before falling lower due to less total light being focused successfully to the solar cell.

4.5 Experimental validation

The measurements as shown in Fig. 11*a* gave a 3.5% current increase and a 6.7% power increase. When adding the reflective film to the refractive homogeniser (Figs. 11*b* and 11*c*), care was taken that the film did not optically stick to the refractive medium

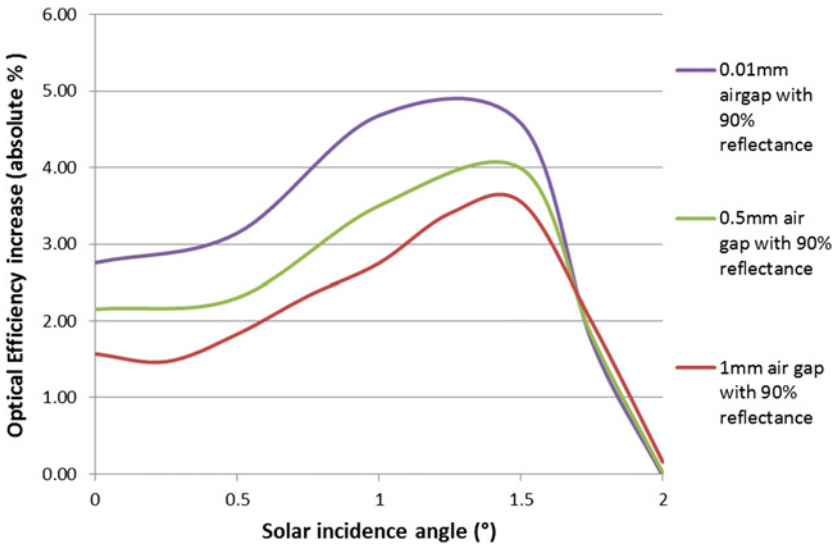

Fig. 6 *Increase in optical efficiency with the addition of the reflective sleeve under different conditions. Here, the base optical efficiency is that of the refractive homogeniser with the same dimensions and no reflective sleeve*

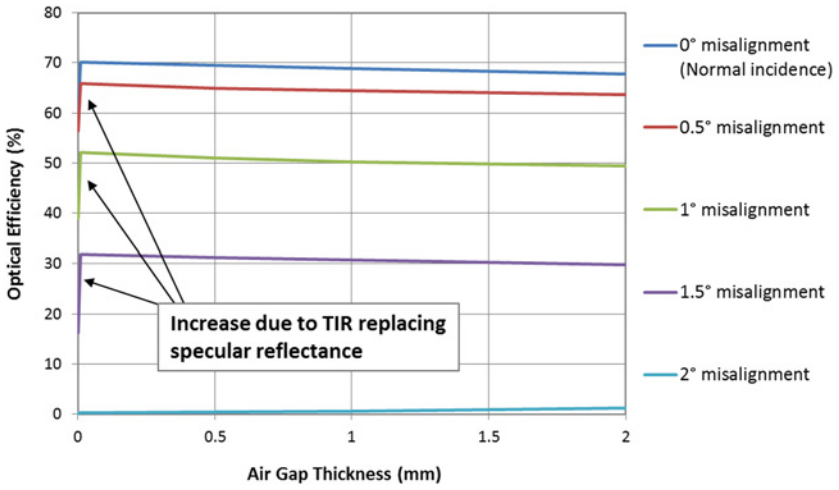

Fig. 7 *Graph of optical efficiency against air gap thickness for different solar misalignment angles*

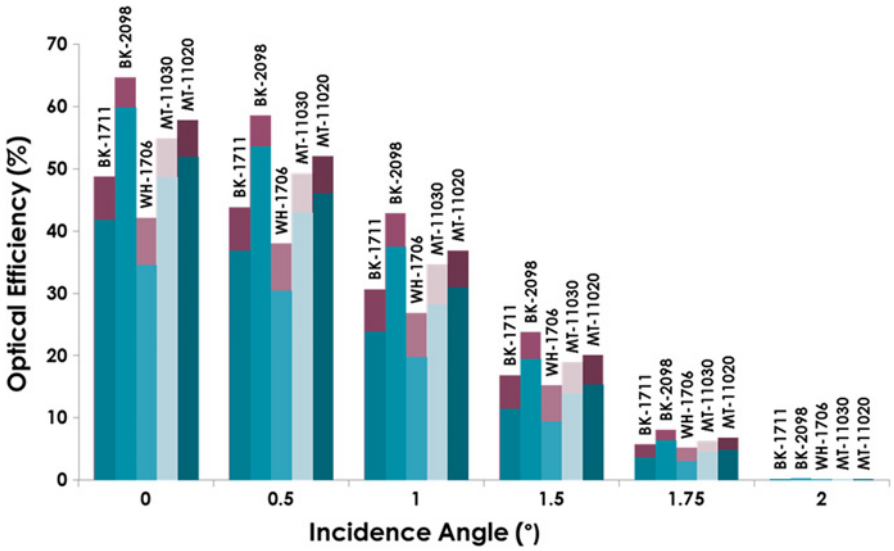

Fig. 8 *Increase in optical efficiency (purple shaded extensions at top of bars) due to the addition of the reflective sleeve to the refractive homogeniser with an air gap of 0.01 mm for increasing BSDF's. The incidence angle of the light is also increased up to 2° to show the effect misalignment has on the benefit of the CRRH in comparison with the performance of a refractive homogeniser (original blue shaded bars excluding extensions)*

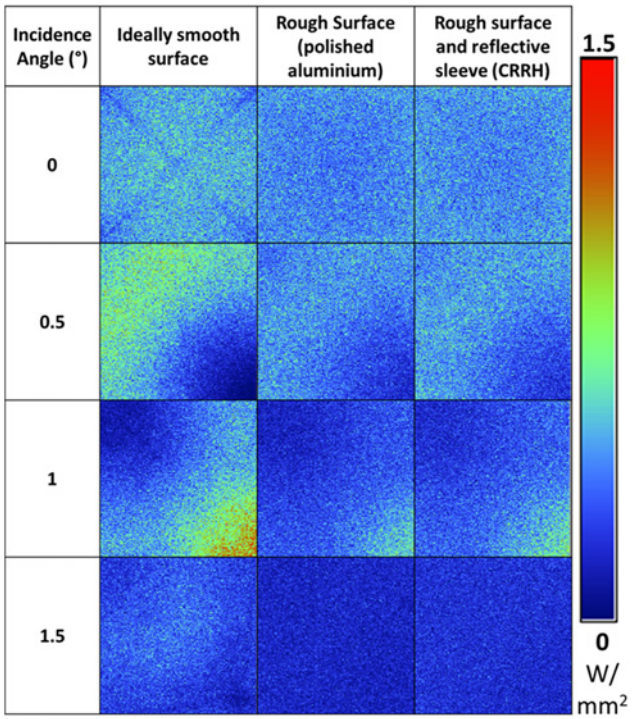

Fig. 9 *Irradiance distribution on solar cell with increasing solar incidence angle (increasing tracking error). Column 1: solar incidence angle on full Cassegrain system. Column 2: the case of 100% reflective dishes and a refractive homogeniser with an ideal surface finish. Column 3: results after the addition of a rough surface finish on the homogeniser. Column 4: same conditions as previous but with the reflective sleeve in place. The tracking error is set for both axes, hence the diagonal focusing*

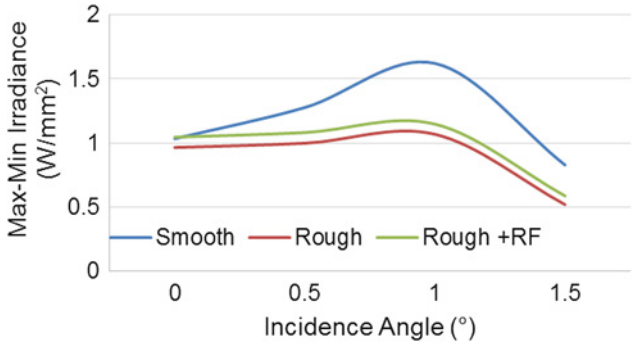

Fig. 10 *Irradiance range (max–min) on the solar cell with increasing solar incidence angle (increasing tracking error) for the smooth refractive homogeniser, the realistically rough refractive homogeniser and CRRH*

and prevent TIR. It was also ensured that the primary optic (Fresnel lens) only focused to the centre of the homogeniser for both tests and the same concentration ratio was maintained. With higher-efficiency primary optics and higher-concentration levels, the final stage optic gains more influence on the overall optical efficiency and performance. These practical measurements confirm the advantage of the CRRH over a plane refractive homogeniser.

5 Conclusion

The CRRH has been presented within the Cassegrain concentrator design. The CRRH has been shown to improve the optical efficiency by a maximum of 7.75% when considering a realistic surface roughness on the homogeniser and reflective optics within the Cassegrain concentrator system. The benefits of the CRRH are

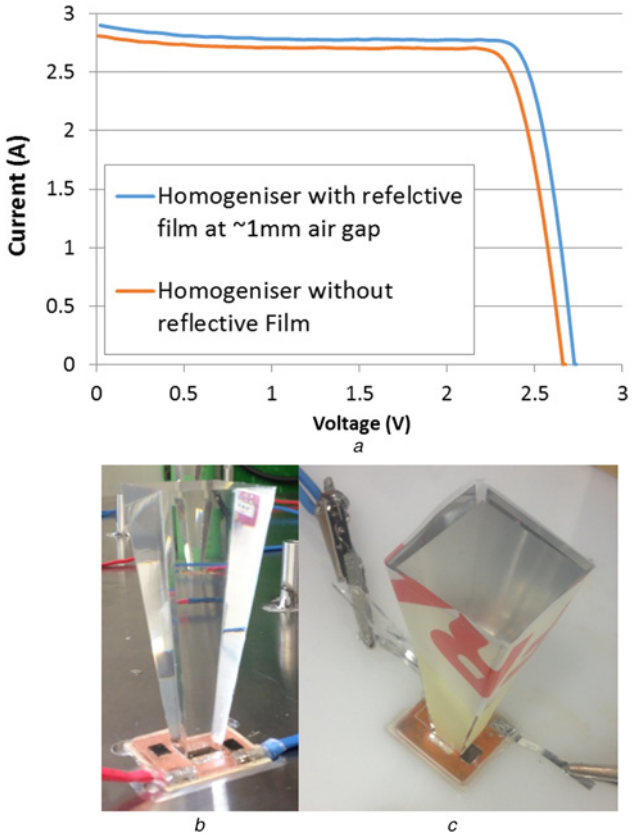

Fig. 11 *Experimental validation*

a I–V trace for the refractive homogeniser with and without the reflective sleeve and air gap
b Refractive homogeniser without reflective sleeve
c With reflective sleeve to make prototype CRRH

limited by the Cassegrain concentrator geometry and by the magnitude of surface roughness on the homogeniser. A high-quality homogenising optic with almost ideal surface smoothness would not benefit from the addition of a reflective sleeve but this is rarely the case due to difficult geometries and expense. Experimental tests confirmed the ray trace simulation analysis and a 6.7% performance improvement with the CRRH in comparison with the original refractive homogeniser was measured. Future work is required to fully understand the benefit conjugate refractive–reflective optics can have for solar concentrator technologies.

6 Acknowledgments

This work has been carried out as a part of BioCPV project jointly funded by the Department of Science and Technology (DST), India (ref. no: DST/SEED/INDO-UK/002/2011) and the Engineering and Physical Sciences Research Council (EPSRC), UK, (ref. no: EP/J000345/1). Authors acknowledge both the funding agencies for the support. In support of open access research all underlying article materials (such as data, samples or models) can be accessed upon request via email to the corresponding author.

7 References

1 Akbari, H., Damon Matthews, H., Seto, D.: 'The long-term effect of increasing the albedo of urban areas', *Environ. Res. Lett.*, 2012, **7**, p. 024004
2 Gaffin, S.R., Imhoff, M., Rosenzweig, C., *et al.*: 'Bright is the new black – multi-year performance of high-albedo roofs in an urban climate', *Environ. Res. Lett.*, 2012, **7**, p. 014029

3 Burg, B.R., Selviaridis, A., Paredes, S., *et al*.: 'Ecological and economical advantages of efficient solar systems'. 'CPV-10', AIP Conf. Proc., 2014, pp. 317–320
4 Canavarro, D., Chaves, J., Collares-Pereira, M.: 'New second-stage concentrators (XX SMS) for parabolic primaries', comparison with conventional parabolic trough concentrators', *Sol. Energy*, 2013, **92**, pp. 98–105
5 Baig, H., Heasman, K.C., Mallick, T.K.: 'Non-uniform illumination in concentrating solar cells', *Renew. Sustain. Energy Rev.*, 2012, **16**, (8), pp. 5890–5909
6 Brunotte, M., Goetzberger, A., Blieske, U.: 'Two-stage concentrator permitting concentration factors up to 300× with one-axis tracking', *Sol. Energy*, 1996, **56**, (3), pp. 285–300
7 Canavarro, D., Chaves, J., Collares-Pereira, M.: 'New optical designs for large parabolic troughs', *Energy Procedia*, 2014, **49**, pp. 1279–1287
8 Winston, R., Miñano, J.C., Benítez, P., *et al*.: 'Nonimaging optics' (Elsevier, 2005)
9 Victoria, M., Domínguez, C., Antón, I., *et al*.: 'Comparative analysis of different secondary optical elements for aspheric primary lenses', *Opt. Express*, 2009, **17**, (8), pp. 6487–6492
10 Coughenour, B.M., Stalcup, T., Wheelwright, B., *et al*.: 'Dish-based high concentration PV system with Köhler optics', *Opt. Express*, 2014, **22**, (S2), p. A211
11 Araki, K., Leutz, R., Kondo, M., *et al*.: 'Development of a metal homogenizer for concentrator monolithic multi-junction-cells'. Conf. Record of the 29th IEEE Photovoltaic Specialists Conf., 2002, 2002, pp. 1572–1575
12 Gordon, J.M., Feuermann, D., Young, P.: 'Unfolded aplanats for high-concentration photovoltaics', *Opt. Lett.*, 2008, **33**, (10), p. 1114
13 Tang, R., Wang, J.: 'A note on multiple reflections of radiation within CPCs and its effect on calculations of energy collection', *Renew. Energy*, 2013, **57**, pp. 490–496
14 O'Gallagher, J., Winston, R.: 'No title test of a trumpet secondary concentrator with a paraboloidal dish primary', *Sol. Energy*, 1986, **36**, (1), pp. 37–44
15 Benítez, P., Miñano, J.C., Zamora, P., *et al*.: 'High performance Fresnel-based photovoltaic concentrator', *Opt. Express*, 2010, **18**, pp. A25–A40
16 Shanks, K., Senthilarasu, S., Mallick, T.K.: 'High-concentration optics for photovoltaic applications', in Pérez-Higueras, P., Fernández, E.F. (Eds.): 'High concentrator photovoltaics: fundamentals, engineering and power plants' (Springer International Publishing, 2015, 1st edn.), pp. 85–113
17 Leutz, R., Fu, L., Annen, H.P.: 'Stress in large-area optics for solar concentrators', in Dhere, N.G., Wohlgemuth, J.H., Ton, D.T. (Eds.): 'SPIE solar energy + technology' (International Society for Optics and Photonics, 2009), pp. 741206–741206–7
18 Jagoo, Z.: 'Tracking solar concentrators' (Springer Nether, 2013, 1st edn.)
19 Bader, R., Haueter, P., Pedretti, A., *et al*.: 'Optical design of a novel two-stage solar trough concentrator based on pneumatic polymeric structures', *J. Sol. Energy Eng.*, 2009, **131**, (3), p. 031007
20 Zanganeh, G., Bader, R., Pedretti, A., *et al*.: 'A solar dish concentrator based on ellipsoidal polyester membrane facets', *Sol. Energy*, 2012, **86**, (1), pp. 40–47
21 Barber, G.J., Braem, A., Brook, N.H., *et al*.: 'Development of lightweight carbon-fiber mirrors for the RICH 1 detector of LHCb', *Nucl. Instrum. Methods Phys. Res. A, Accel. Spectrom. Detect. Assoc. Equip.*, 2008, **593**, (3), pp. 624–637
22 Guo, S., Zhang, G., Li, L., *et al*.: 'Effect of materials and modelling on the design of the space-based lightweight mirror', *Mater. Des.*, 2009, **30**, (1), pp. 9–14
23 Yin, L., Huang, H.: 'Brittle materials in nano-abrasive fabrication of optical mirror-surfaces', *Precis. Eng.*, 2008, **32**, pp. 336–341
24 Leutz, R., Suzuki, A.: 'Nonimaging Fresnel lenses: design and performance of solar concentrators' (Springer Science & Business Media, 2001)
25 Kiontke, S. and Kokot, S.: 'Roughness reduction on aspheric surfaces,' in Classical Optics 2014, OSA Technical Digest (online) (Optical Society of America, 2014), paper OTu2B.4. doi:10.1364/OFT.2014.OTu2B.4 https://www.osapublishing.org/abstract.cfm?uri=OFT-2014-OTu2B.4
26 Brun, C., Buet, X., Bresson, B., *et al*.: 'Picometer-scale surface roughness measurements inside hollow glass fibres', *Opt. Express*, 2014, **22**, (24), p. 29554
27 Asmail, C.: 'Bidirectional scattering distribution function (BSDF): a systematized bibliography', *J. Res. Natl. Inst. Stand. Technol.*, 1991, **96**, (2), p. 215
28 Baig, H.: 'Enhancing performance of building integrated concentrating photovoltaic systems', PhD thesis, University of Exeter, 2015
29 Baig, H., Sellami, N., Mallick, T.K.: 'Trapping light escaping from the edges of the optical element in a concentrating photovoltaic system', *Energy Convers. Manage.*, 2015, **90**, pp. 238–246
30 Baig, H., Sarmah, N., Chemisana, D., *et al*.: 'Enhancing performance of a linear dielectric based concentrating photovoltaic system using a reflective film along the edge', *Energy*, 2014, **73**, (14), pp. 177–191
31 Shanks, K., Sarmah, N., Mallick, T.K.: 'The design and optical optimisation of a two stage reflecting high concentrating photovoltaic module using ray trace modelling'. 'PVSAT-9', 2013
32 Breault Research Organization: 'ASAP technical guide: scattering in ASAP'. Available at http://www.breault.com/sites/default/files/knowledge_base/brotg0922_scatter_1.pdf, accessed October 2015
33 Huang, C.K., Sun, K.W., Chang, W.-L.: 'Efficiency enhancement of silicon solar cells using a nano-scale honeycomb broadband anti-reflection structure', *Opt. Express*, 2012, **20**, (1), pp. A85–93
34 Zhou, G., He, J., Xu, L.: 'Antifogging antireflective coatings on Fresnel lenses by integrating solid and mesoporous silica nanoparticles', *Microporous Mesoporous Mater.*, 2013, **176**, pp. 41–47

[Article 4]

K. Shanks, H. Baig, N. P. Singh, S. Senthilarasu, K. S. Reddy, and T. K. Mallick, “Prototype fabrication and experimental investigation of a conjugate refractive reflective homogeniser in a cassegrain concentrator,” *Sol. Energy*, vol. 142, pp. 97–108, Jan. 2017.

Solar Energy 142 (2017) 97–108

Contents lists available at ScienceDirect

Solar Energy

journal homepage: www.elsevier.com/locate/solener

Prototype fabrication and experimental investigation of a conjugate refractive reflective homogeniser in a cassegrain concentrator

Katie Shanks [a,*], Hasan Baig [a], N. Premjit Singh [b], S. Senthilarasu [a], K.S. Reddy [b], Tapas K. Mallick [a,*]

[a] Environment and Sustainability Institute, University of Exeter, Penryn Campus, Penryn TR10 9FE, UK
[b] Heat Transfer and Thermal Power Laboratory, Department of Mechanical Engineering, Indian Institute of Technology Madras, Chennai 600 036, India

ARTICLE INFO

Article history:
Received 1 September 2016
Received in revised form 21 November 2016
Accepted 22 November 2016
Available online 22 December 2016

Keywords:
Concentrator photovoltaics
Cassegrain
Optical loss
Materials
Temperature
Homogeniser

ABSTRACT

The conjugate refractive reflective homogeniser (CRRH) is experimentally tested within a cassegrain concentrator of geometrical concentration ratio 500× and its power output compared to the theoretical predictions of a 7.76% increase. I–V traces are taken at various angles of incidence and experimental results showed a maximum of 4.5% increase in power output using the CRRH instead of its purely refractive counterpart. The CRRH utilises both total internal reflection (TIR) within its core refractive medium (sylguard) and an outer reflective film (with an air gap between) to direct more rays towards the receiver. The reflective film captures scattered refracted light which is caused by non-ideal surface finishes of the refractive medium. The CRRH prototype utilises a 3D printed support which is thermally tested, withstanding temperatures of up to 60 °C but deforming at >100 °C. A maximum temperature of 226.3 °C was reached within the closed system at the focal spot of the concentrated light. The material properties are presented, in particular the transmittance of sylguard 184 is shown to be dependent on thickness but not significantly on temperature.

Utilising both TIR and standard reflection can be applied to other geometries other than the homogeniser presented here. This could be a simple but effective method to increase the power of many concentrator photovoltaics.

1. Introduction

Concentrator photovoltaic (CPV) designs have been pushing higher concentration ratios to achieve higher conversion efficiencies and cost effectiveness. As the concentration ratio of an optic is increased, the acceptance-angle decreases, making it more difficult to manage the design deviations and uncertainties (optical tolerances) (Baig et al., 2012; Canavarro et al., 2013). A homogeniser optic is typically needed to match beam shape and size to the receiver and improve the optical tolerance of the overall optical system (Baig et al., 2012; Canavarro et al., 2013). Final stage optics within a CPV commonly take the form of a compound Parabolic Concentrator or V-trough but other shapes are being investigated such as the dome lens (Hatwaambo et al., 2008; Shanks et al., 2016c, 2015; Victoria et al., 2009; Winston, 1970). There are homogenising optical designs with varying advantages already available but as designs progress and perhaps become more complex the material, surface quality and solar cell coupling method needs to be further investigated.

One key consideration in all of the above named designs is the material to be used and the resulting surface quality (Fend et al., 2003; Yin and Huang, 2008). Previous simulation work has been carried out to show the importance of considering the surfaced roughness and subsequent light scattering during the design and simulation stages of development (Shanks et al., 2016a). This previous study investigated a cassegrain concentrator design similar to that of SolFocus (Gordon et al., 2008) but focused on the surface quality of the refractive homogenising optic. The system presented here and in the previous work was optimised for acceptance angle (Shanks et al., 2016b). There are many cassegrain concentrators which have been investigated in the past (Chen and Ho, 2013; Chong et al., 2013; Dreger et al., 2014; McDonald et al., 2007; Roman et al., 1995; Terry et al., 2012, 1996; Victoria et al., 2013; Yehezkel et al., 1993) but further insight into the material and manufacturing choices is needed. Cassegrain set ups are known for having slightly lower acceptance angles than their Fresnel lens counterparts but can reach higher concentration ratios and hence why this type of system was chosen to not only understand the

* Corresponding authors.
E-mail addresses: kmas201@exeter.ac.uk (K. Shanks), H.Baig@exeter.ac.uk (H. Baig), premjitmtech@gmail.com (N.P. Singh), S.Sundaram@exeter.ac.uk (S. Senthilarasu), ksreddy@iitm.ac.in (K.S. Reddy), T.K.Mallick@exeter.ac.uk (T.K. Mallick).

http://dx.doi.org/10.1016/j.solener.2016.11.038
0038-092X/

design constraints but see if a new homogeniser would improve the performance, especially for future designs of higher solar concentration levels. The surface roughness of refractive optics which utilise total internal reflection (most homogenisers) causes scattering of incoming light and incomplete TIR despite incident light fulfilling the acceptance angle criteria of the optic. Surface imperfections will also increase the reflection upon entering the refractive optic. The degree of this surface inhomogeneity depends on the manufacturing process and material used with higher quality optical finishes and coatings costing more (Yin and Huang, 2008).

As indicated in the previous theoretical study (Shanks et al., 2016a), high quality glass homogenisers and similar refractive optics which utilise TIR will not suffer much optical loss due to poor surface quality. Glass is the preferred choice of material to achieve very smooth and accurate optical finishes and the inverted pyramid glass homogeniser and CPC optics can be bought off the shelf at reasonable costs. However, more complex prototypes are costly to fabricate using glass and even if glass is used these optics then need to be attached optically to the solar cells using an encapsulate. When coupling a homogeniser to a solar cell as a secondary step, the lateral spillage of the silicone causes significant optical losses from leakage through it. If to avoid spillage the joint is under-filled, the joint could be weaker and possibly result in an air gap also producing optical losses (Benítez et al., 2010). These losses cannot be quantified until full production is achieved. In the present study we have eliminated the step of the optical coupling the solar cell separately with the solar cell by preparing a mould, which allows this.

In this way we can manufacture the V-trough homogeniser, simultaneously join it to the solar cell and reduce alignment errors by using this mould. To do this we use the refractive material Sylguard 184 which is predominantly used as an encapsulate and has the advantage of setting at room temperature. This is important as we should not subject the cell to any unnecessary heating before use and because typical high temperature mould setting can involve expansion and contraction of the material which could damage the solar cell when part of a closed mould such as this.

As already discussed, using an alternative material to glass will most likely result in more surface scattering. To compensate for this we add an outer reflective casing with an air gap to ensure both TIR and standard reflection can occur, trapping scattered rays. This hence becomes the Conjugate Refractive Reflective Homogeniser (CRRH).

Identifying the losses within a homogenizer of a high concentrating photovoltaic system, quantifying them and applying simple solutions towards improving them will improve the performance of the full system. Within the growing area of solar concentrator research there needs to be a clearer understanding of how theoretical designs will perform in real conditions with real optics. For this reason this paper is the experimental counterpart to a previous theoretical study on the CRRH within a cassegrain concentrator (Shanks et al., 2016a). Hence, one of the focuses of this study is to confirm how much of the theoretical predictions could be realised (7.76% theoretical power increase), what materials and manufacturing methods are feasible and their performance in a high temperature environment.

At present, manufacturing processes for optics include precise grinding, milling, polishing, and a variety of coating methods for a smooth finish (Xu et al., 2013). Most current manufacturing processes struggle to produce acceptable priced prototype optics of new specific shapes and reliable accuracy (Kaushika and Reddy, 2000; Tsai, 2013). Here, we have tested plastic mirrors for their advantages in cost, weight and smooth surface quality. One of the challenges of CPV technology is its increased initial investment in comparison to flat plate PV due to the added optics and tracking required (Fraas, 2014). Computer-controlled diamond turning machines, as well as other modern materials and moulding techniques, have significantly improved the design and accuracy of refractive optics such as Fresnel lenses (Leutz and Suzuki, 2001). In this study we have utilised 3D printing and tested a structure for its heat tolerance within a CPV system. 3D printing is a very powerful prototyping tool which needs further testing for use within CPV research. The 3D printed support structure also compensates for the possibly weaker coupling joint of the 1 step moulding. This study, though specific in design and material, highlights a general issue in optics and prototyping and suggests simple but effective methods of compensating for losses due to surface roughness.

2. Theoretical work

A previous study has been undertaken which optimised a cassegrain concentrator design of 500× geometrical concentration (Shanks et al., 2016b). This design was optimised for acceptance angle by investigating the ray displacement at 1° incidence angle for a range of focal length and separation distance parameter of the two reflector dishes in the system. Use of a homogeniser was required to improve the acceptance angle of the cassegrain set up and a refractive homogeniser was chosen instead of a reflective one to take advantage of total internal reflection (TIR). As already discussed this TIR is however only fully effective if the homogeniser surface quality is very smooth. In the previous study, this tall homogeniser optic was found to lean when the system was tilted to track the sun (Shanks et al., 2016b). For all these reasons a new homogeniser optic utilising an outer reflective casing was proposed and investigated also (Shanks et al., 2016a). This previous study focused on the theoretical concept of compensating for surface roughness in the homogeniser by catching refracted rays with a reflective film. Various materials and surface structures were investigated (Shanks et al., 2016a). Manufacturing the optic however needed to be done in a reliable and effective manner. Hence, the reports here utilising 3D printing.

The cassegrain concentrator and its final dimensions can be seen in Fig. 1 (Shanks et al., 2016b). The design aimed to simultaneously obtain a high optical efficiency and a good acceptance angle. The concentrator consisted of a parabolic primary reflector, inverse parabolic secondary reflector and a refractive crossed V-trough homogenising tertiary as shown in Fig. 1. In comparison to the SolFocus design (Gordon et al., 2008), the primary parabolic dish has a higher focal length (270 mm) and a taller homogeniser (75 mm). Everything has also been cut to a square shape to allow compact arrays. Manufacturing uncertainties were considered and various material surface scattering profiles of the optics in the system were simulated (Shanks et al., 2016a). A 3–42% drop in optical efficiency was shown to occur (Fig. 2) depending on the material and scattering profile of the homogeniser.

Hence, the new conjugate refractive-reflective homogeniser (CRRH) was proposed as a solution to improve the homogeniser optical losses. The CRRH utilises the addition of a straight reflective film to the dielectric homogeniser with a 1 mm air gap kept between the dielectric medium and reflective film. The reflective sleeve ensures total internal reflection is maintained for the majority of light rays and the previously lost scattered light is also caught. This simple but effective method to recover rays which fail TIR has been used elsewhere (Baig, 2015). Baig et al. (2015, 2014) discuss the optical losses caused by the encapsulation medium used in connecting low concentration optics to solar cells. Light rays incident in this overlap region do not reflect towards the solar cell but continue through the encapsulation medium until lost.

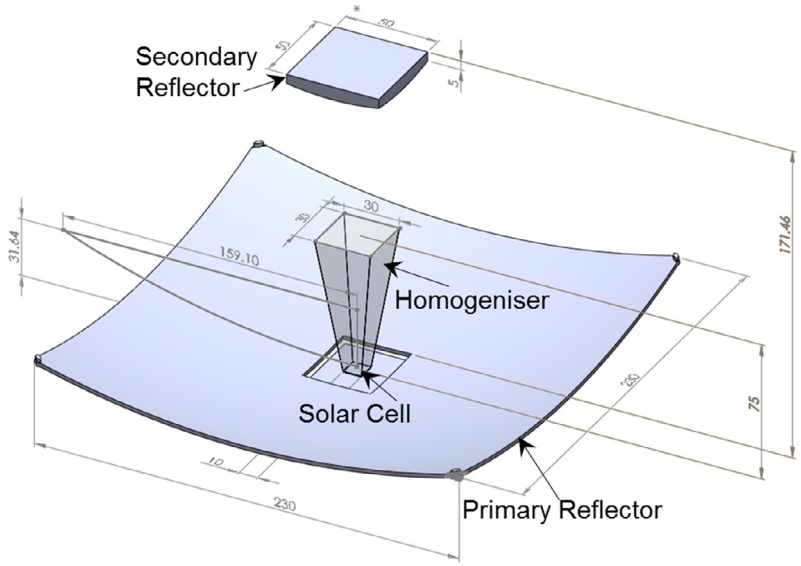

Fig. 1. Cassegrain design with large primary parabolic reflector and secondary parabolic reflector with dimensions in mm. The primary paraboloid has a focal length of 270 mm and the secondary paraboloid a focal length of 70 mm. Both parabolic reflectors are afocal in relation to each other and cut to square shapes for compact array placement.

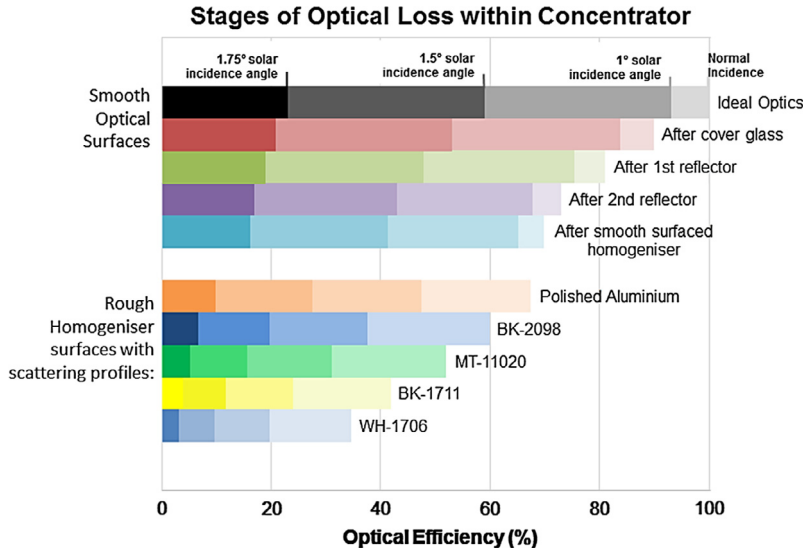

Fig. 2. Theoretical contribution of optical losses from different optical stages/surfaces calculated from ray trace simulations (Shanks et al., 2016a).

Baig et al. overcame the encapsulation issue by adding a strip of reflective film to the bottom edge of the 3D cross compound parabolic concentrator designed for building integration (Baig et al., 2015, 2014). We have expanded on this method by applying reflective film with a 1 mm air gap to all of the TIR active walls of a homogeniser in a high concentration cassegrain concentrator.

The effects of the air gap size and reflective film angle and material was investigated in the previous study (Shanks et al., 2016a). Ultimately, the findings confirmed that the addition of the reflective film did improve the optical efficiency of the optic but its angle and the size of the air gap made little difference. As small air gap as possible is optimum but an air gap is essential to ensure TIR still takes place or there is a significant reduction in optical loss due to multiple standard reflections. Other shapes such as an outer compound parabolic concentrator reflective film could also be investigated. Although the optical efficiency may not improve much by using a CPC shaped reflective casing, the acceptance angle may benefit. A reliable method of manufacturing would still be necessary to ensure the added complexity of a CPC CRRH did not result in excessive cost. The flat reflective film sleeve was chosen in this study due to its simplicity and low cost especially for the prototyping stage of a concentrator. Once proven and manufactured effectively with the best materials, more complex curves can be investigated more effectively.

We have also eliminated the homogeniser to solar cell coupling stage and minimised the encapsulate spillage by moulding everything together at once using the same refractive material. Hence, the conjugate refractive reflective homogeniser (CRRH) as shown in Fig. 3.

In the theoretical study carried out previously (Shanks et al., 2016a), the CRRH (Fig. 3a) increased the overall optical efficiency by a maximum of 7.75% in comparison to that of a standard refractive homogeniser (Fig. 3b) simulated within the same concentrator system. This value depended on the material used and surface

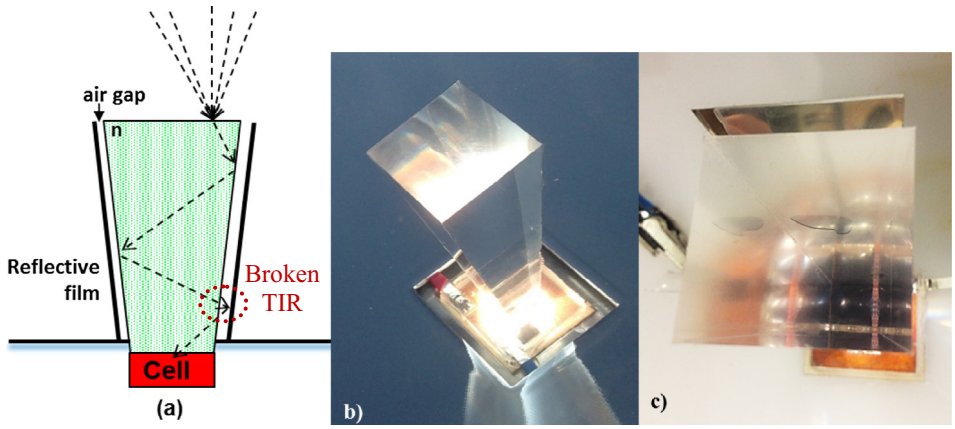

Fig. 3. (a) Diagram of the conjugate refractive reflective homogeniser showing a light ray which eventually does not undergo TIR but is still reflected by the layer of reflective film. (b) Photo of refractive homogeniser attached to 10 mm × 10 mm multijunction solar cell. (c) Photo of refractive homogeniser with reflective film sleeve on one side (making the CRRH) for initial validation results given in (Shanks et al., 2016a). The effect of no air gap (where the reflective film is sticking to the refractive medium half way down the side) which voids TIR and causes non ideal standard reflection can also be seen.

roughness of the refractive part of the homogenisers in use (Shanks et al., 2016a). The CRRH (Fig. 3c) was also validated via practical measurements and a 6.7% power increase was measured under a 1000 W/m^2 solar simulator at normal incidence for the experimental test (Shanks et al., 2016a). This test however used a Fresnel lens set up of a different focal length and wavelength dispersion than that of the simulated cassegrain concentrator. Although the result still validates the benefit of the CRRH, further experimental investigation is required to compare the theoretical to the experimental, especially for varying incidence angle. The reliability of the materials must also be tested experimentally. As mentioned earlier the acceptance angle becomes increasingly important as the concentration ratio increases. Fig. 4b illustrates the different losses within the cassegrain system when the module is misaligned with the sun. The red numbered circles in Fig. 4b highlight the main areas of loss which are otherwise optimised as shown by the lettered red circles in Fig. 4a. These lost rays in Fig. 4b are responsible for the reduced optical efficiency in Fig. 2 at increased solar incidence angles when the optical materials are simulated as ideal but the geometry still loses light.

The CRRH minimises the optical losses at site no. 4 in Fig. 4b but other areas of loss are inevitable with increased solar incidence angle due to the acceptance angle limitations of the design.

High and ultrahigh concentrator designs rely heavily on high accuracy which often leads to high expense. Here, we compare the experimental performance of the CRRH within a 500× cassegrain concentrator to the same system with a standard refractive homogeniser (Fig. 3b). Measurements are taken over a range of solar misalignment angles to show the effect on acceptance angle for this type of system. The experimental results obtained are also compared to the theoretical predictions in the previous study to show how much of the theoretical gain with the CRRH is actually realistically achievable – an important factor sometimes overlooked in theoretical design proposals.

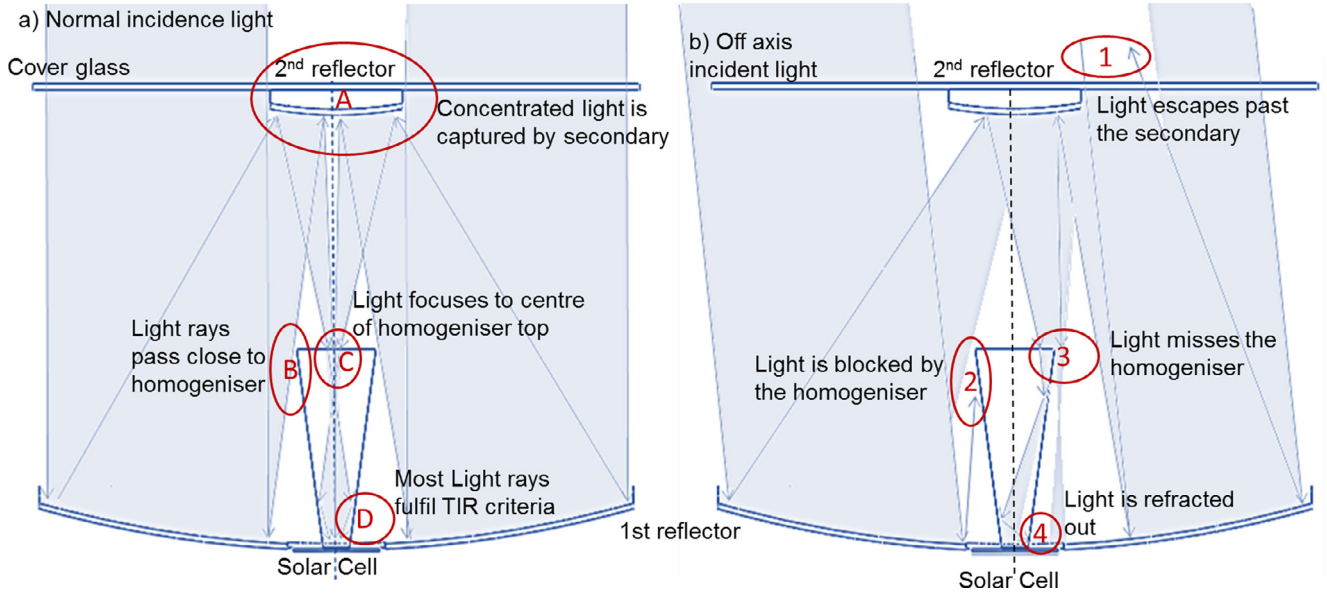

Fig. 4. (a) Diagram of light ray propagation through the cassegrain concentrator when incoming light is normal to the system and components are aligned perfectly towards the sun. Key design features at normal incidence are highlighted with lettered red circles. (b) Diagram of lost light rays due to misalignment with sun. Areas of loss are highlighted with numbered red circles. (For interpretation of the references to color in this figure legend, the reader is referred to the web version of this article.)

3. Materials and manufacturing

Prototypes are difficult to manufacture cost effectively. As mentioned earlier there is always at least some loss with each additional optical stage and component material interface introduced (Fig. 2). Unless very accurate and also expensive manufacturing procedures are employed, these losses increase in the prototyping stage. 90% efficient primary and secondary reflectors in particular were difficult to obtain for this prototype. The low iron glass cover was measured as being ~90% transparent (Fig. 5a), but this can be improved with more expensive glass materials. For this prototype, the manufacturing company 'HLH prototypes' provided very good plastic primary and secondary reflectors but after some initial testing the secondary's had to be swapped for hand polished aluminium reflectors. This was due to the plastic secondary's melting due to the concentrated light incident on them and hence higher temperatures. The reflectance spectra of the primary and secondary materials were measured and shown in Fig. 5b. The primary plastic mirrors have the advantage of being far lighter than their metallic counterparts and also manufactured accurately using CNC machining with no need for repeated post-polishing that is necessary for CNC'd metal. Depending on the polishing method, the specific curvature of the reflective dish can also be lost. The reflective film used in the CRRH was Reflectech's mirror film (Digrazia and Jorgensen, 2010; ReflecTech.Inc, 2014), this reflective film has a very high reflectance as shown in Fig. 5b and is reliable over many years of UV exposure (Digrazia and Jorgensen, 2010; ReflecTech.Inc, 2014). The operating temperature of this film is however recommended to be a maximum of 60 °C, which would be too low if the film was subject to highly concentrated light. In this system the reflective film is used as part of the CRRH and so should only capture scattered light but experimental testing was carried out to confirm this.

The refractive material used for the homogeniser was Sylguard 184, the transmittance of this was measured for different thicknesses as shown in Fig. 5c and d. As expected the increased thickness of the refractive material reduces the transmittance of the light. For the CRRH, the minimum length the light rays could travel from entrance to exit is 75 mm and the maximum is estimated at ~96 mm (Tang and Wang, 2013). The maximum distance also incurs the maximum no. of reflections within the homogeniser without being reflected back out of the homogeniser entrance aperture (Tang and Wang, 2013). With increased incidence angles and more reflections of the side walls of the homogeniser, more distance will be travelled within the refractive medium and hence more absorption will take place. The first prototype of the CRRH involved careful placement of a reflective film sleeve over the original refractive homogeniser (Fig. 6b and c). This method of manufacturing is not practical and there is no way of ensuring the air gap is maintained without checking by eye. In Fig. 6c, it can be seen where the reflective film is in contact with the refractive material causing a puddle like image midway down the homogeniser side wall and voiding TIR. 3D printing was hence employed to manufacture an outer structure which the reflective film could be adhered to as shown in Fig. 6a. In this way, the air gap thickness could be controlled and sustained.

The 3D printed structures were designed using solidworks to leave a 1 mm gap on the inside between the refractive medium and reflective film. The 3D structure was printed as two halves which were then screwed together as shown in Fig. 6a. The nodes at the top opening of the 3D printed structures are to keep the refractive homogeniser centred. The refractive core of the homogeniser was moulded directly onto the solar cell in 1 step to reduce

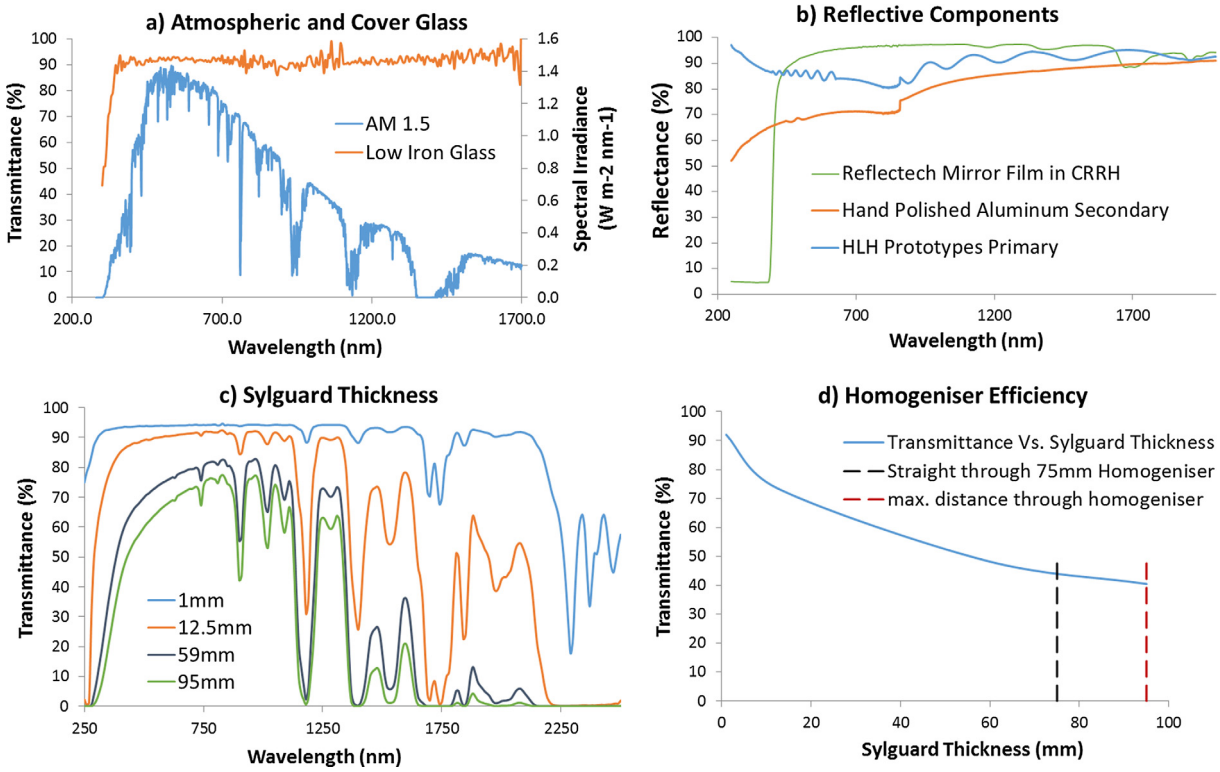

Fig. 5. (a) Cover glass transmittance and atmosphere AM1.5 direct incident irradiance spectrum. (b) Reflectance of the primary and secondary reflector materials. (c) Transmittance spectra for varying thicknesses of sylguard. (d) Transmittance through refractive homogeniser as a function of thickness with estimated minimum and maximum distance the light will travel through the homogeniser. All measurements apart from the AM1.5d were taken with a Perkin Elmer lambda 1050 Spectrophotometer at the University of Exeter, Penryn Campus.

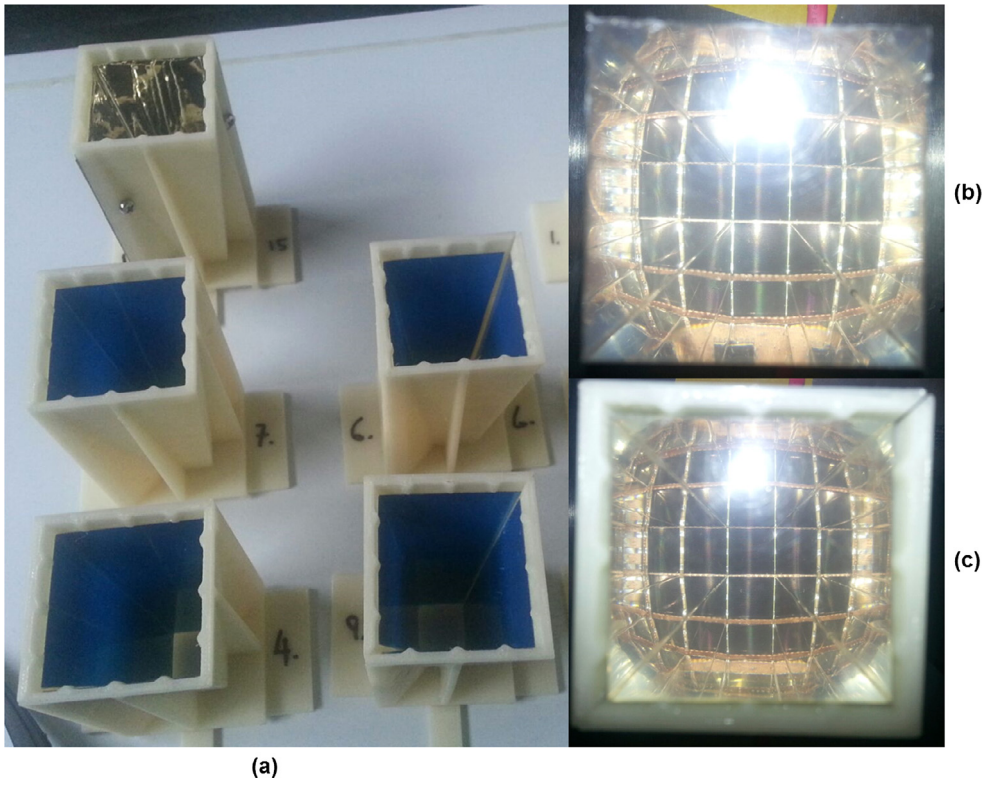

Fig. 6. (a) 3d printed structures with reflective film placed on the inside. A protective blue layer covers the reflective film and is peeled off before use. (b) Standard refractive homogeniser with no reflective film. This is the view from the entry aperture of the homogeniser. (c) Conjugate refractive-reflective homogeniser with 3d structure and reflective film in place. (For interpretation of the references to color in this figure legend, the reader is referred to the web version of this article.)

encapsulate overlap and optical loss, as well as ensuring alignment. This method however also weakens the joint and stability of the homogeniser. When the system is tilted to track the sun during use, the homogeniser may lean to one side and would perhaps stick to the reflective film, voiding TIR or even peeling away from the solar cell itself. These nodes ensure this does not happen and reduce the strain on the joint to the solar cell.

The material used for the 3D printed homogeniser support structure was ABSplus-P430. This is a durable thermoplastic which undergoes heat deflection at 96 °C under 66psi and at 82 °C under 264 psi respectively (Stratasys, 2008). Fig. 6b is a top view of the purely refractive homogeniser and the 1 solar cell reflected in the homogenisers' sides. Due to the reversibility of light paths, the more area seen to be covered by the solar cell and its reflections the more incident light from the sun would reach the solar cell. In this way the improvement can be visually seen when using the CRRH (Fig. 6c) where there is less reflected light and more solar cell coverage. When Fig. 6b and c photos were taken the camera and apparatus was kept in the same place and the only change made was the addition of the reflective sleeve casing (making it CRRH). Visually it can be seen that more light is being absorbed and less reflected back. There is also more solar cell area seen in Fig. 6c near the edges of the refractive medium. This is particularly noticeable at the bottom of Fig. 6c where the reflection of 3 solar cells is seen but at the bottom of Fig. 6b there are only 1 and a half solar cells being reflected. This was confirmed by an increased flux reading from the solar cell.

4. Temperature testing of materials

A complete prototype of the cassegrain set up with the CRRH was subjected to increased temperatures inside a thermal heater to test the ABS plastic of the primary reflector and the CRRH support structure. The full prototype was placed inside a vacuum drying oven (with vacuum mode off) and left for at least 3 h at set temperatures of 60, 70 and 80 °C (not including the time it took for the oven to reach the desired temperature). Higher temperatures were not tested due to the attachment of the solar cell to the CRRH which could be damaged if exposed to higher temperatures. No visual deformation was seen on the CRRH components. When retested under a solar simulator of 1000 W/m^2 there was also no change to the power output after this heat exposure.

The bulk of the homogeniser is made of sylguard which has recommended operational temperature range from −45 °C to 200 °C (Dow Corning Corporation, 2013). The optical transmittance of silicone and encapsulation materials degrades with length of exposer to UV light and excessive heating and cooling (Dow Corning Corporation, 2013; Mcintosh et al., 2009; Miller et al., 2015;

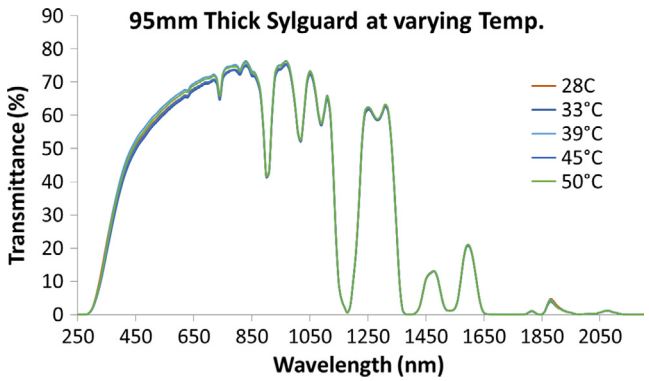

Fig. 7. Transmittance spectra through sylguard at varying temperatures.

Randall Elgin et al., 2007). The transmittance of the sylguard at varying temperatures was measured and the results shown in Fig. 7. There is only a slight difference between these results which is most likely due to soiling and slightly different entrance and exit positions during testing. With curved refractive optics or grooved refractive lenses, the temperature has an effect on the optical properties due to the expansion of the material. In the concentrator tested here the homogeniser has flat refractive surfaces and so the temperature has a negligible effect during operation. It would be expected however that with years of exposure and use, the transmittance quality would decrease.

A 3 by 3 array prototype of the cassegrain concentrator was also built and then tested at the Indian Institute of Technology Madras (IITM) in Chennai as shown in Fig. 8. Under these increased ambient temperatures of around ~30 °C (Nov-Feb), the air temperature inside the 3 by 3 module was measured to be between 50 and 60 °C depending on DNI and duration in sunlight. When the prototype was misaligned with the sun, causing the light to focus on the CRRH 3D printed support structure (Fig. 8a), the plastic material began to melt as shown in Fig. 8b and c. This does not happen when the system is kept aligned within its working range but an improvement to the design would be to fix reflective film or a similar protective layer to shade the 3d printed material from the direct concentrated focusing point. This would ensure the systems components are not at risk of damage if for whatever reason the solar tracker stops working accurately and the system becomes misaligned for >5 min.

As you can see from Fig. 8b, the deformation is localized, confirming that it is only the focal area which is capable of melting the 3d printed plastic. This localization can also be seen in the infrared images shown in Fig. 9. A different plastic cannot be chosen at this time for the 3d printed structure due to the 3d printing process and requirements. Other manufacturing processes could be employed to make the support structure but the accuracy must be within ±0.5 mm. The tapered wall, nodes and feet of the support structure would be difficult to manufacture with a different process and no doubt cost more, especially for small batch prototype orders.

The focal area of the concentrated light was measured to be a far higher temperature than the inside of the module, reaching a maximum of 149 °C with an open (no walls) system and a maximum of 226.3 °C with a closed system (no air ventilation). Thermocouples were used instead of the infrared camera to take all temperature measurements including the focal area temperature as shown in Fig. 9b. The infrared images however also show the overall temperature dispersion within the module and one cassegrain primary was removed to show the difference in temperature when no light concentration takes place (Fig. 9a). From Fig. 9a and b you can see that the temperature of the secondary reflectors, the tops of the homogeniser and the bottom of the

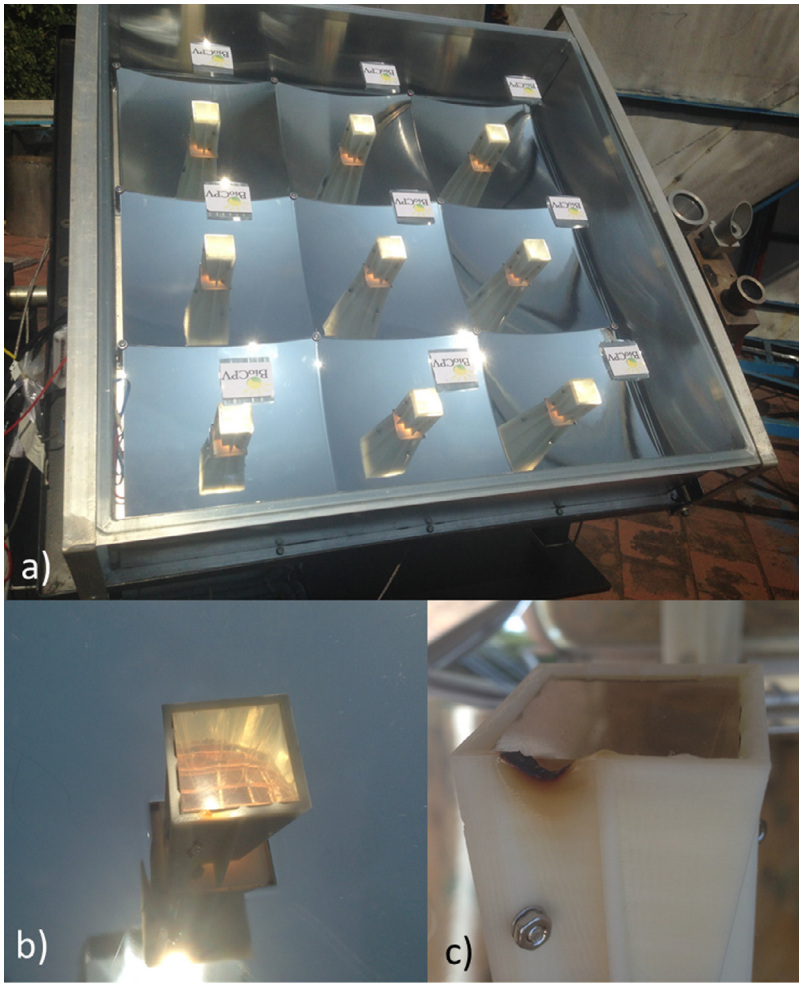

Fig. 8. (a) Photo of complete 3 by 3 prototype with side walls in place (closed) mounted on a 2 axis automatic tracker at IIT Madras, Chennai. (b) Photo of CRRH with concentrated light focusing off-centre onto plastic material of 3d printed support structure and causing burn marks. (c) Close up photo of melting due to >20 min of focused light incident on CRRH plastic support structure.

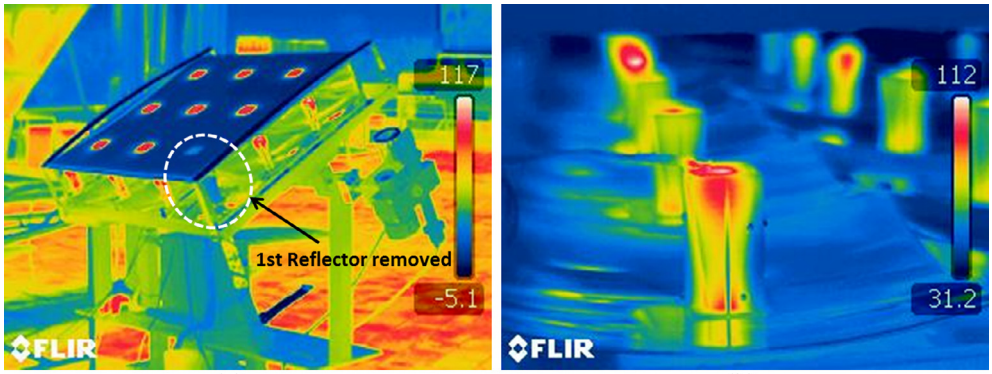

(a) (b)

Fig. 9. (a) Infrared photo of 3 by 3 concentrator prototype with side walls off (open) mounted on solar tracker at IIT Madras, Chennai. The bottom right primary reflector has been removed so there is no concentration of light on the secondary or homogenizer, hence the cooler temperature coloring shown in this corner. (b) Close up of homogenizer situated bottom left of Fig. 8b) with thermocouple used to measure focal area temperature.

homogeniser, near the solar cell, were the higher temperature areas of the system. The high absorption of the homogeniser (Fig. 5c and d) suggests the homogeniser optic to be the most heated part of the system. Prolonged use at these temperatures could damage the sylguard material and transparency over time.

The solar cells themselves were measured using a calibrated K-type thermocouple attached with thermal adhesive to the underside of the cell. Three solar cells were measured, the central, bottom corner and left centre solar cells in the 3 by 3 array. The measured temperatures of the central solar cell varied between 54 and 61 °C for the closed (no air ventilation) system and between 43 and 48 for the open (no walls) system. The left centre cell and corner cell were slightly lower than the central cell temperature but similar to each other and varied between 51 and 57 °C in the closed system. In the open system the middle left and the bottom corner cell temperatures separated more and a temperature of between 40 and 44 °C was measured for the middle left and of 38–40 °C for the bottom corner. These measurements although done with a thermocouple attached to the solar cell assembly are not measuring the direct temperature on the top of the cell which as indicated by the infrared images to be higher. There may be a significant difference even between the top of the solar cell and the bottom of the solar cell due to the concentration of light, insulating homogeniser material and large cooling heat sink on the bottom. As previously suggested, the homogeniser is absorbing most of the thermal radiation but will also be insulating the solar cell. Further detailed thermal analysis would need to be conducted to ensure the operating temperature of the solar cell was not significantly reducing its conversion efficiency. From the difference in temperatures between the open and closed systems, the different cell positions and the rate of heating and cooling of the system it was assumed that the large aluminium heat sink was working effectively at cooling the solar cells, especially with the aid of air movement around the system. The primary reflectors were at a safe lower temperature; hence their bulk plastic material did not melt. With each stage and increase in light concentration, an increase in temperature can also be expected and so 2nd or 3rd stage optics should have a higher working temperature range than the 1st. The location and function of the concentrator system will however have an effect on this.

5. I-V output and incidence angle

The estimated irradiance reaching the solar cell for this prototype is shown in Fig. 10 below. This is resulting from the measured efficiencies of each component being applied to the AM1.5 direct irradiance spectrum (Fig. 5). The low reflectance of the hand polish aluminium secondary reflector over the range ~200–900 nm from Fig. 5 can be seen in Fig. 10 to drop the irradiance over that range down significantly. The main loss however is due to the absorption within the dielectric material used for the CRRH. The transmittance spectra of the homogeniser is shown in Fig. 5c and the average transmittance over 300–1800 nm shown in Fig. 5d. The average transmittance is less than 50% at a thickness of >75 mm. The homogeniser reduces the efficiency significantly in the wavelengths >1100 which the secondary reflector does now. Overall the thick sylgard is the greatest source of loss within the system due to absorption. From Fig. 10 it can be estimated that the optical efficiency is as low as ~35%. Shorter CRRH designs or CRRH optics made of different refractive mediums could have a substantially higher optical efficiency.

The multijunction solar cell used was the 3C42A 10 × 10 mm^2 CPV TJ Solar Cell from Azur Space (Azure Space Solar Power GMBH, 2014). This cell has a wavelength range of ~300–1700 nm and a peak efficiency of 41.5% depending on sun concentration and temperature as shown in Fig. 11.

The solar concentration of the system will be less than 500× which is its ideal geometrical concentration ratio. As can be seen from Fig. 11b, the cell efficiency has a relatively flat relationship with sun concentration at below 500× so the defining parameter for efficiency in this case will be the operating temperature of the solar cell. The temperature of the cell was measured experimentally during operation to vary between 40 and 60 °C which would give a theoretical cell efficiency of ~40.5% but as already suggested a more thorough thermal analysis would be required to know for sure.

The cassegrain concentrator was tested under a continuous type WACOM 1000 W/m^2 class AAA indoor solar simulator (Wacom Electric Company Ltd., 2014) at the university of Exeter Penryn campus with the CRRH and with the standard refractive homogeniser counterpart. I-V traces were taken for a range of alignment angles against the simulated incident light as shown in Fig. 12 below.

The CRRH consistently improved the power output in comparison to the purely refractive homogeniser as shown in Fig. 12. The CRRH increased the Pmax by 3.5% at normal incidence and by 4.5% at 0.5° misalignment. This makes sense as at an increased incidence angle, more light rays should be lost through the side walls of the homogeniser (site 4 in Fig. 4b) and hence the CRRH captures more light and a greater improvement in optical efficiency is seen. At 1° misalignment (the theoretical acceptance

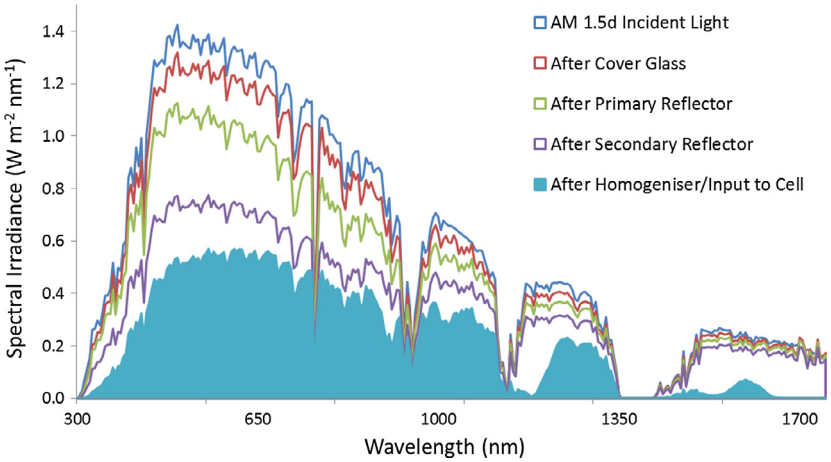

Fig. 10. Graph of irradiance as it filters through the optical stages within the prototype concentrator.

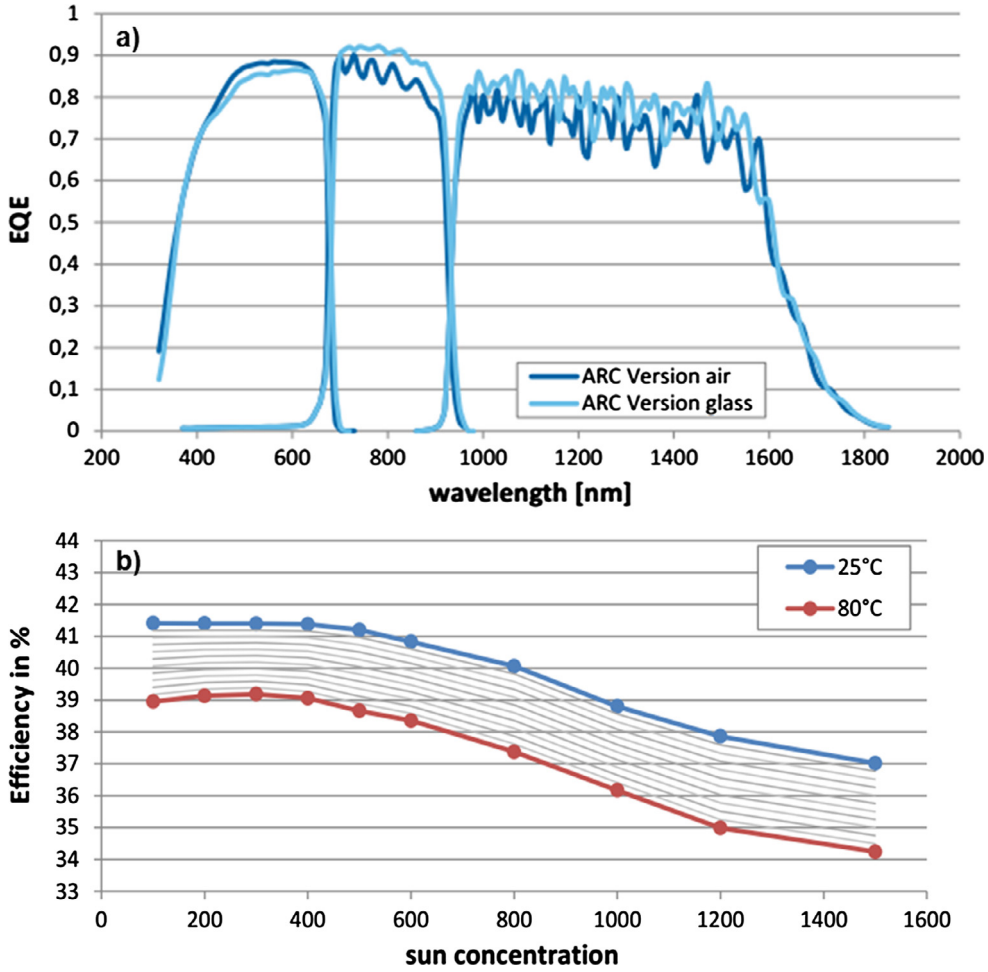

Fig. 11. Graph of conversion efficiency vs. sun concentration for the 10 by 10 mm Azure Space solar cell 3C42 at varying operation temperatures(Azure Space Solar Power GMBH, 2014).

angle of the system), more light is now missing the secondary reflector (site 1 in Fig. 4b) and so the power increases by only 3.7% with the CRRH. At 2 and 3° misalignment the percentage increase in power is 11.3% and 48.7% but this is due to more light being captured at the entrance surface of the CRRH. The CRRH has an entry aperture of 32 mm by 32 mm due to the extra 1 mm air gap added to each side of the original refractive homogeniser of 30 mm by 30 mm entrance aperture. The set-up of the complete cassegrain concentrator is such that light is focused to the centre of the homogenising optic and hence this increased entry aperture effect would only be noticeable when the light began to focus at the edge of the entrance aperture (at 2 or 3° misalignment angles) as shown in Fig. 12b. Any increase in power output is however an advantage. This explains why the power increase of the CRRH in

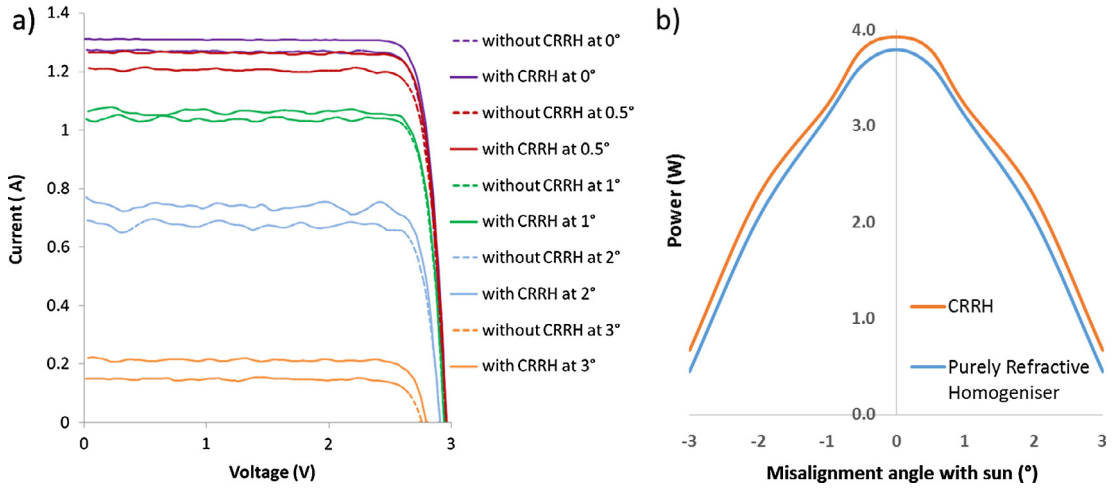

Fig. 12. (a) Comparison of I-V plots for the cassegrain concentrator with a standard refractive homogenizer and with the CRRH at various solar misalignment angles. (b) Power output against full system misalignment angle with normal axis incident light for both homogenizer types.

Fig. 12b stays fairly constant from 2 to 3° despite there being less light incident on the homogeniser optic overall.

The acceptance angle technically does not increase very much from the results shown in Fig. 12b due to the normal incidence power also increasing and hence 90% of that value results in roughly the same acceptance angle as the lower performing pure refractive homogeniser. However, it is clear from Fig. 12a and b that the CRRH outperforms the purely refractive homogeniser. The shape of the CRRH power output in Fig. 12b is slightly unusual but emphasis the stages of loss already discussed in the previous paragraph and in Fig. 4. The optical tolerance of a system is a very important part of a design especially as concentration levels increase for future designs. More complex reflective sleeves consisting of conic curves, grooves or truncated tiling may improve the acceptance angle more significantly. Misalignments in tracker systems are still very common and for high concentration designs can significantly reduce their output from their full potential.

The fill factor for the set up with and without the CRRH was around 0.85 at normal incidence and 0.87 at 1° misalignment and 0.84 at 2–3° misalignment. The absolute efficiency of the system was significantly lower than anticipated due to the low reflection and high absorption of the optics as discussed previously. The temperature of the solar cell could also be reducing the overall efficiency but by how much is not known without a more thorough investigation into the exact temperature of the cell. There are many papers which try to predict the conversion efficiency of solar cells depending on incident irradiance, temperature distribution across the cell, hours of operation and rate of temperature changes during operation.

6. Comparing theoretical predictions to experimental and CAP analysis

The maximum acceptance angle for a 500× geometrical concentration design is 3.59° assuming a refractive index of 1.4 for the homogeniser. The maximum acceptance angle is never attainable due to a variety of non-ideal contributors such as manufacturing errors, temperature effects and material properties. The concentration-acceptance product (CAP) does however give a value of how good the design is in comparison to its theoretical limits. The higher the CAP the more fulfilling the design is for that specific geometric concentration level. A summary table of the optical efficiency, resulting concentration ratio, acceptance angle and the associated CAP is given below (see Table 1).

For this system, the CAP is roughly a third of its ideal if we only look at the optimised design detailed in the previous theoretical studies. This is relatively standard in comparison to other designs of similar concentration ratios. The addition of the CRRH instead of a purely refractive homogeniser slightly increases the CAP. Once the realistic optical efficiency is introduced the CAP falls significantly, especially due to the high absorption of the homogeniser as shown in Fig. 5. Using a different material such as Glass or PMMA should reduce the absorption and improve the performance significantly.

The maximum theoretical optical efficiency increase due to the CRRH was 7.76% in the simulations carried out previously by Shanks et al. (2016a). Experimental measurements with a Fresnel lens set up produced 6.7% but it was suspected that some light entered the air gap in this experiment at normal incidence due to the slightly larger focal area using the Fresnel lens. The maximum experimental increase in power measured from these studies was 4.5% using the cassegrain set up which had a tighter focal spot incident only on the refractive core of the CRRH. The simulated optical efficiency from before assumed a lower absorption for the homogeniser refractive material. In this study sylgard 184 was utilised and had significant absorption losses as shown in Figs. 5c and d and 10, especially in the infrared range. This results in overall a lower optical efficiency of the system and a lower concentration incident on the cell than theoretically suggested. The benefit of the CRRH is expected to increase with concentration ratio as there is more light for it to recapture.

The absorption losses are more significant in the infrared range and in theory these wavelengths would benefit most from the CRRH due to their slightly higher critical angle requirements. This slight increase in critical angle (+0.5° between 589 nm and 1554 nm) as wavelength size increases may or may not be negligible depending on how close to the critical angle the light rays are originally. It is well known that temperature can alter the refractive index and shape of a dielectric optic which in turn can push an optimised design over or under its peak performance parameters. The same could be occurring to some degree in this design as there are such high temperatures present on the homogeniser in particular. A fully optimised homogeniser would just fulfil TIR conditions and no more, achieving the maximum concentration ratio and acceptance angle before optical efficiency decreased too low. In which case anything that could risk changes to the refractive index, angle of incidence or shape of the optic would again alter the optics performance and optical efficiency.

Table 1
Cap analysis of cassegrain concentrator for different optical efficiencies.

Design scenario	Optical efficiency	Effective concentration ratio	Acceptance angle (°)	CAP
Ideal (maximum values possible)	100%	500×	3.59	1.4 (n)
Geometric design (no reflection or absorption losses) (Shanks et al., 2016b)	100%	500×	1.2	0.468
Standard (not conjugate) Refractive Homogeniser (theoretical losses) (Shanks et al., 2016a)	68%	340×	1	0.322
CRRH (theoretical losses) (Shanks et al., 2016a)	71%	355×	1	0.329
CRRH (measured)	~40%	200×	~0.8	0.197

The simulations carried out for this design also did not take into account the conversion efficiency of the solar cell or temperature effects. All of the above contribute to the difference between the theoretical and experimental results. From this study a 4.5% increase in power output is the maximum realistic benefit of the CCRH within a cassegrain concentrator set up of similar concentration and manufactured with similar materials and methods.

7. Discussion and future outlook

The CRRH optic is a simple but effective method to improve the power output of a concentrator system utilising a receiver/homogenising optic. How much the CRRH will benefit the system depends on the input energy to the homogenizer (whether this be due to a higher concentration ratio or optical efficiency of the system) and the manufacturing quality of the homogenising optic. High accuracy manufacturing with very smooth surface finishes for the purely refractive homogenizer should see minimal improvement with the addition of a reflective sleeve to make the CRRH. In this study, the refractive homogenizer was manufactured using sylgard material and a mould made of polished aluminium which is a common method for small optics such as this.

The theoretical analysis suggested a possible increase in power output of 7.76% and the experimental testing carried out in this study gave a maximum of 4.5% power increase. The difference in these values is most likely due to high absorption by the thick homogenizer and possibly the high operating temperature of the solar cell. Small misalignments within the system; and the lower reflectance of the primary and secondary reflectors also reduces the amount of light available to recover if scattered. As previously discussed other effects such as temperature and refractive index change could be altering the optical efficiency and acceptance angle of the homogenizer. It is suggested for future work in high and ultrahigh concentration levels to not only design for manufacturing tolerances but also temperature tolerances. This may mean choosing design variables which actually precede the optimum performance design at room temperature but will continue to fulfill TIR or similar parameter conditions at high operating temperatures where the refractive index has decreased. From this and previous analysis of the CRRH (Shanks et al., 2016a), it would seem the CRRH's benefit to optical efficiency increases with an increase in input light, such as for higher concentration ratio designs. This also makes sense as higher concentration systems are also more prone to diverging focal spots and a wider range of light ray angles incident on the secondary and tertiary optics. It can also be deduced from these experimental results that roughly 40% of a simulated performance increase, due to the CRRH or a similar conjugate refractive reflective optic in comparison to a purely refractive counterpart, can be realized in experimental testing.

The structure of the CRRH could be improved by using a different material for the support structure such as aluminium or similar which can handle the very high temperatures of the focused light. This type of structure however may be heavy depending on the design. A skeletal support structure may not be strong enough to hold the reflective film in place. Sheets of polished aluminium could be used to surround the refractive medium but manufacturing would have to be accurate to ensure the ~1 mm air gap between the two materials. Some kind of node seems to be beneficial to maintain alignment. Perhaps the refractive homogenizer and its matching reflective casing could be manufactured together and then separated slightly. A simple solution to avoid the 3D printed structures melting in this study would be to add a protective layer to the top edge of the CRRH plastic material to diffusely reflect the focused light safely away. Improving the alignment and focusing capabilities of the system would also reduce the risk of the focused light hitting the 3D printed plastic structure. Another improvement would be to have a refractive medium with a higher transmittance or to perhaps try a lens walled approach to reduce absorption losses through the thick homogenizer. Overall this concept of conjugate refractive reflective optics should be researched further for other shapes and their benefit analyzed.

The use of plastic core optics appears to be a valuable option, especially for the prototyping stage of CPV. From these results they are however limited to low concentration optics, primary optics in higher concentration set ups or as support structures not subject to focused light. Their durability with time should however be tested further.

8. Conclusion

The Conjugate Refractive Reflective Homogeniser has been experimentally tested within a 500× geometric concentration cassegrain design. A prototype of the complete system was built and experimentally tested. Measurements showed a 4.5% increase in power. This was ~40% of the theoretical improvement calculated by simulations (7.76%). Temperature testing was also carried out on the components and the 3D printed support structure for the CRRH was found to be inadequate at coping with the direct focused sunlight. However, the resulting deformation in the structure only occurs when there is a misalignment of 2–3° in the system. The high operating temperature should not affect the transmittance of the homogenizer since flat refractive surfaces are used and hence expansion of the refractive medium should not alter the direction of light. Improving the design by using a protective layer on the 3d printed support structure should easily solve this issue. The experimental tests confirmed the CRRH can improve the power output of a cassegrain concentrator of this design and 500× geometric concentration ratio.

Acknowledgments

This work was partly funded by the Newton Bhabha PhD Placement fund and partly by DST, India (Ref No: DST/SEED/INDO-UK/002/2011) and EPSRC, UK, (Ref No: EP/J000345/1) through the BioCPV project. Authors acknowledge all funding agencies for the support. In support of open access research all underlying article materials (such as data, samples or models) can be accessed upon request via email to the corresponding author.

References

Azure Space Solar Power GMBH, 2014. Enhanced Fresnel Assembly - EFA Type: 3C42A – with $10 \times 10\ mm^2$ CPV TJ Solar Cell Application: Concentrating Photovoltaic (CPV) Modules.

Baig, H., 2015. Enhancing Performance of Building Integrated Concentrating Photovoltaic Systems (Article). University of Exeter.

Baig, H., Heasman, K.C., Mallick, T.K., 2012. Non-uniform illumination in concentrating solar cells. Renew. Sustain. Energy Rev. 16, 5890–5909. http://dx.doi.org/10.1016/j.rser.2012.06.020.

Baig, H., Sarmah, N., Chemisana, D., Rosell, J., Mallick, T.K., 2014. Enhancing performance of a linear dielectric based concentrating photovoltaic system using a reflective film along the edge. Energy 73, 177–191.

Baig, H., Sellami, N., Mallick, T.K., 2015. Trapping light escaping from the edges of the optical element in a concentrating photovoltaic system. Energy Convers. Manage. 90, 238–246. http://dx.doi.org/10.1016/j.enconman.2014.11.026.

Benítez, P., Miñano, J.C., Zamora, P., Mohedano, R., Cvetkovic, A., Buljan, M., Chaves, J., Hernández, M., 2010. High performance Fresnel-based photovoltaic concentrator. Opt. Exp. 18, A25–A40. http://dx.doi.org/10.1364/OE.18.000A25.

Canavarro, D., Chaves, J., Collares-Pereira, M., 2013. New second-stage concentrators (XX SMS) for parabolic primaries; comparison with conventional parabolic trough concentrators. Sol. Energy 92, 98–105. http://dx.doi.org/10.1016/j.solener.2013.02.011.

Chen, Y.T., Ho, T.H., 2013. Design method of non-imaging secondary (NIS) for CPV usage. Sol. Energy 93, 32–42. http://dx.doi.org/10.1016/j.solener.2013.03.013.

Chong, K.K., Lau, S.L., Yew, T.K., Tan, P.C.L., 2013. Design and development in optics of concentrator photovoltaic system. Renew. Sustain. Energy Rev. http://dx.doi.org/10.1016/j.rser.2012.11.005.

Digrazia, M., Jorgensen, G., 2010. Reflectech Mirror Film: Design Flexibility and Durability in Reflecting Solar Applications.

Dow Corning Corporation, 2013. Electronics Sylgard ® 184 Silicone Elastomer. http://dx.doi.org/10.1017/CBO9781107415324.004.

Dreger, M., Wiesenfarth, M., Kisser, A., Schmid, T., Bett, A.W., 2014. Development and Investigation of A CPV Module with Cassegrain Mirror Optics, in: CPV-10.

Fend, T., Hoffschmidt, B., Jorgensen, G., Kuster, H., Kruger, D., Pitz-Paal, R., Rietbrock, P., Riffelmann, K.J., 2003. Comparative assessment of solar concentrator materials. Sol. Energy 74, 149–155. http://dx.doi.org/10.1016/S0038-092X(03)00116-6.

Fraas, L.M., 2014. Low-Cost Solar Electric Power. Springer International Publishing, Cham. http://dx.doi.org/10.1007/978-3-319-07530-3.

Gordon, J.M., Feuermann, D., Young, P., 2008. Unfolded aplanats for high-concentration photovoltaics. Opt. Lett. 33, 1114–1116.

Hatwaambo, S., Hakansson, H., Nilsson, J., Karlsson, B., 2008. Angular characterization of low concentrating PV–CPC using low-cost reflectors. Sol. Energy Mater. Sol. Cells 92, 1347–1351. http://dx.doi.org/10.1016/j.solmat.2008.05.008.

Kaushika, N., Reddy, K., 2000. Performance of a low cost solar paraboloidal dish steam generating system. Energy Convers. Manage. 41, 713–726. http://dx.doi.org/10.1016/S0196-8904(99)00133-8.

Leutz, R., Suzuki, A., 2001. Nonimaging Fresnel Lenses: Design and Performance of Solar Concentrators. Springer Science & Business Media.

McDonald, M., Horne, S., Conley, G., 2007. Concentrator Design to Minimize LCOE 6649, 66490B-66490B-11. http://dx.doi.org/10.1117/12.735738.

Mcintosh, K.R., Cotsell, J.N., Cumpston, J.S., Norris, A.W., Powell, N.E., Ketola, B.M., 2009. The Effect of Accelerated Aging Tests on the Optical Properties of Silicone and EVA Encapuslants.

Miller, D.C., Annigoni, E., Ballion, A., Bokria, J.G., Bruckman, L.S., Burns, D.M., Chen, X., Elliott, L., Feng, J., French, R.H., Fowler, S., Gu, X., Hacke, P.L., Honeker, C.C., Kempe, M.D., Khonkar, H., Köhl, M., Perret-Aebi, L.-E., Phillips, N.H., Scott, K.P., Sculati-Meillaud, F., Shioda, T., Suga, S., Watanabe, S., Wohlgemuth, J.H., 2015. Degradation in PV encapsulation transmittance: an interlaboratory study towards a climate-specific test preprint degradation in PV encapsulation transmittance: an interlaboratory study towards a climate-specific test. In: 42nd IEEE Photovoltaic Specialists Conference, New Orleans, Louisiana.

Randall Elgin, Bill Riegler, Rob Thomaier, 2007. How Temperature Effects Transmission of Silicone Encapsulants a Survey of the effects of temperature in optically clear silicones. Photonics Spectra.

ReflecTech.Inc, 2014. ReflecTech Mirror Film Technical [WWW Document]. URL <http://www.reflectechsolar.com/technical.html> (accessed 4.20.16).

Roman, R.J., Peterson, J.E., Goswami, D.Y., 1995. An off-axis cassegrain optimal design for short focal length parabolic solar concentrators. J. Sol. Energy Eng. 117, 51. http://dx.doi.org/10.1115/1.2847742.

Shanks, K., Baig, H., Senthilarasu, S., Reddy, K.S., Mallick, T.K., 2016a. Conjugate refractive–reflective homogeniser in a 500× Cassegrain concentrator: design and limits. IET Renew. Power Gener. 1–8. http://dx.doi.org/10.1049/iet-rpg.2015.0371.

Shanks, K., Sarmah, N., Ferrer-Rodriguez, J.P., Senthilarasu, S., Reddy, K.S., Fernández, E.F., Mallick, T., 2016b. Theoretical investigation considering manufacturing errors of a high concentrating photovoltaic of cassegrain design and its experimental validation. Sol. Energy 131, 235–245. http://dx.doi.org/10.1016/j.solener.2016.02.050.

Shanks, K., Senthilarasu, S., Mallick, T.K., 2016c. Optics for concentrating photovoltaics: trends, limits and opportunities for materials and design. Renew. Sustain. Energy Rev. 60, 394–407.

Shanks, K., Senthilarasu, S., Mallick, T.K., 2015. High-concentration optics for photovoltaic applications. In: Pérez-Higueras, P., Fernández, E.F. (Eds.), High Concentrator Photovoltaics: Fundamentals, Engineering and Power Plants, Green Energy and Technology.. Springer International Publishing, Cham, pp. 85–113. http://dx.doi.org/10.1007/978-3-319-15039-0.

Stratasys, 2008. ABSplus Properties.

Tang, R., Wang, J., 2013. A note on multiple reflections of radiation within CPCs and its effect on calculations of energy collection. Renew. Energy 57, 490–496. http://dx.doi.org/10.1016/j.renene.2013.02.010.

Terry, C.K., Peterson, J.E., Goswami, D.Y., 2012. Terrestrial solar-pumped iodine gas laser with minimum threshold concentration requirements. J. Thermophys. Heat Transf.

Terry, C.K., Peterson, J.E., Goswami, D.Y., 1996. Feasibility of an iodine gas laser pumped by concentrated terrestrial solar radiation. J. Sol. Energy Eng. 118, 136. http://dx.doi.org/10.1115/1.2848006.

Tsai, C.-Y., 2013. Enhanced irradiance distribution on solar cell using optimized variable-focus-parabolic concentrator. Opt. Commun. 305, 221–227. http://dx.doi.org/10.1016/j.optcom.2013.04.052.

Victoria, M., Domínguez, C., Antón, I., Sala, G., 2009. Comparative analysis of different secondary optical elements for aspheric primary lenses. Opt. Exp. 17, 6487–6492.

Victoria, M., Dominguez, C., Askins, S., Anton, I., Sala, G., 2013. Experimental analysis of a photovoltaic concentrator based on a single reflective stage immersed in an optical fluid. Prog. Photovoltaics Res. Appl. http://dx.doi.org/10.1002/pip.2381.

Wacom Electric Company Ltd., 2014. Wacom Product Solar Simulator [WWW Document]. URL <http://www.wacom-ele.co.jp/en/products/solar/normal/> (accessed 11.14.16).

Winston, R., 1970. Light collection within the framework of geometrical optics. J. Opt. Soc. Am. 60, 245. http://dx.doi.org/10.1364/JOSA.60.000245.

Xu, Y.J., Liao, J.X., Cai, Q.W., Yang, X.X., 2013. Preparation of a highly-reflective TiO_2/SiO_2/Ag thin film with self-cleaning properties by magnetron sputtering for solar front reflectors. Sol. Energy Mater. Sol. Cells 113, 7–12. http://dx.doi.org/10.1016/j.solmat.2013.01.034.

Yehezkel, N., Appelbaum, J., Yogev, a., Oron, M., 1993. Losses in a three-dimensional compound parabolic concentrator as a second stage of a solar concentrator. Sol. Energy 51, 45–51. http://dx.doi.org/10.1016/0038-092X(93)90041-L.

Yin, L., Huang, H., 2008. Brittle materials in nano-abrasive fabrication of optical mirror-surfaces. Precis. Eng. 32, 336–341. http://dx.doi.org/10.1016/j.precisioneng.2007.09.001.

[Article 5]

K. Shanks, S. Senthilarasu, R. H. Ffrench-Constant, and T. K. Mallick, “White butterflies as solar photovoltaic concentrators,” *Sci. Rep.*, vol. 5, p. 12267, Jul. 2015.

SCIENTIFIC REPORTS

OPEN

White butterflies as solar photovoltaic concentrators

Katie Shanks[1], S. Senthilarasu[1], Richard H. ffrench-Constant[2] & Tapas K. Mallick[1]

Received: 27 January 2015
Accepted: 12 June 2015
Published: 31 July 2015

Man's harvesting of photovoltaic energy requires the deployment of extensive arrays of solar panels. To improve both the gathering of thermal and photovoltaic energy from the sun we have examined the concept of biomimicry in white butterflies of the family Pieridae. We tested the hypothesis that the V-shaped posture of basking white butterflies mimics the V-trough concentrator which is designed to increase solar input to photovoltaic cells. These solar concentrators improve harvesting efficiency but are both heavy and bulky, severely limiting their deployment. Here, we show that the attachment of butterfly wings to a solar cell increases its output power by 42.3%, proving that the wings are indeed highly reflective. Importantly, and relative to current concentrators, the wings improve the power to weight ratio of the overall structure 17-fold, vastly expanding their potential application. Moreover, a single mono-layer of scale cells removed from the butterflies' wings maintained this high reflectivity showing that a single layer of scale cell-like structures can also form a useful coating. As predicted, the wings increased the temperature of the butterflies' thorax dramatically, showing that the V-shaped basking posture of white butterflies has indeed evolved to increase the temperature of their flight muscles prior to take-off.

Solar concentrators use mirrors and lenses to capture light and direct it towards smaller areas of photovoltaic (PV) material where the solar energy is converted into electricity[1]. In this way the cost of the overall system is reduced by decreasing the area of photovoltaic material required which is typically the most expensive part of a PV solar panel[1,2]. However, the introduction of these optical devices to focus light onto these solar cell(s) can result in very bulky systems. Although solar concentrators can reduce solar energy costs and improve efficiencies, their weight and size therefore often limits their deployment[3,4]. Current solar concentrators vary widely in design and even the simple polishing of metal can result in a reflective mirror finish but such polished surfaces are very heavy and specific curved shapes are difficult and therefore expensive to manufacture[5,6]. Reflective film adhered to plastic mirrors is a second option but this setup often has low reflectivity when applied to complex surfaces[6]. Polymer mirror films are a more recent third method to gain reflectance values of >90% but require specially designed structures to gain the appropriate shapes for a given application[7,8]. Vacuum metalizing is therefore the current best option but this process is highly dependent on the material and surface quality it is bonded with in order to ensure a high quality mirror finish[5,9]. Given the limitations of all existing systems, further study into possible lightweight reflective materials and structures is important. The benefits of a lightweight, easily applied reflective material or coating would not only improve the development of solar concentrator technologies but may also be beneficial to many other disciplines where lightweight highly reflective coatings are desirable.

The white butterflies of the genus *Pieris* take flight before other butterflies on cloudy days when solar inputs to flight muscle warming are limited. This ability to heat up quickly on cloudy days has been anecdotally suggested to relate to the V-shaped posture they adopt whilst basking in cloudy conditions, a process we here term 'reflectance basking'. These white butterflies do indeed show high wing reflectance based upon a unique display of pterin containing nano-beads within their individual wing scales as

[1]Environment and Sustainability Institute, Biosciences, University of Exeter, Falmouth, TR10 9FE, UK. [2]Centre for Ecology and Conservation, Biosciences, University of Exeter, Falmouth, TR10 9FE, UK. Correspondence and requests for materials should be addressed to R.H.F.-C. (email: rf222@exeter.ac.uk) or T.K.M. (email: T.K.Mallick@exeter.ac.uk)

extensively reported by Stavenga *et al.*[10–12], Giraldo *et al.*[13,14] and Morehosue *et al.*[15]. Luke *et al.*[16] expand on this descriptive work by removing the pterin beads and showing that overall reflectance is decreased by a third in the absence of the beads themselves. The precise arrangement of the pterin beads within the scale cell appears critical as it shows a quasi-random pattern that has recently been proposed to be optimum for efficient light manipulation[17].

Here we therefore investigate if the wings, or some derivation thereof, of the white *Pieris* butterflies can be used to develop a novel, lightweight reflective material directly applicable to solar concentrators. To investigate if a consideration of the photonics of butterfly wings is indeed useful in solar concentrator design we chose to first answer five specific questions. First, can we prove practically that the butterflies concentrate light, and indeed heat, onto their thorax? Second, is there an optimum angle with which they accomplish this and which we would therefore have to adhere to in solar concentrator design? Third, does the light reflected by the butterfly wings themselves actually match the input requirements of any given photovoltaic solar cell? Fourth, can whole butterfly wings thus be used directly to increase the output from a given solar cell? Finally, can specific sub-structures from the wing (e.g. a mono-layer of removed scale cells) or bead-like coatings (e.g. a coating of nano-beads with the same orientation and properties of the pterin beads) be used to achieve similarly improved solar cell outputs?

Butterfly wings are in fact surprisingly complex as butterflies not only have pairs of wings that are effectively linked in flight (and overlap at rest) but the scale cells on their wings also show dramatically different morphologies and orientations. Further, these scale cells can exist as complex overlapping layers therefore potentially conferring complex overall optical properties on the whole wing, as detailed extensively by the work of Vukusic *et al.*[18–20] and also by Kolle *et al.*[21]. Such complex naturally occurring structures can be used for various modern applications in a process known as 'biomicry'[22–24], however no studies have yet examined the *Pieris* wing structures as a basis for reflective materials in solar photovoltaic concentrators. Johnsen and Widder[25] showed that the pterin bead size is optimized for light scattering and that the two types of wing scales ('cover' and 'ground' scales) together produce wide-angle scattered light. Stavenga and co-workers also argue that to gain the full reflectance from the pierid wing a complete model including all components of the wing structure would be required. This would initially suggest that a single layer of scale cells or a thin coating of nano-beads correctly orientated would have insufficient optical performance to enhance inputs to a solar cell. One of the central aims of the research described here was therefore to see if a mono-layer of scale cells could recapitulate the reflective properties of the whole wing. Surprisingly, here we show that wings from the large white butterfly do indeed increase the efficiency of photovoltaic cells when the wings are held at a critical optimal angle for the concentration of both heat and light. Further, this whole wing configuration not only dramatically increases the power to weight ratio of the butterfly-solar cell structure but critically similar reflective properties can be achieved from a single mono-layer of removed scale cells. This work suggests that scale cell-like structures or indeed just coatings of correctly oriented nano-beads may be useful in even more lightweight coatings.

Results

Parallels between the V-shape of a basking butterfly and the V-trough concentrator. As white butterflies of the family Pieridae are especially effective at early take-off on cloudy days, and can therefore fly before other groups of butterflies in poor weather, we reasoned that this ability is due to the V-shaped posture they adopt with their wings while 'thermal' basking (Fig. 1a). This V-shaped posture should gather and focus solar energy, reflected by the wings, onto the body (thorax) of the butterfly (Fig. 1b) and thus, increase the temperature of the flight muscles prior to take-off. The V-shaped design of the butterfly is therefore strikingly similar to the V-trough solar concentrator which uses mirrored side walls to focus light towards a small area of photovoltaic material[3,26] (Fig. 1d) thereby increasing the output power of any solar cell to which it is attached[4,27].

Determining the optimal angle at which a butterfly should hold its wings. To directly test the hypothesis that the butterfly uses its wings to increase the temperature of its body and to determine the optimal angle at which the wings should be deployed, we measured the temperature of the butterflies' 'thorax' (at an equivalent position between the open wings) using an infra-red camera (Fig. 1c). Following 10 and 35 second exposure to the equivalent of 'one sun' (light from an artificial source mimicking bright sunlight[28]) we measured the temperature of the butterfly 'thorax' at different wing angles (measured from the vertical or normal). Using this experimental set-up we found that 17° from normal was the optimal angle for the butterfly to hold its wings and that this increased the 'body' temperature by 7.3 °C more than the temperature achieved when the wings were held flat (at 90°) (Fig. 2). These observations support the concept that thermal basking does indeed increase the temperature of the butterfly body and therefore directly implies that a similar experimental design could be useful in improving solar inputs to photovoltaic cells.

Matching the input requirements of a solar cell using different butterfly species. Before we could test this exciting hypothesis, we first needed to match the wavelength range reflected by the butterfly wings to the input requirements of a given solar cell. There have been various studies into how natural structures can affect light[18–21] and butterfly wing structures in particular are well researched[12,29–33] but

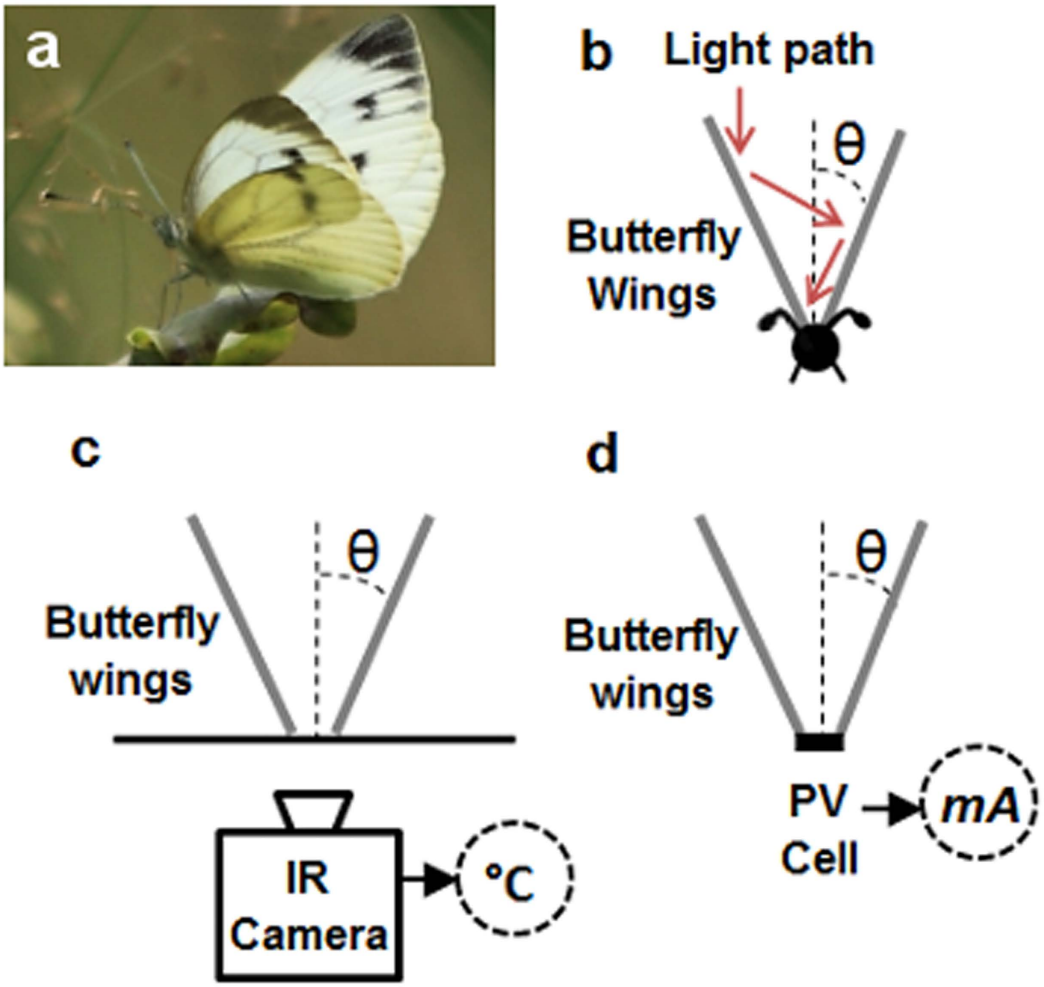

Figure 1. White butterflies as solar concentrators. (**a**), Photograph of large white (taken by Richard ffrench-Constant) with wings in 'V-shape' basking posture. (**b**), Schematic diagram of theoretical light concentration towards thorax via reflection from wings of butterfly. (**c**), Method for measuring wing angle effect on 'body' temperature (°C). (**d**), Method for measuring wing angle effect on current output (mA) from solar cell in place of 'body'.

none of this prior work relates specifically to solar cells. To determine which wings were best matched to a specific solar cell type, we first mapped the reflectance patterns across the forewings of three common *Pieris* species the large white, *P. brassicae*, the small white, *P. rapae*, and the green-veined white, *P. napi* (Fig. 3a–c). These reflectance maps strikingly emphasise the contrast between the low reflectance associated with the black spots present on the butterfly forewings (Fig. 3a,b) with the high reflectance of the surrounding white areas[18,21]. These gradients in reflectance across the wing are explained by well-known differences in the ultrastructure of black and white wing scales in this group[10,11,13,15,34,35]. In the white wing scales the scale windows (gaps in the scale structure) are partially filled with ovoid shaped granules or 'beads' (Fig. 3g). These ovoid beads contain the white pigment pterin which absorbs light in the short-wavelength range but strongly scatters light outside the pigment absorption range[11,13,34–36]. The black scales located in the two black spots lack these pigment carrying beads (Fig. 3h) and the black pigment melanin, which has a broad absorption spectrum, located in the cross-ribs of the scale itself[13,34].

Using the wings of the large white butterfly to increase power output from a solar cell. The highest reflectance came from the forewings of the large white butterfly and this reflectance was also well matched to the input requirements of a mono-crystalline silicon cell (average of 78.9% reflectance over 400–950 nm range, Fig. 3a). We therefore attached the wings of the large white butterfly to a 1 cm × 1 cm mono-crystalline silicon solar cell to test for any increase in output power. Attaching the wings increased the maximum power by 42.3% (from 16.8 mW to 23.9 mW) and when compared to the weight of standard reflective film increased the power to weight ratio 17 fold (Fig. 4a,b). Moreover, a mono-layer of scale cells removed from the wing onto adhesive tape also maintained similar high reflectance properties (62% reflectance from 400–950 nm, maintaining 78.6% of the original reflectance). Suggesting that

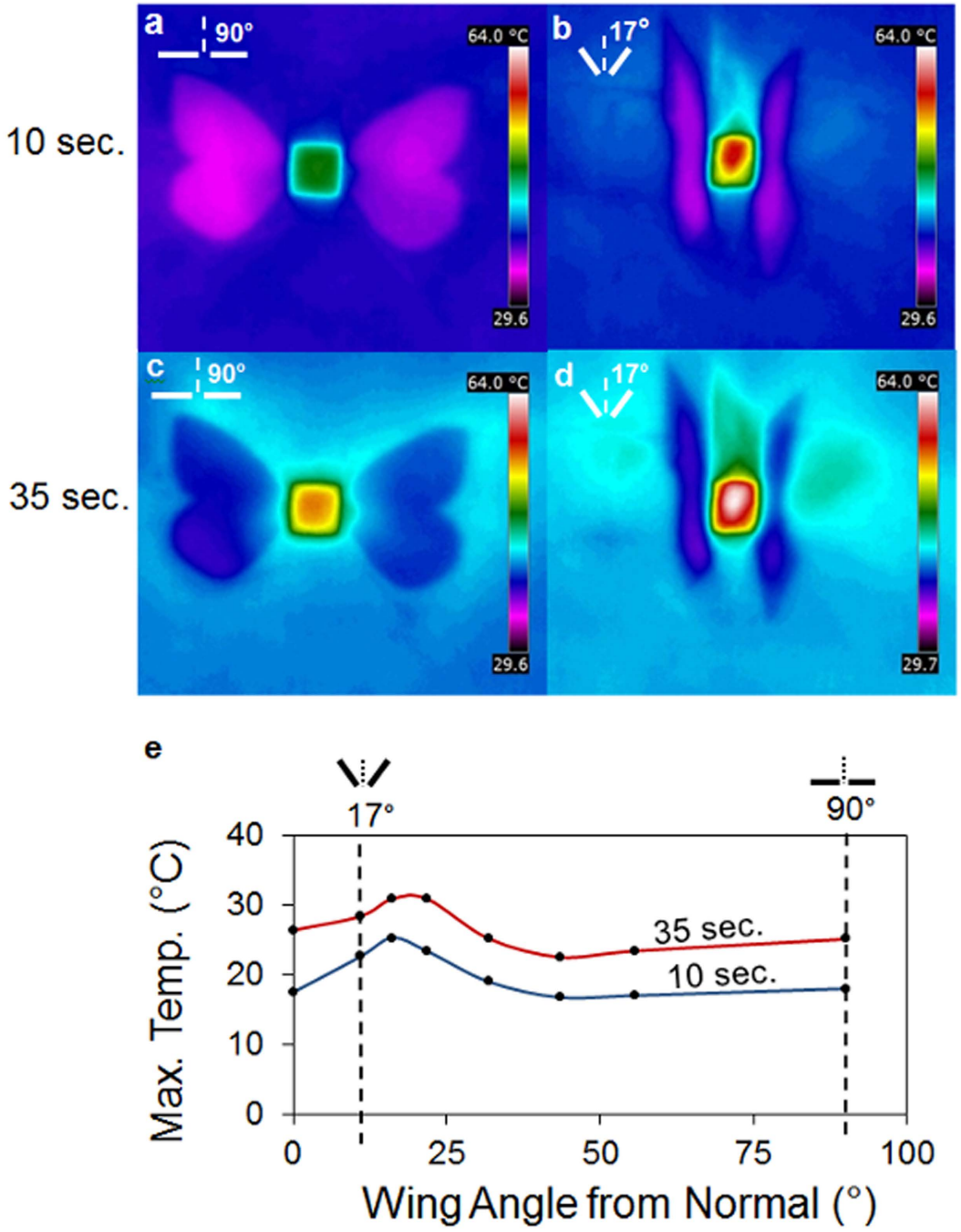

Figure 2. Thermal analysis of butterflies with wings held open (90°) or in a V-shape (17°). (**a**,**b**) Increase in temperature seen following 10 second exposure to one sun equivalent. (**c**,**d**) 35 second exposure to one sun equivalent. Note the dramatic increase in temperature at the equivalent location of the thorax when the wings are held at the optimal basking angle of 17°. (**e**), Graph of 'body' temperature as a function of wing angle for two sunlight exposure times of 10 seconds and 35 seconds.

only a single layer of scale cells is necessary to generate high levels of reflectance, rather than a complex multi-layered structure as found in the wing itself[18,25] and therefore directly increasing their potential utility in making a reflective coating.

Discussion

The V-shaped reflectance basking of the family Pieridae is most definitely comparable to V-trough solar concentrators and even more so when considering studies into the segmented surface structure of solar concentrators as carried out by Zanganeh *et al.*[8], Nilsson *et al.*[26] and more broadly by Sangster *et al.*[37]. Nilsson and co-workers prove that the introduction of micro-structures onto the surface of reflectors has

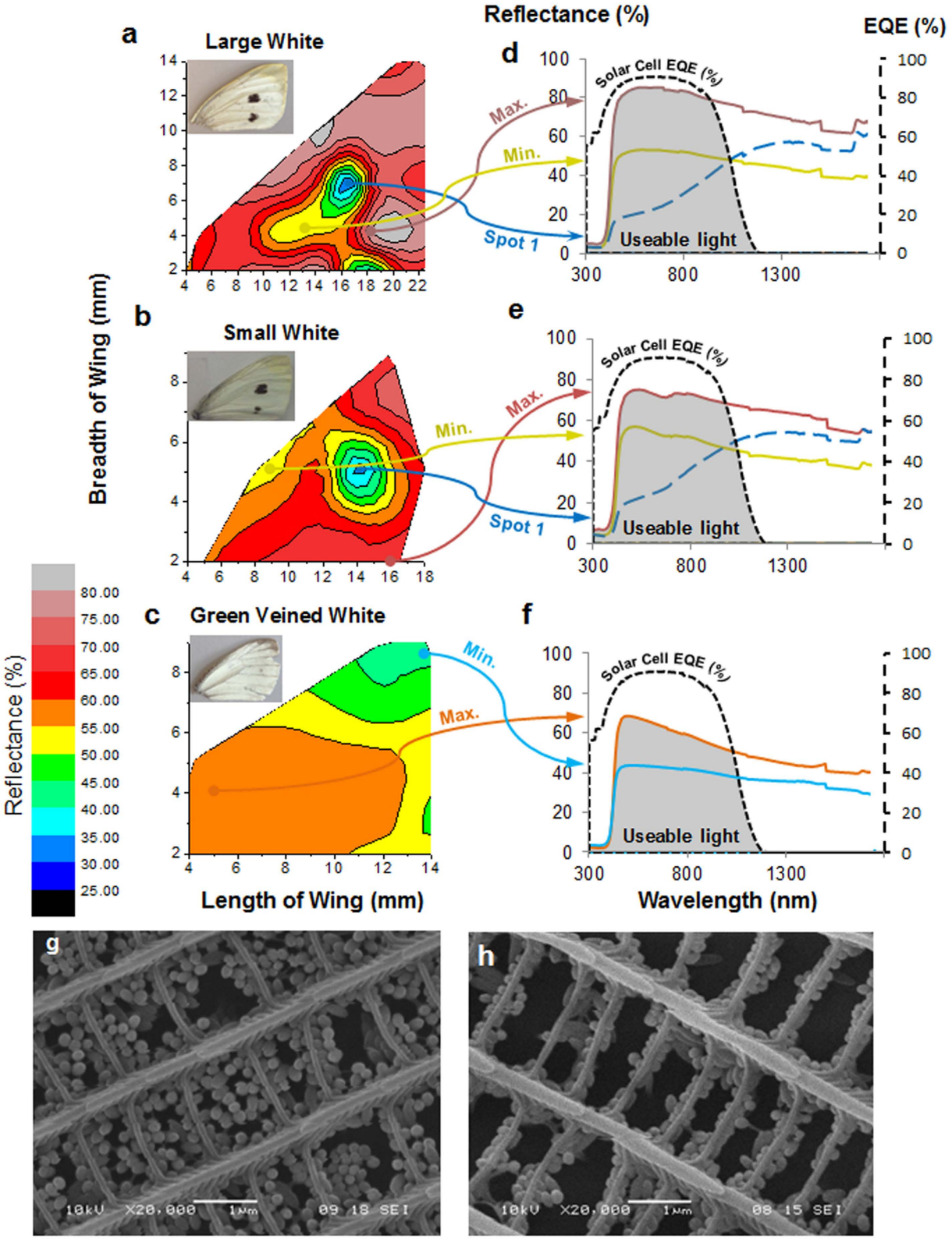

Figure 3. Mapping reflectance across the butterfly wing. Average percentage reflectance map for wings of the large (**a**), small (**b**) and green-veined white (**c**) butterflies. Insets show how each wing appears in normal daylight. (**d,e,f**) Reflectance spectrum for specific notable areas (maximum, minimum and black spot areas). Note how reflectance decreases dramatically over the black 'spots' present of the forewing of females of the large (**d**) and small white (**e**) whose black scales lack the reflecting pigment containing beads, see text for discussion. (**g**), SEM of wing scale containing packed pterin beads. (**h**), SEM of black spot area of wing scale containing significantly less pterin beads.

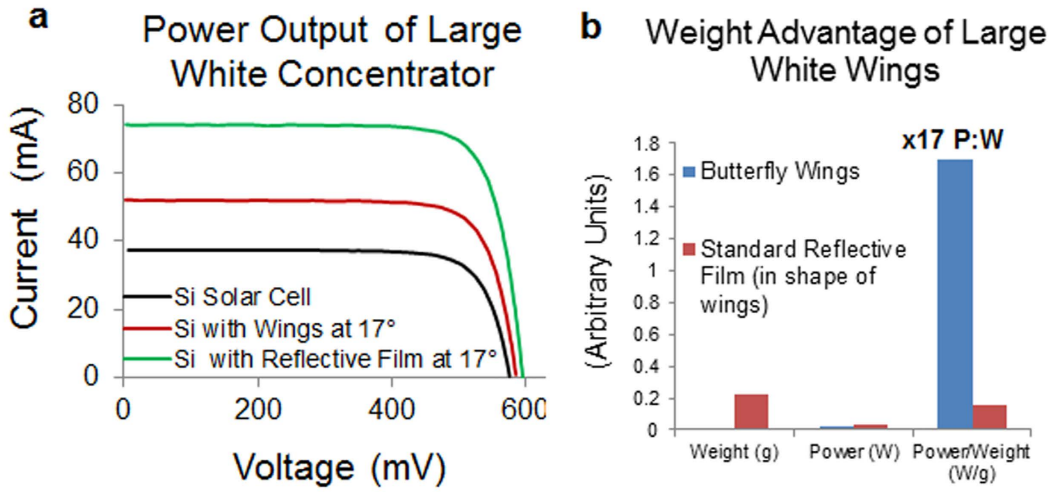

Figure 4. Butterfly wings increase both the output power and the final power to weight ratio of solar cells. (**a**), Power output of a mono-crystalline silicon (Si) solar cell either alone, or with large white wings versus reflective film held at the optimal angle of 17°. (**b**), Histogram representing the relative changes in both power, weight and the subsequent power to weight ratio of large white butterfly wings versus reflective film.

many benefits including a more uniform distribution of light upon the receiver and higher acceptance angles. The wings of the pieridae have a similar micro structure upon their wings due to the 'tiling' of their scales. Both of the aforementioned benefits reported by Nilsson *et al.* may be crucial to the pierid butterflies when basking in overcast diffused light conditions (light is incident from all angles, not just directly from the sun). Further investigation into the acceptance angle of these basking butterfly wings is however required.

In our study the optimum wing angle for light concentration by the butterfly wings was found to be 17° for both the thermal and photovoltaic receiver conditions. This angle does not however indicate with certainty the exact angle with which real butterflies will position their wings due to slight differences in the geometry of our set-up and that of a real butterfly. Specifically, the receiver size and shape in the tested case was a 10 mm by 10 mm square solar cell instead of the thorax/flight muscle area of the butterflies which is in the range of 2 to 3 mm by up to 20 mm (large white). The optimum angle in V-trough concentrators can be influenced by the receiver shape and size, the reflective mirror heights, location (i.e. latitude and longitude of the place) and the solar tracking method used[38–40]. In the case of the pierids, the surface structure of their wings as well as the shape and size of their target area (flight muscles) will predominantly decide the angle with which their wings are held. Other factors however could include: the desired energy/temperature upon flight muscles[41]; the time of year (sun's location, ambient temperature, thorax size[42]); and location (global horizontal irradiance values)[38,43]. This optimum angle does however prove that other receiver dimensions and applications are possible with these wings and that they are not solely optimised for the characteristics of the thorax.

The excellent match between the reflectance spectra of the large white butterfly and the working range of a monocrystalline silicon solar cell ensures that useful light rays are incident upon the solar cell. The butterflies' main aim in reflectance basking is to heat their flight muscles[41] whereas photovoltaic solar cells work less efficiently when heated[44] and so it would have been feasible that the reflected wavelengths would only be harmful IR wavelengths. The reflectance spectra given in Fig. 3a however reassure the use of wavelengths in the 450–950 nm range. These results would indicate that if used in larger concentration systems (500 fold concentration) that receiver cooling would be required to avoid damage to the photovoltaic receiver. This is a common necessity for current concentrator technology at high concentration ratios[44,45].

The I-V output curves show a 42.3% increase in power from the solar cell with attached large white butterfly wings. In terms of increased solar input (solar concentration) this works out as a concentrating effect of 1.3x, compared to the 2x concentration achieved by the reflective film. However in terms of *weight*, the butterfly wings have 17x the power to weight ratio of the reflective film structure. In theory, the maximum concentration ratio possible using the angle of the wings and receiver size with no light loss, would be 7.5 x concentrations. The miss-match in values however is due to the configuration of the wings where most light can be lost to the front and rear where there is no wing coverage. The 2x concentration result from the reflective film wings prove the majority of the loss is due to the wing configuration and not the wings themselves. A different configuration of the wings, with a smaller receiver similar to the butterflies' thorax should result in even higher I-V values with less loss.

In conclusion, these striking results have several implications both for the biology of butterflies and for the design of more lightweight but efficient solar concentrator systems. First, the infra-red measurements of butterfly body temperature confirm the assumption that the thermal basking exhibited by pierid butterflies really does provide an increase in thorax temperature proving that their V-shaped posture is an effective thermal basking method. Second, butterfly wings are both highly reflective and much lighter than any current reflective material. Mimicking these reflective structures with similar power to weight properties will be extremely useful in the design of new reflective materials for use in applications where weight is a limiting issue, such as flight. Third, and perhaps most obviously, this suggests that butterflies have evolved to concentrate light effectively for their needs and supports the idea that any given problem may first have been solved by nature[22–24]. Finally, despite the apparent complexity of the multi-layered array of butterfly scales on the wing, here we have shown that a simple mono-layer of scale cells removed onto adhesive tape is also highly reflective. Taking this analogy to its logical end point, we further speculate that nano-fabrication of a layer of ovoid pigment containing beads will also form a reflective and light weight mimic of a pierid scale cell, provided that the nano-beads are presented in their correct orientation. Not only could this potentially enhance the properties and application of reflective materials but it could also expand the application of technologies such as solar concentrators which are currently severely limited by power to weight issues.

Methods

Light concentration theory. Given that the V-shape is known to concentrate light as long as there is light reflectance and an acute angle between the reflectors then much of the theory of solar concentrators can be applied to the butterflies. The geometric concentration ratio (C) of a solar concentrator can be estimated using Eqn. 1[28] and hence an estimation of the potential concentration ratio of the butterflies and of a combination of butterfly wings and solar cell can be calculated.

$$C = \frac{\text{Light Entry Aperture Area}}{\text{Reciever Area}} \tag{1}$$

$$C_{Butterfly} = \frac{\text{Wing Opening Area}}{\text{Thorax Area}} \tag{2}$$

$$C_{Cell+Wings} = \frac{\text{Wing Opening Area}}{\text{Solar Cell Active Area}} \tag{3}$$

The concentration ratio is a value used to categorise and analyse the efficiency of solar concentrators. The power of light incident on a receiver (P_r on butterfly body or solar cell) is dependent upon the optical efficiency (η_o), concentration ratio (C), incident irradiance on the system (I_i), and the receiver area (A_r), such that:

$$P_r = \eta_0 C I_i A_r \tag{4}$$

In the case of concentrator photovoltaic systems; where the receiver is 1 or more solar cells, the final power output produced from the solar cell(s) would be the efficiency of the cell multiplied by the power incident on the cell(s), (P_r). Similarly the term effective concentration ratio should equal the geometrical concentration ratio minus optical and solar cell losses, or in other words, multiplied by their efficiencies[28] as in Eq.5.

$$C_{eff} = \eta_0 \eta_{cell} C \tag{5}$$

The possible optical losses in the butterfly wing configuration include; light rays incident upon the wings but which are reflected to the front or rear -where there is no wing or body coverage- or even back out the top opening area, and also the efficiency at which the wings reflect the light—the reflectance. Instead of solar cell efficiency, the butterflies presumably would have heat transfer efficiency, dependent on their initial body temperature, incident temperature/energy from sunlight, and the ambient temperature of their environment.

Measurements Performed. The infra-red (IR) camera shots were taken with a FLIR T425 camera positioned underneath a structure consisting of the butterfly wings separated at the base by 10 mm. The wings were positioned manually at varying angles and exposed to 1000 W/m^2 of light from a Wacom AAA continuous solar simulator (model: WXS-210S-20, AM1.5G). The optimum performance was found when θ equaled roughly 17°, which was also the optimum angle for power output of the solar cells. This angle was maintained to compare results. The receiver size and shape in the tested case was a 10 mm by 10 mm square solar cell, although this could have been resized to replicate the butterflies body, this would affect the solar cell performance and perhaps not give as promising results as were obtained. Without the replication of the hairy thorax and exact wing positioning (perhaps more cone like than the

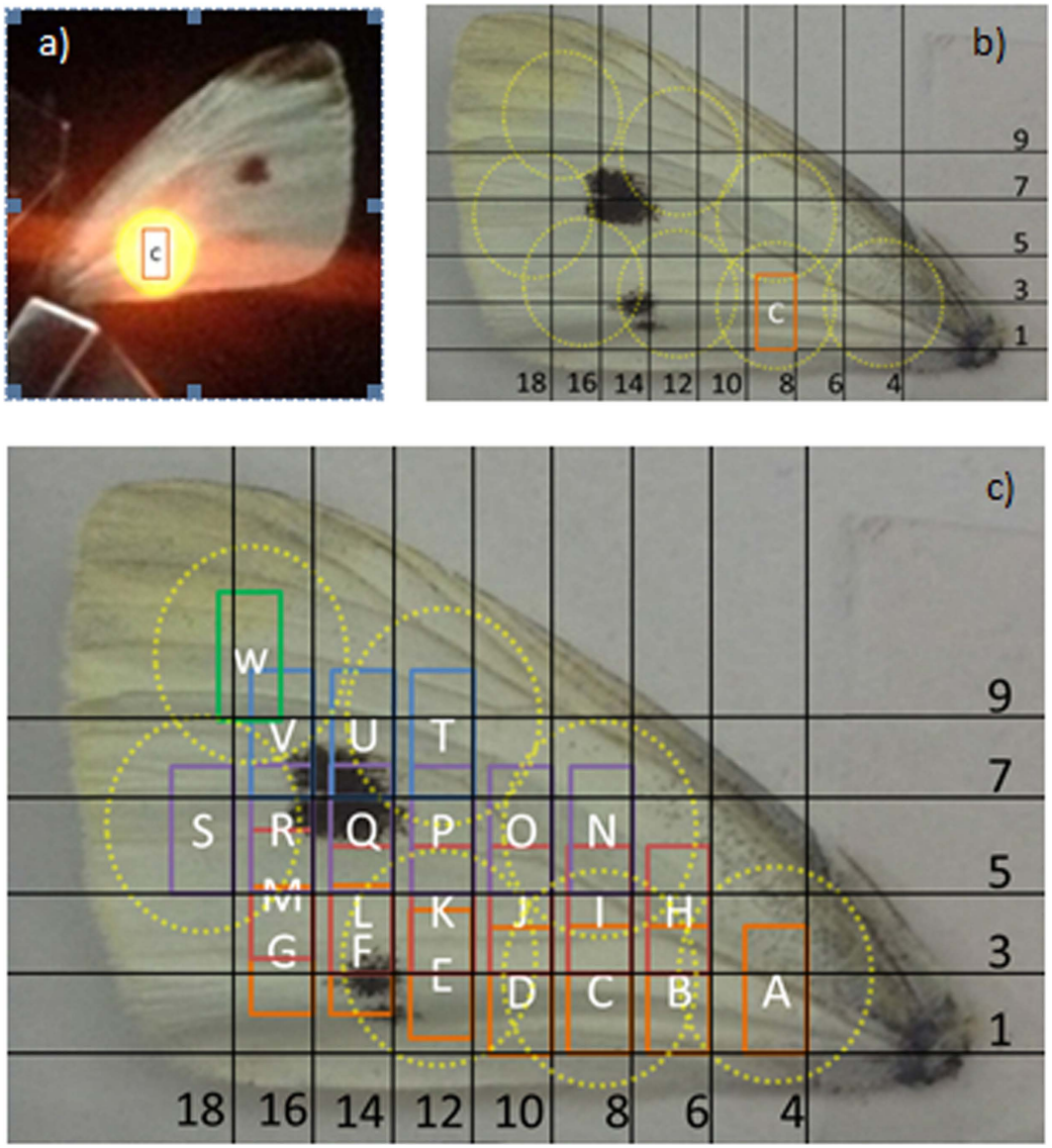

Figure 5. Reflectance mapping method. (**a**), Photograph of forewing placed against integrating sphere at the third measurement position of 8 mm along and 1 mm up (position C). (**b**), An indication of the limit of measurements due to porthole size represented by the yellow dotted circles. (**c**), The full mapping technique with position labels. The exact location of incident beam is not known but confined to the rectangles labelled alphabetically in order of measurements taken.

simple 2D V-shape) the prediction of the butterfly basking wing angle would still not be 100% accurate. The exposure time under the Wacom AAA continuous solar simulator (model: WXS-210S-20, AM1.5G) set at 1000 W/m^2 was noted and IR images recorded after 10 and 35 seconds. A cool down period of at least 7 minutes was allowed between each set of measurements and a base measurement was taken before switching on the solar simulator, later subtracted from measurements to reduce error due to ambient temperature changes.

The reflectance was measured over the wavelength range of 300–1750 nm using a Bentham PVE300 system, the maximum and minimum reflectance spectra are shown in Fig. 3 for the small white, large white and green veined butterfly wing samples. Within this range a wavelength interval of 5 nm was taken and by moving across the wing (x-axis) and up the wing (y axis) in 2 mm steps, the wing was manually mapped as shown in Fig. 5 b,c. The response of the monocrystalline silicon cell (1 cm × 1 cm) was also measured using the Bentham and the external quantum efficiency (EQE) plotted in Fig. 3 graphs a to c, to show the wavelength compatibility between the reflectance spectra of the butterfly wing and working range of the solar cell.

Due to their promising reflectance results, the large white wings were tested further as reflectors in a V-trough CPV systems with a 10 mm × 10 mm solar cell placed between the wings. Figure 4a shows the

results obtained with and without wings as a reflector. Reflective film cut in the same shape as the wings was also measured with the solar cell for comparison. The I–V results were taken of a 10 mm by 10 mm monocrystalline silicon solar cell with the 4 large white wings secured at the base and manually angled under the Wacom AAA continuous solar simulator (model: WXS-210S-20, AM1.5G) at 1000 W/m^2 and using an EKO MP 160 I-V tracer. The monocrystalline silicon solar cells used were from Narec Solar, now known as Solar Capture Technologies. 'Standard' reflective film used was RF-015A from Qingdao Lingding Technology Ltd.

Performance calculations for butterfly wings as solar photo voltaic concentrators. Using equation (3) the theoretical concentration ratio of the wings at 17 degrees from normal with a 100 mm^2 receiver area is calculated as 7.5x. In ideal conditions with 100% optical efficiency this would translate into the short circuit current of the solar cell without concentration (1 sun) being increased from 36.985 mA to 277.388 mA with concentration from the wings (7.5 suns). When incorporating reflectance loss, using the average reflectance taken for the large white wing samples over the monocrystalline silicon cells response range, 78.9%, the short circuit current under concentration from the wings should be 218.86 mA but practical measurements gave 52 mA. This mis-match in theoretical to practical values suggests there is a large percentage of light lost to the front and rear of the configuration but again it should be remembered that in the case of the pierids, the receiver size is much smaller and hence there is less space for light rays to be lost to the front or rear.

Using the short circuit results gained from the practical testing and working backwards, the effective concentration ratio of the butterfly wings with the solar cell is 1.3x and with the reflective film cut in the shape of the wings is 2.0x proving the majority of the loss is due to configuration and not the wing's themselves. A different configuration of the wings, with a smaller receiver similar to the shape and size of the butterfly body should result in higher I-V values with less loss. Solar concentration will increase the receiver (solar cell) temperature which can lead to a decrease in their performance but for low concentration levels (up to 10x) this is not usually, and was not in these experiments, an issue but may need to be considered under longer exposure times.

References

1. Winston, R., Miñano, J. C., Benítez, P., Shatz, N. & Bortz, J. C. *Nonimaging Optics*. *Nonimaging Opt*. 317–394 (Elsevier, 2005). doi: 10.1016/B978-012759751-5/50013-0
2. Mallick, T. & Eames, P. Design and fabrication of low concentrating second generation PRIDE concentrator. *Sol. Energy Mater. Sol. Cells* **91,** 597–608 (2007).
3. Maiti, S., Sarmah, N., Bapat, P. & Mallick, T. K. Optical analysis of a photovoltaic V-trough system installed in western India. *Appl. Opt.* **51,** 8606–14 (2012).
4. Tang, R. & Liu, X. Optical performance and design optimization of V-trough concentrators for photovoltaic applications. *Sol. Energy* **85,** 2154–2166 (2011).
5. Barber, G. J. *et al.* Development of lightweight carbon-fiber mirrors for the RICH 1 detector of LHCb. *Nucl. Instruments Methods Phys. Res. Sect. A Accel. Spectrometers, Detect. Assoc. Equip*. **593,** 624–637 (2008).
6. Jagoo, Z. *Tracking Solar Concentrators*. (Springer, 2013) (Date of access: 14/05/2015) at <http://link.springer.com/content/pdf/10.1007/978-94-007-6104-9.pdf>
7. Bader, R., Haueter, P., Pedretti, a. & Steinfeld, a. Optical Design of a Novel Two-Stage Solar Trough Concentrator Based on Pneumatic Polymeric Structures. *J. Sol. Energy Eng.* **131,** 031007 (2009).
8. Zanganeh, G., Bader, R., Pedretti, a., Pedretti, M. & Steinfeld, a. A solar dish concentrator based on ellipsoidal polyester membrane facets. *Sol. Energy* **86,** 40–47 (2012).
9. Guo, S., Zhang, G., Li, L., Wang, W. & Zhao, X. Effect of materials and modelling on the design of the space-based lightweight mirror. *Mater. Des.* **30,** 9–14 (2009).
10. Stavenga, D. G., Giraldo, M. a & Hoenders, B. J. Reflectance and transmittance of light scattering scales stacked on the wings of pierid butterflies. *Opt. Express* **14,** 4880–90 (2006).
11. Stavenga, D. G., Stowe, S., Siebke, K., Zeil, J. & Arikawa, K. Butterfly wing colours: scale beads make white pierid wings brighter. *Proc. Biol. Sci.* **271,** 1577–84 (2004).
12. Stavenga, D. G., Leertouwer, H. L. & Wilts, B. D. Coloration principles of nymphaline butterflies - thin films, melanin, ommochromes and wing scale stacking. *J. Exp. Biol.* **217,** 2171–80 (2014).
13. Giraldo, M. A. & Stavenga, D. G. Sexual dichroism and pigment localization in the wing scales of Pieris rapae butterflies. *Proc. Biol. Sci.* **274,** 97–102 (2007).
14. Giraldo, M. A. & Stavenga, D. G. Wing coloration and pigment gradients in scales of pierid butterflies. **37,** 118–128 (2008).
15. Morehouse, N. I., Vukusic, P. & Rutowski, R. Pterin pigment granules are responsible for both broadband light scattering and wavelength selective absorption in the wing scales of pierid butterflies. *Proc. Biol. Sci.* **274,** 359–66 (2007).
16. Luke, S. M., Vukusic, P. & Hallam, B. Measuring and modelling optical scattering and the colour quality of white pierid butterfly scales. *Opt. Express* **17,** 14729–43 (2009).
17. Smith, A. J., Wang, C., Guo, D., Sun, C. & Huang, J. Repurposing Blu-ray movie discs as quasi-random nanoimprinting templates for photon management. *Nat. Commun.* **5,** 5517 (2014).
18. Vukusic, P. Manipulating the flow of light with photonic crystals. *Phys. Today* **59,** 82–83 (2006).
19. Vukusic, P. & Sambles, J. R. Photonic structures in biology. *Nature* **424,** 852–855 (2003).
20. Vukusic, P. Structural colour: Elusive iridescence strategies brought to light. *Curr. Biol.* **21,** R187–R189 (2011).
21. Kolle, M. *et al.* Mimicking the colourful wing scale structure of the Papilio blumei butterfly. *Nat. Nanotechnol.* **5,** 511–515 (2010).
22. Potyrailo, R. a. *et al.* Morpho butterfly wing scales demonstrate highly selective vapour response. *Nat. Photonics* **1,** 123–128 (2007).
23. Dewan, R. *et al.* Studying nanostructured nipple arrays of moth eye facets helps to design better thin film solar cells. *Bioinspir. Biomim.* **7,** 016003 (2012).
24. Huang, C. K., Sun, K. W. & Chang, W.-L. Efficiency enhancement of silicon solar cells using a nano-scale honeycomb broadband anti-reflection structure. *Opt. Express* **20,** A85–93 (2012).

25. Johnsen, S. & Widder, E. The physical basis of transparency in biological tissue: ultrastructure and the minimization of light scattering. *J. Theor. Biol.* **199,** 181–98 (1999).
26. Nilsson, J., Leutz, R. & Karlsson, B. Micro-structured reflector surfaces for a stationary asymmetric parabolic solar concentrator. *Sol. Energy Mater. Sol. Cells* **91,** 525–533 (2007).
27. Uematsu, T. *et al.* Design and characterization of flat-plate static-concentrator photovoltaic modules. *Sol. Energy Mater. Sol. Cells* **67,** 441–448 (2001).
28. Cooke, D. *et al.* Sunlight brighter than the Sun. *Nature* **346,** 802 (1990).
29. Leertouwer, H. L. Colourful butterfly wings: scale stacks, iridescence and sexual dichromatism of Pieridae. **67,** 158–164 (2007).
30. Stavenga, D. G. & Arikawa, K. Evolution of color and vision of butterflies. *Arthropod Struct. Dev.* **35,** 307–18 (2006).
31. Shawkey, M. D., Morehouse, N. I. & Vukusic, P. A protean palette: colour materials and mixing in birds and butterflies. *J. R. Soc. Interface* **6 Suppl 2,** S221–S231 (2009).
32. Vukusic, P., Sambles, R., Lawrence, C. & Wakely, G. Sculpted-multilayer optical effects in two species of Papilio butterfly. *Appl. Opt.* **40,** 1116–1125 (2001).
33. Vukusic, P. & Hooper, I. Directionally controlled fluorescence emission in butterflies. *Science* **310,** 1151 (2005).
34. Yagi, N. Note of electron microscope research on pterin pigment in the scales of pierid butterflies. *Annot. Zool. Jpn.* **27,** 113–114 (1954).
35. Giraldo, M. a & Stavenga, D. G. Wing coloration and pigment gradients in scales of pierid butterflies. *Arthropod Struct. Dev.* **37,** 118–28 (2008).
36. Rutowski, R. L., Macedonia, J. M., Morehouse, N. & Taylor-Taft, L. Pterin pigments amplify iridescent ultraviolet signal in males of the orange sulphur butterfly, Colias eurytheme. *Proc. Biol. Sci.* **272,** 2329–2335 (2005).
37. Sangster, A. J. *Electromagnetic Foundations of Solar Radiation Collection*. (Springer International Publishing, 2014). doi: 10.1007/978-3-319-08512-8
38. Fernández, E. F., Almonacid, F., Ruiz-Arias, J. A. & Soria-Moya, A. Analysis of the spectral variations on the performance of high concentrator photovoltaic modules operating under different real climate conditions. *Sol. Energy Mater. Sol. Cells* **127,** 179–187 (2014).
39. Sarmah, N., Richards, B. S. & Mallick, T. K. Evaluation and optimization of the optical performance of low-concentrating dielectric compound parabolic concentrator using ray-tracing methods. *Appl. Opt.* **50,** 3303–10 (2011).
40. Hughes, M. D., Maher, C., Borca-Tasciuc, D.-A., Polanco, D. & Kaminski, D. Performance comparison of wedge-shaped and planar luminescent solar concentrators. *Renew. Energy* **52,** 266–272 (2013).
41. Kohane, M. J., Watt, W. B. & Sciences, B. Flight-muscle adenylate pool responses to flight demands and thermal constraints in individual Colias eurytheme (Lepidoptera, pieridae). *J. Exp. Biol.* **3154,** 3145–3154 (1999).
42. Karlsson, B. & Johansson, A. Seasonal polyphenism and developmental trade-offs between flight ability and egg laying in a pierid butterfly. *Proc. Biol. Sci.* **275,** 2131–6 (2008).
43. Chai, P. & Srygley, R. B. The Predation and the Flight, Morphology, and Temperature of Neotropical Rain-Forest Butterflies. *Am. Nat.* **135,** 748–765 (2014).
44. Micheli, L., Sarmah, N., Luo, X., Reddy, K. S. & Mallick, T. K. Opportunities and challenges in micro- and nano-technologies for concentrating photovoltaic cooling: A review. *Renew. Sustain. Energy Rev.* **20,** 595–610 (2013).
45. Micheli, L., Sarmah, N., Luo, X., Reddy, K. S. & Mallick, T. K. Design of A 16-Cell Densely-packed Receiver for High Concentrating Photovoltaic Applications. *Energy Procedia* **54,** 185–198 (2014).

Acknowledgements

This work has been supported by EPSRC, UK, (Ref No: EP/J000345/1), and BBSRC grant BB/H014268. The funders had no role in study design, data collection and analysis, or preparation of the manuscript.

Author Contributions

R. ff-C, S.S., T.K.M. and K.S. jointly conceived the study, the experiments therein and participated in manuscript preparation. K.S. performed all practical experimentation.

Additional Information

Competing financial interests: The authors declare no competing financial interests.

How to cite this article: Shanks, K. *et al.* White butterflies as solar photovoltaic concentrators. *Sci. Rep.* **5**, 12267; doi: 10.1038/srep12267 (2015).

[Article 6]

K. Shanks, J. P. Ferrer-Rodriguez, E. F. Fernández, P. Pérez-Higueras, S. Senthilarasu, and T. K. Mallick, "A reliable Ultrahigh Concentrator utilising multiple primary Fresnel Lenses and a Sapphire Reciever Optic," *Optica*, 2017 *(submitted).*

Research Article

optica

A reliable Ultrahigh Concentrator utilising multiple primary Fresnel Lenses and a Sapphire Reciever Optic

KATIE SHANKS[1A*], JUAN P. FERRER-RODRIGUEZ[2], EDUARDO F. FERNÁNDEZ[2], FLORENCIA ALMONACID[2], PEDRO PÉREZ-HIGUERAS[2], S. SENTHILARASU[1], TAPAS MALLICK[1B*]

[1]*Environmental and Sustainability Institute, University of Exeter Penryn Campus, Penryn, TR10 9FE, UK*
[2]*Centre for Advanced Studies in Energy and Environment, University of Jaen, Campus las Lagunillas, Jaen 23071, Spain*
**Corresponding author: [A]Kmas201@exeter.ac.uk, [B]T.K.Mallick@exeter.ac.uk*

Received XX Month XXXX; revised XX Month, XXXX; accepted XX Month XXXX; posted XX Month XXXX (Doc. ID XXXXX); published XX Month XXXX

Ultrahigh concentrator photovoltaics hold both a great potential in reducing the cost of photovoltaic energy and to higher conversion efficiencies. The challenges in their design and manufacturing however have not yet permitted a >3000x reliable system. Here we propose an ultrahigh concentrator photovoltaic design of 5800x geometrical concentration ratio based on multiple primary Fresnel lenses focusing to one central solar cell. The final stage optic is of a novel design, made of sapphire, to accept light from four different directions and focus the light towards the solar cell. The extremely high geometrical concentration of 5800x was chosen in anticipation of the losses accompanied with ultrahigh concentration due to alignment difficulties. Two scenarios are also simulated, one with state of the art optics (achromatic Fresnel lenses and 98% reflective mirrors) and one of standard, relatively cheap optics. An optical efficiency of ~75% is achieved in simulations if high quality optics are utilised, which gives an effective concentration ratio of just over 4300x. Simulating standard optical constraints with less accurate optics results in an optical efficiency of ~55% which translates to an effective concentration ratio of ~3000x. In this way the quality of the optics can be chosen depending on the trade of between cost and efficiency with room for future advanced optics to be incorporated at a later date. The optical efficiency of each component is simulated as well as experimentally measured to ensure the accuracy of the simulations. An acceptance angle of 0.4° was achieved for this design which is considered good for such a high concentration level. Such a design could be the breakthrough in concentrator photovoltaic research for reaching higher concentration ratios. The use of flat optics to ease manufacturing and alignment is a simple but effective method to achieve a reliable system that will achieve ultrahigh concentration even at 55% optical efficiency. Such a design will be of use in investigations of concentration, concentrator solar cell development, temperature effects and more; achieving ultrahigh concentration levels not yet tested.

OCIS codes:

http://dx.doi.org/10.1364/optica.99.099999

1. Introduction

One trend in concentrator photovoltaic (CPV) technology is towards systems of higher concentration levels [1–3]. This is due to their ability to increase cell conversion efficiencies and reduce cell size, also reducing the photovoltaic cost contribution to the full system [4,5]. Multi-junction solar cells are pushing higher and higher efficiency records within relatively short time spans and need equally progressive concentrator optical designs to match. The main design constraint for the optics of high (100-2000suns) and ultra-high (>2000 suns) CPV systems is the difficulty to achieve a high tolerance design which is simultaneously of a high optical efficiency. This is ultimately due to the limits of etendue but are also affected by material availability and manufacturing accuracy [5–8]. Temperature is another key issue in ultrahigh concentration designs but as long as the light distribution upon the cell is distributed relatively uniform and there is sufficient cooling (passive or active), then it is manageable. There has already been research into the effect of high temperatures on Fresnel lenses [9–11] and the ability of passive cooling plates to accommodate ultrahigh concentration ratios [12,13].

Fresnel lenses as a primary concentrating optic have a relatively good acceptance angle and optical efficiency in comparison to the cassegrain design utilising conic primary reflectors [1]. If used alone, a single medium Fresnel lens is limited in concentration ratio by chromatic aberration to ~1000 suns ([14]. Achromatic Fresnel lenses

made of 2 mediums as described by Languy et al. [14] and Guido et al. [5] can achieve higher concentration ratios but are still to reach full scale manufacturing. The other option for ultrahigh concentration is to incorporate multiple concentrating optics in a singular system but too many can significantly reduce the optical efficiency and tolerance (due to manufacturing and alignment error). In this paper we present an ultrahigh design of geometric concentration ratio >5800x in anticipation of high optical losses and to compare the effects of different quality optics. In this way this study will not only present a new type of ultrahigh concentrator that can be built with current standard optics but also with developing state of the art optics to reach optimal performance. In theory, by deprioritising the optical efficiency it should also be easier to achieve a good acceptance angle for the system.

Another constraint in achieving ultrahigh concentration ratios is fabrication limits, the size of Fresnel lens or conic mirror required would be costly and difficult to manage. To overcome this we propose the use of 4 Fresnel lens's focusing to 1 central PV cell with the aid of other redirecting and concentrating optics. A similar method has been adopted by Ferrer-Rodriguez et al. who recently proposed a design consisting of 4 cassegrain style reflectors which were angled to focus onto a central receiver optic and PV cell [15]. The design had a geometrical concentration ratio of 2304x, an optical efficiency of 73% (resulting in an effective concentration ratio of 1682x) and an acceptance angle of 0.61°. Here we aim to achieve a higher effective concentration ratio and an acceptance angle achievable by current tracking systems (>0.1°). Due to the high accuracy required for ultrahigh concentration optics, we have aimed for a relatively simple design (flat mirrors utilised for redirection) and pooled both ray trace simulations and practical testing to ensure nothing is underestimated (such as manufacturing uncertainty).

If reliable easy to manufacture ultrahigh concentrator photovoltaics were demonstrated then the cost effectiveness and further development of CPV technologies would expand greatly. The initial costs of CPV technology are still too high and the benefit of higher concentration systems has been clouded by high prototyping costs and in field challenges. This design takes advantage of the long developed Fresnel lens and achieves ultrahigh concentration is a simple but effective way. Similar designs could be used simply to test more advanced concentrator solar cells or investigate temperature challenges. Overall, the proposed design should be of useful to many in the area of CPV and optical research and the design is simple enough to be adapted and investigated for other applications (e.g. thermal).

2. Design

For this design we chose 4 square Fresnel lenses (PMMA on glass) with focal lengths of ~46cm and aperture areas of 21cm by 21cm each. For the receiver we use the Azure Space 5.5x5.5 mm multi-junction solar cell. This gives us a geometric concentration ratio of 5831x and an effective concentration of >4102.7 if >70% optical efficiency is obtained. In order to gather the light towards the centre we propose the use of flat mirrors and a central refractive optic made up of 4 dome lenses as shown in figure 1.

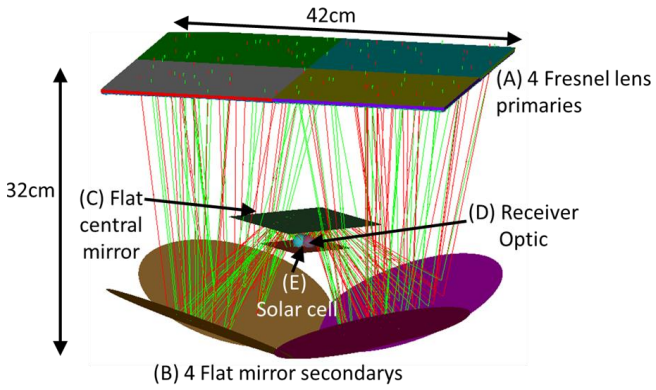

Fig. 1. Ray trace diagram of ultrahigh concentrator showing 4 square Fresnel lenses focusing towards 4 angled flat reflectors. The light it reflected again by a central flat mirror onto a central refractive optic made of 4 spherical lenses completing concentration onto the solar cell receiver. The green and red rays represent 400nm and 1600nm light respectively.

In order to keep the design as simple as possible and minimise loss due to manufacturing inaccuracies flat mirrors were used instead of conically shaped ones. By using flat mirrors the reflectance can be very high (~97%) even in the prototyping stage since no complicated shapes are involved which would either be expensive to manufacture or very difficult to attach reflective film to. Accurately manufacturing large smooth shapes of metal is also very challenging if intending on using vacuum metalizing methods to coat the metal into a mirror [16]. Aligning the mirrors with their specific angle of inclination will also be easier if they are flat. A central flat mirror as the third optical stage was also chosen but mainly due to the unique quarter boundaries experienced by this design as the light rays travel close to the centre (figure 2A). As shown in figure 2A, any optic located close to the centre of the design (centre of the 4 Fresnel lenses when viewed from above) must only fill 90° of the plane or be a continuous revolution. For example a half ball lens fully cantered in the middle of the Fresnel lenses would be acceptable but this does not focus the angled incoming light to the centralised solar cell.

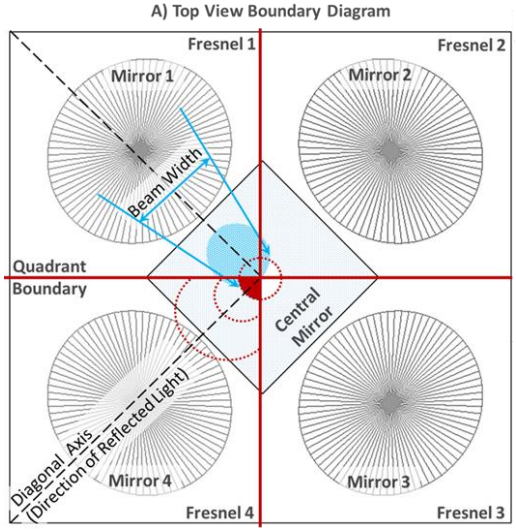

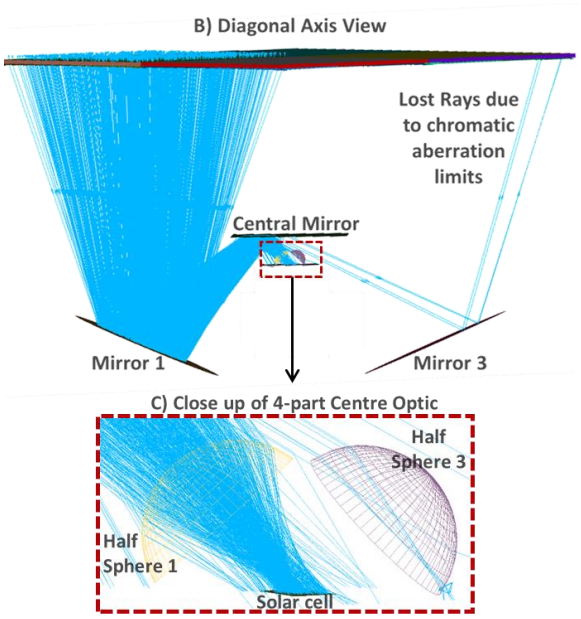

Fig. 2. A) Top view diagram of the optical systems 4 quadrants and how light focuses onto the central mirror. The dotted red curves show examples of how an increase in the size of an offset optic will still be constrained by the quadrant boundaries. B) Ray trace diagram viewing the diagonal face of the system where light can be seen focusing from the Fresnel lens onto the first flat mirror then the central flat mirror until finally hitting the refractive lenses. The effect of chromatic aberration is also shown. C) Close up of the 4-part centre lenses showing only lenses 1 and 3 for simplicity.

Offset lenses can focus the incoming light to a centralised solar cell but they must fit within their quadrant. This is one of the key challenges of this design linked to the width of the incoming light beam (figure 2A). Due to the concentration level, the limits of chromatic aberration from the Fresnel lenses and the use of only flat mirrors up until this point, the beam width overlaps into the other quadrants, especially when there is misalignment with the sun or in the optics assembly. Using the flat central mirror overcomes the boundary concern and it was ensured that its size and position did not block any rays coming from the Fresnel lens as shown in figure 2B.

The final stage optic is made of 4 truncated half sphere lenses aligned to face the incoming light as shown in figure 2C. Ideally this final optic will be made of a high refractive material such as sapphire in order to reach maximum ultrahigh concentration and optical efficiency. It was also preferred to keep this refractive final stage optic small to minimise absorption losses. Larger lenses of a smaller refractive index may have worked but would also be positioned further from the solar cell and result in substantial absorption loses along with added weight and cost to the built system. Half spheres were chosen for this design due to their relatively good acceptance angle [17] and simple shape which will be beneficial during manufacturing.

3. Quality and Efficiency of Optical Components

Due to the accuracy required for ultrahigh concentrator optics, thorough simulations as well as some measured optical properties (figure 3) were carried out to ensure the design was modelled accurately. The quality of the optics plays a significant role in the achieved optical efficiency [16,18–20] and so two scenarios are given for this system – standard quality and state of the art quality optics (figure 4). The standard scenario assumes a standard PMMA on glass Fresnel lens as measured in figure 3A (~88%), 95% reflective mirror film as measured in figure 3B and a refractive centre optic made of sapphire (n=~1.76) of estimated optical efficiency ~85% [21].

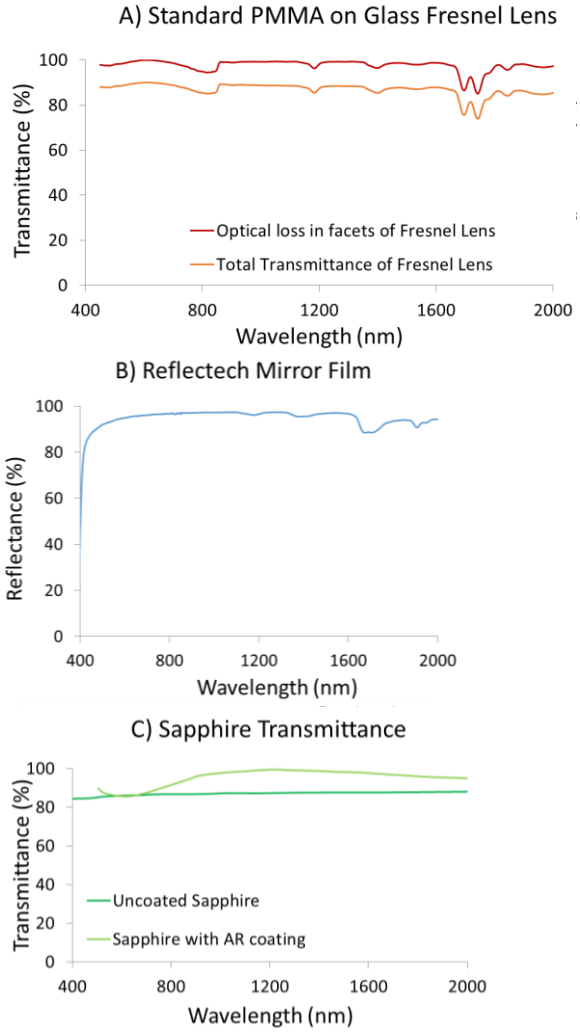

Fig. 3. A) Measured transmittance of Fresnel lens using pane of glass as a reference to measure scattering within facets. B) Measured reflectance of Reflectech mirror film. C) Transmittance of common Sapphire and Sapphire with antireflection coating [22].

The transmittance of a standard Fresnel lens is typically ~88% (figure 3A) and for an achromatic Fresnel lens ~86% if manufactured as suggested by Guido et al. [5]. Although an achromatic lens has a slightly lower transmittance, for this proposed design it would regain the scattered light due to chromatic aberration shown in figure 2B and C. A reflectance of >95% should be easily achievable with flat mirrors in place. The reflectance of one of Reflectech's mirror films is shown to have slightly above this for most of the wavelength range absorbed by the intended solar cell (400-1600 nm) in figure 3B.

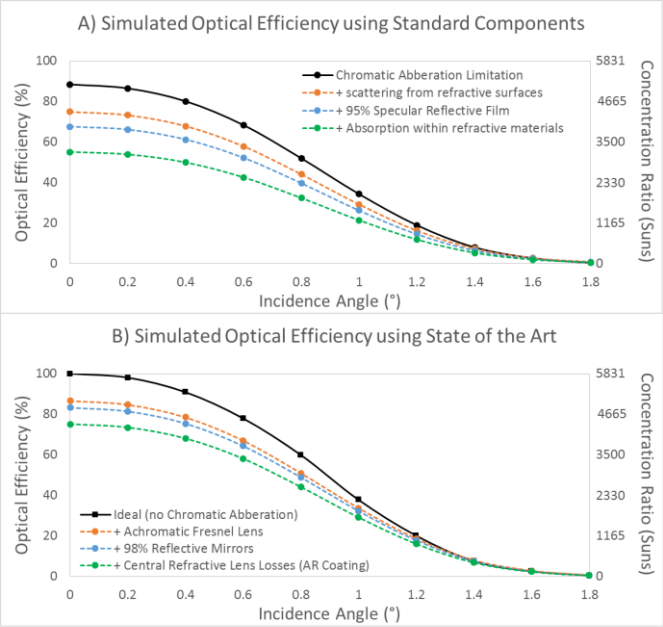

Fig. 4. A) Simulated optical efficiency of the concentrator using standard components including a silicon on glass Fresnel lens, flat 95% reflective mirrors and an uncoated sapphire centre optic. B) The simulated optical efficiency of the system if top of the range components are utilised including an achromatic Fresnel lens made of two refractive index materials on glass, 98% silver mirrors and a high quality sapphire centre optic with an antireflective coating.

The transmittance of sapphire is often given to be ~85-90% as shown in figure 3C depending on the growth method, surface quality, thickness and temperature [21]. This 15% loss is attributed to both scattering upon refraction into the material and due to absorption within the material. During ray trace modelling scattering and absorption effects were simulated as accurately as possible without measurements of the actual optic to be used. These simulations suggest a scattering of ~8-14% depending on the angle of incidence and surface roughness and an internal absorption of ~8-10% depending on material composition. These results match relatively well with the properties of Sapphire reported in the literature although there are slight variations [21,23–25].

One key unknown attribute is the surface quality of the Sapphire optic which could reduce the optical efficiency in figure 4A by another 4-7% [21,26]. One of the interesting points of Sapphire however is that its transmittance can be significantly increased due to the application of antireflective (AR) coatings [21,24,25]. This is assumed in figure 4B however depending on which antireflective coating is applied it may reduce the transmittance in other parts of the spectra still absorbed by the solar cell.

In figure 4B the use of achromatic Fresnel lenses, 98% reflective silver mirrors and a high quality Sapphire centre optic with AR coating increases the optical efficiency to 75.03% from the standard version of 55.12%. These values relate to an effective concentration of 4373x and 3214x respectively. The state of the art scenario is however the best possible case. If an antireflective coating is not used the optical efficiency should reduce by a further 4.8% (absolute) in figure 4B. Both scenarios are given to show that a prototype of this system should likely fall within these two scenarios. It should also be noted that if further corners were cut during prototype manufacturing (e.g. a cheaper low refractive index center optic used) although this would significantly reduce the optical efficiency to ~35% this would still result in an effective ultrahigh concentration ratio of 2000x. The resulting distribution upon on the cell area should also be more uniform and have an improved acceptance angle which may be necessary depending on the application and location. The disadvantage of such a low optical efficiency system would be the waste of area used, a smaller system of higher optical efficiency could obtain the same output but could still cost more due to the accuracy required. Depending on the aim of the design - to be most cost effective, most area efficient, or most optically efficient- different quality optics can be used.

Table 1. Concentration-acceptance angle product (CAP) analysis table depending on quality of optics used

Simulated Design Scenario	Optical Efficiency	Effective Concentration Ratio (C_{Eff})	Acceptance Angle (°) (α)	Effective CAP $(\sqrt{C_{Eff}}\ \sin\alpha)$
Ideal (max. theoretical)	100%	5831x	1.32 (Entendue limit)	1.76 (n)
Geometric Design (No optical loss)	100%	5831x	0.4	0.53
State of the art optics (simulated)	75%	4373x	0.4	0.46
Standard optics (simulated)	55%	3207x	0.4	0.40

4. Irradiance Distribution

For ultrahigh concentration the irradiance distribution and temperature of the solar cell is very important. Due to the 4 separate input of beams in this design, the irradiance distribution can be manipulated slightly more than usual. Depending on the angle and off-axis position of the components the irradiance distribution can change as shown in figure 5 below.

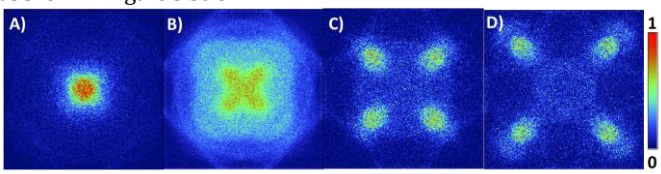

Fig. 5. Normalised Irradiance distribution upon solar cell of size 5.5 by 5.5mm. A) Most focused and aligned configuration of optics. B)-D) Increasing off cantered position of half spheres which make up centre optic. Each distribution is normalised to its maximum value.

The most aligned, in focus configuration resulted in figure 5 A) for the irradiance distribution upon the cell. This would most likely damage the solar cell under prolonged use. By adjusting the components in and out of focus with each other and further off axis from the centre more diffused irradiance distributions could be obtained as shown in figures 5 B)-D). This however also slightly reduced the optical efficiency and acceptance angle of the system. Figure 5B) was chosen as the optimum configuration with only a 2% drop in optical efficiency. The authors note however that with further experimental testing it may be that another configuration proves to be better overall. For example the advantage of having peaks in the corners of the solar cell may make the current and temperature dissipate slightly faster being closer to the edge of the cell. More research into this however is required.

The irradiance distribution as a function of incidence angle for the design is shown in figure 6.

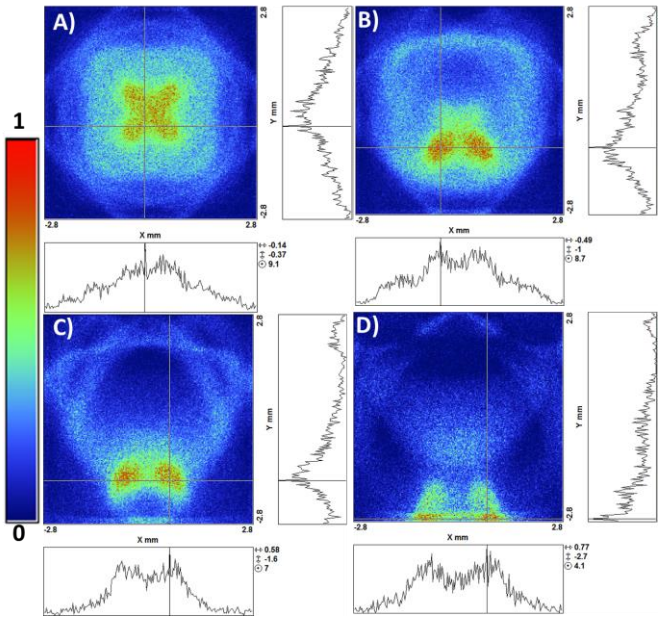

Fig. 6. Normalised Irradiance distribution on 5.5 by 5.5 mm solar cell for A) normal incidence, B) 0.4° incidence angle, C) 0.8° incidence angle and D) 1.2° incidence angle. The distributions are normalised to their own maximums and are not comparable in intensity, only relative distribution. The local maximums are shown with the crossed lines and the cross section of the intensity through these positions are shown to the side of the distributions.

As can be seen from the line profiles in figure 6 the irradiance distribution doesn't peak sharply but is a relatively gradual decline. The distribution in figure 6C might be an issue. This is when there is a misalignment of 0.8°. Similarly in figures 6D the distribution is very nonuniform and could be damaging to the solar cell if kept at this state. If the solar cell is however kept uniformly cool then the irradiance distribution shouldn't cause too much damage to the 5.5 by 5.5mm solar cell. Experimental testing is required to investigate this further especially due to the ultrahigh concentration levels. The maximum irradiance in each distribution reduces as expected with increased incidence angle. The maximum in figure 6A is 18, in B is 16.9, in C is 16.4 and in D is 12.96. These are the values with which each distribution was normalised to also to maintain the amount of information readable in each distribution.

5. Design Comparison and Discussion

A comparison table is given below (Table 2) which compares the presented design to others in the literature. As can be seen higher concentration ratios can achieve higher concentration acceptance products (CAPs) but tend to have lower optical efficiencies. This may be due to the higher number of optical stages or due to the higher priority given to maintaining an adequate acceptance angle. The number of stages shown in table 2 includes the entrance and exit of light through optics, also including the cover glass as these interfaces will contribute to scattering and light ray deviation which in turn contributes to the acceptance angle of the system as well as the optical efficiency. In this way, although the ultrahigh Fresnel lens concentrator contains 2 flat mirrors which might seem unnecessary, the number of optical stages is similar to the cassegrain ultrahigh concentrator but with the advantage that the flat optics will be far easier to manufacture and position with high accuracy in comparison to the curved mirrors of the ultrahigh cassegrain design. The manufacturing difficulty is a qualitative measurement based on the need for large smooth curved optics. These are avoided in the ultrahigh Fresnel lens where only a small dome shaped central optic is present. There is also room for the presented design to be miniaturized such as the mini cassegrain concentrator designed by Dreger et al. [27] where a smaller solar cell would be used and the optics can be downscaled which should be accompanied by reductions in cost or increases in optical quality.

Table 2. Concentration-acceptance angle product (CAP) analysis table depending on quality of optics used.

Concentrator Design Type	Ultrahigh Concentrator under study (Sim.)	4-off-axis Cassegrain [15] (Sim.)	Dome shaped Fresnel Lens [28](Sim.)	Mini-Cassegrain Concentrator [27] (Exp.)
Geometric Concentration Ratio	5831X	2304X	506X	1037X
Acceptance Angle (°)	0.4	0.61	0.5	0.75
Geometric CAP	0.533	0.51	0.20	0.42
Optical Efficiency	75%	73%	90%	80%
Effective Concentration Ratio	4373X	1682X	455.4X	800X
Effective CAP $\left(\sqrt{C_{Eff}}\sin\alpha\right)$	0.46	0.44	0.19	0.37
Solar Cell Size	5.5x5.5mm2	5x5mm2	1.4x1.4mm2	1x1mm2
No. of Optical Stages (including entry/exit of cover glass)	5	5	3	4
Manufacturing Difficulty	Medium	High	Medium-High	Medium

6. Conclusion

An ultrahigh concentrator photovoltaic system is presented and the different cases for non-ideal optics have been analyzed. The design takes advantage of flat mirrors and easy manufacturing methods in line with current and state of the art optical capabilities. The system can achieve an optical efficiency of 75% which is >4300x or if poorer quality optics are utilized then an optical efficiency of 55% is obtained which translates to >3000x. The system has an acceptance angle of 0.4° which is very good for such levels of ultrahigh concentration and of a relatively simple design. The design should be easy to manufacture and will be very useful in pushing CPV technology to higher concentration ratios. A comparison to other designs was also undertaken and shows ultrahigh concentration designs, especially the one presented here, achieving higher concentration acceptance products.

Funding

EPSRC (EP/P003605/1) through the Joint UK-India Clean Energy Centre (JUICE). In the support of open access research all underlying materials (such as data, samples or models) can be accessed upon request via email to the corresponding author.

REFERENCES

1. K. Shanks, S. Senthilarasu, and T. K. Mallick, "Optics for Concentrating Photovoltaics: Trends, limits and opportunities for materials and design," Renew. Sustain. Energy Rev. **60**, 394–407 (2016).
2. A. Vossier, D. Chemisana, G. Flamant, and A. Dollet, "Very high fluxes for concentrating photovoltaics: Considerations from simple experiments and modeling," Renew. Energy **38**, 31–39 (2012).
3. A. Cristóbal, A. Martí Vega, and A. Luque López, eds., *Next Generation of Photovoltaics*, Springer Series in Optical Sciences

(Springer-Verlag Berlin Heidelberg, 2012), Vol. 165.
4. J. M. Gordon, E. a. Katz, D. Feuermann, and M. Huleihil, "Toward ultrahigh-flux photovoltaic concentration," Appl. Phys. Lett. **84**, 3642 (2004).
5. G. Vallerotto, Victoria, Marta, S. Askins, R. Herrero, C. Dominguez, I. Anton, and G. Sala, "Design and modeling of a cost-effective achromatic Fresnel lens for concentrating photovoltaics," Opt. Express **24**, 89–92 (2016).
6. K. Shanks, S. Senthilarasu, and T. K. Mallick, "High-Concentration Optics for Photovoltaic Applications," in *High Concentrator Photovoltaics: Fundamentals, Engineering and Power Plants*, P. Pérez-Higueras and E. F. Fernández, eds., 1st ed., Green Energy and Technology (Springer International Publishing, 2015), pp. 85–113.
7. F. Languy and S. Habraken, "Nonimaging achromatic shaped Fresnel lenses for ultrahigh solar concentration.," Opt. Lett. **38**, 1730–2 (2013).
8. R. Winston and J. M. Gordon, "Planar concentrators near the étendue limit.," Opt. Lett. **30**, 2617–9 (2005).
9. T. Hornung, M. Steiner, and P. Nitz, "Estimation of the influence of Fresnel lens temperature on energy generation of a concentrator photovoltaic system," Sol. Energy Mater. Sol. Cells **99**, 333–338 (2012).
10. T. Hornung, A. Bachmaier, P. Nitz, and A. Gombert, "Temperature and wavelength dependent measurement and simulation of Fresnel lenses for concentrating photovoltaics," in R. B. Wehrspohn and A. Gombert, eds. (International Society for Optics and Photonics, 2010), p. 77250A.
11. T. Hornung, P. Kiefel, and P. Nitz, "The distance temperature map as method to analyze the optical properties of Fresnel lenses and their interaction with multi-junction solar cells," in (AIP Publishing, 2015), Vol. 1679, p. 70001.
12. L. Micheli, E. F. Fernández, F. Almonacid, T. K. Mallick, and G. P. Smestad, "Performance, limits and economic perspectives for passive cooling of High Concentrator Photovoltaics," Sol. Energy Mater. Sol. Cells **153**, 164–178 (2016).
13. L. Micheli, L. Micheli, E. F. Fernandez, and F. Almonacid, "Enhancing Ultra-High CPV Passive Cooling Using Least- Material Finned Heat Sinks," in *CPV-11* (2015).
14. F. Languy, C. Lenaerts, J. Loicq, T. Thibert, and S. Habraken, "Performance of solar concentrator made of an achromatic Fresnel doublet measured with a continuous solar simulator and comparison with a singlet," Sol. Energy Mater. Sol. Cells **109**, 70–76 (2013).
15. J. P. Ferrer-Rodriguez, E. F. Fernandez, F. Almonacid, and P. Perez-Higueras, "Optical Design of a 4-Off-Axis-Unit Cassegrain Ultra- High CPV Module with Central Receiver," Opt. Lett. **41**, 3–6 (2016).
16. K. Shanks, N. Sarmah, J. P. Ferrer-Rodriguez, S. Senthilarasu, K. S. Reddy, E. F. Fernández, and T. Mallick, "Theoretical investigation considering manufacturing errors of a high concentrating photovoltaic of cassegrain design and its experimental validation," Sol. Energy **131**, 235–245 (2016).
17. M. Victoria, C. Domínguez, I. Antón, and G. Sala, "Comparative analysis of different secondary optical elements for aspheric primary lenses," Opt. Express **17**, 6487–6492 (2009).
18. K. Shanks, H. Baig, S. Senthilarasu, K. S. Reddy, and T. K. Mallick, "Conjugate refractive–reflective homogeniser in a 500× Cassegrain concentrator: design and limits," IET Renew. Power Gener. 1–8 (2016).
19. L. Yin and H. Huang, "Brittle materials in nano-abrasive fabrication of optical mirror-surfaces," Precis. Eng. **32**, 336–341 (2008).
20. R. J. Roman, J. E. Peterson, and D. Y. Goswami, "An Off-Axis Cassegrain Optimal Design for Short Focal Length Parabolic Solar Concentrators," J. Sol. Energy Eng. **117**, 51 (1995).
21. V. Pishchik, L. A. Lytvynov, and E. R. Dobrovinskaya, "Properties of Sapphire," in *Sapphire: Material, Manufacturing, Applications* (Springer US, 2009), pp. 55–176.
22. J. W. Leem and J. S. Yu, "Superhydrophilic Sapphires for High-Performance Optics," Opt. Express **20**, 769–773 (2012).
23. I. H. Malitson, "Refraction and Dispersion of Synthetic Sapphire," J. Opt. Soc. Am. **52**, 1377 (1962).
24. C. Gödeker, U. Schulz, N. Kaiser, and A. Tünnermann, "Antireflection coating for sapphire with consideration of mechanical properties," Surf. Coatings Technol. **241**, 59–63 (2014).
25. S. Bruns, M. Vergöhl, T. Zickenrott, and G. Bräuer, "Deposition of abrasion resistant single films and antireflective coatings on sapphire," Surf. Coatings Technol. **290**, 10–15 (2016).
26. A. Duparré, J. Ferre-Borrull, S. Gliech, G. Notni, J. Steinert, and J. M. Bennett, "Surface characterization techniques for determining the root-mean-square roughness and power spectral densities of optical components.," Appl. Opt. **41**, 154–171 (2002).
27. M. Dreger, M. Wiesenfarth, A. Kisser, T. Schmid, and A. W. Bett, "Development And Investigation Of A CPV Module With Cassegrain Mirror Optics," in *CPV-10* (2014).
28. A. Akisawa, M. Hiramatsu, and K. Ozaki, "Design of dome-shaped non-imaging Fresnel lenses taking chromatic aberration into account," Sol. Energy **86**, 877–885 (2012).

[Article 7]

Shanks, K., Senthilarasu, S., Mallick, T.K.: 'High-Concentration Optics for Photovoltaic Applications', in Pérez-Higueras, P., Fernández, E.F. (Eds.): 'High Concentrator Photovoltaics: Fundamentals, Engineering and Power Plants' (Springer International Publishing, 2015, 1st edn.), pp. 85–113

High-Concentration Optics for Photovoltaic Applications

Katie Shanks, Sundaram Senthilarasu and Tapas K. Mallick

Abstract The concept of a high-concentration optical system is introduced detailing the various design types and focusing only on those aimed at photovoltaic (PV) applications. This will include point focus, line focus, imaging, nonimaging, and the classical cassegrain set-up. The theory of high-concentration optics is explained in terms of idealised concepts and maximum limits for each concentrator type and combination. The optical system is broken down into the different stages and materials possible in a high-concentration configuration. The physics of reflective and refractive optics are described, and their associated errors, advantages and a brief overview of past milestones, and recent research trends in the area of high-concentration PVs are presented. Current primary and secondary optics are geometrically explained covering Fresnel, parabolic, heliostat, compound parabolic, hyperboloid, v-trough, and dome-shaped optics. This chapter also covers examples of new secondary optics, such as the three-dimensional crossed-compound parabolic concentrator and the square elliptical hyperboloid concentrator. The aim of this chapter is to provide the basic optical behaviour of high-concentration designs aimed at PV applications considering their geometry, materials, and reliability.

1 Introduction

1.1 Concentrator Concepts

High-concentration optics are in the range of 100–2000 suns [1], a recently modified definition due to their need for dual axis tracking. The development of solar concentrator technology over the years has included improvements in concentration solar cells, cooling systems, and optical accuracy. The concentration ratio

K. Shanks (✉) · S. Senthilarasu · T.K. Mallick
Environment and Sustainability Institute, University of Exeter, Penryn Campus, Penryn, Cornwall TR10 9FE, UK
e-mail: kmas201@exeter.ac.uk

P. Pérez-Higueras and E.F. Fernández (eds.), *High Concentrator Photovoltaics*, Green Energy and Technology, DOI 10.1007/978-3-319-15039-0_4

definition also lacks conformity because this can be linked to the geometrical concentration ratio, optical concentration ratio (similar to optical efficiency), or intensity concentration ratio (flux concentration ratio) [2]. Care should be taken when a concentrating system is being described what is being used, although often it is the designed geometrical concentration ratio quoted along with an optical efficiency, which, when multiplied, should give the flux concentration ratio.

In terms of a concentrator PV (CPV) system, multiple concentrator optics (including low concentration devices <10 suns) can be involved. In this way a high-concentrator PV (HCPV) system can be classified as a single-stage, two-stage, or greater-stage system, although fewer stages are desired to decrease complexity and additional uncertainties. The preferred outline of a high-concentration optical system within an HCPV system consists of primary and secondary optics. The primary optics initially collect incident light, and typical examples include the Fresnel lens and the parabolic reflector. The secondary optics are of medium to low concentration and can be referred to as "receiver optics" when in optical contact with the PV. These secondary optics can increase the concentration of the system but are used more often with the aim of improving the system's acceptance angle and the irradiance distribution on the PV. Receiver optics introduced to a concentrator design which improve the irradiance distribution are also suitably referred to as homogenisers. Two examples of different HCPVs are given in Fig. 1.

CPV systems can be categorised in a variety of ways such as concentration ratio, primary optic type, tracking method, geometry, and number of stages. Figure 1a could be described as a two-stage refractive concentrator consisting of a primary

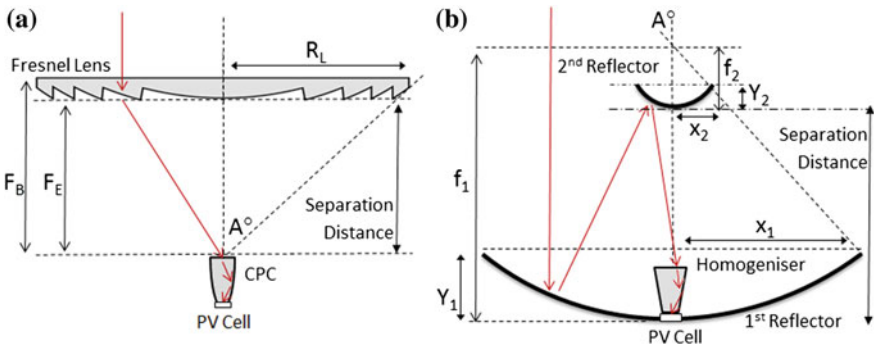

Fig. 1 **a** Primary Fresnel lens with secondary compound parabolic concentrator (CPC). Parameters that may be considered during the design of such a system are given: radius of the Fresnel lens R_L, back focal length F_B; effective focal length F_E; and separation distance and maximum angle of incident rays on the secondary, A. **b** A classical cassegrain set-up of a primary parabolic dish reflector with a hyperboloid secondary reflector and crossed V-trough dielectric filled homogeniser as a receiver optic. Example of design parameters to be considered in a cassegrain are shown: primary paraboloid's radius x_1; depth of the paraboloid y_1; and focal length f_1. Similarly, examples for the secondary are hyperboloid radius x_2; depth y_2; and focal length f_2. The separation distance between the two reflectors is again displayed as is the maximum incidence angle of light on the secondary A, which can relate the two reflectors' geometry

Fresnel lens and secondary CPC. Figure 1b shows the classic cassegrain set-up, which typically consists of a parabolic primary reflector, a secondary paraboloid or hyperboloid secondary, and a tertiary crossed V-troughed dielectric filled homogeniser. In both of these, if the original two-dimensional (2D) geometries were translated linearly, then they would be described as "line-focus systems." Figure 1a would become a linear Fresnel lens with a linear (or 2D) CPC focusing on a line of solar cells, and Fig. 1b would become a parabolic trough similarly focusing on linear optics and receivers. A line-focus CPV system, also referred to as a 2D design, is normally used for solar thermal concentrator systems where the receiver may be a transparent pipe carrying water or another liquid medium to be heated. There is often a point-focus version to every line-focus geometry and vice versa, where by way of rotational or translational symmetry the original 2D design is transformed into a three-dimensional (3D) one. Terms such as "crossed" or "rotated" could be used to describe how a 2D profile has been transformed into a 3D optic. A point-focus collector can be deliberately designed not to be symmetrical across any obvious axis, but an uneven irradiance distribution on the cell would be expected. Due to the popularity of line-focus systems with thermal heating, and the rareity of high-concentration linear optics [3], point source systems will be addressed more than linear systems in this chapter. It should also be obvious that with point-focus optics, a dual-axis tracking system is preferred for maximum performance, and a line-focus optical concentrator would require a single-axis tracking system.

Optics can also be classified as imaging or nonimaging where the former describes an optic that refracts light from an object in such a way as to maintain the image but produce a smaller form at the focal plane [4]. Nonimaging optics, such as the CPC and the nonimaging Fresnel lens, were designed later and tailored specifically for the collection of solar rays. This means that they were designed specifically to obtain high optical efficiencies and highly uniform flux distribution output and to cope with the characteristics of solar light [4]. This list of aims, however, does not necessarily require the same image to be replicated at the focal plane, and thus typically the image is distorted at the focal plane, and the term "nonimaging optics" was given. Nonimaging concentrators with very large numerical apertures (small aperture ratio or *f*-number) would have very large aberrations if used as image-forming systems [2]. Geometrical aberrations in the classic sense cause imaging optics to perform at a nonideal level. Image-forming concentrators must treat each ray in a similar fashion to replicate the image at the receiver.

This means all rays that pass through an imaging optic will be reflected once or pass through a refractive boundary only once along with all of the other rays. In this way, rays at varying angles or different incident positions, which would be lost, cannot be treated differently in an attempt to keep them within the system. Nonimaging concentrators such as the CPC, however, can apply different conditions to different rays and obtain ideal performance. Purely imaging optics are, however, capable of approaching the thermodynamic limit and even possibly attaining flux

levels greater than a nonimaging one; for both types, careful and tailored design decides which is optimum [5].

The ideal solar concentrating optical system would have 100 % optical efficiency, an output of uniform irradiance distribution (matching in shape and size to the PV receiver), maximum acceptance angle, high optical tolerance, and durability (hence high reliability). It would also preferably be cheap to manufacture, lightweight, and easy to install. Each type of CPV system has advantages and disadvantages, and it is important to know the application and location to choose the most appropriate design.

1.2 Optical Physics Basics

1.2.1 Concentration Ratio

The concentration of an optic or system of optics can be defined as low (<10 suns), medium (10–100 suns), high (100–2000 suns), or ultrahigh (>2000 suns) concentration [1]. Under normal conditions, the maximum concentration ratio ($C_{\max}$) achievable on Earth due to the divergence of light from the Sun is 46,000× for a 3D system (full tracking) and only 216× for a 2D system (single-axis tracking) as calculated from the Sun's diameter [2, 6]. The resulting Eqs. (1) and (2) consider that the concentrator is immersed in refractive index, n, (for air this becomes 1) and θ_i as the input angle (i.e., effective solar angular radius: 4.7 mrad or 0.267°) [2, 6]:

For a linear concentrator, the maximum concentration equation is shown:

$$C_{\max} = \frac{n}{\sin \theta_i} \tag{1}$$

and for a point-focus concentrator:

$$C_{\max} = \left(\frac{n}{\sin \theta_i}\right)^2 \tag{2}$$

If we now use θ_o to represent the output (absorber) angle and NA to denote the numerical aperture ($NA = n \sin \alpha$), then the above can be written [7]:

$$C_{\max} = \left(\frac{n \sin \theta_o}{n \sin \theta_i}\right)^2 = \left(\frac{NA_o}{NA_i}\right)^2 \tag{3}$$

The previous equation can be used to calculate the maximum concentration possible of an optic by using the maximum acceptance angle as θ_i. Fresnel-reflective losses from the absorber can be avoided by limiting the θ_o to $<\pi/2$ [2, 7], but some antireflective coatings of solar cells can still have greater

reflectance values for off-axis incident light rays. The concentration ratio of a linear concentrator is usually given as the ratio of the transverse input and output dimensions [2]. As expected, the point-focus equivalent of a line-focus concentrator will always have an increased geometrical concentration ratio, but it is much easier to achieve an ideal concentrator design in 2D geometry such has been performed for the CPC. An ideal concentrator works perfectly for all rays within the acceptance angle.

The current concentration ratio range for commercial HCPV is 100–1000 suns [8]. Specific concentration limits for each type of concentrator is discussed in later sections.

1.2.2 Ideal Conditions and the Classic Cassegrain

Most optical concentrators are initially based on, or initially designed on, idealised concepts and conditions, and then they are developed to consider more accurately the practical environment. First assumptions may include the condition of incoming radiation from the Sun to be parallel and a specific irradiance value (e.g., 1000 W $/m^2$). The optical components are also idealised, assuming 100 % specular reflectance for mirrors, all wavelengths to be fully refracted for lenses, and no thermal effects on shape [9]. It would be difficult to include all uncertainties in the first steps of optical design, but some are essential and can significantly alter results. One must consider that these practical uncertainties are especially important at greater concentration ratios (which are more sensitive to error) and when incorporating multiple stages (errors build on each other) where these uncertainties intensify (see Fig. 2).

The line and spot in line- and point-focusing optics can only ever be realised in an idealized mathematical model. Manufacturing uncertainties (surface roughness and slope errors) and alignment errors (tracking error and component misalignment) give an effective distribution of errors for the system, which contribute to the Gaussian diameter seen in real measurements [3]. Parabolic reflectors are concentrators intended for distant sources (parallel light sources) where all incident light is reflected into the focal point. In this way, parabolic mirrors are popularly used in telescopes. The Sun is an extended source, not a point light source, with a light divergence of 4.7 mrad (0.27°) and where solar rays are not exactly parallel, but instead each ray can be described as a cone. This effect is amplified by multiple stage concentrators [10–12].

The classical cassegrain (shown in Fig. 1b) uses a primary parabolic-shaped reflector and a hyperboloid secondary. Other conic curves have been tried for the primary and secondary, but a hyperboloid secondary is preferred to allow greater optical tolerance. A cassegrain consisting of a parabolic primary and secondary is based on the theory of parabolas: Any parallel light incident on a parabolic dish will be reflected at such an angle as to pass through the focal point of that parabola. In this way, with a parabolic primary and secondary of coincident focal points, the

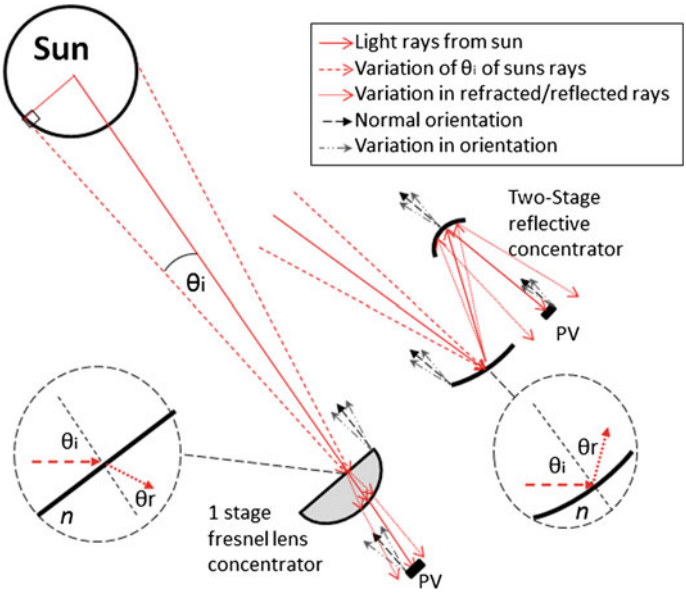

Fig. 2 Light rays from the Sun are shown to not be parallel, incident on a single-stage refractive concentrator and a two-stage reflective concentrator. Focus is given to the variation of incidence angle of a light ray from the Sun after refraction or reflection, which can cause final light rays missing the PV receiver. Magnifications of the incident rays undergoing refraction and reflection are also shown and labelled

parallel light would be concentrated and reproduced, thus giving a uniform irradiance distribution on a solar cell placed in the base of the first reflector. As mentioned, light from the Sun is not parallel, and so the paraboloids would need to be positioned off focus (afocal) to compensate, or another design such as the parabololoid-hyperboloid one could be used instead. Many have researched and commercialised the cassegrain design, and it holds the advantage of an upward-facing receiver. This can be easier to cool and structure without extensive shadowing on the primary. For HCPVs, shadowing within the cassegrain causes the loss of 1 sun, which is not significant compared with the hundreds of suns an HCPV is designed to produce. The dark image produced on the PV receiver may, however, affect the PVs efficiency. The shadow is $1/C$ of the total area where C is the geometrical concentration ratio.

Low optical tolerance is associated with the cassegrain design because it uses two reflective stages, thus compounding the reflective error and the uncertainty in incidence angle of the light rays (see Fig. 2). It often requires a tertiary optic to improve the acceptance angle, but there are methods to avoid this such as decreasing the path length of light rays within the system. This decreases the effect of error on the final light ray position [13]. The cassegrain reflector arrangement allows the PV receiver to be mounted below the main reflector. This geometry gives

easy access to the receivers during replacement and thus drastically lowers maintenance costs. Furthermore, the whole optical geometry can be designed using ray tracing and is usually considered a compact solar concentrator. The minimum aspect ratio of the cassegrain design has been calculated as one fourth [2], but the same has yet to be proven for a cassegrain design with a nonimaging (hence different ray path lengths) primary and/or secondary [10].

The final hurdle in any concentrator optic development is manufacturing and practical testing. Unless the design has a sufficiently high optical tolerance then errors in geometry replication and alignment will decrease the performance. Practical considerations—such as fluctuations in temperature, moisture, wind, and shadowing—can also affect results as expected.

1.2.3 Optical Tolerance, Etendue, and Solar Tracking

One of the main challenges of concentration optics is the decrease in acceptance angle as concentration ratio is increased due to etendue. Optical tolerance refers to all possible alignment uncertainties within the optical system including component misalignment, cell position uncertainty, and tracking error. For high and ultra-high concentrator optics, this is difficult to overcome without compromising another attribute such as optical efficiency or irradiance distribution. Conventionally, the acceptance angle of an optical system is taken to be the offset angle from normal solar incidence, which achieves 90 % of the normal incidence power. This value may be different for $\theta > 0$ and $\theta < 0$ in an asymmetric concentrator (or one with asymmetric errors). If the acceptance angle is maximised, then it decreases the need for highly accurate and more expensive optics, structure, and tracking. A minimum requirement for the angular tolerance, θ_t, and hence the acceptance angle of a system, is to exceed the effective solar angular radius, θ_i. Assuming that $\sin\theta_t \approx \theta_t$, the following equation is formed [14]:

$$\theta_t \leq \frac{n \sin\theta_o}{\sqrt{C_g}} - \theta_i \tag{4}$$

The acceptance angle or optical tolerance for high-concentration devices, such as parabolic dishes and Fresnel lenses, without additional optics can be expected to be very low ($\pm \approx 0.5^\circ$ or less) [15–17]. However, there are exceptions to this with increasing focus on improving acceptance angles for HCPVs [13].

High-concentration optics have the limitation of requiring continuous tracking. The acceptance angle can be determined from the variation of optical efficiency as a function of the incident angle of the input light rays. However, there is slight variation in the value at which to measure the acceptance angle (e.g., 95–80 % of the normal incidence maximum). During practical testing, the short circuit current or power output can be used to measure acceptance angle, but each gives slightly differing results [18].

During the day the Sun is viewed as having a daily rotation about its north-south axis. It then also has a seasonal north-south motion of $\pm 23^{\circ}27'$ away from the equator [19]. Due to the Earth's axial tilt and elliptical orbit, the Sun's noontime position also slightly changes. Jagoo [19] give the derivation for the Sun's position equation as well as a comparison of the theoretical azimuth and theoretical altitude with measured values at different times of the day. Single-axis trackers follow the east–west motion of the Sun during the day but are unable to fully consider the seasonal variation. Dual-axes trackers give optimal performance year-round. However, trackers introduce their own error and cost and are less resistant to natural extremes, which could permanently damage the system. Dynamic trackers use sensors to generate a differential signal when the device is not positioned optimally for available incident light. Although easy to build and maintain, these devices fail to discriminate between the obscured Sun and a bright spot in a broken cloud [19]. The chronological tracker maintains the receiver normal to the Sun using a built-in clock and is typically single-axis. This type of tracker requires frequent manual adjustments, thus making it difficult to accurately follow both daily and seasonal variations and only works over a portion of the time because it rotates 15°/h.

1.2.4 Reflection and Refraction

Snell's law of refraction dictates that any ray travelling through a medium with refractive index n_1, which is then incident on the surface of another medium of refractive index n_2, will have a path described by:

$$n_1 \sin \alpha_1 = n_2 \sin \alpha_2 \tag{5}$$

where α_1 and α_2 are the angles the ray makes with the normal of the surface before (angle of incidence) and after refraction (angle of refraction). Snell's law can also be applied to the case of reflection where the refractive medium is replaced by a mirror. In this scenario, the ray will continue to stay in the same medium of refractive index n_1, and so Eq. (5) becomes Eq. (6) where α_2 is referred to as the angle of reflection:

$$\begin{aligned} n_1 \sin \alpha_1 &= n_1 \sin \alpha_2 \\ \alpha_1 &= \alpha_2 \end{aligned} \tag{6}$$

Total internal reflection (TIR) occurs when a light ray comes into contact with a less optically dense medium (lower refractive index) than the medium it is currently travelling in and if the angle of incidence is greater than the critical angle for TIR. The critical angle for TIR can be calculated using Snell's law by letting $\theta_2 = \frac{\pi}{2}$ and rearranging for θ_1, which now represents the critical angle θ_c:

$$\theta_c = \sin^{-1}\left(\frac{n_2}{n_1}\right) \tag{7}$$

When a mirror is placed against the surface of a lens (n_2 now > n_1), TIR is lost, and the rays will be reflected with the mirror's reflectance properties (approximately 90 %). By leaving an air gap between the two materials both the TIR and refracted rays, which do not meet the TIR criteria (otherwise lost), are kept within the optical system.

The surface of both reflective and refractive surfaces must be smooth to avoid the scattering of light. The previous equations assume optically smooth interfaces between two lossless media, but light can be partially or fully absorbed, refracted, and reflected. For lenses, a rough finish will decrease TIR or alter the refraction direction intended; for mirrors, a greater proportion of the light will be diffusely reflected (scattered) instead of specularly reflected (direct). On a very smooth surface, lines normal to neighbouring points along that surface are parallel to each other, and multiple light rays reflect specularly, all with the same definite angle pertaining to Eq. (6). In diffuse reflection, all of the reflected rays still behave in accordance with the law of reflection, but the roughness of the surface means normals along the surface vary. Because the angle of incidence depends on the normal line at the exact point a ray hits, the incident angles for a set of parallel rays will not be the same, and each reflected ray will have a different angle of reflection, hence scattering occurs.

Gaussian scattering can be applied to optical surfaces using Eq. (8) within simulations to produce more accurate irradiance distributions, which will be affected by nonideal factors in the optics [20].

$$R(\alpha) = R_0 \exp\left[-0.5(\alpha/\sigma)^2\right] \tag{8}$$

where R_0 is the radiance in the specular direction, and σ is the SD of a Gaussian distribution in degrees (0.2).

High-concentration optics very rarely will be able to use any diffuse irradiance. Most materials exhibit a mixture of specular and diffuse reflection along with absorption and transmittance (refraction); examples are given in Materials for HCPV Optics . For most interfaces, the fraction of light increases with increasing angle of incidence until, in scenarios capable of TIR, the critical angle is surpassed.

The refractive index is also wavelength dependent, and although this variation can be negligible at certain solar energy wavelengths and for relevant materials, for high-concentration optics it can compromise the refractive optical design, thus limiting the concentration ratio (such as for Fresnel lenses) and affecting the reliability of the system by way of the optical efficiency, acceptance angle, and irradiance distribution.

Most solar concentrators will be encased for protection including a transparent cover material forming the input aperture of the collector system. There are two parallel interfaces for this as well as any other panes used (e.g., air/glass and

glass/air) with reflection at each interface. Every transparent material exhibits some absorption due to the interaction of incident radiation with the molecular structure of the medium. Norton [21] discussed the effect of incidence angle on the transmittance of light and indexed sources of material data to replicate the theoretical absorbance/transmittance as well as strength and other properties important for solar collectors.

When using a refractive optic, care must be taken that TIR does not work against the design by reflecting light backwards instead of toward the receiver. This is negligible when the optic is in optical contact with the solar cell, but errors in the interface (mismatched slopes, grooves, cracks, bubbles) will allow for air ($n = 1$) and unwanted reflection. Antireflection coatings for solar cells are common, but information about the angle of incidence required is limited. The coating could decrease reflection for approximately normal incident rays but increase it for wide-angled rays. For final-stage refractive optics, which have a greater portion of output rays at wide angles, the overall energy incident on the solar cell would be decreased.

1.3 Historical Overview

1.3.1 HCPV Optical-Design Milestones and Current Trends

John Hadley introduced parabolic mirrors into practical astronomy in 1721 when he used one to build a reflecting telescope with little spherical aberration [22]. Before that, telescopes used spherical mirrors. The first reported use of an external flat reflector in a solar thermal concentrator was in 1911 by Shuman for a water-pumping system powered by a flat-plate reflector assembly [21]. Lighthouses also commonly used parabolic mirrors to collimate a point of light from a lantern into a beam before being replaced by more efficient Fresnel lenses in the Nineteenth century [23]. Augustin Jean Fresnel was the first to discover the use of Fresnel lenses in 1822 as glass collimators in lighthouses [24, 25]. Only when less costly materials such as poly(methylmethacrylate) (PMMA) were discovered were Fresnel lenses implemented as solar energy collectors in the 1950s. In the late 1970s, the first modern Fresnel lens CPV system was built at Sandia National Laboratories [26]. Interest in Fresnel lense solar concentrators increased in the second half of the twentieth century [4].

In the 1960s, Giovanni Francia was the first person to apply the Fresnel reflector concentrator concept for industrial thermal processes in Italy [27]. The compound parabolic concentrator (CPC) was the first 2D concentrator ever designed, also in the 1960s, but the theory was not explicitly explained until the 1970s when the generalized entendue was derived [2].

Regarding concentration measurements, since the first ultra-high flux measurements were performed at the University of Chicago in 1988, there has been very rapid progress including experimental investigation of laser pumping and materials

processing experiments performed at the National Renewable Energy Laboratory High-Flux Solar Furnace and the Weizmann Institute Solar Tower [2].

Concentrating solar technologies have passed the testing and small-scale power-production phases and are now being commercialised [19]. A noticeable trend in large solar concentrator designs is the shift from continuos surfaces to segmented surfaces of optics, e.g., using many smaller flat or circular facets to make a large parabolic dish. Evidence shows that this is now one method to improve the performance of reflector concentrators as shown by Zanganeh et al. [28]. Solar dish concentrators based on ellipsoidal polyester membrane facets and V-groove reflectors have been showing improved irradiance distributions whilst still obtaining optical efficiencies of >80 % [28]. Nilsson et al. [11] proposed a stationary asymmetric parabolic solar concentrator with a microstructured reflector surface; three different microstructures were tested for their effect on irradiance distribution and optical efficiency. The highest optical efficiency reached 88 %, and all distributions decreased distribution peaks. For high concentration, an array of small concentrators per cell module is the safer design considering manufacturing, maintenance, damage, and replacement [9], and it is the same for systems with mulitple concentrators per cell.

Third-generation organic PVs have begun to be tested under concentrated sunlight as well. Organic PVs are a potentially low-cost, lightweight, and flexible alternative to inorganic PVs, but they have poor durability. Under concentration levels <10 suns, the short-circuit current increases with concentration in a linear fashion, whereas the open circuit voltage increases logarithmically [29]. At >10 suns, heating of the organic PV material causes a decrease in the open circuit voltage [29]. At present only low-concentration optics—such as light funnels, wedges, luminescent concentrators, and small reflective dishes—are being used with organic PVs.

2 Primary Optics

The majority of HCPV concentrators will be point focus and require two-axis tracking. They are well suited for large field installations in the 10–100-MW range [8] rather than smaller scale systems or for domestic use. High-concentration optics are only suited to sunny areas where direct sunlight is available due to their high dependency on normal incident light rays and specular reflectance rather than diffuse.

2.1 Fresnel Lens

The most developed refractive concentrator is the Fresnel lens, which is made up of a chain of prisms (see Fig. 3) where each prism contributes a section of the slope of the lens surface but without the material of the full body of a conventional singlet [4].

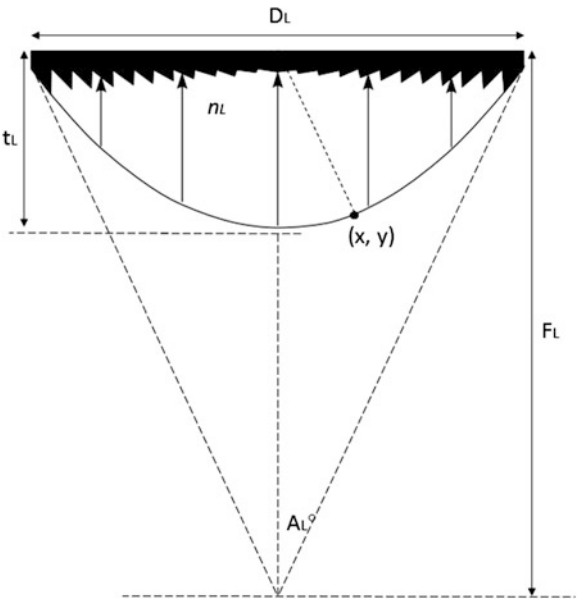

Fig. 3 The conversion from a conventional convex lens to a compact Fresnel lens by way of truncation. Dimensions and geometry of the lens are shown: diameter of the lens D_L; original thickness t_L; original focal length (which is now termed the "back focal length" of the Fresnel lens) F_L; refractive index of the lens n_L; and the maximum angle of concentration A_L

According to Fermat's principle that all rays have an equal path length, then the following equation can be obtained for a full-bodied aspheric convex lens [26]:

$$F_L + (n_L + 1)t_L = \sqrt{(F_L - y_L)^2 + x^2} + n_L y \tag{9}$$

By substituting $D_L/2$ for × and the thickness of the lens t_L for y, the following equation relates the focal length to the thickness [26]:

$$\frac{t_L}{D_L} = \frac{\sqrt{F_L^2/D_L^2 + 1/4} - F_L/D_L}{n_L - 1} \tag{10}$$

For a solid lens, only the angular orientations of the outer surfaces on which light is incident and transmitted are relevant to the focusing action. The thickness of the inner medium is not important and in fact absorbs more energy the longer the light travels in the medium. So by collapsing the convex lens down to minimise the thickness, the rays should approximately still focus in the same area but require less lens material to do so.

The centre of curvature of each ring in a Fresnel lens can be designed to recede along the axis according to its distance from the centre to eliminate spherical aberration. Fresnel reflection causes approximately 8 % loss within the Fresnel lens, and for easy mold removal any vertical lines shown in a Fresnel diagram are typically actually inclined at 2° [26].

In a Fresnel lens, the discretisation and the sharp edges of the prisms, which are absent in the convex, are a source of unwanted diffracted rays. Consequently, the Fresnel lens is a much poorer imaging lens than the original smooth convex lens; however, as stated previously, imaging of the source is not necessary in power collection. This small percentage of loss is greatly outweighed by the relative lightness and compactness of the Fresnel lens. The convex lens would not be used in a commercial HCPV system as a primary optic. In general, high-concentrating Fresnel lenses are actually also avoided commercially because in large structures mainly formed from glass, such lenses are still considered unwieldy, heavy, and expensive [9]. This gives more reason for modular designs with Fresnel lenses focusing toward very small solar cells ($100\ mm^2$) or all focusing to one PV receiver.

The *f*-number (relative aperture) of a Fresnel lens is the focal length over the diameter. Because the *f*-number is increased, the irradiance is decreased. They are typically point-focus circular-faced lenses, although line-focus Fresnel lenses have been designed, and they can be cut to square shapes to increase the packing factor. The maximum concentration ratio of a single Fresnel lens, which is limited by chromatic aberration, is approximately 1000× [30]. However, by combining a diverging polycarbonate (PC) lens and a converging PMMA lens, the concentration limit can be increased up to 8500× [31].

There are two types of Fresnel lens: imaging and nonimaging [12]. The nonimaging Fresnel lens has a lower manufacturing cost, but the performance is far from optimum due to the low acceptance angle and decreased geometrical optical efficiency [32]. However, nonimaging Fresnel lenses are considered less sensitive to chromatic aberration, especially when the design process considers multiple wavelengths such as in the case of the domed Fresnel lens [17]. In the case of imaging Fresnel lenses, the output image can be altered by aberrations due to inaccurate manufacturing of the prism tips and grooves [4]. However, acceptance angles close to the theoretical maximum and 100 % geometrical optical efficiencies are [32–34]. For both types, ray-tracing software can be used to improve the optical efficiency, acceptance angle, chromatic aberration, spot shape, and flux uniformity. For Fresnel lenses, there is a compromise to be made between module thickness and the above mentioned list of attributes, which increase as thickness decreases [23].

The irradiance distribution for Fresnel lenses, such as for many concentrator optics, is originally a Gaussian shape, which is difficult to match to a square solar cell. However, an asymmetrical curved Fresnel lens, which has very good uniform irradiance (ratio of maximum and minimum irradiance points <2), is possible [32]. There are significant manufacturing problems with this type of Fresnel lens due to the nonsymmetric design and problems in molding the curved lens [32]. A hybrid Fresnel-based concentrator with a significantly improved uniformity, compared with a traditional Fresnel lens, can be obtained by tailoring the order of the Fresnel prisms as shown in Fig. 4 (adapted from Zhuang and Yu [35]).

The use of an aspheric lens (Fresnel or not) to obtain high concentration by eliminating spherical aberration is widely known, and the profile can be calculated using Fermat's principle. When considering chromatic aberration, ray-tracing

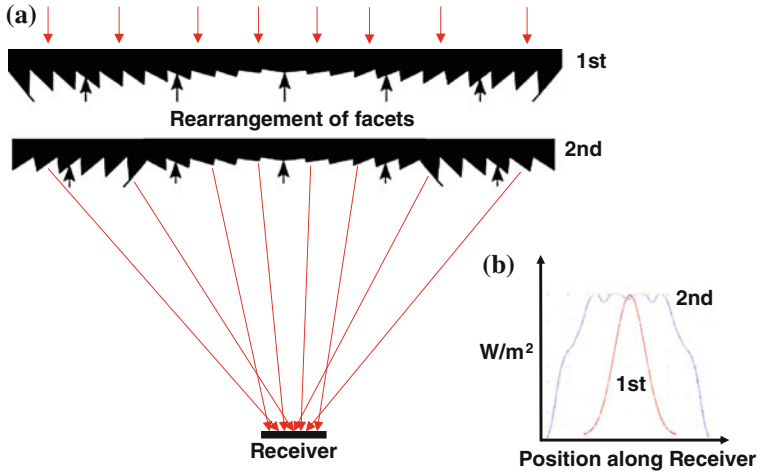

Fig. 4 **a** Diagrammatic representation of improved Fresnel-based concentrator and **b** irradiance distribution profile on the receiver [35]

methods or calculations involving two or more wavelengths are an effective method to decrease the dispersion of the focus beam. A dome-shaped nonimaging Fresnel lense can be made in such a way with improved optical efficiency and less transmission of infrared rays, which may or may not be beneficial to the PV material being used.

Fresnel lenses offer high optical efficiencies and low production costs, which explains their development as PV concentrators over the years.

2.2 Parabolic Reflectors

The point-focus parabolic dish and line-focus parabolic trough can be concave or convex (inverse) where the active side (that which is used to redirect the light) faces the source. The parabolic dish is a paraboloid of revolution, a surface obtained by revolving part of a parabola about its axis of symmetry. The parabola shown in Fig. 5 may be represented in cartesian coordinates by:

$$D_r^2 = 8\, F_r\, t_r \tag{11}$$

and:

$$4\tan(A_r/2) = \frac{2x}{F_r} \tag{12}$$

As shown in Fig. 1b, when two parabolas have coincident focal points and hence the same angle A, then the following equation relates the two:

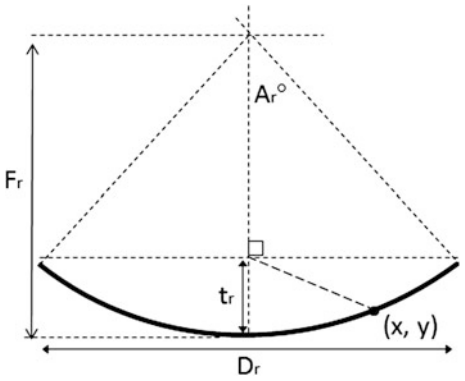

Fig. 5 Dimensions and geometry of a parabolic curve reflector in two dimensions

$$\frac{x_1}{f_1} = \frac{x_2}{f_2} \tag{13}$$

Parabolic troughs are usually designed for low to medium concentration ratios with a half-acceptance angle two to three times the apparent angular width of the Sun's disk. The maximum concentration ratio of a parabolic trough concentrator, which can attain high optical efficiency and high acceptance angles without the aid of a secondary optic, is limited to $\sim 70\times$ [36]. Beyond this, the parabolic trough is suitable for concentrations up to 200 suns and although possible, it is rarely used for HCPV applications [3]. The use of a second concentrator is needed to bring the concentration value as close to the limit as possible. Therefore, the usual approach is to take advantage of the low aspect ratio values of focusing primary optics and use second-stage concentration at the receiver to increase the overall concentration value. Parabolic trough concentrators are the most proven and commercially tested solar thermal concentrator technologies, and the California Mojave Desert has nine large commercial-scale solar power plants in operation [19], but the parabolic dish is used for HCPV systems.

Large paraboloids are difficult to manufacture accurately, and sometimes smaller flat or conic mirror facets are arranged to approximate the paraboloid shape. The trough is inherently easier to manufacture and can be performed so by bending a flat reflective sheet [3].

A parabolic dish (point-focusing) solar collector is advantageous compared with other collector systems due to the absence of cosine losses and the increased concentration ratio compared with the line-focusing parabolic trough [37]. The 3D parabolic dish can be thought of as the most efficient high-concentration optic with the fewest restrictions, but maximizing their full potential is very expensive compared with the point-focus Fresnel lens [19]. Parabolic dishes have greater optical efficiencies than that of the linear Fresnel reflector or central receivers where cosine losses ensue.

As for their performance at high-concentration ratios, although parabolic reflectors on their own can reach high optical efficiencies or have relatively uniform

irradiance distribution (by matching receiver size to beam radius), they cannot perform both unless other optical stages are used due to the gaussian shape of light from the Sun [38, 39].

Parabolic mirrors for dish power-generation systems are generally constructed from one large parabola per dish, although less expensive techniques, such as forming the dish from an array of small mirrors, are becoming more common [9].

2.3 Linear Fresnel Reflector and Heliostat Fields

Linear Fresnel reflectors (LFRs) implement flat mirrors in strips at increasing tilt positions at further distances from the receiver (usually positioned above the LFR). Most LFR systems are solar thermal, and research into receiver shapes and areas has been conducted. They have been classed as low-concentration optics in the past, but they can be used as medium concentrators. To reach greater concentrations, bent or parabolic mirrors are needed in place of the flat mirrors, and hence LFRs are sometimes not considered as high-concentration optics, but their parabolic or similarly curved counterparts would be. The central receiver set-up has the advantage of being a stationary fixed receiver, which is easy to structure and support, and it decreases the weight and strain on moving optics. This can be adoptable for any collector field-tower receiver set-up, and typical support tower heights are up to 10 × 15 m tall [9].

Abbas et al. [40] reviewed LFRs and described how the variation of the total power impinging onto the receiver and its flux map along the day has traditionally been identified as a major handicap for LFR technology. This problem is first due to the optical efficiency of the solar field, which varies more than in trough collectors [41], as well as the change on total radiation falling within the field, which is caused by the zenith angle.

The linear Fresnel reflector has the ability to "reshape" the mirror surface, which is a major advantage compared with the trough system. Solar movement across the sky can be compensated for by simple adjustment of the mirror elements rather than requiring movement and control of the reflector/receiver unit as a whole. This simplifies the support and tracking structure leading to fewer implementation costs [9].

Linear Fresnel reflector systems have relatively low initial cost, and because the reflector strips are ground-mounted, wind loads on the reflector strips are low.

Fields of heliostats are similarly used for thermal power towers and some smaller-scale PV central receivers have gained growing interest, but at present their use as HCPV optics is rare. Plans for space solar-concentrator optics, which would direct light toward solar fields on Earth, consist of a lightweight array of heliostat mirror satellites in a constellation in low Earth orbit (1000 km). Although this may seem far-etched, NASA is developing a solar sail due to be finished by 2015. The Earth-based solar fields, which would receive the extra 6 $kWh/m^2/day$, are already being constructed [8]. This idea involves taking advantage of the dawn-to-dusk

sunsynchronous orbit adopted, i.e. a near-polar orbit of inclination angle 99° rotating at 1°/d, to remain consistently normal to the Sun's rays.

On the Earth's surface, each heliostat has a dual-axis tracking system, and the overall field usually takes on a circular or semicircular array [21].

3 Secondary and Final-Stage Optics

In high-concentration optics, secondary optics are necessary for high performance and high reliability. Due to the low optical tolerance of HCPVs, this is important even during prototype stages where manufacturing and alignment is perhaps not optimum. This is even more important for optical systems of multiple stages, such as the cassegrain, and as the concentration ratio is increased. As one can imagine, tertiary optics are common depending on the design of the optical system, and a wide range of shapes is used. Reflective secondary optics tend to have increased flux uniformity and colour-mixing effects, but dielectric secondariness using TIR can withstand more internal reflections without much loss [42]. Too many reflections in both optics results in severe light ray loss by way of Fresnel losses, not meeting TIR criteria, or in light being reflected back (opposite direction of receiver). The three main families of final stage optics are the dome-shaped lens, the compound parabolic concentrator (CPC), and the light funnels (light cones). Although all are capable of increasing the concentration ratio, irradiance distribution, and/or acceptance angle on the solar cell(s), the optimum receiver optic will depend on the design and constraints of the system.

Nonimaging secondary optics can improve the irradiance uniformity and eliminate shadowing better than imaging secondary optics for certain systems. The nonimaging secondary optic can be formed by rotating a segment of curve from a linear, quadratic, and even cubic order function [10].

3.1 The Revolved Conics

This section refers to the ellipsoid, paraboloid, hyperboloid, and even the sphere (the circle can be argued to be and not be a true conical shape) as revolved conics producing 3D point source optics. These are typically used as the second stage of reflection in the cassegrain set-up described earlier, and thus their size should be kept low to avoid shadowing effects on the primary. Although these secondary optics will share the same advantages and disadvantages as the larger primary versions, due to their smaller size they are easier to manufacture accurately. They will also undoubtedly introduce their own errors into the optical system, but these too are easier to minimise on a small scale than in the high-concentrating versions. The revolved conics are imaging optics, and so microscopic and macroscopic imperfections will increase the focusing point diameter and cause lower concentration.

As mentioned in the Introduction, high concentration is difficult to achieve with line-focusing optics, but the combination of two linear optics can produce an overall point focus capable of high-concentration ratios up to 2000 suns [3]. This is performed by the primary linear optic focusing in one plane along its length to create a line focus and then the secondary linear optic focusing that line to a point. In this set-up, the path of most rays within the optical system are longer than in the conventional point source counterpart, and so further beam spread is incurred as is increased shadowing from the oblong secondary optic, but accurate manufacturing is more economic.

A 2D profile of a dome lens can be designed that redirects all incoming rays from the first-stage (and possibly second-stage) optic toward the cell. The 3D lens is then rotated around the optical axis. The dome lens typically uses less material than a CPC and can be easier to manufacture [20]. The significant advantage of the dome-shaped lens is the uniform irradiance distribution it can provide on the cell [20]. A ball lens can also be used as a secondary optic, but this would perhaps still require a tertiary optic at the receiver. Due to the ball lens 3D symmetry, any expansion due to heat should not affect the performance of the ball lens to redirect the light rays to the intended destination. However, the weight and support of the ball lens is more difficult to accommodate.

The paraboloid, ellipsoid, and hyperboloid mirrors are typically used as secondary reflectors wherein the latter is more tolerable to errors and hence can improve the acceptance angle of a system when replacing a secondary paraboloid. The ellipsoid, semisphere, and sometimes even flat mirrors are used in arrays to emulate a larger parabolic dish with simultaneously high optical efficiency and irradiance distribution.

Many novel secondary optics have been aimed at improving irradiance distribution on the PV receiver, but most of these require the input aperture to be fully illuminated, which—although possible in HCPVs—does then limit the acceptance angle.

3.2 The CPC and Its Variations

The 2D profile of the CPC can be described as having focal points of both parabola sides located at the intersection between the opposite parabola and the receiver. The compound parabolic concentrator is designed using the edge-ray principle and is considered an ideal concentrator in two dimensions. This means that no rays within the acceptance angle are lost, and hence it achieves maximum theoretical concentration. All rays entering at the extreme collecting angle are conserved on the output exit aperture with no loss of rays. The length is bound by the extreme rays at θ_i where both rays reach the receiver. The focal length can be given as [2]:

$$f = \frac{a'}{1 + \sin\theta_i} \tag{14}$$

where α' is half the exit aperture.

The overall length is [2]:

$$L = \frac{a(1 + \sin\theta_i \cos\theta_i)'}{\sin^2\theta_i} \tag{15}$$

And the entry aperture diameter in:

$$a = \frac{a'}{\sin\theta^i} \tag{16}$$

From Eqs. (16) and (1), the CPC matches the maximum theoretical concentration ratio. In the ideal 2D CPC design, the rays incident on the rim of the exit aperture are said to be at the boundaries of failure regions, which in 3D designs are realised for skew rays. A 3D CPC can be made from revolving the 2D profile (circular), by crossing two linear CPCs (square), or by more complex computation methods for specific geometries such as the rotationally asymmetrical compound parabolic concentrator [43].

In the 3D CPC (Fig. 6a, b), there is a 3-fold infinity of rays as opposed to the 2-fold infinity in the 2D design, and the rays outside the meridian sections can no longer be guaranteed accommodation in the same way as the 2D rays (because the light ray can now be skewed) and hence be reflected out of the CPC.

The linear dielectric-filled CPC can also be designed to account for the acceptance angle inside the dielectric due to refraction using:

$$\sin\theta_i\ (n - (2/n)) \quad \text{or} \quad \sin\theta_i'(1 - (2/n^2)) \tag{17}$$

From this equation, it is preferable to choose refractive materials with a refractive index greater than the square root of 2, but in the case of 3D, rays will still be lost. The dielectric-filled CPC takes advantage of TIR and increases the collecting angle for the same length as a reflective CPC. Thus, this gives the possibility of a higher acceptance angle or shortening of the CPC [2].

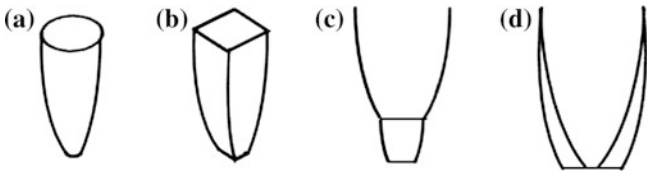

Fig. 6 Variations of CPC. **a** Revolved CPC. **b** Crossed CPC. **c** CCPC. **d** Lens-walled CPC

The CCPC (Fig. 6b) has been found to be an ideal concentrator for a half acceptance angle of 30° and outperforms the revolved CPC as a static solar concentrator at 3.6× concentration [44]. The square-apertured CCPC is also preferable due to its higher packing factor when arrayed side by side, and less PV material is wasted in manufacturing because of the efficiency of cutting square PV cells rather than circular ones. However, the CCPC, like the CPC, does not have a good output irradiance distribution for a flat receiver, and hot spots can reach 50× the energy of the incident rays [44]. The CCPC can be classed as a new type of secondary optic for HCPV systems, which requires further study.

In attempt to decrease the amount of material required in a CPC (the high length-to-width ratio) and hence decrease the weight and expense depending on the material used, the two-stage CPC [CCPC (see Fig. 6c)] is an option. The first stage is in the air with a regular reflective CPC; then, instead of a solar cell at the exit aperture, there is another transparent material filled CPC using TIR. Another method to decrease the length of the CPC is to use truncation, i.e., removing part of the entrance aperture end, which tends to a gradiant of 0. By doing so, there is little decrease in the concentration ratio with a sizeable decrease in the length. Truncation can increase the half acceptance angle of a CPC, but it also decreases the geometrical concentration ratio. The maximum concentration ratio can only be achieved by a full-height CPC without truncation [21]. Larger-opening angles can decrease wind-induced deviations, manufacturing tolerances, and sagging effects, whist through optimisation they can still yield high acceptance angles [36].

CPCs can absorb direct and diffuse solar radiation, and, as low concentration devices, their acceptance angle is much greater than that of high-concentration systems. Correspondingly, optical efficiency decreases slowly within the range of the acceptant angle the CPC is designed for, but it decreases rapidly beyond this range. The main disadvantage of the CPC is the very nonuniform irradiance distribution it outputs with a very high peak in the centre [20]. The lens-walled CPC (see Fig. 6d) is designed such that the the two parabolic curves of the 2D CPC profile are each rotated from the light-entry side to create a type of wedge shape with parabolic curves. The optical efficiency is lower than the original filled CPC or mirrored CPC, but the irradiance distribution is somewhat improved. The lens-walled CPC is also capable of higher acceptance angles [45]. One design of the lense-walled CPC reports $\sim$65 % optical efficiency at 0° incidence, which decreases slightly to $\sim$60 % at 20° from normal [45].

For an ideal CPC the exploitable part of the diffuse irradiance is 1/c but this contribution to a high concentrating system is negligible.

3.3 Light Funnels

Light funnels (light cones or homogenisers) all follow a funnel shape (Fig. 7) and are typically used in the same fashion as a funnel where their prime aim is to capture more stray light due to errors and redirect them toward the receiver. Light

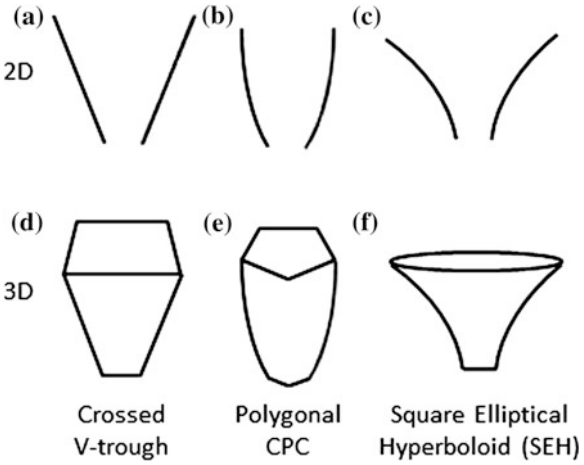

Fig. 7 Examples of 2D profiles and possible 3D transformations. **a** V-trough. **b** CPC. **c** Compound hyperbolic concentrator. **d** 3D square-apetured V-trough. **e** Polygonal apertured CPC. **f** Hyperboloid with an elliptical entry aperture and square-exit aperture

funnels can first be described by their 2D curves (Fig. 7a–c) where the side walls will be flat (V-trough), hyperbolic, or elliptical. However, the most popular cones are the CPC, as described previously, and simple V-shaped cones in order to save on manufacturing costs and decrease complexity. Further variations are possible when the 2D profile (V-shaped, CPC-shaped, or hyperbolic curved as shown in Fig. 7a–c) is translated into 3D where circular, square, or polygonal entry apertures can be realised (Fig. 7d–f). In this way we obtain the square-faced V-trough, the circular cone, the elliptical cone, and many more complex variations. Merged forms, including the circular-square cone, which has a circular entry merged with a square exit, are possible as well. Square solar cells are more common than circular, and hence square-exit faces are usually desired, but there are plenty of examples of circular cells with circular optics [42, 46].

At present, light funnels are all used in the same fashion in HCPVs which, as described, is to funnel light toward the receiver with the receiver being a solar cell, an array of solar cells, or possibly another type of low concentration optic that is attached to the solar cell(s) (specifically the two-stage CPC design and any variations would fit this description). In arrangements with an array of solar cells, the HCPV system will only work as efficiently as the lowest-performing cell. Hence, errors in irradiance distribution or tracking can severely limit the system's full potential. There is less risk of this happening with an accompanying optic or array of optics attached to the receiver.

The light cones are simple forms of nonimaging devices, some of which have been used for many years [2]. The advantage of these light cones is by far their simplicity yet effectiveness at increasing acceptance angle. They are not ideal optics; many of the light rays, even within a critical angle of incidence, can still be lost. In all of the designs there is a compromise between entry aperture width, which allows a greater acceptance of deviated rays, and slope or height of the walls. A smaller gradient in the walls results in smaller reflection angles, hence more

reflections and rays not meeting TIR criteria or reflecting backward out of the system. Similarly, if the height is increased to maintain the wall slope whilst increasing aperture width, then the ray will travel longer in the light funnel and incur a greater number of reflections resulting in the same problems.

The equation:

$$2y = (\pi/2) - \theta_1 \tag{18}$$

can be used to determine the length of a cone for a given entry aperture diameter, but some rays within θ_i can still be reflected out of the cone. The 2D V-trough is far from ideal as depicted by earlier literature [2]. The identification rays that are reflected out of axisymmetric cone shaped concentrators can be performed according to the procedure outlined by Winston et al. [2] for the CPC. The optical efficiency of a cone for rays within the acceptance angle is approximately 80 % with smaller-angled cones performing closer to ideal concentrators. A V-trough concentrator will have very high acceptance angles when its geometrical concentration ratio is <2 [47]. The crossed V-trough (inverted pyramid) and similar square-shaped light funnels are the simplest but most effective method to couple a circular primary optic with a square cell as well as homogenizing the irradiance distribution on the cell.

The square elliptical hyperboloid (SEH), which is based on the ideal trumpet concentrator, has recently been developed with an elliptical-entry aperture connected to a square-exit aperture by way of hyperbolic curves (Fig. 7f) [48]. A concentration ratio of 6× for the SEH is the optimum for use as a stationary solar concentrator despite its low optical efficiency of 55 %. The main use of this type of concentrator, however, is for building integrated PV applications, and its performance as a final-stage light funnel still has to be tested. The SEH designed for 4× concentration ratio has a greater optical efficiency of 68 % and may be more suited to HCPV optical systems.

One particular type of optic, which has no concentration effect and is purely for ensuring that rays travel toward the receiver, is the straight-forward light pipe or light rod. The light rays are focused onto the surface in the same way as in a light funnel, but the width of the entry aperture is not greater than that of the receiver. The light rod would be used in optical systems where it is beneficial to position the solar cell outside the optical system or not in the location of focused rays (cooling purposes). The light rod can transport the light rays to the cell and act as a homogeniser to distribute rays evenly. If we ignore this homogenising effect, which would improve the performance of the cell, then technically the acceptance angle would be the same as when the receiver was placed at the entry-aperture position of the light rod. For that reason, it cannot be called a light funnel or cone that directly improves the acceptance angle. Depending on the condition of the focusing light rays, it may only improve the irradiance distribution by a small factor and will somewhat decrease the optical efficiency due to absorption and if too many internal reflections are incurred. The light rod is hence the simplest method purely to reposition the cell.

4 Materials for HCPV Optics

A critical task in any concentrating optic design is identifying the best possible materials. Ideally a material would have high optical efficiencies (90–100 % reflection or transmittance), high thermal and ultraviolet (UV) tolerance, physical durability against environmental conditions, and overall economical to produce. In some systems using both a refractive element and a reflective element, both refractive and reflective issues must be addressed, but with careful design they may complement each other. For example, a secondary mirror optic may correct for primary lens aberrations as long as they are not severe. Generally, reflective materials are more cost-effective than refractive materials [10].

4.1 Refractive Optics

Glass can withstand high temperatures and is typically the best choice for high-quality accurate optics. Most plastic materials have less effective light-transmission properties compared with glass and tend to degrade with heat and UV exposure. Glass can be used over decades in some applications (regular maintenance, such as cleaning, is still required), whereas plastics typically last for only a few years [21]. The combination of strength, flexibility, and light weight, however, makes plastics more attractive with an overall aim to save money on capital and running costs (less-expensive solar tracker systems are required for lighter systems). Polymers—such as PMMA, which has a refractive index of 1.49 (very close to that of glass)—are often used in solar concentrators with good solar spectrum matching and resistances to ageing. PMMA remains thermally stable up to at least 80° [4] and is perhaps the most popular polymer used in CPVs. Polyethylene is used widely in other areas, such as a plastic film, but it has a short lifetime of only 1 year [21]. Polyamide, polystyrene, acrylics, and PC have been investigated (at least as covers for flat-plate collectors), but more research is required, especially regarding their durability. Durability is a topic that lacks data in many areas. Testing requires several years to pass, although some advanced weathering simulations are possible as is modelling. High levels of temperature, humidity, and solar radiation have, however, been proven to accelerate ageing with thermal effects proving most detrimental.

The properties of plastic films are dependent on the length of the polymer chain: Longer chains result in less brittle material. However, degradation due to heating, light exposure, oxidation, and mechanical breaking (scratches and repeated flexing) split these long polymer chains [21].

Fresnel lenses have traditionally been manufactured out of PMMA, which, due to the dispersion curve, makes shorter wavelengths converge faster than longer wavelengths and hence causes longitudinal chromatic aberration (LCA). Fresnel lenses may be manufactured by hot-embossing, casting, extruding, laminating, compression-moulding, or injection-moulding thermoplastic PMMA [49]. Optical

or mirror-grade PMMA material may come from the automotive, lighting, or skylight industries. Applicable formulations of optical-grade poly(dimethylsiloxane) (PDMS) material are shared with the aerospace, electronics, and light-emitting diode industries. A heavier lens technology consists of acrylic or silicone facets patterned on a glass superstate as researched in the late 1970s [50, 51]. PMMA and PDMS can be adhered to a glass superstate and patterned as a Fresnel lens. PC is sometimes suggested as an alternative to PMMA due to its significantly greater resilience, which prevents mechanical fracture and fatigue. However, PC has a smaller spectral bandwidth, less optical transmittance, and lower resistance to scratches [52]. It suffers more from optical dispersion, chromatic aberration, and solar-induced photo oxidation [53–56].

PMMA has a transmittance of $\sim$95 % and has a low glass-transition temperature meaning that high-temperature treatments, such as calcination, which is a preparation method of antireflective and antifogging coatings, cannot be used on PMMA material. Zhou et al. [57] successfully fabricated antifogging and antireflective coatings on Fresnel lenses by way of spin-assembling silica nanoparticles without any high-temperature posttreatments and reached a transmittance of 98.5 %. Super hydrophilic coatings (antifogging) can effectively prevent water condensation on transparent substrates, which can alter light concentration in CPV systems. Another way to achieve an antireflective property on PMMA (refractive index = 1.49) is to layer a single coating of refractive index 1.22. However, at present there are no bulk materials that possess such a low refractive index [57], but nanoporous coatings have voids leading to a lower refractive index and better antireflective properties [57].

As mentioned previously, the acceptance angle decreases with greater concentration ratios. To combat this trade-off between concentration ratio and half acceptance angle in CPCs, a large refractive index dielectric medium could be used to form the solid concentrator instead of the common mirror one. However, this increases the weight and amount of material required for manufacturing. The lens-walled CPC, which uses less material and thus decreases the weight, has a lower optical efficiency partly due to the low transmissivity of the lens material chosen for the lens-walled CPC and so could be improved with different materials.

Computer-controlled diamond turning machines, as well as other modern materials and molding techniques, have significantly improved the design and accuracy of refractive optics such as Fresnel lenses [24]. Similarly, computer-aided design and machining has improved the quality of reflective optics, but in both cases good-quality prototyping can be expensive when requiring smooth and accurate geometries.

4.2 Reflective Optics

Reflective concentrators do not suffer from selective wavelength absorption and dispersion associated with dielectric lenses. They use less material than any other equal concentration system because they are not filled with an optical material.

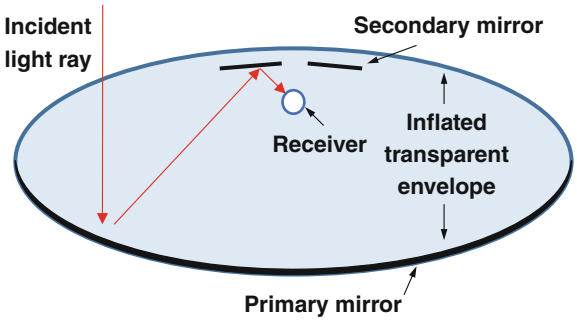

Fig. 8 Diagram of inflatable solar concentrator optics for solar thermal application. The primary mirror consisting of a silicone coated fiberglass fabric with an aluminum mirror layer [59]

They are, however, said to be more prone to manufacturing errors and are less tolerant to slope error than lenses.

In general, the optical efficiency of reflective concentrators is a coupled function of both the geometry and the mirror reflectivity. A common approximation for the effect of reflectivity on optical efficiency follows from the pioneering work of Rabl [58].

Polymer mirror films can be used as a low-cost option for reflective surfaces and have low weight and costs compared with a curved glass or polished aluminium mirror. They are, however, difficult to apply, especially to 3D shapes, and if not properly applied will not replicate the intended curve or line intended.

V-trough concentrators are one of the easiest-constructed of all low-concentrating systems: They can be fabricated from a single aluminium sheet. Bader et al. [59] attempted to lower the manufacturing costs of solar concentrators by investigating the use of pneumatic polymer mirrors. By applying slight pressure over an inflatable elastic enclosure, two opposing cylindrical curved surfaces were obtained. These encompassed a transparent foil on one side and a silicone coated fibreglass fabric with an aluminium mirror sheet on the other side as shown in Fig. 8.

Wind-induced vibrations were eliminated due to the use of a concrete structure, which is more rigid and stronger than conventional metallic frames. Self-cleaning scratch-resistant foils were applied easily, and the high-quality mirror foils were well protected from the environment. There is a high potential for a cost decrease due to the cheaper and lightweight materials, which can also be easily transported. The concrete structure would be built on site. The cylindrically shaped optics, which suffer from optical aberration, were corrected somewhat with the use of a tailor-made secondary specular reflector incorporated in tandem with the primary cylindrical mirror. However, the resulting prototype was only suitable for thermal receivers, but it shows the variance of materials possible and how they may be used to reach high solar concentrations.

Parabolic reflectors designed for high concentrations in particular can be costly to build on such a large scale. They require stronger structures and more expensive solar trackers due to their weight and high accuracy requirement. A silvered mirror using smooth glass produces a common mirror with reflectivity >85 %. The smooth glass is covered from the back and sealed with an oxidation layer. These types of mirrors are only applicable as flat reflectors. Curves—such as the parabolae, hyperbolae, ellipse, or circular—are extremely difficult and hence costly to manufacture with accuracy. Manufacturing processes used include precise grinding, milling, polishing, and a variety of coating methods for a mirror finish. Flab et al. have manufactured a mirror with a reflectivity >94 %, which is successfully being used in Colorado [19].

Jagoo et al. constructed a very low cost parabolic dish with basic tools using wood, cement, silicone paste, and fibreglass [19]. A chrome polymer reflector with an adhesive back was used for this application. It had the advantages of high weathering durability, and the system reflected 82 % of the incident sunlight. Fiberglass is cheap, impermeable, and easy to use and mould.

Alanod is a reflective thin film comprised entirely of aluminium that has a total reflectivity of 95 %. Samples coated with a polymeric chemical to protect the alumina layer can survive for a few years. ReflecTech mirror film is a polymer-based film for concentrating sunlight in solar energy arrays. The film has an overall reflectivity of 94 % and is immune to water and UV radiation.

5 Conclusion

High-concentration optics for PV applications require all types of optics including low-concentration and nonconcentration devices. As the geometric concentration ratio is increased, the acceptance angle is decreased and errors in alignment, manufacturing, reflectivity, and refraction are more noticeable. The use of smaller optics to replicate a high-concentrating optic is becoming more popular as a means to achieve high optical efficiency as well as high irradiance uniformity on the receiver. Receiver optics are essential to increase the acceptance angle, and an array of possible optics have been outlined herein. The Fresnel lens and parabolic dish maintain the most popular form of high-concentrating optic for PV applications. A variety of possible materials has been given for both reflective and refractive optics along with manufacturing methods. Depending on the constraints of a project, different concentrator types, geometries, materials, and manufacturing methods will be chosen as optimum, but tailoring a design to an application is always important, especially for high-concentration optics for PV applications. This chapter provided many options for concentrator design and manufacturing and explains the basic optical behaviour and materials used today.

References

1. Chemisana D, Mallick T (2014) Building integrated concentrated solar systems. In: Enteria N, Akbarzadeh A (eds) Solar energy sciences and engineering applications, 1st edn. CRC Press, pp 545–788
2. Winston R, Miñano JC, Benitez P (2005) Nonimaging optics. Elsevier, London
3. Murphree QC (2001) A point focusing double parabolic trough concentrator. Solar Energy 70 (2):85–94
4. Xie WT, Dai YJ, Wang RZ, Sumathy K (2011) Concentrated solar energy applications using fresnel lenses: a review. Renew Sustain Energy Rev 15(6):2588–2606
5. Luque A, Andreev VM (2007) Concentrator photovoltaics. Springer, Berlin
6. Chaves J (2008) Introduction to nonimaging optics. CRC Press, Boca Raton
7. Goldstein A, Gordon JM (2010) Double-tailored nonimaging reflector optics for maximum-performance solar concentration. J Opt Soc Am A Opt Image Sci Vis 27 (9):1977–1984
8. Fraas LM (2014) Low-cost solar electric power. Springer International Publishing, Cham
9. Sangster AJ (2014) Electromagnetic foundations of solar radiation collection. Green energy and technology. Springer International Publishing, Cham
10. Chen YT, Ho TH (2013) Design method of non-imaging secondary (NIS) for CPV usage. Solar Energy 93:32–42
11. Nilsson J, Leutz R, Karlsson B (2007) Micro-structured reflector surfaces for a stationary asymmetric parabolic solar concentrator. Solar Energy Mater Solar Cells 91(6):525–533
12. Winston R, Miñano JC, Bentez P, Shatz N, Bortz JC (2005) Nonimaging optics. Elsevier, Melbourne
13. Dreger M, Wiesenfarth M, Kisser A, Schmid T, Bett AW (2014) Development and investigation of a CPV module with cassegrain mirror optics. In: CPV-10
14. Goldstein A, Gordon JM (2011) Tailored solar optics for maximal optical tolerance and concentration. Solar Energy Mater Solar Cells 95(2):624–629
15. Julio Chaves. Introduction to Nonimaging OpticsÂ (Google eBook). CRC Press, 2008
16. Goldstein A, Gordon JM (2011) Tailored solar optics for maximal optical tolerance and concentration. Solar Energy Mater Solar Cells 95(2):624–629
17. Akisawa A, Hiramatsu M, Ozaki K (2012) Design of dome-shaped non-imaging fresnel lenses taking chromatic aberration into account. Solar Energy 86(3):877–885
18. Yamdt MD, Cook JPD, Hinzer K, Schriemer H (2014) Optical channel variability and acceptance angle in CPV modules studied by active I-V response. In: CPV-10
19. Jagoo Z (2013) Tracking solar concentrators. Springer, The Netherlands
20. Victoria M, Domnguez C, Antón I, Sala G (2009) Comparative analysis of different secondary optical elements for aspheric primary lenses. Opt Express 17(8):6487–6492
21. Norton B (2014) Harnessing solar heat, volume 18 of lecture notes in energy. Springer, Netherlands
22. Wilson RN (2004) Reflecting telescope optics I. Springer, Berlin
23. Miller DC, Kurtz SR (2011) Durability of fresnel lenses: a review specific to the concentrating photovoltaic application. Solar Energy Mater Solar Cells 95(8):2037–2068
24. Leutz R, Suzuki A (2001) Nonimaging fresnel lenses: design and performance of solar concentrators. Springer, New York
25. Yeh N (2010) Analysis of spectrum distribution and optical losses under fresnel lenses. Renew Sustain Energy Rev 14(9):2926–2935
26. Luque A, Hegedus S (2003) Handbook of photovoltaic science. Wiley, England
27. Silvi C (2009) The pioneering work on linear fresnel reflector concentrators (LFC's) in Italy. In: Solarpaces conference. Italian Group for the History of Solar Energy (GSES)
28. Zanganeh G, Bader R, Pedretti A, Pedretti M, Steinfeld A (2012) A solar dish concentrator based on ellipsoidal polyester membrane facets. Solar Energy 86(1):40–47

29. Tromholt T, Katz EA, Hirsch B, Vossier A, Krebs FC (2010) Effects of concentrated sunlight on organic photovoltaics. Appl Phys Lett 96(7):073501
30. Languy F, Fleury K, Lenaerts C, Loicq J, Regaert D, Thibert T, Habraken S (2011) Flat fresnel doublets made of PMMA and PC: combining low cost production and very high concentration ratio for CPV. Opt Express 19(3):A280–94
31. Languy F, Habraken S (2013) Nonimaging achromatic shaped fresnel lenses for ultrahigh solar concentration. Opt Lett 38(10):1730–1732
32. González JC (2009) Design and analysis of a curved cylindrical fresnel lens that produces high irradiance uniformity on the solar cell. Appl Opt 48(11):2127–2132
33. Leutz R, Suzuki A, Akisawa A, Kashiwagi T (1999) Design of nonimaging fresnel lens for solar concentrators. Solar Energy 65:379
34. Kritchman EM, Friesem AA, Yekutieli G (1979) Highly concentrating fresnel lenses. Appl opt 18:2688–2695
35. Zhuang Z, Yu F (2014) Optimization design of hybrid fresnel-based concentrator for generating uniformity irradiance with the broad solar spectrum. Opt Laser Technol 60:27–33
36. Canavarro D, Chaves J, Collares-Pereira M (2013) New second-stage concentrators (XX SMS) for parabolic primaries; comparison with conventional parabolic trough concentrators. Solar Energy 92:98–105
37. Palavras I, Bakos GC (2006) Development of a low-cost dish solar concentrator and its application in zeolite desorption. Renew Energy 31(15):2422–2431
38. Baig H, Heasman KC, Mallick TK (2012) Non-uniform illumination in concentrating solar cells. Renew Sustain Energy Rev 16(8)5890–5909
39. Shanks K, Sarmah N, Mallick TK (2013) The design and optical optimisation of a two stage reflecting high concentrating photovoltaic module using ray trace modelling. In: PVSAT-9
40. Abbas R, Muñoz Antón J, Valdés M, Martnez-Val JM (2013) High concentration linear Fresnel reflectors. Energy Convers Manage 72:60–68
41. Morin G, Dersch J, Platzer W, Eck M, Häberle A (2012) Comparison of linear fresnel and parabolic trough collector power plants. Solar Energy 86(1)1–12
42. Jaus J, Peharz G, Gombert A, Pablo J, Rodriguez F, Dimroth F, Eltermann F, Wolf O, Passig M, Siefer G, Hakenjos A, Riesen S, Bett AW (2009) Development of flatcon modules using secondary optics. IEEE, pp 1931–1936
43. Abu-Bakar SH, Muhammad-Sukki F, Ramirez-Iniguez R, Mallick TK, Munir AB, Yasin SHM, Rahim RA (2014) Rotationally asymmetrical compound parabolic concentrator for concentrating photovoltaic applications. Appl Energy 136:363–372
44. Sellami N, Mallick TK (2013) Optical efficiency study of PV crossed compound parabolic concentrator. Appl Energy 102:868–876
45. Guiqiang L, Gang P, Yuehong S, Jie J, Riffat SB (2013) Experiment and simulation study on the flux distribution of lens-walled compound parabolic concentrator compared with mirror compound parabolic concentrator. Energy 58:398–403
46. Andreev V, Ionova E (2003) Concentrator PV modules of "all-glass" design with modified structure. In: Proceedings of 3rd world conference on photovoltaic energy conversion, 2003
47. Tang R, Liu X (2011) Optical performance and design optimization of V-trough concentrators for photovoltaic applications. Solar Energy 85(9):2154–2166
48. Sellami S, Mallick TK (2013) Optical characterisation and optimisation of a static window integrated concentrating photovoltaic system. Solar Energy 91:273–282
49. Leutz R, Fu L, Annen HP (2009) Stress in large-area optics for solar concentrators. In Dhere NG, Wohlgemuth JH, Ton DT (eds) SPIE Solar Energy + Technology. International society for optics and photonics, pp 741206–741206–7
50. Egger JR (1979) Manufacturing fresnel lens master tooling for solar photovoltiac concentrators
51. Lorenzo E, Sala G (1979) Hybrid silicone-glass Fresnel lens as concentrator for photovoltaic applications. In: Proceedings of the silver jubilee congress 1:536–539
52. Miller DC, Kempe MD, Kennedy CE, Kurtz SR (2009) Analysis of transmitted optical spectrum enabling accelerated testing of CPV designs preprint. In: SPIE
53. John E Greivenkamp. *Field Guide to Geometrical Optics*. 2004

54. Kasarova SN, Sultanova NG, Ivanov CD, Nikolov ID (2007) Analysis of the dispersion of optical plastic materials. Opt Mater 29(11):1481–1490
55. Andrady A (1997) Wavelength sensitivity in polymer photodegradation. Polymer 128:47–94
56. Andrady AL, Hamid SH, Hu X, Torikai A (1998) Effects of increased solar ultraviolet radiation on materials. J Photochem Photobiol B Biol 46:96–103
57. Zhou G, He J, Ligang X (2013) Antifogging antireflective coatings on fresnel lenses by integrating solid and mesoporous silica nanoparticles. Microporous Mesoporous Mater 176:41–47
58. Rabl A (1976) Comparison of solar concentrators. Solar Energy 18(2):93–111
59. Bader R, Haueter P, Pedretti A, Steinfeld A (2009) Optical design of a novel two-stage solar trough concentrator based on pneumatic polymeric structures. J Solar Energy Eng 131 (3):031007

[Article 8]

N. Sarmah, K. Shank, L. Micheli, K. S. Reddy, and K. M. Tapas, “Design and Optical Performance Analysis of a Reflective Type High Concentrating Photovoltaic System,” in *9th International Conference on Concentrator Photovoltaic Systems (CPV-9)*, 2013.

Design and Optical Performance Analysis of a Reflective Type High Concentrating Photovoltaic System

Nabin Sarmah[1], Katie Shank[1], Leonardo Micheli[1], K. S. Reddy[2], Tapas K Mallick[1*]

[1]*Environment and Sustainability institute, University of Exeter, Cornwall campus, Penryn, Cornwall, EH10 9EZ, United Kingdom*
[2]*Heat Transfer and Thermal Power Laboratory, Department of Mechanical Engineering IIT Madras, Chennai – 600036, India*

**Corresponding author: email: t.k.mallick@exeter.ac.uk; Tel: +441326259465*

Abstract: High concentrating photovoltaic system can enhance the commercial deployment of the PV technologies with higher solar energy to electrical conversion efficiency. A high concentrating set-up with 500× concentration ratio has been designed and optical simulation has been carried out for system optimisation. Simulation study results an optical efficiency of 76.7% with a well distributed energy flux at the receiver within the uniformity of ± 13%.

Keywords: HCPV, ray-tracing, optical simulation
PACS: 42.79.Ek, 88.40.hj

INTRODUCTION

Concentrating photovoltaic (CPV) is the only technology in power generation which aims to achieve over 50% efficiency in coming years. Compared to the commercial flat plat modules CPV can reduce by increasing the overall system efficiency and by reducing the area of expensive solar cell material. The use of high efficiency multijunction solar cell (~43%) in a concentrating system results the higher system efficiency compared to the flat plate PV system [1]. Many high concentrating designs for solar energy applications have been designed and commercialised so far [2,3], however an optimum concentrator design with high optical efficiency is required to increase the overall system efficiency and to reduce the over cost of the unit power output. The refractive (lens based) and reflective type (such as mirror based) system have disadvantages of lower optical efficiencies due to the fuzziness at the receiver and optical losses. The non-uniform distribution of the concentrated light at the receiver is another major challenge for the CPV research community.

Another challenge of the high concentrating CPV system is the cost effective cooling system to maintain low operating temperature of the solar cell. High operating temperature of the solar cell can drastically reduce the power output the solar cell [4]. So a well designed high concentrating system with passive cooling can result in enhancing its system performance.

In this work a CPV system of concentration ratio of 500× has been designed to increase the overall system performance. The designed concentrating system has been optimised for higher optical efficiency and uniform distribution of energy flux.

DESIGN OF THE CPV SYSTEM

The complete CPV system design uses array of specially designed parabolic reflector for each solar cell with a secondary reflector. The dimension of each solar cell is 10mm × 10mm. The schematic design concept of the concentrating system with a primary concentrator and secondary reflector is shown in figure.1. The primary concentrator is a parabolic dish with a square shape aperture opening to create a square shaped image of the sun. This design in expected to reduce the optical losses by concentrating all the incoming solar irradiance on the solar cell. A

secondary reflector is used to guide the concentrated light to the solar cell on the base plate and to attain homogeneous distribution of light at the receiver. The reason to opt this design with the secondary reflector is to use a novel passive cooling system with micro- and nano-fin structure at the bottom plate with a large area heat-dissipation.

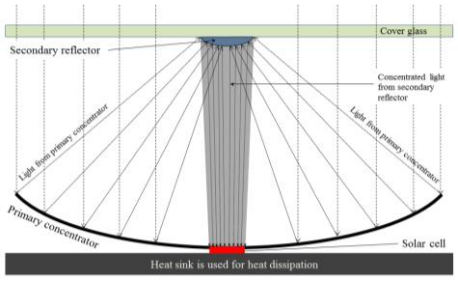

FIGURE 1. A schematic diagram of the CPV system with primary concentrator and secondary reflector.

The design parameters of the primary concentrator have been chosen considering the required concentration ratio, rim angle and the size of secondary concentrator (figure.2 (a)). The receiver area of the system (for one solar cell, located at the centre of the primary) is considered as 11mm × 11mm, to fit the solar cell of dimension 10mm × 10mm. In this study the dimension of the solar cell is termed as active receiver area and all the analysis has been carried out for active receiver area.

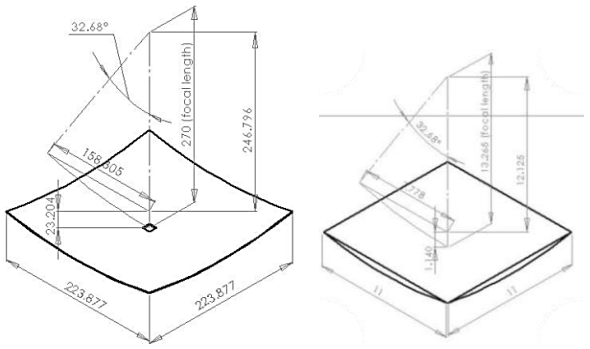

(a) (b)

FIGURE 2. Dimension and design specifications of (a) primary concentrator (b) secondary reflector.

For the secondary reflector design a study has been carried out with different designs and based on the design parameters an inverse parabolic secondary reflector has been designed. The initial study for the optimization of the design parameter of the primary concentrator and the secondary reflector has been carried out considering the total energy collected at the receiver, which is represented by the average irradiance in the figure 3.

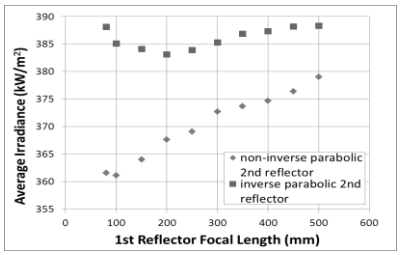

FIGURE 3. Variation of average irradiance (at the receiver) with the focal length of the primary concentrator.

It is observed that the inverse parabola has better properties to collect concentrated light as a secondary reflector compared to the conventional dish type parabolic secondary reflector. In case of inverse parabolic design the average irradiance at the receiver is found to be decreasing initially with the increase in focal length of the primary concentrator. However beyond 200mm, the average irradiance increases for higher focal length of the primary concentrator, until 450mm and stabilises. With this basic initial study the inverse parabolic reflector has been considered for further optical simulation and analysis. The design specification has been optimized with the further analysis on the basis of energy flux distribution at the receiver. The design specifications and dimensions of the primary concentrator and secondary reflector is shown in figure 2 (b).

OPTIAL SIMULATION FOR DESIGN OPTIMISATION

A systematic analysis of the energy flux distribution at the receiver of the concentrating system has been carried out using a ray tracing software 'OptisWorks' for optimization of the system.

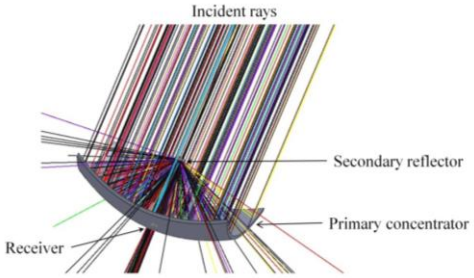

FIGURE 4. A representation ray trace diagram with 100 rays for the CPV system.

The concentrator parameters has been optimised with an detailed optical performance analysis with the variation of the focal length of the primary concentrator and secondary reflector, separation of the primary and secondary reflector and the rim angle of the system. A representation ray trace diagram with 100 incident rays is shown in figure.4.

The 3D optical simulation results show a maximum optical efficiency of 77.4%, considering all the possible losses with the real case scenario and manufacturing errors in the system. The study with the variation of the primary concentrator focal length the optical efficiency varies due to the escaping of light from the system or because of the light concentrating outside the active receiver area. The detail of energy flux distribution at the receiver is discussed in the following section. It is found that the optical efficiency of the system is lowest with the primary reflector of focal length 200mm as shown in figure.5. This drop in optical efficiency is mainly because of the sharp intensity peaks outside the active receiver area. However the variation of optical efficiency is within 77.4% to 76.4% for the change in focal length of the primary concentrator from 75mm to 450mm.

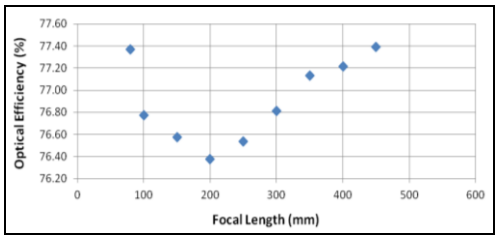

FIGURE 5. Variation of optical efficiency with the focal length of the primary concentrator.

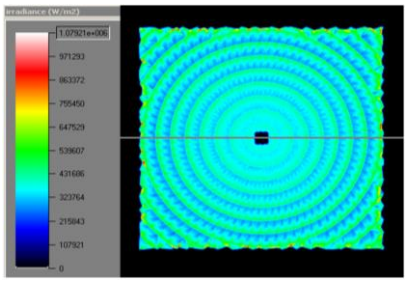

FIGURE 6. Energy flux distribution contour at the receiver of the CPV system for the primary concentrator with foal length 200mm.

The energy flux distribution at the active receiver area has been investigated for optimization of the parameters for primary concentrator and secondary reflector. It is observed that the energy flux at the receiver varies significantly with the change in focal length of the primary concentrator. The study for the energy flux distribution at the active receiver area has been carried out for the range of focal length of the primary concentrator from 75mm to 450mm. It found that, for the primary concentrator of focal length 200mm, the energy flux distribution is within ± 20% excluding the sharp intensity peak at the edges of the receiver. The energy flux distribution at the receiver with 200mm focal length of the primary concentrator is shown in figure.6.

With the increase in focal length of the primary concentrator the energy flux distribution changes significantly, resulting the distribution within ± 13% for the focal length 270mm. This also excludes some high peaks on the solar cell which is ~630kW/m^2. The energy flux distribution at the receiver of the CPV system with the primary concentrator of focal length 270mm is shown in figure.7.

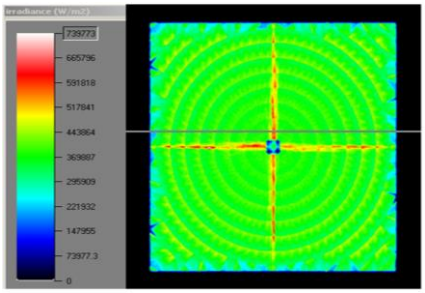

FIGURE 7. Energy flux distribution contour at the receiver of the CPV system for the primary concentrator with foal length 270mm and

Onsidering the optical efficiency and energy fux distribution at the active receier areas of the system, the primary conentrator with the focal length 270mm is found to be the optimum for this system. However during the optmisation study the parameters of the secondary reflector needed to be changed and the optimum focal length for the seondary reflector is found to be 13.27mm.

ASSOCIATED UNCERTAINITY AND TOLERANCE

There are uncertianities associated with the performance of the CPV system effected by the other parameters. Such unceertainities includes the tracking error and the dirversion of the solar irradiance. Proper analysis of the effect of these parameters will help in better desiging of the CPV system to achieve higher optical efficiency.

Effect of Diversion of Solar Irradiance

Although the optimum design has been found for incoming parallel light, natural sunlight has a divergence of ±0.27°. By changing the lambertian light source to have a half limit angle of 0.27° instead of 0° which was used to produce parallel light, irradiance results were obtained for naturally diverging light. This effect dropped the optical efficiency of the significantly to 4%. A further optimisation of the design parameters has been carried out to achieve an optical efficiency higher than 80% with the non-uniformity of energy flux distribution within ± 15%. The optimization study with the similar process mentioned above has been carried out by varying dimension of the secondary reflector and the focal length. This also results in increase in the dimension of the primary concentrator. The assembly of modified primary concentrator and secondary reflector and their specifications is shown in figure.8. The modified optimum assembly achieves an optical efficiency of 86.02% with an insignificant compromise in energy flux distribution at the receiver.

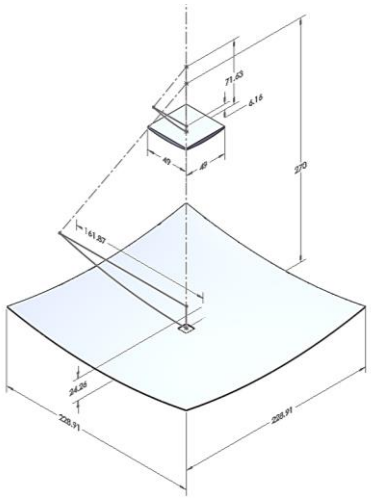

FIGURE 8. Assembly specifications and dimensions of the primary concentrator and secondary reflector after modification for uncertainties.

Effect of Tracking Error

In a efficient high concentrating system the tracking error should be limited to ± 0.1˚ [5]. This enables to deliver approximately 90% of the rated power output. Optical efficiency study shows that the with the designed CPV system, ± 0.1˚ error in tracking can lead to 26.7% drop in optical efficiency (figure.9). A further design modification is needed to deal with the tracking error of higher degrees.

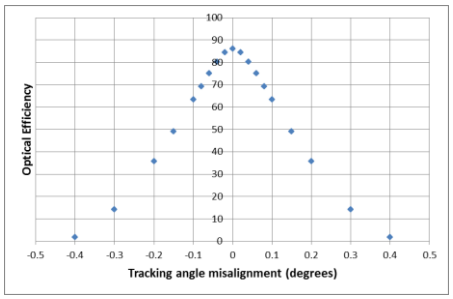

FIGURE 9. Variation of optical efficiency with tracking error.

CONCLUSION

A high concentrating reflective type CPV system has been designed and optical performance has been carried out for design optimisation. Simulation study results a maximum optical efficiency of 77.4% with the initial design considerations. However, optimum design with ideal case scenario results 76.7% with a well distributed energy flux at the receiver within the uniformity of ± 13%. Uncertainty with the real case scenario leads to further modification design parameters, which result in increase in optical efficiency to 86.02% with a compromise in energy flux distribution at the receiver.

ACKNOWLEDGMENTS

This work has been carried out as a part of BioCPV project jointly funded by DST, India *(Ref No: **DST/SEED/INDO-UK/002/2011**)* and EPSRC, UK, *(Ref No:* **EP/J000345/1***)*. Authors acknowledge both the funding agencies for the support.

REFERENCES

1. M. A. Green, K. Emery, Y. Hishikawa, W. Warta and E. D. Dunlop, Prog. Photovolt: Res. Appl., 21: 1–11 (2013)
2. A. Goldstein and J. M. Solar Energy Materials and Solar Cells, 95: 624–629 (2011).
3. M. Li, X. Ji, G. L. Li, Z. M. Yang, S. X. Wei, L.L. Wang, Solar Energy: 85, 1028–1034 (2011).
4. A. Royne, C. J. Dey, D. R. Mills, Solar Energy Materials and Solar Cells, 86: 451-483 (2005).
5. B. M. Davis, T. Williams, M. Martínez, D. Sanchéz "Understanding Tracker Accuracy and its Effects on CPV", International Conference on Solar Concentrators 5: 16-19 November 2008, Palm Desert, CA.

[Article 9]

K. Shanks, N. Sarmah, and T. K. Mallick, “The Design and Optical Optimisation of a Two stage Reflecting High Concentrating Photovoltaic Module using Ray Trace Modelling,” in *PVSAT-9*, 2013, pp. 4–7.

The Design and Optical Optimisation of a Two stage Reflecting High Concentrating Photovoltaic Module using Ray Trace Modelling

Katie Shanks*, Nabin Sarmah and Tapas K Mallick
School of Engineering & Physical Sciences
Heriot-Watt University; Riccarton; EH14 4AS; UK

*Corresponding author: email: kmas1@hw.ac.uk, T: +44(0)7824558670

Abstract

The design and optical optimisation of a 500 suns concentrating photovoltaic system (CPV) to use with a high efficiency 10mm x 10mm multi-junction solar cell is presented. The advantage of using a multi-junction solar cell is the higher electrical conversion efficiency, which enhances the harvesting of the solar energy compared to that of a non-concentrating flat plate PV system. In this study, a concentrating system with a semi-parabolic dish is designed to use with a secondary parabolic reflector. It was found that increasing the radius and focal length of both reflectors improved optical efficiency and an inverse parabolic design of the secondary reflector is more advantageous than a non-inverse design. Results were obtained first for the case of a parallel light source and then with the introduction of practical uncertainties such as diverging light, misalignment, off focus and tracking error effects. Initial parallel light results gave an optimised optical efficiency of 76.63% from a source set to 1000 W/m^2 irradiance. Considering ±0.27° divergence of solar irradiance resulted in an optimised optical efficiency of 86.02% but at the cost of less uniform flux distribution upon the receiver. An absolute uncertainty of ±12.68% due to manufacturing and solar tracking error was also calculated.

Introduction:

The photovoltaic is a promising renewable energy technology but with a disadvantage of higher cost per unit energy output compared to that of conventional energy sources. Common commercially available flat plate solar modules have a maximum efficiency of ~23% [1] and although this value is increasing with the use of multi-junction solar cells which can reach up to ~40% efficiency, the cost of such photovoltaic material is expensive [1]. Thus a payback period of ~15 years or longer depending on the location is expected regardless of the conversion efficiency of the solar cell used. Concentration Photovoltaics can increase system efficiency without needing large quantities of expensive material for multi-junction solar cells and is also an effective method to lessen the demand on the silicon market [2]. There have been many proposed concentrator designs [3-5], however better concentrator system design and detailed research into the accuracy is required in the optics of solar systems, including error analysis of such designs to optimise for the highest efficiency in practical operation. Alexis Vossier et al. [6] proposed next generation 4-6 junction cells should be operated at ultrahigh concentration in order to lower CPV electricity costs. This will require optical optimisation to ensure uniform irradiance upon the intended PV material and avoid hot-spot heating which has been proven to cause irreversible destruction of the solar cell structure [7].
This study has been undertaken to design an optimised solar concentrator through the use of detailed ray trace modelling and analysis.

Concentrator Design Concept:

The proposed concentrator design employs the use of a primary parabolic collector and a smaller secondary parabolic reflector, both with co-incident focal points shown in Figure 1.

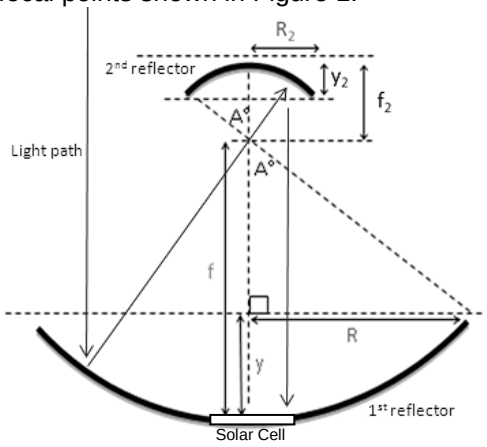

Figure 1: Theoretical focusing of parallel incident light using parabolic reflectors.

Angle A is the maximum angle light can make with the central axis after reflection

from the primary reflector and so should be the minimum angle of the secondary reflector to ensure no light loss. The light hence received at the 10mm x 10mm solar cell placed in the base of the primary reflector will receive a uniform irradiance distribution where the concentration level depends on the open face area of the primary reflector.

Design Method and Calculations:

By limiting the secondary reflector open face area to that of the 11mm x 11mm receiver space made in the primary reflector base for the solar cell, shadowing effects were eliminated for the case of parallel incident light. Both parabolic reflectors were cut to square faces to reduce the optical losses in a square shaped solar cell. The radius of the secondary reflector was hence calculated to be 7.78mm. The required radius of the primary reflector to reach a concentration of 500 suns was calculated to be 158.31mm. Due to the relationship formed between both reflectors when angle A is kept equal as shown in Figure 1, the focal length of the secondary reflector is 0.049 times the focal length of the primary reflector.

Optical simulations were carried out following these restrictions for varying focal lengths of the primary reflector and for an inverse and non-inverse parabolic design for the secondary reflector.

Ideal Case Scenario Results:

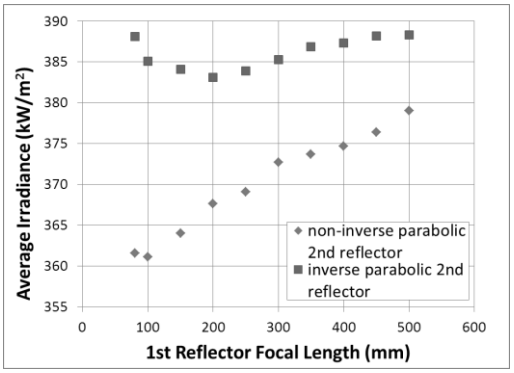

Figure 2: Recieved average irradiance at 10mm x10mm active area of solar cell.

The inverse parabolic reflector design was chosen to be more advantagous than the non-inverse parabolic design for the secondary reflector due to higher average irradiance levels, hence higher optical efficiencies, and a smaller system size as the focal point is located outside the system as shown in Figure 3.

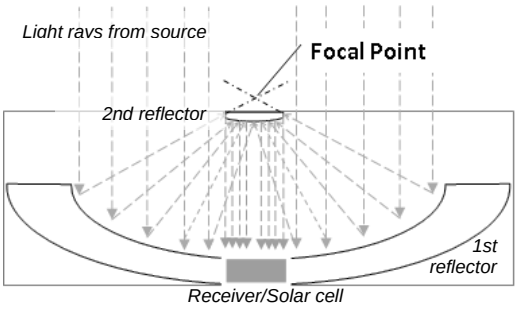

Figure 3: System Set-up for Inverse parabolic secondary reflector design.

Irradiance peaks were found to form along the x=0 and y=0 of the irradiance distribution for the inverse parabolic reflector. For the non-inverse parabolic reflector these peaks formed on the boundary of the distribution which was not included in 10mm x10mm active cell area. Hence received irradiance was higher for the inverse rather than non-inverse secondary reflector design. These peaks were found for focal lengths of 200 mm and above for the primary reflector. As the primary reflector focal length as increased, the x=0 and y=0 irradiance peaks increased whilst the remaning area of irradiance decreased and unified. These irradiance peaks are potential hot-spot risks. The optimum irradiance distribution was found for a primary reflector focal length of 270 mm with an optical efficiency of 76.63% (Figure 4).

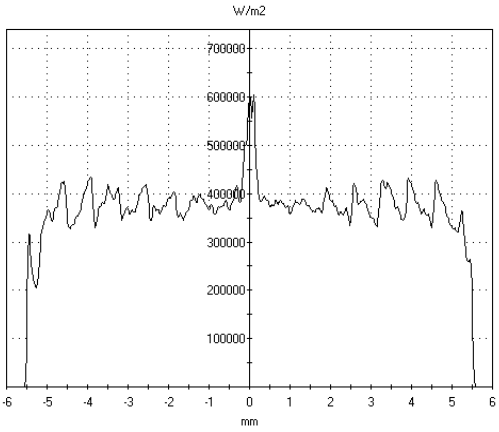

Figure 4: Irradiance line profile for inverse parabolic secondary reflector and primary reflector focal length of 270 mm.

Simulating Practical Uncertainties:

Considering the natural divergence of solar light, ±0.27°, the simulated light rays diverged after reflecting from the secondary reflector so as they were not directly incident upon the solar cell which resulted in an optical efficiency drop to ~4%. Deliberate vertical separation of the

focal points of the two reflectors did not compensate for this divergence as expected due to the small radius and focal length of the secondary reflector. The second reflector radius was investigated and an increase in radius was found to allow a higher degree of convergence and hence a higher optical efficiency as shown in Figure 5.

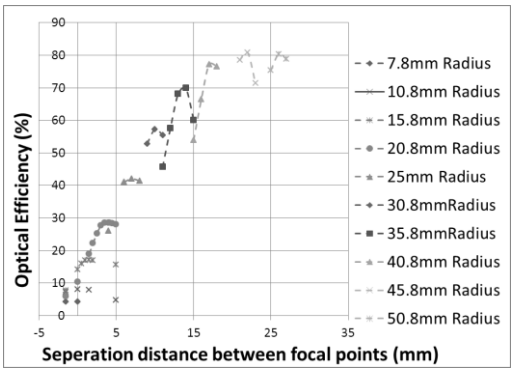

Figure 5: Effect of increasing second reflector radius.

The increase in optical efficiency was due to the increased focusing of the irradiance distribution upon the solar cell which, due to the solar light divergence, was Gaussian in shape. For uniform irradiance distribution a second reflector radius of 30mm was found to be most effective but had an optical efficiency of 55%. As the radius was increased, less of the cell active area was illuminated and so a compromise had to be made between high optical efficiency and uniform irradiance distribution. A radius of 42mm for the secondary reflector was chosen as optimum, with a positive focal point separation distance of 18.5mm and a first reflector radius of 228.91 mm to maintain 500 suns concentration. An optical efficiency of 86.02% was obtained and an irradiance distribution shown in Figure 6.

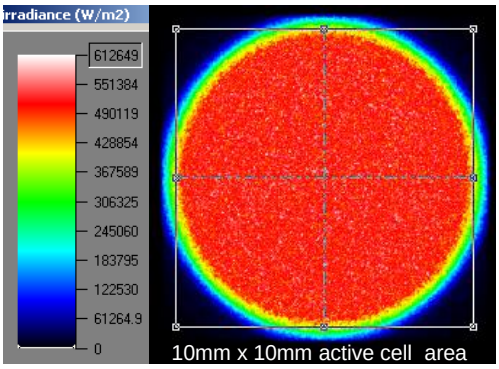

Figure 6: Irradiance distribution at the solar cell due to a secondary reflector radius of 42 mm.

The lack of irradiance at each corner of the solar cell active area could degrade the performance of the solar cell but further practical testing is required.

Solar Tracking Uncertainty:

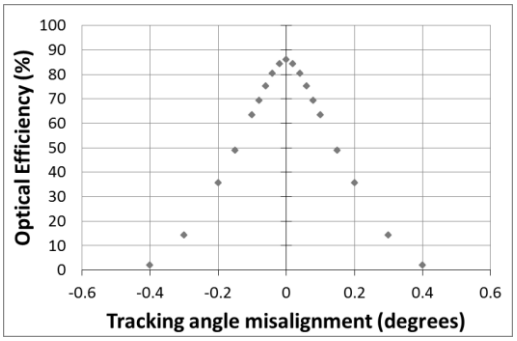

Figure 7: Simulated effect of tracking error in both axes.

Due to the symmetry of the design the tracking inaccuracy effect, as shown in Figure 7, was mirrored on all sides and decreased with increasing offset tracking angle. In typical high concentration systems tracking accuracy must be in the ± 0.1° range to deliver approximately 90% of the rated power output. [8-10] A tracking variation of 0.1°-0.2° from the median is common although dependent on degree of alignment, tuning and calibration of the tracking system. [10] The proposed system requires an increased degree of tracking accuracy of ±0.06° to lower the absolute error range in optical efficiency to ±10.90%.

Manufacturing Uncertainty:

The positioning error in the secondary reflector with respects to the primary reflector can be described in the horizontal and vertical separation distance between the focal points of both reflectors. An alteration in vertical separation from the optimum 18.5mm between the two reflectors resulted in a decrease in optical efficiency due to the irradiance distribution spreading out. Assuming a manufacturing positioning accuracy of ±0.1mm, the optical efficiency will vary by ±0.69% (absolute value).

An error in the horizontal positioning of the secondary reflector had a similar effect to the solar tracking inaccuracy where the irradiance distribution would be moved across the cell area in the opposite direction of the implemented error. Assuming again an accuracy of ±0.1mm resulted in an absolute optical efficiency error of ±1.09%.

Overall System Uncertainty:

The combination of errors is difficult to ascertain theoretically especially with sources of error not considered such as the final module enclosures glass cover reflectance, temperature variation within the enclosure, weather variation, time of day and site location. The direct addition of the uncertainties was employed to maximise uncertainty predictions and compensate for errors not considered, although the errors detailed earlier could compensate for each other if in the appropriate directions. A total uncertainty range of 12.68% was calculated for the optical efficiency of the optimised design considering solar divergence.

Conclusion

An optimised optical efficiency of (86.02 ± 12.68) % was found for the proposed two stage reflecting high concentrating photovoltaic module using ray trace modelling. The design will require a higher degree of manufacturing and tracking accuracy due to the use of two parabolic reflectors. Any theoretical optical modelling carried out for solar concentrator systems should always consider ±0.27° diverging light conditions due to the large difference in results for parallel light. Parabolic reflectors of large radiuses are desirable as the results obtained here suggest they greatly improve light manipulation control and so can obtain higher optical efficiency's and more uniform irradiance if used accordingly. Detailed optical efficiency optimisation as well as a comprehensive error analysis due to tracking and manufacturing uncertainty has also been carried out in this study. Experimental analysis of the designed concentrating system is to be carried out to validate theoretical modelling. It will also be interesting to investigate the effect of non-uniform distribution of energy flux and hot spot formation. The results presented provide a good characterisation of how the irradiance distribution is altered by design dimensions for parabolic reflectors and could be used to measure in detail the size and severity of hot spots with irradiance distribution uniformity.

References

1. Green, M. A., Emery, K., Hishikawa, Y., Warta, W. and Dunlop, E. D. (2013), Solar cell efficiency tables (version 41). Prog. Photovolt: Res. Appl., 21: 1–11. doi: 10.1002/pip.2352
2. F. Muhammad-Sukki, R. Ramirez-Iniguez, S.G. McMeekin, B.G. Stewart & B. Clive, “Solar Concentrators”, International Journal of Applied Sciences (IJAS), Volume 1: Issue 1
3. Weiss W, Rommel M. Process heat collectors. State of the art within Task 33/ IV. IEA SHC-Task 33 and SolarPACES-Task IV: solar heat for industrial processes; 2008.
4. Alex Goldstein, Jeffrey M. Gordon, Tailored solar optics for maximal optical tolerance and concentration, Solar Energy Materials and Solar Cells, Volume 95, Issue 2, February 2011, Pages 624–629.
5. M. Li, X. Ji, G.L. Li, Z.M. Yang, S.X. Wei, L.L. Wang, Performance investigation and optimization of the Trough Concentrating Photovoltaic/ Thermal system, Solar Energy, Volume 85, Issue 5, May 2011, Pages 1028–1034.
6. Alexis Vossier, Daniel Chemisana, Gilles Flamant, Alain Dollet, "Very high fluxes for concentrating photovoltaics: Considerations from simple experiments and modelling", Renewable Energy, Volume 38, Issue 1, February 2012, Pages 31–39.
7. Michael, S, & Edson L., M., 'Review: Detection and analysis of hot-spot formation in solar cells', Solar Energy Materials And Solar Cells, 94, pp106-113
8. Julia Chaves, "Introduction To Nonimaging Optics",: Boca Raton : CRC Press, 2008., Harvard Library Bibliographic Dataset
9. Winston, R, & Koshel, R 2008, Nonimaging Optics And Efficient Illumination Systems V : 10-11 August 2008, San Diego, Californina, USA / Roland Winston, R. John Koshel, Editors ; Sponsored And Published By SPIE,: Bellingham, Wash. : SPIE, c2008., Harvard Library Bibliographic Dataset
10. M. Davis, T. Williams, M. Martínez, D. Sanchéz (2008), "Understanding Tracker Accuracy and its Effects on CPV", International Conference on Solar Concentrators 5 : 16-19 November 2008, Palm Desert, CA.

[Article 10]

K. Shanks, N. Sarmah, K. S. Reddy, and T. Mallick, “The design of a parabolic reflector system with high tracking tolerance for high solar concentration,” in *AIP -10th International Conference on Concentrator Photovoltaic Systems (CPV-10)*, 2014, October 2015, pp. 211–214.

The design of a parabolic reflector system with high tracking tolerance for high solar concentration

Katie Shanks and Kmas201@exeter.ac.ukNabin SarmahK. S. ReddyTapas Mallick

Citation: **1616**, 211 (2014); doi: 10.1063/1.4897063
View online: http://dx.doi.org/10.1063/1.4897063
View Table of Contents: http://aip.scitation.org/toc/apc/1616/1
Published by the American Institute of Physics

The Design Of A Parabolic Reflector System With High Tracking Tolerance For High Solar Concentration

Katie Shanks[1*], Nabin Sarmah[1], K. S. Reddy[2] and Tapas Mallick[1]

1Environmental and Sustainability Institute, University of Exeter Penryn Campus, Penryn, TR10 9FE, UK
2Heat Transfer and Thermal Power Laboratory, Department of Mechanical Engineering, Indian Institute of Technology Madras, Chennai 600 036, India
**Kmas201@exeter.ac.uk,*

Abstract. A compact high concentrating photovoltaic (HCPV) module based on cassegrain optics is proposed; consisting of a primary parabolic reflector, secondary reflector and homogeniser. The effect of parabolic curvatures, reflector separation distance and the homogeniser's height and width on the tracking tolerance has been investigated for optimisation. In this type of HCPV, the addition of a solid transparent homogeniser to the two stage reflector design greatly improves the tracking tolerance. Optical simulation studies show high optical efficiencies of 84.82 – 81.89 % over a range of ±1 degree tracking error and 55.49% at a tracking error of ±1.5 degrees.

Keywords: Solar Concentrator Design Optical Efficiency Optimization Tracking Error Tolerance Acceptance Angle
PACS: 88.40.-j, 88.40.F-; 88.40.fc; 88.40.fm; 88.40.fr; 88.05.Bc; 42.15.-i; 42.15.Dp; 42.15.Eq; 42.79.Bh; 42.79.Ek;

INTRODUCTION

The higher the concentration ratio of a solar concentrator system, the more dependent upon tracking accuracy it becomes. Solar tracking tolerances for two staged reflecting high concentration designs typically ranges between ± 0.1° to ± 0.6° [1-3] but with the addition of a flux homogeniser this can be greatly improved as shown by Gordon et al.[4,5] and Mcdonald et al. [6]. The two main aims of solar concentration systems are to reduce the cost of solar power by replacing expensive photovoltaic material with relatively cheap optical devices, and to increase the efficiency limit of single junction and multi-junction solar cells [2, 7]. However, with an increase in concentration ratio, the solar tracking accuracy required also increases, resulting in the need for expensive tracker systems which offset the cost benefit.

This study has been undertaken to understand in greater detail the contribution parameters within the cassegrain design make on the systems tracking tolerance. A parabolic type solar concentrator was optimized through Monte Carlo ray trace analysis to obtain >80% optical efficiency (including reflection and absorption losses) and a well distributed irradiance upon the receiver over a range of ±1° tracking error. The optical efficiency is maintained >55% up to ±1.5° tracking error.

DESIGN CONCEPT

A two-stage reflector type concentrator was explored due to the advantages of compactness and having an upward facing receiver [1]. The basic design for this solar concentrator employs a Cassegrain set up as shown in Fig. 1 to produce a concentrated uniform irradiance distribution upon a solar cell placed in the base of the 1st reflector.

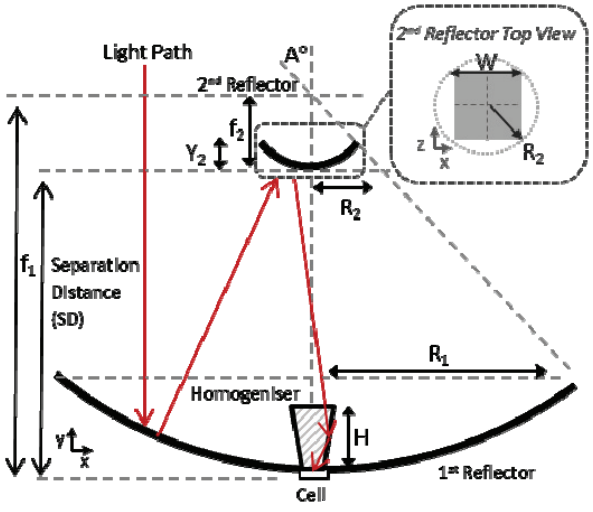

FIGURE 1. Theoretical light path through optics with all dimensions labelled.

Light rays from the sun however have a divergence of ± 0.27°. This can be compensated for by separating the focal points of both reflectors (no longer afocal)

10th International Conference on Concentrator Photovoltaic Systems
AIP Conf. Proc. 1616, 211-214 (2014); doi: 10.1063/1.4897063

and finding the optimum secondary reflector position with respects to the primary reflector.

The focal point, f, Radius, R, and depth, y, of a parabola are related through Eq. 1 [8].

$$R^2 = 4fy \tag{1}$$

It should also be noted that square cut parabolic reflectors were chosen for the primary and secondary reflectors to increase the packing factor when arranged in an array system. In this way, the width, W, of a reflector is related to the radius, R, through Pythagoras (Fig. 1). In Fig. 1 angle A is the maximum angle light can make with the vertical and still pass through the focal point. It determines the utmost limit that light can strike the inside curve of the primary reflector and is related to the reflector's parabolic parameters via Eq. 2 [8].

$$\frac{f_1}{2R_1} = \frac{1}{4\tan\left(A/2\right)} \tag{2}$$

The secondary reflector hence must be positioned or have a width that accommodates all rays. The width of the secondary reflector was chosen to be 50mm as a suitable size and weight that will not incur too much shadowing or difficulties in manufacturing.. The following relationship was formed to calculate the separation distance (SD) between the two reflectors required to collect all rays given the secondary reflector width and primary collector focal length and radius:

$$SD = f_1 - \left(\frac{0.5W}{\tan\left(2\tan^{-1}\left(\frac{R_1}{2f_1} \right) \right)} \right) \tag{3}$$

The radius of the primary reflector, R_1, can also be dependent on the width, W, to ensure a concentration ratio of 500x is reachable when including the secondary reflector shadowing area.

SEPARATION DISTANCE

Combinations of varying primary and secondary reflector focal lengths were simulated first without the homogeniser, investigating the displacement of the final ray positions due to a 1 degree tracking error. The separation distance was also changed, calculated using Eq. 3 above, taking R_1 as 159mm and the secondary reflector width, W, as 50mm.

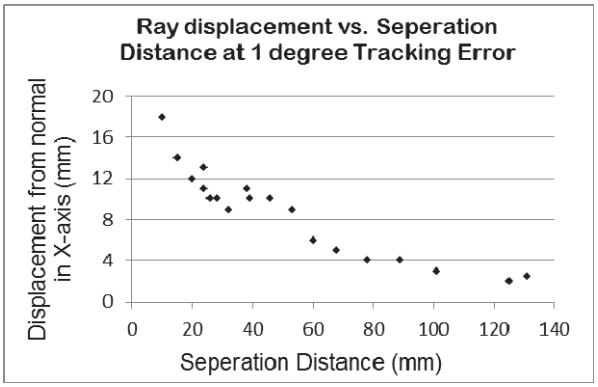

FIGURE 2. The effect of varying separation distance on Ray displacement from normal sun alignment whilst at 1° tracking error.

Larger separation distances result in lower ray displacement and hence a higher tracking tolerance as shown in Fig. 2. The separation distance is linked to the primary reflector focal length which counter intuitively must be decreased to gain a higher tracking tolerance/acceptance angle. This is due to the need to converge the light rays to the cell size with the secondary reflector which entails increasing the secondary reflector focal length but then displacing it further from the primary reflector. However, this has limitations, including the width of the secondary reflector as mentioned earlier.

The homogeniser was hence introduced as a means to let the rays focus and diverge before the receiver but still be redirected to the cell active area. The homogeniser is a crossed V-trough as shown in Fig. 3 with square entry and exit aperture areas.

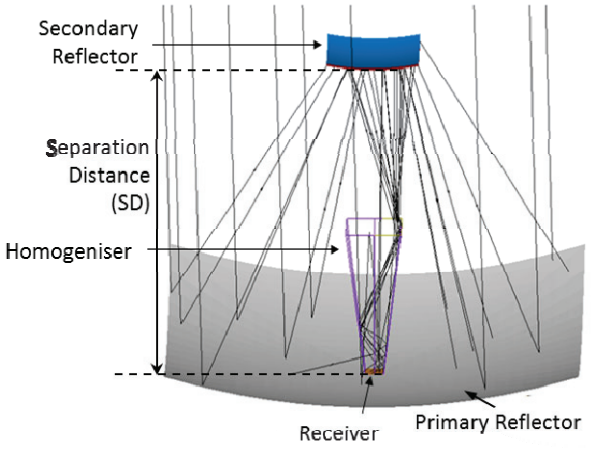

FIGURE 3. 3D ray trace diagram of incident rays at an angle of 1.5° and a solid transparent homogeniser with TIR within which catches otherwise lost rays.

HOMOGENISER

The focal lengths of the primary concentrator and secondary reflector were varied with a metal homogeniser (mirrored sides). The reflectivity was taken to be 95% and from the results found in Fig. 2, larger separation distances are desired, meaning taller Homogenisers are required. However this too has a limit due to the conditions of TIR at the walls of the homogeniser. Ideally the output face of the homogeniser, where the solar cell is placed, is the exact size of the cell active area to avoid losses. An output face of 10.1mm x 10.1mm was taken, instead of the 10mm x 10mm cell area, as a tolerance measure.

A shortlist of parameter combinations were found from various simulation testing and shown in Fig. 4.

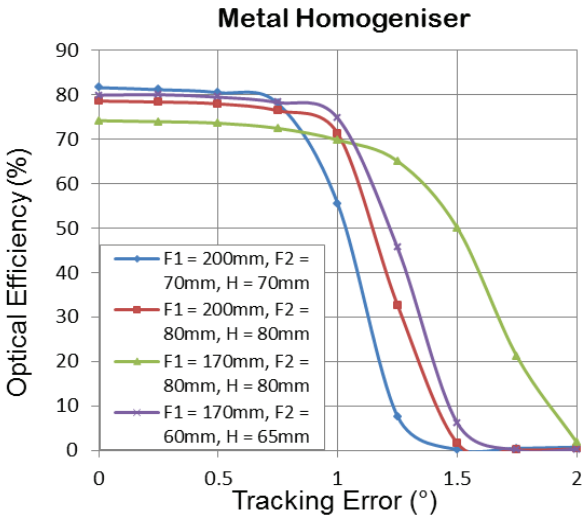

FIGURE 4. Optical Efficiency vs. tracking error. F1 and F2 are the 1st and 2nd reflectors focal lengths; H is the homogeniser height and SD is the Separation Distance. The Homogeniser entry and exit aperture width was 20mm and 10.1mm respectively for all.

The relatively low initial optical efficiency at normal incidence in Fig.4 is due to the reflection loss at the primary reflector, secondary reflector, and third stage homogeniser. The sharp decline in optical efficiency from 1 degree to 1.5 degrees seen is due to an increase in the number of reflections within the homogeniser, (reflective losses), and because of light passing by the homogeniser (diverging by > 10mm from normal in x-axis).

The tracking tolerance was hence improved by simulating a solid (BK7) transparent homogeniser utilising TIR and testing various heights and widths. For this, the focal lengths with the highest optical efficiency in Fig. 4 (F1=200mm, F2=70mm) were used.

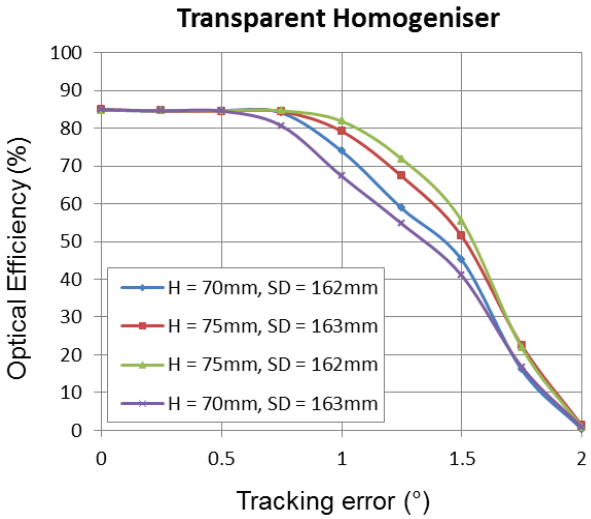

FIGURE 5. Graph of optimum parameter combinations for tracking tolerance. Entry aperture width = 30mm for all, H represents Homogeniser height and SD represents separation distance.

The most promising system parameter combination was chosen to be that with a homogeniser height of 75mm, an input width of 30mm and a separation distance between the two reflectors of 162mm. This configuration maintains an optical efficiency of 84.82 – 81.89 % over ± 1 degree tracking error and 55.49% optical efficiency at a tracking error of 1.5 degrees. The irradiance distribution of each set of parameter configurations was also recorded, all of which followed a similar trend with increasing tracking error as shown below in Fig. 6.

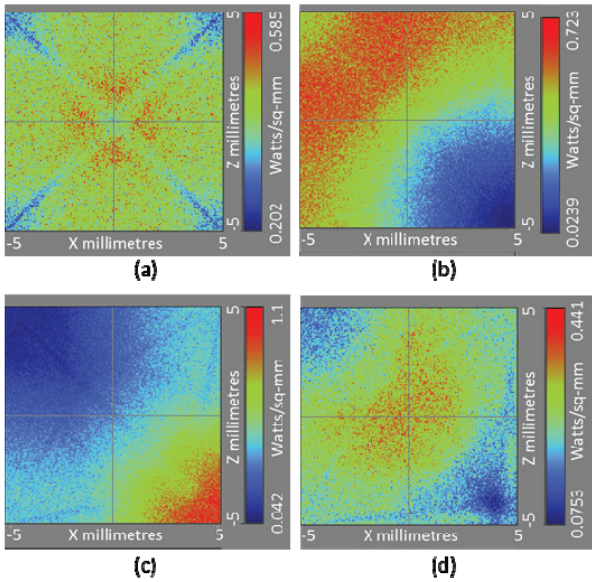

FIGURE 6. The irradiance distribution upon the receiver with increasing tracking error for the chosen

system parameter configuration with: (a) No tracking error; (b) 0.5 degree tracking error; (c) 1 degree tracking error and (d) 1.5 degree tracking error.

ERROR ANALYSIS

The optical efficiency drops from 81.89% to 79.21% due to a ±1mm vertical error at a tracking error of ±1°. These as well as the accuracy of the homogenisers' exit aperture dimensions and its alignment with the cell are the main sources of loss for this design.

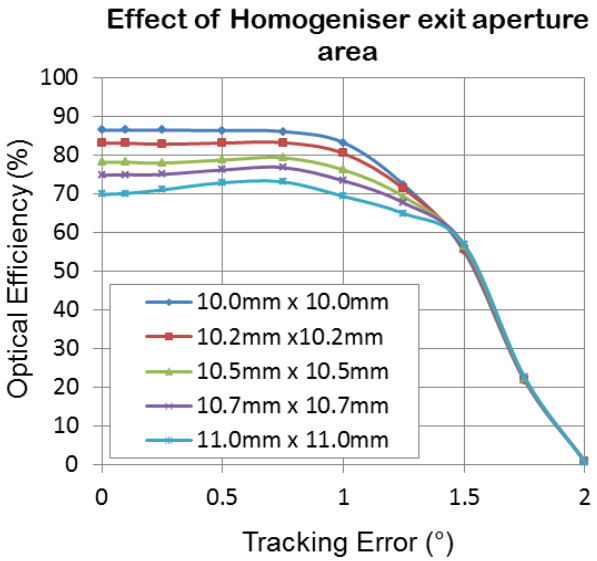

FIGURE 7. Decrease in optical efficiency due to mismatch of exit aperture area and cell area.

Perfect alignment with the cell and a homogeniser exit aperture of 10 x 10 mm obtains a maximum of 86.46% optical efficiency. With a 0.1mm alignment tolerance, the exit aperture dimensions, 10.1mm x 10.1mm, produces a maximum of 84.82% optical efficiency and decreases by ~1.7% (absolute value) for every 0.1mm increase in the area dimensions.

CONCLUSION

The tracking tolerance and optical efficiency of a cassegrain type solar concentrator was optimized through the use of monte carlo ray tracing to achieve high optical efficiencies of 84.82% (including reflection and absorption losses) at normal incidence, 81.89% at ±1° tacking error and 55.49% at ±1.5° tracking error. The optimized design was found to be with a primary parabolic reflector of focal length 200mm and a secondary inverse parabolic reflector of focal length 70mm placed 162mm from the primary collector. The optimized system required a solid transparent homogeniser of height 75mm with an entry aperture of 30mm x 30mm and exit aperture of 10.1mm by 10.1mm. The parameter relationships given, such as the equation for separation distance would be useful even as a preliminary stage in optimisation processes of two stage reflecting systems utilising a parabolic primary. The detailed analysis of the proposed system may be beneficial in the design of parabolic reflector systems, as well as single stage lens systems (that focus onto a homogeniser), as a guideline to help improve an aspect of the system dependent on alignment, focusing area or uncertainties.

ACKNOWLEDGMENTS

This work has been carried out as part of the BioCPV project jointly funded by DST, India and EPSRC, UK. Authors acknowledge both the funding agencies for the support.

REFERENCES

1. Luque-Heredia, J.M. Moreno, P.H. Magalhaes, R. Cervantes, G. Quemere, and O. Laurent, "Inspira's CPV Sun Tracking", in *Concentrator Photovoltaics*, A. Luque, and V. Andreev, ed. Springer Series in Optical Sciences, **130**, 221-250, (2007).
2. J.M. Gordon, "Concentrator Optics", in *Concentrator Photovoltaics*, A. Luque, and V. Andreev, ed. (Springer Series in Optical Sciences, **130**, 113-132, (2007).
3. A. Akisawa, M. Hiramatsu, and K. Ozaki, "Design of dome-shaped non-imaging Fresnel lenses taking chromatic aberration into account," Sol. Energy, **86**, 877–885, (2012).
4. Jeffrey M. Gordon, Daniel Feuermann, Pete Young; Maximum-performance photovoltaic concentration with unfolded aplanatic optics. Proc. SPIE 7043, High and Low Concentration for Solar Electric Applications III, 70430D (September 09, 2008);
5. Alex Goldstein and Jeffrey M. Gordon, "Double-tailored nonimaging reflector optics for maximum-performance solar concentration," J. Opt. Soc. Am. A **27**, 1977-1984 (2010).
6. Mark McDonald ; Chris Barnes; Spectral optimization of CPV for integrated energy output. Proc. SPIE 7046, Optical Modeling and Measurements for Solar Energy Systems II, 704604 (August 28, 2008).
7. H. Doeleman, "Limiting and realistic efficiencies of multi-junction solar cells", University of Amsterdam, (2012).
8. Richard Aufmann, Vernon C. Barker and Richard Nation, *College Algebra and Trigonometry*, Cengage Learning, (2010).

[Article 11]

K. Shanks, H. Baig, and T. K. Mallick, “The Conjugate Refractive-Reflective Homogeniser in a 500X Cassegrain Concentrator : Design and Limits Optical Surface Losses,” in *11th Photovoltaic Science Application and Technology Conference (PVSAT-11)*, 2015, October.

The Conjugate Refractive-Reflective Homogeniser in a 500X Cassegrain Concentrator: Design and Limits

Katie Shanks[1*], Hasan Baig[1] and Tapas K. Mallick[1]
[1]Environment and Sustainability Institute, University of Exeter Penryn Campus, Penryn, Cornwall, TR10 9FE, UK
[*] Corresponding Author kmas201@exeter.ac.uk

Abstract

In this study we present the conjugate reflective refractive homogeniser (CRRH) in a 500X Cassegrain photovoltaic concentrator. The optic is a crossed v-trough filled with a refractive medium and walled with reflective film, leaving an air gap between the two to achieve both TIR and reflection of escaped rays. This simple shape ensures easy manufacturing and produces a relatively uniform irradiance distribution upon the receiver. Results are given for both the ideal 100% reflection and the more realistic 90% reflection scenarios. The surface quality of the homogenising optic is simulated as a realistic rough surface which increases light loss. The CRRH hence traps these rays and increases optical efficiency by a maximum of 6%. These simulations have already been practically confirmed though further research is required. The conjugate reflective refractive homogeniser will increase optical accuracy in many ways including the acceptance angle.

Introduction There is a growing interest in concentrating photovoltaic (CPV) technologies due to their reduced need for PV material and higher potential efficiencies. Not only can CPV systems be the answer to reducing the cost of solar power but they are also more environmentally friendly than regular flat plate PV panels. This is due to two reasons; CPV technology uses less semiconductor components, and CPV technology has a smaller impact on the albedo change in an area than flat plate PV panels [1]. Other advantages of concentrating photovoltaics (CPV) include their ability to reduce system costs and to increase the efficiency limits of solar cells.

As the concentration ratio of an optic is increased, it becomes more difficult to maintain a high optical efficiency, uniform irradiance distribution, and an acceptable optical tolerance for the system [2]. Non-uniform illumination has a detrimental impact on the solar cell performance [3]. Hence a secondary optic/homogeniser element is needed relax the demand on the system's accuracy [4,5].

Some secondary concentrator optics include the compound parabolic concentrator (CPC) [6], the dome lens [7], the ball lens [8] and various homogenising light funnel geometries [9–11]. These typically take on the shape of an inverted cone or pyramid but there are also elliptical and hyperbolic optics [6,12,13].

One key consideration in all of the above named designs is the material to be used and the resulting surface quality.

Optical Surface Losses One commonly utilised and widely researched concentrator design is the Cassegrain concentrator. In this design, shown in figure 1, surface imperfections on the primary and secondary dishes will reduce the reflectance.

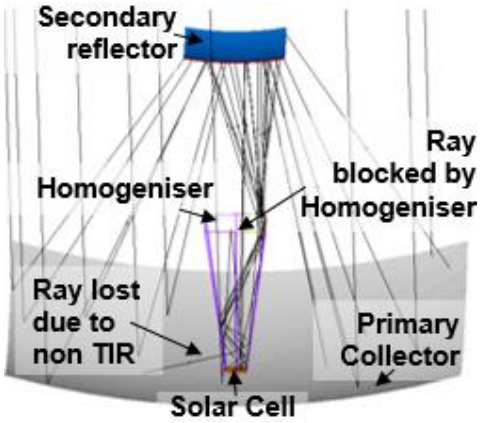

Fig. 1: Ray Trace Simulation of Cassegrain concentrator at a tracking error of ±1.75°. Lost rays are shown.

A reflective homogeniser optic would similarly suffer, especially when the system is misaligned as more reflections will occur within. A refractive medium takes advantage of total internal reflection (TIR) but surface imperfections will cause refraction loss. This includes when the rays initially refract into the homogeniser and a small portion of energy is reflected instead of refracted. A simple but effective method to recover rays which fail TIR at the homogeniser walls is to use a

reflective sleeve with an air gap [14]. Hence, the conjugate refractive reflective homogeniser (CRRH) could prove to be an improved homogeniser.

Parameters and Limits

A previous study has been carried out to determine the dimensions of the primary and secondary reflectors as well as the homogeniser dimensions [15]. Overall, the design has a good acceptance angle of >1°. The homogeniser geometry is set such that a perfect surface should only loose a negligible percentage of energy due to light rays not meeting TIR (>0.01%). However a perfect surface, as well as perfect corners does not exist.

Light rays pass very close to the outer edge of the homogeniser and in fact some are blocked as shown in figure 1 when the system is misaligned with the sun. This limits the air gap and thickness of the reflective sleeve but would not be the case for other designs (e.g. Fresnel lens). In this study, an air gap of 1mm was set between the refractive medium n and the reflective film as shown in figure 2. The solar cell size was 1cm x 1cm and the geometrical concentration ratio was 500X.

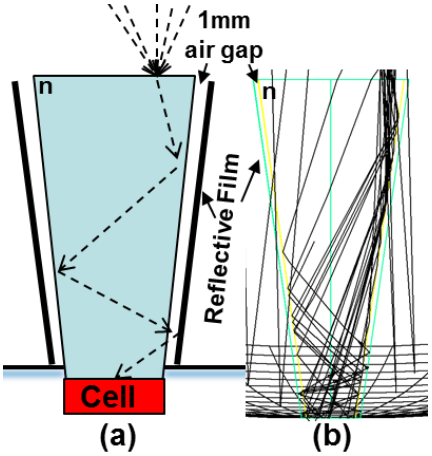

Fig. 2: (a) Diagram showing theoretical performance of CRRH. (b) Ray trace diagram confirming refracted light rays are caught by reflective film.

Simulation method Simulations were carried out using Breault's ASAP ray tracing software. The source was set to imitate energy from the sun with 1000w/m^2 and a divergence angle of ±0.27°. Simulations were run assuming first the scenario of perfect surface qualities and 100% reflectance and transmittance. This is shown in figure 4 and confirms that no light rays are lost within the system at normal incidence. 10% reflectance loss is then assumed for the two reflective dishes to show the strong impact on optical efficiency this has. The losses incurred when the light rays refract into the homogenisers entry aperture are included next and finally a surface roughness is added to the homogeniser material. The homogeniser material is set as SHOTT BK7, with a dispersion curve as shown in figure 3. This is a commonly used medium and has a higher refractive index than others such as PMMA. The homogeniser will be made out of a material with a similarly stable and high refractive index (to improve TIR within).

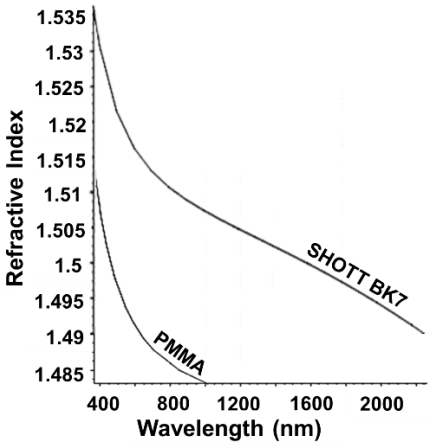

Fig. 3: Dispersion function of PMMA and SHOTT BK7.

The surface roughness chosen was that of standard polished aluminium, following the Harvey model. This model was chosen as the homogeniser will be moulded from an aluminium casing with polished inner surfaces.

Simulations with and without a 90% reflective film placed 1mm from the homogeniser walls are shown in figures 5-7. These simulations assumed again a 100% ideal reflectance from the primary and secondary reflectors, so as to focus solely on the benefit of the CRRH regardless of the performance of other components.

Results and discussion

As can be seen from figure 4, the addition of a 10% reflection loss on both dishes causes a significant drop in optical efficiency. There are various methods to improve reflection such as using silver (~97% reflectance). The loss due to some energy being reflected when the light rays are refracting into the homogeniser entry aperture is small and can be improved

with antireflection coatings or even special textures of the homogeniser surface.

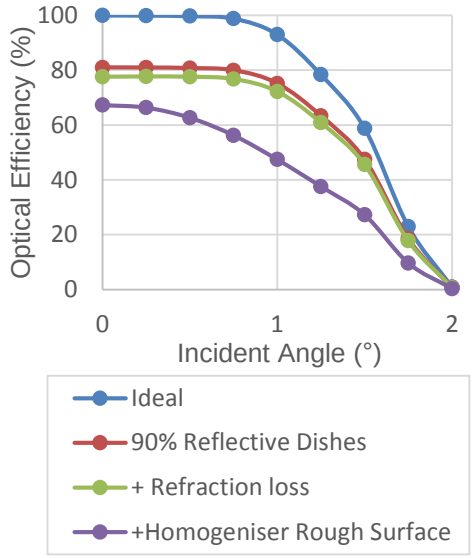

Fig. 4: Optical efficiency while adding surface losses in stages.

The surface roughness is the next main factor causing a drop in optical efficiency and lowering the acceptance angle. This is essentially due to the increase in the solar misalignment angles, the rays reflect more within the homogeniser against the rough surfaced walls and are more likely to refract instead of undergoing TIR. For this reason the conjugate refractive-reflective homogeniser improves optical efficiency by 3% at normal incidence and more so at increased incidence angles. This is as high as 6% over the 1 and 1.5 degree region as shown in figure 5. Although this is a significant gain, other manufacturing methods can result in smoother surface finishes with less light loss.

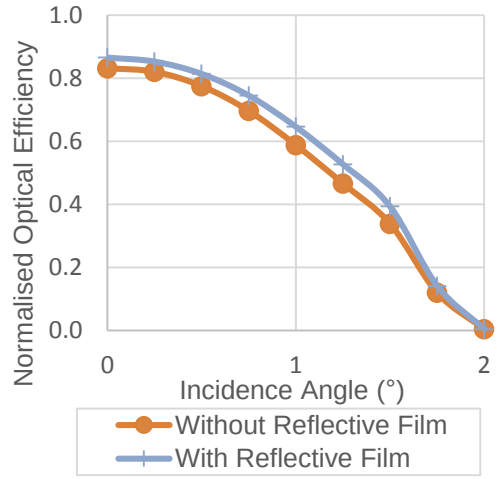

Fig. 5: Optical efficiency increase due to addition of reflective sleeve with increasing off-axis misalignment with the sun.

For higher quality optics, the CRRH would not add significant benefit. In fact, in the case of this Cassegrain design, the addition of the reflective sleeve decreases (by a negligible amount) the optical efficiency as it blocks slightly more rays on their way to the secondary dish reflector (shown in fig.1).

The reflective film was assumed to have a reflectance of 90% and of course higher reflectance films will provide an even better improvement upon optical efficiency. The reflective film sleeve however was chosen as a simple, cheap and effective method to improve optical efficiency without resorting to expensive manufacturing procedures or coatings for the optic and/or mould.

Irradiance distribution

The irradiance distribution upon the solar cell is also affected by the surface roughness of the homogeniser as shown in figure 6.

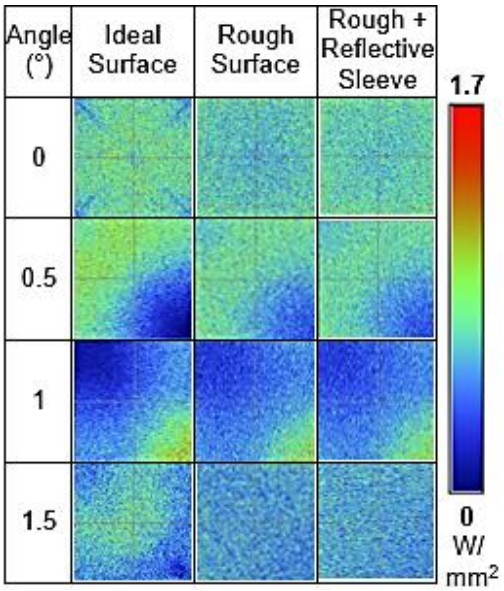

Fig. 6: Table of irradiance distribution upon solar cell with increasing solar incidence angle (increasing tracking error). Column 2: the case of 100% reflective dishes and a refractive homogeniser with an ideal surface finish. Column 3: Results after the addition of a rough surface finish upon the homogeniser. Column 4: Same conditions as previous but with the reflective sleeve in place. The tracking error is set for both axes, hence the diagonal focusing.

The irradiance distribution is somewhat improved due to the slight diffusion of the rays from the rough surface of the homogeniser. In the case of the conjugate refractive reflective homogeniser, when

the reflective sleeve is added, the irradiance distribution is negligibly different to that without the reflective sleeve. The difference between the maximum and minimum irradiance values are given in figure 7. This shows a purely smooth and ideal optic to have the least homogeneous distribution, the addition of the rough surface modelling has the most homogeneous irradiance distribution, and the CRRH has a slightly lessened level of evenly distributed irradiance upon the cell. As expected, with a higher misalignment angle, the distribution is less even, especially at 1°, before falling lower due to less total light being focused successfully to the solar cell.

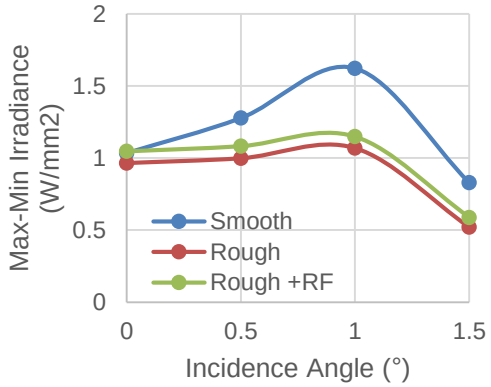

Fig, 7: Graph difference between max. and min. irradiance simulated upon the solar cell against increasing solar incidence angle. Trends given for an ideal smooth homogeniser surface (smooth), a rough homogeniser surface (rough), and the rough homogeniser surface with a reflective film sleeve (rough + RF).

Conclusion The conjugate refractive reflective homogeniser has been presented within the Cassegrain concentrator design. The CRRH has been shown to improve the optical efficiency by as much as 6% when considering a realistic surface roughness upon the homogenising optic. The benefits of the CRRH are limited by the Cassegrain concentrator geometry and by the magnitude of surface roughness upon the homogeniser. A high quality homogenising optic with almost ideal surface smoothness would not benefit from the addition of a reflective sleeve. Future work will be carried out but so far there has been a confirmation of a 6% performance improvement with the CRRH in comparison to the original refractive homogeniser.

References

[1] Akbari H, Damon Matthews H, Seto D. The long-term effect of increasing the albedo of urban areas. Environ Res Lett 2012;7:024004.

[2] Canavarro D, Chaves J, Collares-Pereira M. New second-stage concentrators (XX SMS) for parabolic primaries; Comparison with conventional parabolic trough concentrators. Sol Energy 2013;92:98–105.

[3] Baig H, Heasman KC, Mallick TK. Non-uniform illumination in concentrating solar cells. Renew Sustain Energy Rev 2012;16:5890–909.

[4] Brunotte M, Goetzberger A, Blieske U. Two-stage concentrator permitting concentration factors up to 300x with one-axis tracking. Sol Energy 1996;56:285–300.

[5] Canavarro D, Chaves J, Collares-Pereira M. New Optical Designs for Large Parabolic Troughs. Energy Procedia 2014;49:1279–87.

[6] Winston R, Miñano JC, Benítez P, Shatz N, Bortz JC. Nonimaging Optics. Elsevier; 2005.

[7] Victoria M, Domínguez C, Antón I, Sala G. Comparative analysis of different secondary optical elements for aspheric primary lenses. Opt Express 2009;17:6487–92.

[8] Coughenour BM, Stalcup T, Wheelwright B, Geary A, Hammer K, Angel R. Dish-based high concentration PV system with Köhler optics. Opt Express 2014;22:A211.

[9] Araki K, Leutz R, Kondo M, Akisawa A, Kashiwagi T, Yamaguchi M, et al. Development of a metal homogenizer for concentrator monolithic multi-junction-cells. Conf. Rec. Twenty-Ninth IEEE Photovolt. Spec. Conf. 2002., IEEE; 2002, p. 1572–5.

[10] Gordon JM, Feuermann D, Young P. Unfolded aplanats for high-concentration photovoltaics. Opt Lett 2008;33:1114.

[11] Tang R, Wang J. A note on multiple reflections of radiation within CPCs and its effect on calculations of energy collection. Renew Energy 2013;57:490–6.

[12] O'Gallagher J, Winston R. No TitleTest of a trumpet secondary concentrator with a paraboloidal dish primary. Sol Energy 1986;36:37–44.

[13] Benítez P, Miñano JC, Zamora P, Mohedano R, Cvetkovic A, Buljan M, et al. High performance Fresnel-based photovoltaic concentrator. Opt Express 2010;18:A25–40.

[14] Baig H, Sellami N, Mallick TK. Conjugate Refractive-Reflective based Building integrated Concentrating Photovoltaic (BiCPV) system. Energy (Under Review).

[15] Shanks K, Sarmah N, Mallick TK. The Design and Optical Optimisation of a Two stage Reflecting High Concentrating Photovoltaic Module using Ray Trace Modelling. PVSAT-9, 2013.

[Article 12]

P. Pérez-Higueras, J. P. Ferrer-Rodríguez, K. Shanks, F. Almonacid, and E. F. Férnández, “Thin photovoltaic modules at ultra high concentration,” in *AIP -11th International Conference on Concentrator Photovoltaic Systems (CPV-11)*, 2015, no. 1679, p. 130004.

Thin photovoltaic modules at ultra high concentration

Pedro Pérez-Higueras' , Juan Pablo Ferrer-Rodríguez, Katie Shanks, Florencia Almonacid, and Eduardo F. Férnández

Citation: **1679**, 130004 (2015); doi: 10.1063/1.4931564
View online: http://dx.doi.org/10.1063/1.4931564
View Table of Contents: http://aip.scitation.org/toc/apc/1679/1
Published by the American Institute of Physics

Thin Photovoltaic Modules at Ultra High Concentration

Pedro Pérez-Higueras[1, a)], Juan Pablo Ferrer-Rodríguez[1], Katie Shanks[2], Florencia Almonacid[1] and Eduardo F. Férnández[1, 2]

[1]*Center of Advanced Studies in Energy and Environment (CEAEMA) IDEA Research Group, University of Jaén, Campus Lagunillas, 23071 Jaén, Spain*
[2]*Environment and Sustainability Institute, University of Exeter, Penryn, Cornwall, TR10 9EZ, United Kingdom*

[a)]Corresponding author: pjperez@ujaen.es

Abstract. A new design concept of high concentration photovoltaic (HCPV) module is studied both by ray-tracing simulation and by building a prototype. This set-up is based on the idea of concentrating sunlight from different optical units to a single commercial multi-junction solar cell, which is located in a different plane than that of the primary optics (e.g. Fresnel lenses). A two-optical-unit set-up, as a first approach, is built and measured with the solar simulator "Helios 3198". These results are compared to the measurement results of the single-unit of one Fresnel lens and the same solar cell. The feasibility of this new design has been confirmed theoretically and practically.

INTRODUCTION

The cost of large scale conventional photovoltaic installations decreased in the last years to such a point that it can be considered a low-cost renewable energy technology. Depending on annual sunshine, conservative scenarios predict power costs between €0.04/kWh and €0.06/kWh for the year 2025 [1]. Similarly, HCPV systems have shown a great potential for reducing the levelized cost of electricity (LCOE) which is expected to be in the range of €0.045/kWh and €0.075/kWh for the year 2030 at locations with high solar irradiation (2000 kWh/m^2/year - 2500 kWh/m^2/year [2]). This shows the difficulty in making HCPV compete with PV. Therefore, if HCPV technology is wanted to play an important role in the future of renewable energy, it is necessary to continue efforts in research and development to make this technology more competitive. One of the key factors which promote and make the HCPV modules more competitive (aside from increasing the cell's efficiency [3]) is to increase the concentration ratio: this will reduce the use of semiconductor material. The cost of HCPV system has been found to decrease as the concentration level increases [4,5]. Another possible factor to lower costs is to diminish the size, depth and weight of the total generator system of a HCPV power plant, for a given module's optical concentration ratio and a total installed power: this will reduce the cost and requirements of the trackers, also manufacturing costs, logistics costs, etc. For that, one possibility is to decrease the module's surface by increasing its efficiency. Another possibility is to reduce the module's depth through new thinner optical module's designs while maintaining constant the optical efficiency. The development of more compact modules has been also signaled by different companies as one key issue to reduce the cost of HCPV systems [6,7].

To achieve these two factors at the same time: get high concentration levels and make lighter and more compact modules, different companies and research centers are developing new kinds of concentration modules. For example, Semprius [8] uses 600μm × 600μm micro-transfer printed cells for modules with a concentration of x1111. The use of microcells reduces the optical path of the module, so, instead of being around 40-60 cm deep HCPV module, a typical depth for modules with concentration greater than x1000, Semprius' module is only 6.6 cm deep. Also, the use of optical devices to split the spectral distribution has already demonstrated its potential to get modules with higher efficiencies [9,10]. Others possible designs are continuously being discussed by the scientific community in order to get more competitive modules.

11th International Conference on Concentrator Photovoltaic Systems
AIP Conf. Proc. 1679, 130004-1–130004-8; doi: 10.1063/1.4931564

We are working on a new concept of concentrator modules in order to simultaneously achieve both requirements above, increasing the concentration ratio and reducing the size of the module while using commercial multi-junction cells (of 3x3 or 5x5mm^2 approximately [11]). These Thin Photovoltaic Modules at Ultra-High Concentration (UHCPV), are based on the idea of sending several concentrated light beams coming from different primary optical elements (like different units of Fresnel lens) onto a single solar cell. Moreover, the direction of propagation of the concentrated light inside the module is rotated 90º so that the module's size is reduced. Therefore, the solar cell's plane is no more parallel to that of the sunlight receiving surface.

DESCRIPTION OF THE DESIGN CONCEPT

An example of a design fulfilling the above description (Patent ES2493740 A1, University of Jaen) consists of an n-optical-unit system composed by n-Fresnel lenses and corresponding n-mirrors. Each one of these mirrors sends the concentrated light to the same multi-junction solar cell (see Fig. 1) changing 90º the direction of propagation of the light beam. A tertiary optical element (e.g. a prism) may be needed in order to homogenize the incoming light on the cell.

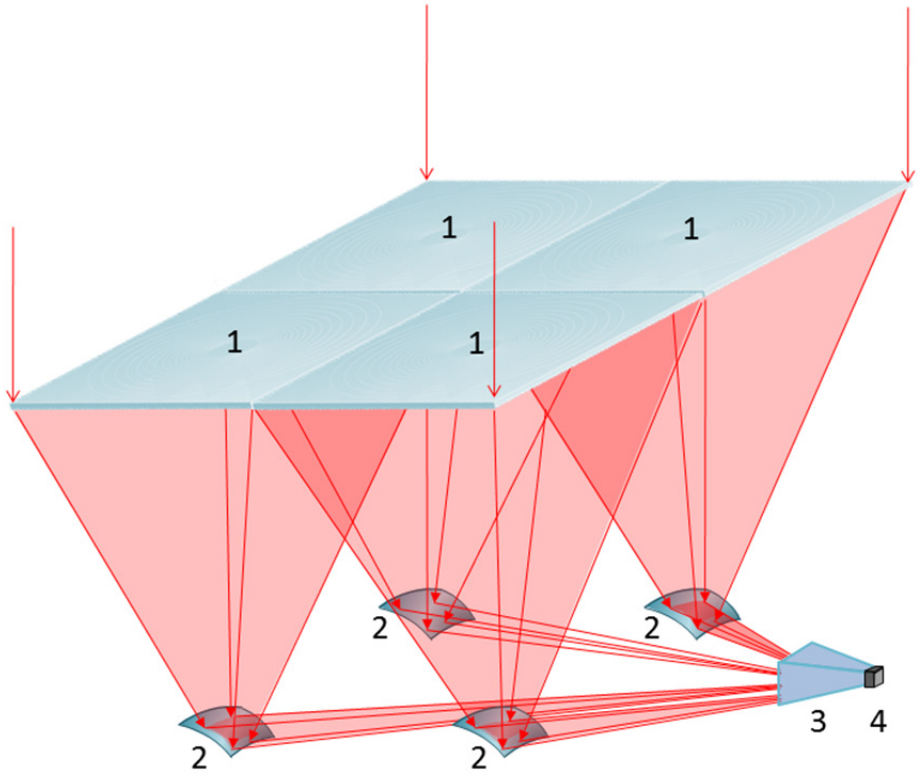

FIGURE 1. Concentration system made up of: (1) four primary refractive optical elements, (2) four secondary reflexive optical elements, (3) a tertiary homogenizer optical element and a single solar cell (4) –patented by University of Jaen.

Please note that the solar cell is located in a middle plane and rotated 90º in respect to the Fresnel lenses plane, which allows to reduce size and depth whereas the concentration ratio is highly increased.

A design of an intermediate step consisting of a two-optical-unit set-up and only one solar cell is studied in this paper. For this case only, commercial planar mirrors are used in order to analyze the feasibility of this idea.

DESIGN OF A TWO-OPTICAL-UNIT MODULE

A two-optical-unit system has been analyzed by using TracePro (Lambda Research Corporation) software. The design has been maintained quite simple: two Fresnel lenses and two planar mirrors (Fig. 2).

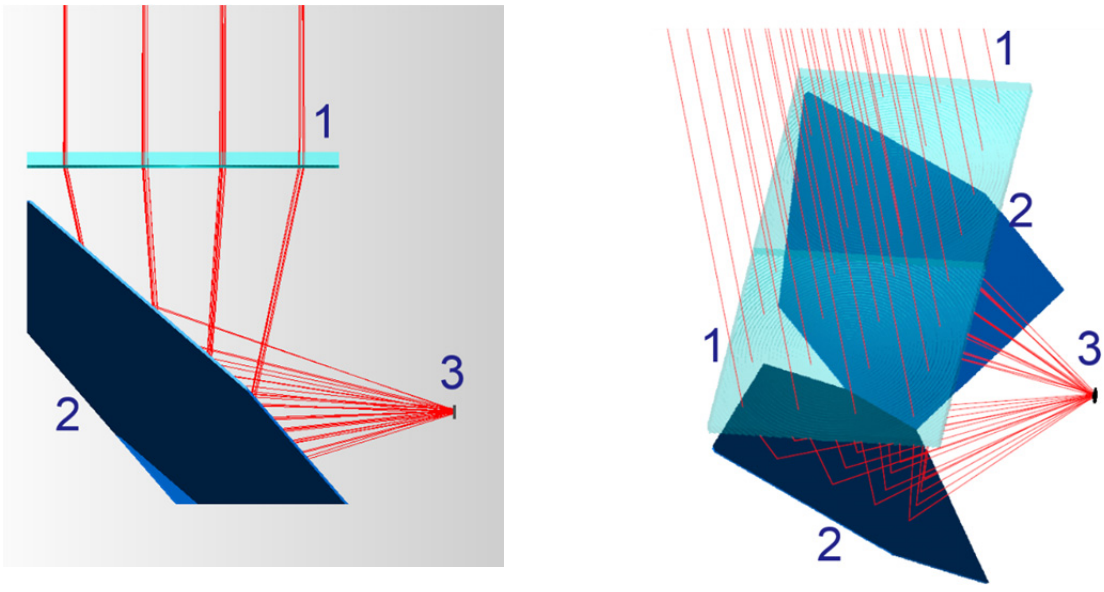

(a) (b)

FIGURE 2. Ray tracing simulation of the two-optical-unit system consisting of two Fresnel lenses, two planar mirrors and a solar cell. Lateral view (a). Another view (b). (1) Fresnel lenses. (2) Planar mirrors. (3) Multi-junction solar cell. Note that the normal to the solar cell´s surface is perpendicular to the optical axis of each Fresnel lens. Simulation made with TracePro software.

Both planar mirrors have been adjusted in order to send the light onto the cell, which is located in a middle plane between the two Fresnel lenses. The normal axis of the solar cell is perpendicular to the optical axis of each Fresnel lens. Both reflected light beams intersect each other just at the same point where the solar cell is located. In this simulation no others optical elements, like a homogenizer, are included.

The Fresnel lenses are of 120mm side and of 210mm focal distance, whereas the Azur Space solar cell is of 5.5mm length. Therefore, the geometrical concentration ratio of this two-optical-unit set-up is 952 suns.

EXPERIMENTAL

A set-up based on the two-optical-unit design was built (see Fig. 3). Each planar mirror is oriented in order to send light coming from each respective Fresnel lens onto the multi-junction solar cell. Note that the direction of propagation of both concentrated light beams is changed 90º after reflecting on each planar mirror.

The two-optical-unit module was measured in the CPV solar simulator “Helios 3198” [12] located at Center of Advanced Studies in Energy and Environment (CEAEMA) of the University of Jaén. Also a mono-module with only one lens and with the same solar cell and same kind of Fresnel lens (called “single-lens prototype”) was measured in the CPV solar simulator in order to compare the result with that of this two-optical-unit set-up [13,14,15]. The fine adjustment of the system was manually made and it was very difficult to position all the elements so that all the light reached the solar cell. See in Fig. 3 both light beams joined together in a single light spot. In future developments, a tertiary optical element would be needed in order to avoid any light mismatching on the solar cell.

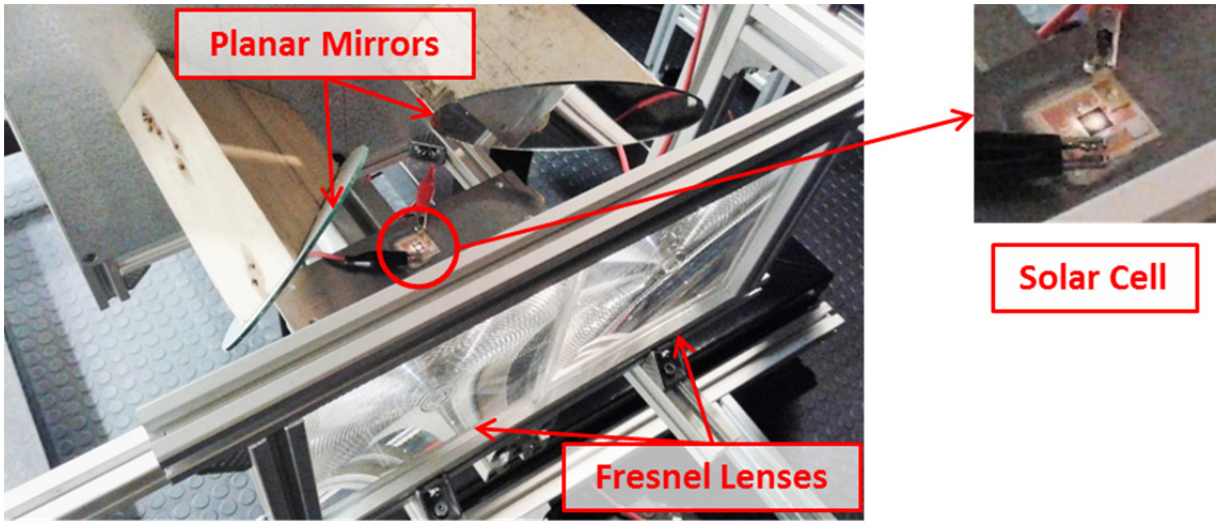

FIGURE 3. Set-up of a two-optical-unit module mounted in the CPV solar simulator "Helios 3198" and a photograph of the illuminated multi-junction solar cell of area 5.5x5.5mm^2. The light spot on the solar cell when having aligned the set-up to the collimated light coming from the modeling lamp of the solar simulator is also shown.

MEASUREMENT RESULTS

I-V curves were taken by using the same solar cell: for the single lens plus the solar cell and for the "two-optical-unit set-up". Figure 4 contains both I-V curve indoor measurements at an effective direct irradiance of 850W/m^2 when illuminating the same solar cell.

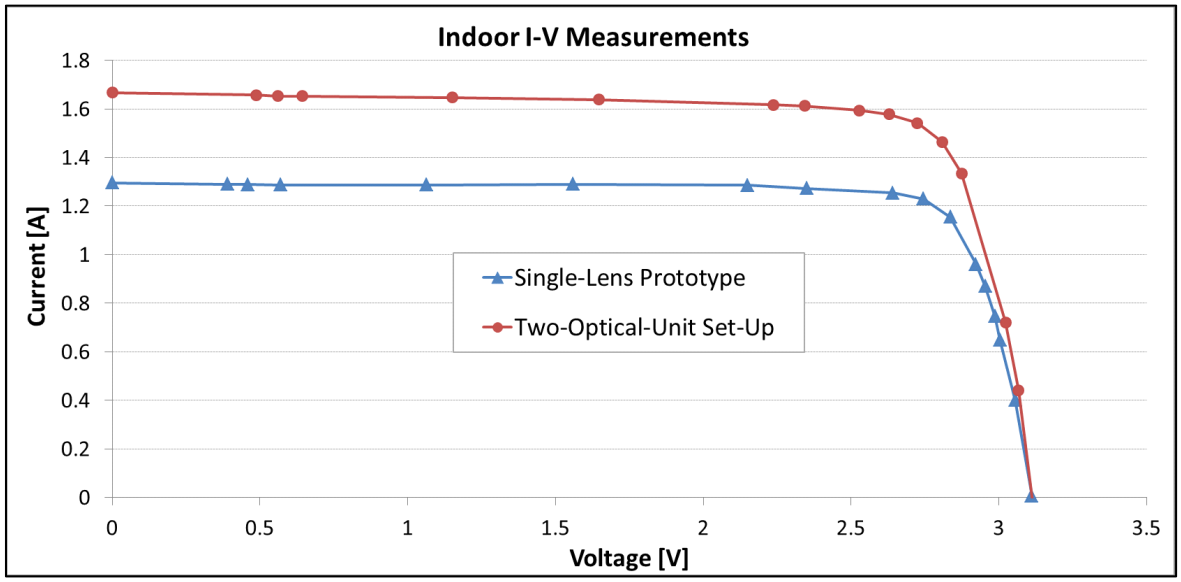

FIGURE 4. Comparative I-V curve indoor measurements of (round markers) "two-optical-unit set-up" and (triangle markers) the "single-lens prototype" taken at an effective direct irradiance of 850W/m^2. Both I-V curves are of the same solar cell and with the same kind of Fresnel lens.

A summary of the I-V indoor measurement results is shown in Table 1. The efficiency of the "two-optical-unit set-up" is lower than that of the "single-lens prototype". The whole two-lens surface has been taken into account in the calculation of the efficiency of the two-optical-unit set-up.

TABLE 1. Summary of indoor I-V measurement results of both experiments.

Effective DNI = 850W/m^2	Single-Lens Prototype	Two-Optical-Unit Set-Up
V_{OC} [V]	3.1	3.1
I_{SC} [A]	1.30	1.67
P_{mpp} [W]	3.4	4.2
V_{mpp} [V]	2.7	2.7
I_{mpp} [A]	1.23	1.54
Fill Factor [%]	83.6	81.0
Efficiency [%]	27.5	17.2
Concentration [suns]	476	952

ANALYSIS OF RESULTS

Both measurement experiments, the "single-lens prototype" and the "two-optical-unit set-up", have similar values of voltage. The fill factor is slightly lower for the two-optical-unit set-up due to the less illumination homogeneity on the cell, since the sum of both light spots is, in our case, less homogeneous than a single light spot [16]. The current values are greater for the last experiment but not high enough to lead to a similar value of efficiency as by the single-lens prototype. The efficiency decrease is only linked to the optical efficiency, since thermal effects are negligible in the measurements taken with this pulsed-solar simulator (the flash has a duration of ca. 2ms [12]). The efficiency decrease from 27.5% to 17.2% in the "two-optical-unit set-up" is due to some different factors:

1. Imperfect fine adjustment between the optical elements.
2. Reflection losses on the standard planar mirrors.
3. Reflection losses on the solar cell due to the increase of the angle of the incoming rays.
4. Non-uniform illumination on the solar cell (decreasing fill factor).

As explanation for each reason listed above, let us consider:

- 1) It would be necessary to build a more complex set-up in which all the optical elements (the two lenses, the two mirrors and the solar cell) were more accurately adjustable by using e.g. accurate positioning stages for most of the elements, and also for determining the 3D orientation of the mirrors.
- 2) Because this is only a feasibility analysis, standard planar mirror were used. For a utility design, first surface mirrors are needed in order to improve the optical efficiency of the system.
- 3) Usually in many other designs of HCPV modules, the optical axis of a Fresnel lens is perpendicular to the solar cell. In our prototype, the direction of propagation of the light beam impinging the solar cell subtends around 45º respect to the normal of the solar cell's surface. It causes a loss of optical efficiency as deduced by the optical Fresnel relations when increasing the incident angle [17].
- 4) In order to collect more light rays and to homogenize the light on the solar cell, a homogenizer prism may be needed in a last optical stage before the solar cell.

CONCLUSIONS AND FUTURE DEVELOPMENTS

The feasibility of the basic idea that will allow a high increase in the concentration ratio whilst reducing the size of the HCPV modules, has been proved in an intermediate design step. Nevertheless, it is critical to optimize the optical efficiency of the prototypes before considering them a reasonable alternative to current designs.

For future n-optical-unit systems, special mirrors and a special homogenizer have to be designed to achieve competitive optical efficiencies.

ACKNOWLEDGMENTS

This work is part of the project ENE2013-45242-R supported by the Spanish Economy Ministry, and by the European Regional Development Fund / Fondo Europeo de Desarrollo Regional (ERDF / FEDER).

ANNEX. APPLICATION EXAMPLE FOR REDUCING THE DEPTH OF HCPV MODULES

To reduce the HCPV modules' depth, one possible application is the use of n-optical-unit elements. The initial conventional HCPV case is compared with two other examples in which the n-optical-unit design is applied by increasing the number of units per solar cell (see Tables 2, 3 and 4 and Fig. 5, 6 and 7). Please note that this is only a theoretical gross approximation to illustrate the module's depth reduction, i.e. optical and efficiency losses due to the increase of the number of optical units per solar cell are not consider. Moreover, the f-number is maintained constant for the three different examples below. The calculation are at CSTC (DNI=1000W/m^2, T_{cell}=25ºC and AM=1.5 low AOD).

TABLE 2. Data summary of an imaginary example of a commercial 1000X module of ca. 1 m^2 surface and 31% efficiency. Data for the cells and lenses used and for the whole module are shown.

Cells		**Lenses**		**Module**	
Dimensions	1 cm x 1 cm	Dimensions	36 x 36 cm	Dimensions	0.72 m x 1.44 m
Surface	1 cm^2	Surface	1296 cm^2	Surface	1.04 m^2
Concentration	1000X	Efficiency	85%	Concentration	1000X
Power	40 W	Lenses for		No. of Lenses	8
Efficiency	40 %	each cell	1	No. of Cells	8
				Power	320 W
				Efficiency	31 %
				Depth	**0.48 m**

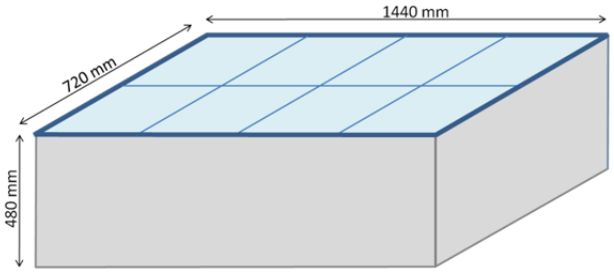

FIGURE 5. Schema of an imaginary example of a commercial 1000X module of ca. 1 m^2 surface and around 31% efficiency.

TABLE 3. Data summary of an imaginary example of a commercial 1000X module of ca. 1 m^2 surface and 31% efficiency. Data for the cells and lenses used and for the whole module are shown. This module is compound of a series of four-optical-unit elements. The module's depth is reduced by half.

Cells		**Lenses**		**Module**	
Dimensions	1 cm x 1 cm	Dimensions	18 x 18 cm	Dimensions	0.72 m x 1.44 m
Surface	1 cm^2	Surface	324 cm^2	Surface	1.04 m^2
Concentration	1000X	Efficiency	85%	Concentration	1000X
Power	40 W	Lenses for		No. of Lenses	32
Efficiency	40 %	each cell	4	No. of Cells	8
				Power	320 W
				Efficiency	31 %
				Depth	**0.24 m**

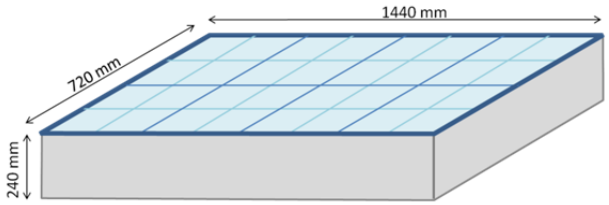

FIGURE 6. Schema of an imaginary example of a commercial 1000X module of ca. 1 m^2 surface and around 31% efficiency. In this case, this module is compound of a series of four-optical-unit elements. The module's depth is reduced by half.

TABLE 4. Data summary of an imaginary example of a commercial 1000X module of ca. 1 m^2 surface and 31% efficiency. Data for the cells and lenses used and for the whole module are shown. This module is compound of a series of sixteen-optical-unit elements. The module's depth is reduced by quarter.

Cells		Lenses		Module	
Dimensions	1 cm x 1 cm	Dimensions	9 x 9 cm	Dimensions	0.72 m x 1.44 m
Surface	1 cm^2	Surface	81 cm^2	Surface	1.04 m^2
Concentration	1000X	Efficiency	85%	Concentration	1000X
Power	40 W	Lenses for		No. of Lenses	128
Efficiency	40 %	each cell	16	No. of Cells	8
				Power	320 W
				Efficiency	31 %
				Depth	**0.12 m**

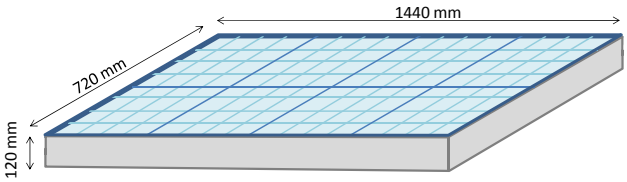

FIGURE 7. Schema of an imaginary example of a commercial 1000X module of ca. 1 m^2 surface and around 31% efficiency. In this case, this module is compound of a series of sixteen-optical-unit elements. The module's depth is reduced by quarter.

REFERENCES

1. J. N. Mayer et al., *Current and Future Cost of Photovoltaics. Long-term Scenarios for Market Development, System Prices and LCOE of Utility-Scale PV Systems* (Fraunhofer ISE, Study on behalf of Agora Energiewende, Freiburg, 2015).
2. S. P. Philipps, A. W. Bett, K. Horowitz and S. Kurtz, *Current Status of Concentrator Photovoltaic (CPV) Technology* (NREL and Fraunhofer ISE, Springfield, 2015), pp. 12–13.
3. P. Pérez-Higueras, E. Muñoz, G. Almonacid and P. Vidal, "High Concentrator Photovoltaics efficiencies: Present status and forecast," *Renewable and Sustainable Energy Reviews*, 15(4): 1810-1815, (2011).
4. M. Yamaguchi, T. Takamoto, K. Araki, M. Imaizumi, N. Kojima, and Y. Ohshita, "Present and Future of High Efficiency Multi-Junction Solar Cells," in CLEO: 2011 - *Laser Applications to Photonic Applications*, OSA Technical Digest (CD) (Optical Society of America, 2011), paper CMT5.
5. Ortiz, E. and Algora, C., "A high-efficiency LPE GaAs solar cell at concentrations ranging from 2000 to 4000 suns." *Progress in Photovoltaics: Research and Applications*, 11: 155–163. doi: 10.1002/pip.476 (2003).
6. Furman, B.; Menard, Etienne; Gray, A.; Meitl, M.; Bonafede, S.; Kneeburg, D.; Ghosal, K.; Bukovnik, R.; Wagner, W.; Gabriel, J.; Seel, S.; Burroughs, S., "A high concentration photovoltaic module utilizing micro-transfer printing and surface mount technology," *Photovoltaic Specialists Conference (PVSC), 2010 35th IEEE*, vol., no., pp.000475,000480, 20-25 (2010).
7. morgansolar.com
8. Scott Burroughs, Kanchan Ghosa1, Peter Krause and Michael Fiedler, "First Year Performance Results from a Unique Micro-cell based HCPV RD&D System Installed in Tucson, Arizona" *26th European Photovoltaic Solar Energy Conference and Exhibition*, pp. 172-175, Hamburg (Germany) (2011).
9. Wang, X. et al., "Lateral spectrum splitting concentrator photovoltaics: Direct measurement of component and submodule efficiency". *Progress in Photovoltaics: Research and Applications,* 20(2), pp. 149-165 (2012).
10. Broderick, L. Z. et al., "Design for energy: Modeling of spectrum, temperature and device structure dependences of solar cell energy production". *Solar Energy Materials and Solar Cells,* Volume 136, p. 48–63 (2015).
11. Pérez-Higueras, P., Fernández, E., Almonacid, F. & Rodrigo, P., "Flat Photovoltaic Modules at Ultra High Concentration. Amsterdam", *29th European Photovoltaic Solar Energy Conference and Exhibition* (2014).
12. C. Domínguez, I. Antón and G. Sala, "Solar simulator for concentrator photovoltaic systems", *Optics Express*, 16(19), 14894-14901 (2008).

13. E. F. Fernández, P. Pérez-Higueras, A. Garcia Loureiro and P. Vidal, "Outdoor evaluation of concentrator photovoltaic systems modules from different manufacturers: First results and steps," *Progress in Photovoltaics: Research and Applications*, 21(4): 693-701 (2013).
14. F. Almonacid, E. F. Fernández, P. Rodrigo, P. Pérez-Higueras and C. Rus-Casas, "Estimating the maximum power of a High Concentrator Photovoltaic (HCPV) module using an Artificial Neural Network," *Energy*, **53**: 165-172 (2013).
15. P. Rodrigo, E. F. Fernández, F. Almonacid and P. Pérez-Higueras, "Models for the electrical characterization of high concentration photovoltaic cells and modules: A review", *Renewable and Sustainable Energy Reviews*, **26**: 752-760 (2013).
16. Baig, H., Heasman, K.C., Mallick, T.K. "Non-uniform illumination in concentrating solar cells", *Renewable and Sustainable Energy Reviews*, 16 (8), pp. 5890-5909 (2012).
17. E. Hecht, *Optics* (Addison Wesley Longman, 1999), pp. 112-140.

[Article 13]

K. Shanks, S. Senthilarasu and Tapas K. Mallick, “Reliability Investigations for Built Ultrahigh Concentrator Prototype,” *13th International Conference on Concentrator Photovoltaic Systems (CPV-13)*, 2017. (Abstract accepted).

Reliability Investigations for a Built Ultrahigh Concentrator Prototype

Katie Shanks[1a*], S. Senthilarasu[1b], Tapas Mallick[1c*]

[1]Environmental and Sustainability Institute, University of Exeter Penryn Campus, Penryn, TR10 9FE, UK

[a*]Kmas201@exeter.ac.uk, [c*]T.K.Mallick@exeter.ac.uk

1. Introduction

Multi-junction concentrator solar cells are reaching >40% efficiencies under high concentration ratios. In order to reach their full potential and to continue developing solar concentrator technology to achieve higher power outputs and cost effectiveness, higher concentration designs should be investigated. Ultrahigh solar concentration (>2000x) poses many potential advantages as well as many challenges. Here we present an ultrahigh concentration design with a geometric concentration ratio of 5800x and a theoretical acceptance angle of 0.4°. This results in a geometric concentration-acceptance product (CAP) value of 0.53 when not including reflection and absorption losses. This suggests the geometric design is very good in comparison to CAP values for high concentration designs which are similar or less [1]. The design takes advantage of 4 primary Fresnel lenses, 2 flat redirecting flat mirror stages and a final refractive central optic coupled to a 5.5 by 5.5mm solar cell. However, the manufacturing and experimental performance of the built design is likely to fall far below the theoretical predictions. High accuracy manufacturing and optical quality would be very expensive for such high concentration levels and dampens the cost effectiveness of ultrahigh concentrators. As anticipated the built prototype had a low optical efficiency of ~40% but this resulted in a reliable 2000x concentrator system. Experimental analysis of the optics and overall concentrator performance is carried out to find if overall a low optical efficiency ultrahigh concentrator system can still provide a more reliable power output than a high optical efficiency high concentrator system. A general comparison of cost and power output per area is also given. Suggestions to improve the optical efficiency and achieve high performing ultrahigh concentrators are also given.

2. The design

The full design is shown in figure 1a and takes advantage of multiple primary Fresnel lenses instead of 1 large Fresnel lens which would be difficult to manufacture. A similar cassegrain type ultrahigh concentrator has been designed by Ferrer-Rodriguez et. al. but its effective concentration fell below 2000x and the design requires specially curved reflector optics which may be difficult to manufacture and align [2]. Highly reflecting and accurate flat mirrors are easier and far less expensive to manufacture and align. However to reach the concentration required a final stage central optic made of 4 dome lenses was needed. The optic was manufactured using a combination of bought and moulded lenses to produce the final shape as shown in figure 1b and c.

3. Concentration-acceptance Product

A CAP analysis on the performance of the ultrahigh concentrator design was undertaken and is shown in table 1. The maximum acceptance angle achievable due to the limits of étendue [3] is 1.32° and assuming the 4-dome receiver optic would be made out of a higher refractive index material such as sapphire for best performance. Ray trace simulations suggest an acceptance angle of 0.4° is achievable using these optics but it is unknown yet how different methods of manufacturing may affect the acceptance angle. Using state of the art achromatic Fresnel lenses and 97% reflective mirrors and a high quality sapphire central optic would give 75% optical efficiency as shown in table 1. Using standard Fresnel lenses and less optically efficient mirrors and a central optic made of lower refractive index than sapphire will give ~55% optical efficiency. A built prototype should perform between these two predictions but the acceptance angle may also decrease due to alignment issues and manufacturing errors. There is also the possibility that only the optical efficiency will suffer and the acceptance angle could perhaps increase depending on how the light is distributed from the optics.

References

[1] P. Benítez, J. C. Miñano, P. Zamora, R. Mohedano, A. Cvetkovic, M. Buljan, J. Chaves, and M. Hernández, "High performance Fresnel-based photovoltaic concentrator.," *Opt. Express*, vol. 18, pp. A25–A40, 2010.

[2] J. P. Ferrer-Rodriguez, E. F. Fernandez, F. Almonacid, and P. Perez-Higueras, "Optical Design of a 4-Off-Axis-Unit Cassegrain Ultra- High CPV Module with Central Receiver," *Opt. Lett.*, vol. 41, no. 0, pp. 3–6, 2016.

[3] A. Goldstein and J. M. Gordon, "Tailored solar optics for maximal optical tolerance and concentration," *Sol. Energy Mater. Sol. Cells*, vol. 95, no. 2, pp. 624–629, Feb. 2011.

Simulated Design Scenario	Optical Efficiency	Concentration Ratio	Acceptance Angle (°)	CAP
Ideal (maximum theoretical limits)	100%	5831x	1.32	1.76 (n)
Geometric Design (No reflection of absorption losses)	100%	5831x	0.4	0.53
State of the art components (simulated)	75%	4373x	0.4	0.46
Standard component losses (simulated)	55%	3207x	0.4	0.40

Table 1: Concentration-acceptance angle product (CAP) analysis table depending on quality of optics used.

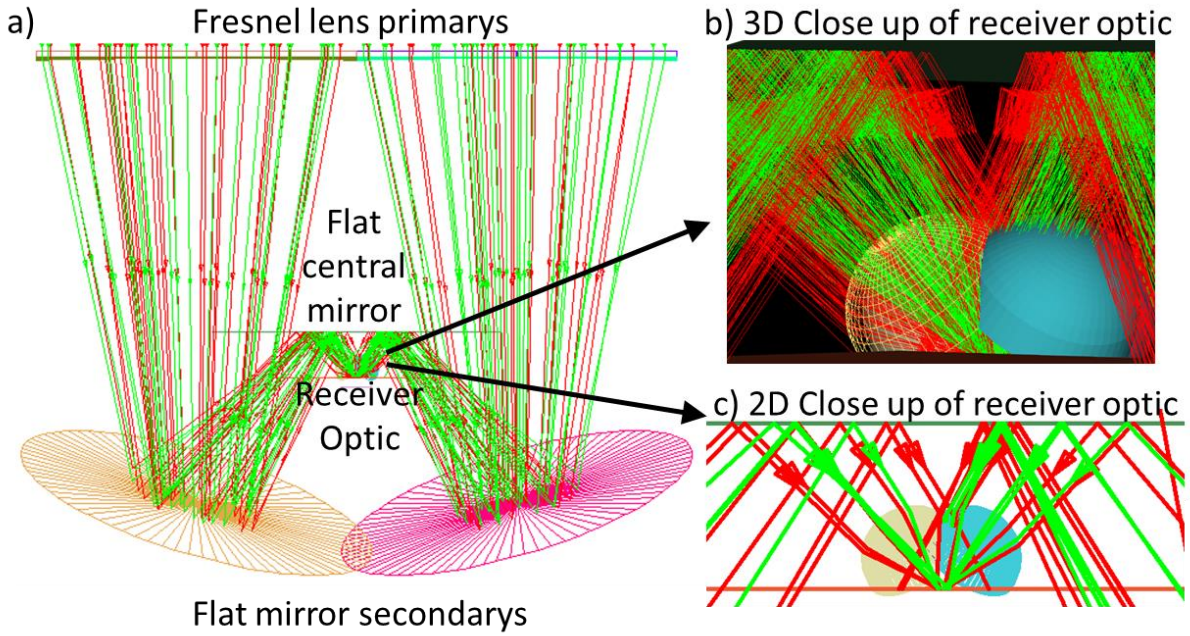

Figure 1: Ray trace simulations of a) full ultrahigh concentrator side view showing rays of 300 and 1800nm (green and red). b) 3D close up of central 4-dome optic which concentrates rays onto 5.5 by 5.5mm solar cell and c) 2D close up of receiver optic showing less rays and more clearly the central focusing point and the challenges of the width of the incoming light onto the central receiver optic.